Deciphering the molecular mechanisms underlying the pathobiology of esophageal squamous cell carcinoma

by

Hai-feng Zhang

A thesis submitted in partial fulfillment of the requirements

for the degree of

Doctor of Philosophy in Medical Sciences - Shantou in

Laboratory Medicine and Pathology

University of Alberta

ABSTRACT

Esophageal squamous cell carcinoma (ESCC) is one of the most lethal cancers worldwide, largely due to a high frequency of tumor invasion/metastasis, chemoresistance and recurrence. In this study, we explored from different perspectives the molecular mechanisms behind these aggressive features of ESCC. **1)** microRNAs are small non-coding RNAs that suppress gene expression at the post-transcriptional level, the deregulation of which have been shown to promote invasion/metastasis. We found that the miR-200b/200a/429 cluster was frequently downregulated in ESCC, which significantly correlated with unfavorable prognosis in ESCC patients. miR-200b suppressed the invasiveness of ESCC both *in vitro* and *in vivo.* Quantitative mass spectrometry identified 57 putative miR-200b targets, including Kindlin-2, which was found to mediate the role of miR-200b in the regulation of ESCC invasiveness by modulating the cytoskeletal and the adhesive machinery. **2)** STAT3 has been widely recognized as an oncogene, whereas accumulating evidence from both experimental and clinical studies has suggested that STAT3 may also carry a tumor suppressor role. We hypothesized that the interplay between the two STAT3 isoforms, STAT3α and STAT3β, may be the key determinant of the opposing roles of STAT3 in cancer biology. We revealed that while STAT3β substantially increased the tyrosine^{705}-phosphorylation, nuclear translocation and promoter occupancy/DNA-binding of STAT3α, it significantly decreased the transcription activity of STAT3 and its tumorigenic potential in ESCC cells. STAT3β also decreased the cancer stem cell population, and markedly sensitized ESCC cells to 5-flurouracil (5-FU) and cisplatin both *in vitro* and *in*

vivo. We found that the STAT3β-induced increase in phospho-STAT3α^{Y705} (pSTAT3α^{Y705}) is attributed to the decreased binding and dephosphorylation of STAT3α by PTP-MEG2, a protein tyrosine phosphatase. We found a significant correlation between the expression of STAT3β and pSTAT3α^{Y705} and a longer survival in ESCC patients. Importantly, the prognostic value of pSTAT3α^{Y705} was dependent on the expression status of STAT3β. **3)** The presence of cancer stem cells within a tumor has been linked to chemoresistance and cancer recurrence. Using a lentiviral reporter expressing GFP and luciferase under the control of SRR2 (Sox2 regulatory region 2), two subpopulations of cells (*i.e.* GFP- and GFP+) were identified in ESCC based on the reporter responsiveness. Compared with RU (reporter-unresponsive) cells, RR (reporter-responsive) cells displayed a higher capacity in forming tumorspheres, contained a higher proportion of stem cell-like CD44^{High} cells and were more chemoresistant to cisplatin. Importantly, we revealed that ROS (reactive oxygen species) induced by H_2O_2 was able to convert the less stem-like RU cells to the more stem-like RR cells. We found that the PI3K/AKT pathway activates MYC to promote the stemness in RR cells, which also mediates the ROS-induced RU-to-RR conversion. To conclude, this study has provided insights into the molecular mechanism underlying the pathobiology of ESCC, which may provide valuable prognostic and therapeutic targets in ESCC.

PREFACE

Some of the research conducted for this thesis forms part of an international research collaboration, led by Professor Raymond Lai at the University of Alberta, with Professor Li-Yan Xu being the lead collaborator at Shantou University Medical College.

The patient samples were obtained and processed from Shantou, China, the research projects, of which this thesis is a part, received research ethics approval in 2010 from both the ethical committee of Shantou Central Hospital and that of Shantou University Medical College. Written informed consent was obtained from all surgical patients to use resected samples for research. The animal studies were performed in Shantou, China, in accordance with the Institutional Animal Care and Use Committee of Shantou University. Moreover, the grant that supported this research project, of which this thesis is a part, also received research ethics approval from the University of Alberta Research Ethics Board, Project Name: The clinical and biological significance of Sox2 in breast cancer"; Ethical application number: Pro00044942; Date: May 8, 2014.

Chapter 1 of this thesis has been published as:

1). **Zhang HF,** Xu LY, Li EM. A Family of Pleiotropically Acting MicroRNAs in Cancer Progression, miR-200: Potential Cancer Therapeutic Targets. Curr Pharm Des 2014;20:1896-903. I was first author of this paper, and contributed to this work as outlined on page 1 of this thesis.

2). **Zhang HF,** Lai R. STAT3 in cancer: friend or foe? Cancers (Basel) 2014;6(3):1408-40. I was first author of this paper, and contributed to this work as outlined on page 1 of this thesis.

Chapter 2 of this thesis has been published or submitted for publication as:

1). **Zhang HF,** Zhang K, Liao LD, Li LY, Du ZP, Wu BL, Wu JY, Xu XE, Zeng FM, Chen B, Cao HH, Zhu MX, Dai LH, Long L, Wu ZY, Lai R, Xu LY, Li EM.

miR-200b suppresses invasiveness and modulates the cytoskeletal and adhesive machinery in esophageal squamous cell carcinoma cells via targeting Kindlin-2. *Carcinogenesis* 2014;35:292–301. I was first author of this paper, and contributed to this work as outlined on page 115 of this thesis.

2). **Zhang HF,** Alshareef A, Wu CS, Li S, Cao HH, Lai R. Xu LY, Li EM. Loss of miR-200b promotes invasion via activating the Kindlin-2/Integrin β1/AKT pathway in esophageal squamous cell carcinoma: an E-cadherin-independent mechanism. Oncotarget. 2015 Aug 20. [Epub ahead of print]. I am first author of this paper, and contributed to this work as outlined on page 115 of this thesis.

Chapter 3 of this thesis has been submitted for publication as:

Zhang HF, Chen Y, Wu CS, Wu ZY, Tweardy DJ, Alshareef A, Liao LD, Xue YJ, Wu JY, Chen B, Xu XE, Gopal K, Gupta N, Li EM, Xu LY, Lai R. The interplay between STAT3α and STAT3β dictates the dual role of STAT3 in esophageal squamous cell carcinoma. *Clin Cancer Res* 2015. (Accepted). I am the first author of this paper, and contributed to this work as outlined on page 192 of this thesis.

Chapter 4 of this thesis represents work that will be included in a manuscript in preparation:

Zhang HF, Wu CS, Alshareef A, Gopal K, Gupta N, Li EM, Xu LY, Lai R. The PI3K/AKT/c-MYC axis promotes the acquisition of cancer stem-like features in esophageal squamous cell carcinoma. (2015, Submitted to The Journal of Pathology). I am the first author of this paper, and contributed to this work as outlined on page 251 of this thesis.

ACKNOWLEDGEMENTS

I am grateful to all the individuals who have guided and supported me during the journey towards the PhD. Foremost, I would like to thank my supervisor, Dr. Raymond Lai, who not only taught me how to write papers professionally, but also inspired me enormously in doing research, such as how to interpret unexpected data from different perspectives, and how to establish a hypothesis/model and use it to predict the outcomes. Equally important, I would like to thank my co-supervisor Dr. Li-Yan Xu, as well as Dr. En-Min Li, who have constantly guided and supported me during my graduate studies. They have witnessed me learning research all the way back from the first day when I got to know how to use a pipet. Thank them for giving me numerous opportunities to attend international conferences to interact with researchers from all around the world.

I would also like to thank my supervisory committee members, Dr. Jun-Hui Bian and Dr. Robert Ingham, for their constant and invaluable support throughout my PhD program. I'm grateful to all the time and input you have given to my projects, which has significantly helped me in completing this journey.

To Dr. Paul Melancon, the chair of the UA-Shantou Steering Committee, for guiding me as a foreign graduate student from the first day since I entered the PhD program. To Dr. Monika Keelan, the Graduate Studies Coordinator, for

giving me very thoughtful guidance and support throughout my studies in the University of Alberta.

Thank you to Dr. Minjie Luo, consultant of Shantou University Medical College in the Li Ka Shing Foundation, for kindly supporting my PhD studies. I also would like to thank Dr. Jian-Jun Zhang for your patient guidance in the initial stage of this program. To Dr. Joan Kale for teaching me English language for my studies abroad.

To all the current and past members of the Lai Lab who have provided me enormous help in both research and daily life. My special thanks to my colleagues and friends Abdulraheem Alshareef and Chengsheng Wu, for their support in the lab as well as their invaluable friendship. Thank you to Dr. Karen Jung for being such a nice and warmhearted colleague. Thank Ying Zhang, my long-time classmate and colleague, for all your support these years.

I'm grateful to Shantou University Medical College, and the Li Ka Shing Foundation for their generous financial support needed during my PhD studies. Thank the Key Laboratory of molecular Biology for High Cancer Incidence Coastal Chaoshan Area for its support. Thank the Canadian Institutes of Health Research (CIHR), the National Natural Science Foundation of China (NSFC), and the NSFC-Guangdong Joint grants for funding the research projects.

Table of Contents

List of Abbreviations

3'UTR – three prime untranslated region

5-Aza-dC – 5-Aza-2'-deoxycytidine

5-FU – 5-fluorouracil

ALK – anaplastic lymphoma kinase

ALCL – anaplastic large cell lymphoma

APC – adenomatous polyposis coli

BCL2 – B-cell lymphoma 2

Cyto – cytoplasmic

c-MYC – V-myc avian myelocytomatosis viral oncogene homolog

CRC – colorectal cancer

CSCs – cancer stem cells

C-terminal – carboxy terminal

CTEN – C-terminal tensin-like

Co-IP – co-immunoprecipitation

DMEM – Dulbecco's modified Eagle's media

DN – dominant negative

DNMT – DNA methyltransferase

Dox – doxycycline

ECL – enhanced chemiluminescence

EMT – epithelial-to-mesenchymal transition

ERK – extracellular signal-related kinase

ESCC – esophageal squamous cell carcinoma

F – phenylalanine

FA – focal adhesion kinase

FAK – focal adhesion kinase

FBS – fetal bovine serum

FITC – fluorescein isothiocyanate

FN1 – fibronectin 1

FACS – fluorescent activated cell sorter

FITC – fluorescein isothiocyanate

GFP – green fluorescence protein

GLI1 – glioma-associated oncogene homolog 1

GSK – glycogen synthase kinase

H2O2 – hydrogen peroxide

H&E – Hematoxylin and eosin

HDAC1 – histone deacetylase 1

HEK – human embryonic kidney

HMECs – human microvascular endothelial cells

HUVECs – human umbilical vein endothelial cells

IGF-1R – insulin-like growth factor 1 receptor

IHC – immunohistochemistry

IL – interleukin

IP – immunoprecipitation

JAK – Janus kinase

MAPK – mitogen-activated protein kinase

MAX – MYC-associated factor X

Mcl1 – myeloid cell leukemia sequence 1

MEK – mitogen-activated protein kinase

MET – mesenchymal-to-epithelial transition

Min – multiple intestinal neoplasia

miRNA – microRNA

MTS – 3-(4,5-dimethylthiazol-2-yl)-5-(3-carboxymethoxyphenyl)-2-(4-sulfophenyl)-2H-tetrazolium

NADPH – Nicotinamide adenine dinucleotide phosphate

NAC – N-acetyl-L-cystein

NPM-ALK – nucleophosmin fused to anaplastic lymphoma kinase

N-terminal – amino terminal

N/A – not available

ns – not significant

P/p – phospho/phosphorylation

p-Y – phosphorylated tyrosine

PARP1 – poly (ADP ribose) polymerase 1

PBS – phosphate buffered saline

PCR – polymerase chain reaction

PI – propidium iodide

PI3K – phosphatidylinositide 3-kinase

PIAS3 – protein inhibitors of activated STAT3

PRC – polycomb repressor complex

PTCH – patched

PTEN – phosphatase and tensin homolog

PTPs – protein tyrosine phosphatases

ROS – reactive oxygen species

RR – reporter responsive

RTK – receptor tyrosine kinase

RU – reporter unresponsive

SDS-PAGE – sodium docedyl sulfate-polyacrylamide gel electrophoresis

SH2 – Src homology2

SHP1 – Src homology region 2 domain-containing phosphatase-1

SHP2 – Src homology region 2 domain-containing phosphatase-2

siRNA – small interfering RNA

SILAC (stable isotope labeling with amino acids in cell culture)

SRC – v-Src avian sarcoma (Schmidt-Ruppin A-2) viral oncogene homologue

SRR2 – Sox2 regulatory region 2

STAT – signal transducer and activator of transcription

SOCS – suppressors of cytokine signaling

Sox2 – SRY (sex determining region Y)-box 2

LGL – large granular lymphocytic leukemia

CLPD-NKs – chronic lymphoproliferative disorders of natural killer cells

Tet – tetracycline

TRAIL – TNF-related apoptosis inducing ligand

tTa – Tetracycline-transactivator

UV – ultraviolet

VEGF – vascular endothelial growth factor

Y – tyrosine

List of Tables

List of Figures

Chapter 1

General Introduction

This chapter has been modified from the two publications shown below:

1. **Zhang HF,** Xu LY, Li EM. A Family of Pleiotropically Acting MicroRNAs in Cancer Progression, miR-200: Potential Cancer Therapeutic Targets. Curr Pharm Des 2014;20:1896-903.

2. **Zhang HF,** Lai R. STAT3 in cancer: friend or foe? Cancers (Basel). 2014;6(3):1408-40.

Zhang HF is the first author of both review papers and did the writing of the manuscripts. For the first publication, Dr. Xu LY and Dr. Li EM supervised and provided valuable suggestions during the preparation of the manuscript. For the second publication, Dr. Lai R supervised the preparation of the manuscript, and critically revised the manuscript before and after the submission.

1.1 Esophageal squamous cell carcinoma

Esophageal cancer is one of the deadliest malignancies, with an estimated 482,000 new cases and 407,000 deaths worldwide in 2008, represents the sixth leading cause of cancer-related death [1-2]. Esophageal cancer is approximately three times more prevalent in males than in females, partly due to the fact that tobacco smoking and alcohol drinking, two critical risk factors for ESCC, are more common in males than in females [3]. The absence of the serosa and the presence of the extensive lymphatics in the esophagus are probably some of the contributing factors to the high frequency of local invasion and metastasis in ESCC. At the time of the diagnosis of esophageal cancer, more than 50% of patients have either unresectable tumors or radiographically visible metastases, resulting in a very poor prognosis of this type of malignancy [3]. A previous survey has shown that despite the use of multimodal treatments, the overall 5-year survival rate for patients with esophageal cancer was only about 14% [3-4]. Esophageal cancer is histologically divided into esophageal squamous cell carcinoma (ESCC) that originates from the flat squamous cell layer lining the cavity of esophagus, and esophageal adenocarcinoma that develops from the mucus-secreting glands in the esophagus. ESCC is the most prevalent type of esophageal cancer worldwide, which constitutes the vast majority of esophageal cancer cases in China, whereas adenocarcinoma is the predominant type of esophageal cancer in the Western world [1-2].

Six regions in China have been identified as high-risk regions for esophageal cancer, including Linxian of Henan province, Cixian of Hebei province,

Yangcheng of Shanxi province, Huaian of Jiangsu province, Yanting of Sichuan province and Chaoshan area of Guangdong province [5]. Among the six areas, Chaoshan area is the only high-risk region for ESCC that localizes in the coastal region of China (**Figure 1.1**) [6,7]. While tobacco smoking and alcohol drinking were found to be highly associated with a higher risk of ESCC, diferent risk factors were revealed in these ESCC hotspots in China [3]. Epidemiology studies have indicated that unique diet factors, such as consumption of fermented fish sauce and drinking very hot tea are significant risk factors for ESCC in the Chaoshan region [6,7]. The Linxian area of Henan province is another ESCC hotspot that has been extensively studied as to what are the major risk factors for ESCC development. Poor overall nutritional status and deficiencies in vitamins have been shown to be critical contributors for the prevalence of ESCC in this area [3]. However, less is known about the specific ESCC risk factors in other hotspots. In the present study, the ESCC patient samples are collected from one of the cancer centers in the Chaoshan region.

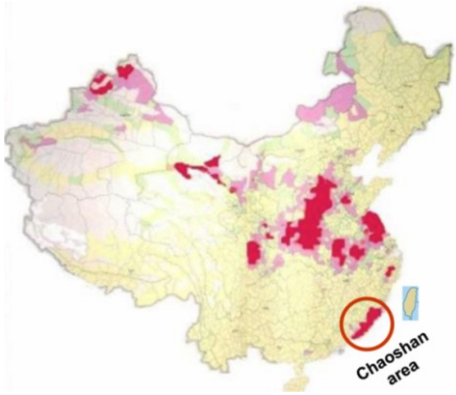

Figure 1.1 Overview of the ESCC hotspots (labeled with red) in China (cited from the website: http://dceg.cancer.gov/news-events/linkage-newsletter/2014-11/research-publications/china-partnership). The circled area is the Chaoshan area, where the clinical samples of this study were collected.

During the last few years, our understanding of the pathobiology of ESCC has increased exponentially, attributing to the findings of multiple large-scale genomic analyses [8-12]. In these studies, over ten susceptibility loci and a spectrum of mutations were discovered in ESCC. For instance, by genotyping 1,077 individuals with ESCC and 1,733 control subjects of Chinese Han descent, Wang and colleagues revealed that *PLCE1* at 10q23 and *C20orf54* at 20p13 were susceptibility loci in ESCC [8]. Another study led by Lin and colleagues uncovered nine new ESCC susceptibility loci at chromosomes 4q23, 16q12.1, 17q21, 22q12, 3q27, 17p13, 18p11, 2q22 and 13q33. Importantly, the susceptibility loci at the 4q23 locus, which includes the *ADH* (Alcohol dehydrogenase) cluster, had a significant interaction with alcohol drinking in their association with ESCC risk [9]. Moreover, they also confirmed the known association of the *ALDH2* (aldehyde dehydrogenase 2) locus on 12q24 to ESCC, and drinkers with both of the *ADH1B* and *ALDH2* risk alleles increased the chance of developing ESCC by 4-fold [9]. The other genomic studies commonly revealed that the well-known tumor-associated genes such as *TP53, RB1, CDKN2A, PI3KCA, NFE2L2 and NOTCH1* were frequently mutated in ESCC, and recurrent mutations were also found in multiple histone modification genes such as *EP300, KMT2D, KMT2C and CREBBP* [10-12]. Besides, previously uncharacterized mutated genes such as *FAT1, FAT2, ZNF750, ADAM29, FAM135B,* and *FBXW7* were found in ESCC [10-12]. Based on these large-scale genomic studies in ESCC, major abnormalities were identified in various signaling pathways such as the RTK, MAPK, PI3K, Wnt, cell cycle, Hippo, and Notch pathways, and the epigenetic regulation were also frequently deregulated by multiple molecular mechanisms [10-12].

1.2 microRNAs (miRNAs) in cancer

1.2.1 Background

miRNAs are small non-coding RNAs that regulate gene expression at the post-transcriptional level mainly by binding specifically to the 3'-untranslated regions (3'-UTRs) of mRNAs and inhibiting their translation via inducing the RNA-induced silencing complex [13, 14]. Recently, miRNAs have also been shown to modulate gene expression by targeting the coding regions as well as 5'-UTRs of their target mRNAs [15-18]. Our current knowledge indicates that miRNAs regulate virtually all types of cellular processes, such as cell differentiation, proliferation, motility, metabolism and apoptosis; by doing so, miRNAs participate in multiple developmental and physiological processes [19, 20]. However, aberrant expression of miRNAs is associated with the pathogenesis of various diseases, and our understanding of the role of miRNAs in cancer has increased dramatically during the last decade [21]. In addition, miRNAs also mediate the roles of critical oncogenes and tumor suppressor genes in different stages of cancer progression [22,23]. For instance, MYC can activate the expression of the miR-17-92 cluster, which augments tumor angiogenesis by targeting Tsp1 and CTGF [22]. The miR-34 family members were demonstrated as crucial mediators of the strong tumor suppressive function of p53 in cancer by targeting CDK4 and MET, thereby repressing cell cycle progression and cell proliferation [23].

miRNAs, together with DNA methylation and histone modifications (e.g. methylation and acetylation) represent the three major aspects of epigenetics. Since genetic mutation is an irreversible process, whereas epigenetic

modifications abnormalities are reversible, at least to varying degrees, restoration of epigenetic aberrancies have been shown to be an attractive approach in cancer therapies [24-27]. In recent years, DNA methylation inhibitors like 5-azacytidine (azacitidine) and 5-aza-2'-deoxycytidine (decitabine) and histone deacetylase (HDAC) inhibitors like suberoylanilide hydroxamic acid (SAHA) have been approved for the treatment of certain types of cancer [28-31]. After about a decade of extensive research, miRNAs have also been shown to be promising tools or targets in cancer therapeutic intervention [32, 33].

1.2.2 The miR-200 family

1.2.2.1 Introduction

The miR-200 family (denoted as miR-200s herein) is comprised of 5 members that are encoded within two clusters located on separate chromosomes: the miR-200b-200a-429 cluster (miR-200b cluster) on chr1p36 and the miR-200c-141 cluster on chr12p13 **(Figure 1.2A)**. The five members can be subdivided into two groups according to their seed sequences (about 6-8 nucleotides in length at the 5' end of a mammalian miRNA): miR-200a and miR-141 (AACACUG) comprise one group and miR-200b/c and miR-429 (AAUACUG) comprise another **(Figure 1.2B)**, and due to the similarity of their seed sequences, similar target genes may be shared. Recently, miR-200s has been demonstrated to play potent tumor suppressive roles in multiple types of solid tumors [34-42]. miR-200s also play important roles in suppressing the self-renewal of cancer stem cells, and thus participate in the initiation of tumors [39-42]. By targeting the key components of the VEGF signaling

pathway, such as VEGF-A, FLT1/VEGFR1, KDR/VEGFR2 and ETS1, miR-200s are also involved in the angiogenesis network, which may facilitate the maintenance of tumors [43-47]. Importantly, miR-200s are currently recognized as central negative regulators of epithelial-to-mesenchymal transition (EMT), through which they modulate the invasion and metastasis of cancers [34-38]. Moreover, the involvement of miR-200s in the chemotherapeutic resistance of cancer cells has also been reported [48-56]. Collectively, the information described above indicates that miR-200s participate in virtually all stages of tumor progression, including: tumor initiation, tumor maintenance, malignant metastasis and chemoresistance. Therefore, restoration of miR-200s could serve as a promising therapeutic approach against cancer. Nevertheless, a recent study revealed a metastasis enhancing effect of miR-200s in breast cancer, demonstrating that although miR-200s suppress cancer cell invasion in the first step of the complicated cascades of metastasis, miR-200s enhance the colonization of disseminated cancer cells in distant organs [57, 58]. Here, we will specifically describe: 1) the reported findings on the function of miR-200s in different stages of cancer progression; 2) pharmaceutical approaches that can be employed to manipulate the expression of miR-200s to treat cancers; 3) cautions that should be taken when considering miR-200s as cancer therapeutic targets.

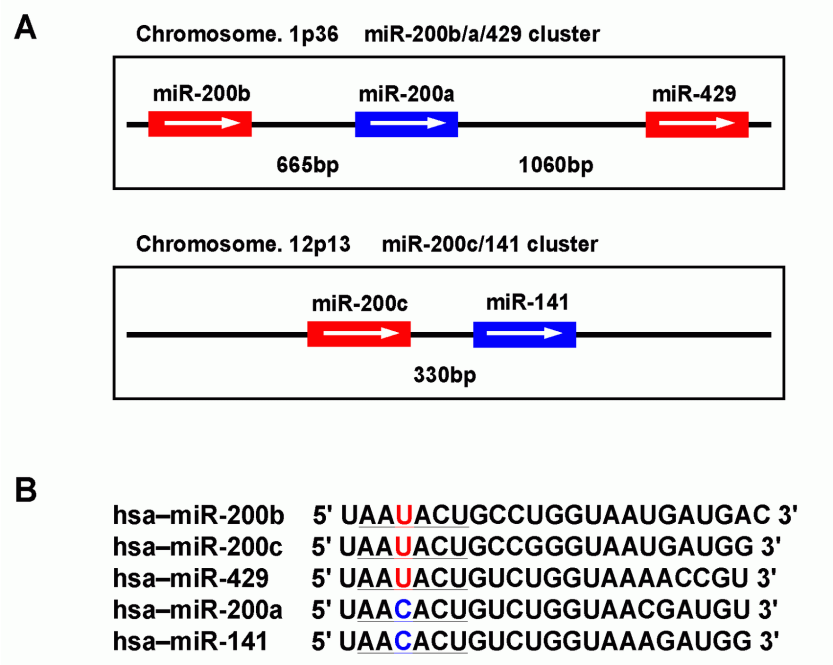

Figure 1.2 Overview of the chromosomal localization and the sequences of the miR-200 family members. (A) Schematic representations of the chromosomal localization of the miR-200 family members. The miR-200b/a/429 cluster (including miR-200b, miR-200a and miR-429) members are encoded on chromosome 1p36, and the miR-200c/141 cluster (including miR-200c and miR-141) members are encoded on chromosome 12p13. (B) The five members of the miR-200 family have high sequence similarities. According to the similarity of the "seed sequence" (sequences underlined), the miR-200 family members are divided into two groups.

1.2.2.2 Downregulation of miR-200s Promotes Cancer Cell Stemness

Cancer stem cells are a group of cancer cells with stem-like properties that represent only a small minority of neoplastic cells within a tumor, and have been demonstrated to be "tumor initiating cells" [59, 60]. Recently, Shimono *et al*. discovered that miR-200s were downregulated in breast cancer stem cells, and overexpression of miR-200c diminished the tumor initiation capacity of these cells [39]. In this study, miR-200c was shown to target the 3'UTR of

BMI1, an essential gene that regulates self-renewal and differentiation of multiple stem cell types, including hematopoietic, brain, and mammary stem cells [61-63]. Wellner *et al*. demonstrated that miR-200s are important mediators of the tumor-initiating capacity of ZEB1 in pancreatic and colorectal cancers [40]. Notably, miR-200s were shown to suppress cancer stem cell properties by targeting BMI1 as well as other stem cell factors, such as KLF4 and SOX2 [40]. Moreover, the repression of miR-200s expression was shown to be important during cancer stem cell formation in an inducible oncogenesis model [41]. This study revealed that miR-200b inhibited the formation of cancer stem cells by directly targeting SUZ12, a subunit of a polycomb repressor complex [41]. Overexpression of miR-200b or depletion of its target SUZ12 not only blocked the formation and maintenance of mammospheres, but also strongly suppressed tumor growth and prolonged remission in mouse xenografts, especially in combination with chemotherapy reagents [41].

Intriguingly, both of the two stemness related targets of miR-200s mentioned above (*i.e.* BMI1 and SUZ12) are subunits of the polycomb repressor complex (PRC), which is composed of two distinct members, PRC1 and PRC2, which directly regulate key developmental factors that maintain embryonic stem cell self-renewal and pluripotency [64-66]. Specifically, BMI1 is a subunit of PRC1, while SUZ12 is a subunit of PRC2. The upregulation of these PRC factors has been frequently observed in aggressive tumors [67-69]. Collectively, the evidence clearly shows that miR-200s modulate the formation of cancer stem cells by regulating the expression of PRC factors and other stem cell factors,

and by doing so, this family of miRNAs is involved in tumor initiation processes **(Table 1.1)**.

Table 1.1 The function and targets of miR-200s in cancer

Cancer type	Target gene(s)	Functions of miR-200s	References
Breast cancer	ZEB1/2, SIRT1	Inhibit EMT, enhance chemosensitivity	[34-37, 52, 79, 105-107]
	BMI1, SUZ12	Inhibit cancer stem cell formation	[39-42]
	MSN, FN1, PLCG1	Inhibit migration/invasion and anoikis	[108, 109]
	WAVE3, FHOD1, PPM1F	Regulate cytoskeleton reorganization	[110, 111]
	SEC23, ZEB2	Promote cancer metastasis	[57, 58]
Lung cancer	ZEB1/2	Inhibit EMT and metastasis	[81, 112, 113]
	FLT1	Inhibit invasion and metastasis	[45]
	E2F3	Enhance chemosensitivity to docetaxel	[56]
HCC	ZEB1/2	Inhibit EMT and migration/invasion	[114]
ATC	Unverified	Inhibit EMT and migration/invasion	[115, 116]
Colorectal cancer	ZEB1, ETS1, FLT1	Inhibit EMT and metastasis	[34, 38, 88, 117]
Pancreatic cancer	ZEB1/2	Inhibit EMT, enhance chemosensitivity	[34, 50, 95, 97]
	BMI1	Inhibit cancer stem cell self-renew	[40]
PNET	ZEB1	Inhibit EMT, invasion and metastasis	[80]
Endometrial cancer	TUBB3	Enhance chemosensitivity	[49, 51]
Prostate cancer	ZEB1/2	Inhibit EMT and cancer stem cells	[118, 119]
	SLUG	Inhibit EMT and tumorigenesis	[77]
Gastric cancer	ZEB1/2, CTNNB1	Inhibit EMT and cell proliferation	[120-123]
Lymphoma	CCNE2	Involved in the disease progression	[124]
Ovarian cancer	MAPK14	Control oxidative stress response	[125]
	ZEB1/2	Inhibit EMT, promote transformation	[38, 126, 127]
	TUBB3	Induce sensitivity against paclitaxel	[49, 51, 92]
Bladder cancer	ZEB1/2	Inhibit EMT, enhance chemosensitivity	[48, 128]
	ERRFI-1	Enhance sensitivity to EGFR therapy	[48]
HNSCC	ZEB1/2, CTNNB1, BMI1	Inhibit cell growth, migration/invasion	[129, 130]
Meningiomas	ZEB1/2, CTNNB1	Inhibits tumor growth	[131]

Esophageal cancer	PPP2R1B	Induce chemoresistance	[132]
Melanoma	MARCKS	Promote invasiveness	[133]
PDAC	EP300, ZEB1	Promote proliferation and metastasis	[134, 135]

HCC: Hepatocellular carcinoma; ATC: Anaplastic thyroid cancer; PNET: pancreatic neuroendocrine tumor; HNSCC: Head and neck squamous cell carcinoma; PDAC: pancreatic ductal adenocarcinoma.

1.2.2.3 Loss of miR-200s Promotes Tumor Maintenance by Augmenting Angiogenesis

Recently, in both endothelial cell models and cancer cell models, several groups of researchers have demonstrated that miR-200s members regulate the expression of multiple proteins in the angiogenesis regulatory network [43-47]. Chan *et al.* discovered that the pro-angiogenic effects induced by hypoxia or Hif-1α stabilization were mediated by the suppression of miR-200b expression in human dermal microvascular endothelial cells [43]. Further investigation revealed that miR-200b hampered the pro-angiogenic effects of hypoxia by targeting ETS1, a key transcription factor that promotes angiogenesis [43]. miR-200b was also shown to directly target and inhibit the expression of KDR/VEGFR2 in both human microvascular endothelial cells (HMECs) and human umbilical vein endothelial cells (HUVECs) [43, 44]. Moreover, other two key components of the VEGF signaling pathway such as VEGF-A and FLT1/VEGFR1 have also been identified as targets of miR-200b [44, 45]. Ectopic expression of miR-200b or miR-200c has been shown to diminish the tube-formation ability of both HMECs and HUVECs [44]. VEGF-A and KDR/VEGFR2 have also been shown to be the targets of miR-200s in other physiological and pathological models, *e.g.* cutaneous wound angiogenesis and diabetic retinopathy [46, 47].

Despite the potent regulatory power of miR-200s on the VEGF signaling network, direct evidence demonstrating the functional effects of miR-200s on tumor angiogenesis is still lacking **(Table 1.1)**. Given the indispensable role of angiogenesis in tumor maintenance, miR-200s may serve as invaluable therapeutic targets in cancer treatment, although more lines of evidence are required.

1.2.2.4 miR-200s Influences Cancer Cell Invasion and Metastasis by Regulating EMT

EMT is a biological process in which polarized epithelial cells that are closely adjoined by specialized membrane structures (*e.g.* tight junctions, adherens junctions, desmosomes and gap junctions) convert into isolated, non-polarized, motile and invasive mesenchymal cells [70-72]. This process is accompanied by a switch in epithelial markers (including E-cadherin and cytokeratins) and mesenchymal markers (including vimentin, N-cadherin and fibronectin) [70-72]. EMT has been observed in the invasive front of various cancers, and the acquisition of a mesenchymal phenotype is often correlated with poor prognosis in cancer patients [73-75]. Currently, miR-200s members are regarded as master regulators of EMT [76]. Downregulation of miR-200s was shown to promote EMT by targeting three key transcription factors that suppress the expression of E-cadherin, such as ZEB1, ZEB2 and SLUG [34-38, 77]. Intriguingly, all these EMT-inducing transcription factors were demonstrated to suppress the expression of miR-200s by specifically binding to the E-box elements within the promoter regions [34, 35, 77]. Therefore, a self-reinforcing regulatory loop is formed between ZEB1, ZEB2, SLUG and

miR-200s, which has been shown to determine the epithelial or mesenchymal status of cancer cells [34-38, 77]. Moreover, other targets of miR-200s, *e.g.* BMI1 and SIRT1, were also shown to mediate the regulatory impact of miR-200s on EMT [78, 79].

Governed by the feedback regulatory mechanisms described above, downregulation of miR-200s has been reported to enhance the aggressive properties of various cancers, including breast cancer, colorectal cancer, bladder cancer, gastric cancer, hepatocellular carcinoma, pancreatic cancer, prostate cancer and lung adenocarcinoma **(Table 1.1)**. Reintroduction of miR-200s in these cancers has been shown to induce epithelial phenotypes characterized by the gain of E-cadherin expression and reduced invasive properties (described in Table 1.1). Remarkably, a strong correlation was observed between miR-200s and the mesenchymal or epithelial phenotype across the NCI-60 set of cancer cell lines derived from nine different human cancers (*i.e.* breast, colon, melanoma, lung, brain, blood, ovarian, prostate and renal) [38]. In clinical studies, a strong correlation between miR-200s, ZEB1/2 and the EMT status was observed in breast cancer [36].

Multiple *in vivo* studies conducted in mouse models further verified the essential roles played by the ZEB1/2—miR-200s regulatory loop in cancer metastasis [80, 81]. Olson *et al*. investigated the microRNA dynamics in different stages of tumorigenesis in a mouse model of pancreatic neuroendocrine tumors, and revealed that the miR-200s—ZEB1—E-cadherin axis was specifically deregulated in metastasis-like tumors; miR-200s and E-

cadherin expression were reduced and ZEB1 expression was upregulated in metastasis-like primary tumors and liver metastases compared to primary tumors [80]. Another study performed in a lung adenocarcinoma mouse model demonstrated that the expression of miR-200s was markedly repressed in metastasis-prone tumors relative to metastasis-incompetent tumors [81]. Enforced expression of the miR-200b-200a-429 cluster in metastasis-prone tumor cells strongly abrogated their capacity to undergo EMT and metastasize in syngeneic mice, and the miR-200s—ZEB1/2—E-cadherin axis was shown to mediate the observed effects [81].

In addition to the feedback loops illustrated above, several recent studies have identified another novel self-reinforcing regulatory loop between miR-200s and the Notch signaling pathway. miR-200s was shown to control the Notch signaling pathway in multiple cancer models by directly targeting multiple activators of Notch pathway, such as the Notch ligand Jagged1 and the mastermind-like coactivators Maml2 and Maml3 [82, 83]. Intriguingly, Notch activation (by Jagged2, another ligand of Notch) was also demonstrated to suppress the expression of miR-200s in lung adenocarcinoma cells [84]. Therefore, a reciprocal regulatory loop between miR-200s and Notch signaling pathway was established. In biological function studies, the miR-200s/Notch regulatory loop influenced the invasive, metastatic and the self-renew capacities of cancer cells [82-84].

Notably, it is currently well-recognized that EMT is a reversible process: after being successfully disseminated into distant organs with the assistance of the

EMT process, cancer cells usually undergo mesenchymal-to-epithelial transition (MET), a process that is the reverse of EMT, to facilitate the subsequent settlement and proliferation of the cancer cells at secondary locations [85]. This theory has been validated in the metastasis process in multiple cancer types, including prostate cancer, breast cancer and colorectal cancer [86-88]. Recent studies have shown that miR-200s are involved in the dynamic transition between the mesenchymal and epithelial status of cancer cells to fuel the malignant traits of tumors [88, 89]. Hur *et al*. revealed that miR-200c was significantly downregulated in primary colorectal cancer with metastasis compared with thoese without metastasis, which facilitated the EMT process by upregulating of ZEB1, ETS1 and FLT1 in these cells [88]. However, the reduced expression of miR-200c was restored once the metastatic colorectal cancer cells arrived at distant organs, which was accompanied by downregulation of ZEB1 and the induction of MET [88]. Such a switch from a mesenchymal to an epithelial phenotype was demonstrated to allow the metastatic cells to regain their proliferative potential and resume growth at the secondary metastatic sites [88]. In agreement with this finding, another study also documented the increase of miR-200b and E-cadherin, a surrogate marker of EMT, in the distant metastases of breast cancer [89].

To sum up, these discoveries have pinpointed the significant roles played by miR-200s in the EMT and MET processes during the multi-step metastatic cascade, and the multiple self-reinforcing loops that modulate miR-200s expression strongly augmented the pivotal position of miR-200s in the invasion and metastasis of cancers **(Figure 1.3)**.

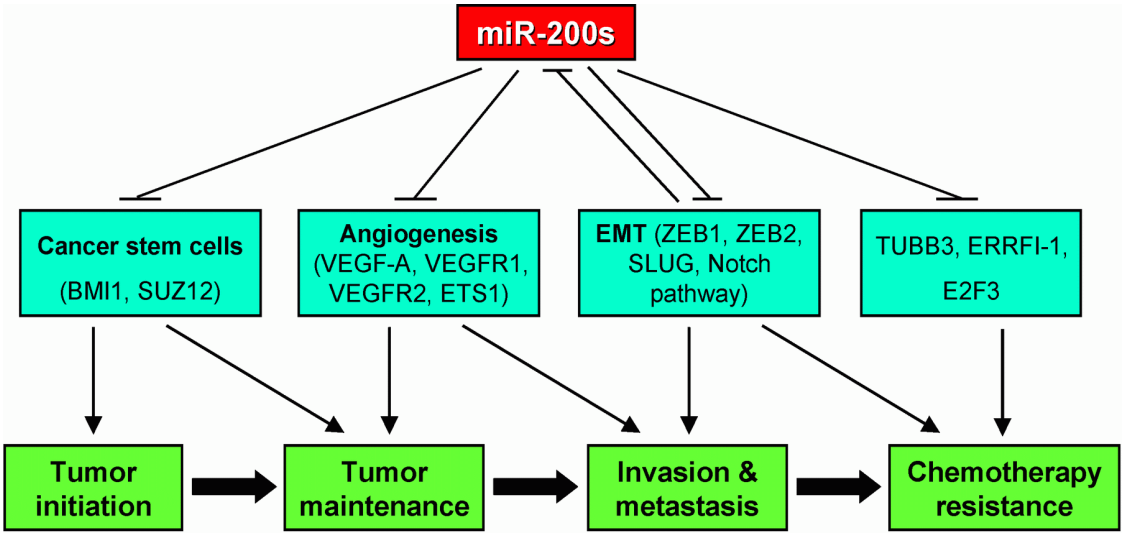

Figure 1.3 A schematic representation of the function of miR-200 family (miR-200s) in different stages of cancer progression. By directly targeting the genes involved in the formation of cancer stem cells, angiogenesis, EMT and chemoresistance, miR-200s have been shown to play important roles throughout the progression of cancers, including tumor initiation, tumor maintenance, invasion/metastasis and chemoresistance. Notably, multiple self-reinforcing regulatory loops are formed between miR-200s and their targets that play key roles in EMT. It is also notable that certain biological processes participate multiple stages of malignant progression. Specifically, cancer stem cells are responsible for both tumor initiation and tumor maintenance, angiogenesis is a process that contributes to both tumor growth and tumor metastasis, and the EMT process not only confers high invasive/metastatic properties to cancer cells, but also facilitates the chemoresistance of tumors.

1.2.2.5 Deregulation of miR-200s is Associated With Chemoresistance

Since EMT is also associated with the acquisition of chemoresistant phenotypes in cancer cells [90, 91], mounting evidence has shown that the EMT process initiated by the loss of miR-200s plays a causal role in cancer cell chemoresistance **(Table 1.1)**. In addition, multiple genes specifically associated with chemoresistance to certain drugs have been shown to be

targets of miR-200s. For instance, Adam *et al*. found that all five members of miR-200s were downregulated in mesenchymal-like bladder cancer cell lines compared to epithelial cells [48]. Overexpression of miR-200 not only reversed the EMT phenotype by targeting ZEB1/2, but also conferred sensitivity of the bladder cancer cells to EGFR therapy by suppressing the expression ERRFI-1, another direct target of miR-200s [48]. Moreover, by targeting TUBB3, miR-200c increased the sensitivity of female reproductive cancers, including breast cancer, ovarian cancer and endometrial cancer, to microtubule-targeting agents [49, 51, 92]. In a clinical study, Sun *et al*. showed that reduced expression of miR-200b correlated with the chemoresistance observed in 86 patients with tongue cancer [78]. Furthermore, as shown in **Table 1.1**, miR-200s was also associated with the chemosensitivity of many other cancer types, *e.g.* doxorubicin- or cisplatin-resistant breast cancer [52, 93, 94], docetaxel-resistant human non-small cell lung carcinoma and lung adenocarcinoma [54, 56], hydroxycamptothecin-resistant gastric cancer [55] and gemcitabine-resistant pancreatic cancer [50, 95]. Therefore, the manipulation of miR-200s expression may serve as a promising tool to treat cancers, especially for cancers that possess chemoresistance.

1.2.2.6 Activation of miR-200s Expression by Pharmaceutical Approaches in Cancer Cells

Given the crucial and pleiotropic roles played by miR-200s in cancers, researchers have been prompted to search for effective pharmaceutical approaches to modulate the expression of miR-200s. Li *et al*. demonstrated

certain types of “natural agents”, such as 3,3-diindolylmethane (DIM) or isoflavone, could upregulate the expression of miR-200b and miR-200c in pancreatic cancer cells, which increased the sensitivity of chemoresistant pancreatic cancer cells to gemcitabine [50]. Meanwhile, the expression of ZEB1 and vimentin was decreased, suggesting that the EMT process regulated by miR-200s may have mediated the anti-cancer effects of these “natural agents” [50]. Recently, a study performed by Sarkar and colleagues indicated that an herbal extract curcumin or its analogue difluorinated-curcumin (CDF) could increase miR-200b and miR-200c expression, and this was shown to correlate with a potent increase of the gemcitabine sensitivity of pancreatic cancer cells [95-97]. Further mechanistic investigation suggested that the observed therapeutic effect of the pharmaceutical agents and miR-200s was mediated by an increase in PTEN expression and a decrease in MT1-MMP (Membrane type-1 matrix metalloproteinase) expression [96, 97]. In addition to the “natural agents” mentioned above, garcinol, an herbal extract derived from *Garcinia indica* that has been reported to have anti-cancer properties [98-100], was shown to have the ability to stimulate miR-200b and miR-200c expression, which reversed EMT in aggressive breast cancer cells [101]. Consistently, treatment with miR-200 inhibitors could reverse the anti-invasive effects of garcinol [101]. Taken together, these findings suggest that the activation of miR-200s by means of natural pharmaceutical treatment appears to be a promising approach for cancer therapeutics.

1.3 STAT3 in cancer

1.3.1 Background

The roles and significance of STAT3 in cancer biology have been extensively studied for more than a decade. Mounting evidence has shown that constitutive activation of STAT3 is a frequent biochemical aberrancy in cancer cells, and this abnormality directly contributes to tumorigenesis and shapes many malignant phenotypes in cancer cells. Nevertheless, results from more recent experimental and clinicopathologic studies have suggested that STAT3 also can exert tumor suppressor effects under specific conditions. Importantly, some of these studies have demonstrated that STAT3 can function either as an oncoprotein or a tumor suppressor in the same cell type, depending on the specific genetic background or presence/absence of specific coexisting biochemical defects. Thus, in the context of cancer biology, STAT3 can be a friend or foe. Nevertheless, the underlying mechanisms remain unclear.

1.3.2 The normal functions of STAT3

STAT3 belongs to a family of transcription factors that transduces the cellular signals from a host of cytokines and soluble growth factors such as the IL-6 family cytokines, epidermal growth factor and platelet-derived growth factor [136,137]. In the canonical pathway, ligation of cytokines to their respective cell-surface receptors induces dimerization and auto-phosphorylation of various tyrosine residues of Janus kinases (JAKs), which then serve as the docking sites for the inactive, monomeric STAT3 molecules. The JAK-bound STAT3 molecules are then phosphorylated by JAKs at the tyrosine residue 705 ($STAT3^{Y705}$), a crucial event for the subsequent dimerization and activation of STAT3. Subsequently, the phosphorylated STAT3 (pSTAT3)

molecules form homodimers, which migrate to the nuclei where they bind to the promoters of various target genes and regulate their transcriptions [136,137]. Many STAT3 targets, such as Survivin, Cyclins and the Bcl-2 family proteins, are known to promote cell proliferation and survival [136,138,139]. In recent years, accumulating evidence has suggested the existence of the non-canonical pathway, in which the functions of STAT3 are independent of the phosphorylation of $STAT3^{Y705}$ or its nuclear translocation [140].

STAT3 has important and diverse biological functions in normal cells, and details can be found in a number of excellent reviews [141-143]. Briefly, its biological importance is highlighted by the observation that *STAT3* gene ablation in mice results in embryonic lethality that occurs 6-7 days after conception [144]. Studies using conditional *STAT3* knockout mice have provided evidence that STAT3 is required for the development and differentiation of various tissue types, such as the skin, immune system, liver, mammary gland, thymus and nervous system [141]. For example, ablation of *STAT3* in keratinocytes was found to impair migration of keratinocytes and skin remodelling [145]. In another study, deletion of *STAT3* in the mammary glands was found to suppress apoptosis of the glandular epithelial cells and lead to delayed glandular involution [146]. STAT3 is critical to the development and biology of T-cells. In one specific study in which STAT3 was conditionally ablated in all stratified epithelia including the thymic epithelia, there was a dramatic increase in apoptosis in thymocytes; in addition, STAT3-depleted thymocytes were more susceptible to apoptosis induced by dexamethasone and γ-irradiation [147]. In another study, STAT3 was shown

to be important in mediating the anti-apoptotic effect of IL-6 in the presence of a low-serum culture environment [148].

1.3.3 The oncogenic potential of STAT3

1.3.3.1 An overview

The oncogenic roles of STAT3 have been well-recognized and reviewed in the literature [136-140], and only a brief summary will be provided here. Some of the first evidence supporting the oncogenic role of STAT3 came from studies using *STAT3C*, which is a constitutive active STAT3 mutant construct [149-151]. STAT3C contains two cysteine substitutions at the residues A661 and N663, leading to the formation of disulfide bridges between two STAT3 molecules and mimicking STAT3 homodimerization that occurs in the normal activation process [149]. It has been demonstrated that STAT3C can effectively induce malignant transformation [149-151], and that STATC can transcriptionally increase the expression of many genes that are important in promoting cellular proliferation, resistance to apoptosis, angiogenesis, immune evasion, invasion and metastasis, all of which are hallmarks of cancer [136-140]. Inappropriate activation of STAT3 has been revealed in various types of solid and hematological cancers, and blocking the STAT3 signaling pathway by various means is effective in killing cancer cells in many experimental models [138, 139, 152]. More recently, STAT3 has been implicated in the self-renewal of cancer stem cells [153-157]. For instance, it was found that STAT3C cooperates with the embryonic stem cell marker Sox2 to initiate the malignant transformation process in esophageal basal cells [157].

To reinforce the concept that STAT3 is oncogenic when it is inappropriately or constitutively activated, many laboratories have shown that the dominant negative STAT3 mutant construct, often labeled STAT3-DN in the literature, can effectively mediate cell cycle arrest and/or induce apoptosis in cancer cells [158-160]. STAT3-DN is generated by substituting the Y705 residue with phenylalanine, and thus, STAT3 cannot be phosphorylated. STAT3-DN is believed to exert its biological effects by competing with the endogenous STAT3 molecules for the binding sites on JAKs and other STAT3 activating proteins, thereby limiting the activation of endogenous STAT3. Many studies that had used other means of STAT3 inhibition (*e.g.* siRNA and small peptides) produced similar results, as reviewed by Wang *et al.* [161].

Constitutive activation of STAT3, which has been demonstrated in a broad spectrum of solid and hematological cancers, often correlates with an unfavorable prognosis in cancer patients [137,139,162]. A few recent publications are used to illustrate this point. In a cohort of 262 gastric tumor samples, Xiong *et al.* found that patients carrying tumors with phosphorylated $STAT3^{Y705}$ (or pSTAT3) expression had significantly shorter overall survival compared with those carrying tumors without pSTAT3 [163]. In a study of colorectal cancer, pSTAT3 expression was found to significantly correlate with the depth of tumor invasion, status of lymph node, metastasis and tumor stage [164]. Huang *et al.* also reported that a high expression of *STAT3* mRNA or pSTAT3 protein significantly correlates with a short overall survival and event-free survival in a cohort of patients with diffuse large B-cell lymphoma [165]. STAT3 activation was found to predict a worse clinical

outcome in many other types of cancer, such as cervical cancer [166], esophageal squamous cell carcinoma [167,168], head and neck squamous cell carcinoma [169,170] and thymic epithelial cancer [171].

1.3.3.2 Mechanisms underlying the constitutive activation of STAT3 in cancer

In normal cells, physiologic activation of STAT3 in response to extracellular signals such as growth factors and cytokines is a transient event, largely due to the existence and operation of various negative feedback mechanisms [172,173]. The constitutive activation of STAT3 in cancer cells represents a biochemical aberration, and there are at least four mechanisms shown to contribute to this abnormality: 1) loss of the negative regulation of STAT3; 2) excessive stimulation of STAT3; 3) positive feedback loops that sustain persistent STAT3 activation; 4) somatic mutations that confer a hyperactive property to STAT3.

1.3.3.2.1 Loss of the negative regulation of STAT3

To avoid inappropriately sustained activation of STAT3, there are multiple negative regulators that can promptly silence STAT3 signalling. The suppressors of cytokine signaling (SOCS) and protein tyrosine phosphatases (PTPs) are two families of proteins that carry out this important function [173-175]. The SOCS family of proteins is made up of eight members in mammalian cells, including SOCS1-7 and the cytokine-inducible SH2 protein, all of which have been shown to regulate cell growth, differentiation and survival, and to modulate dendritic cell functions, inflammatory response and

hematopoiesis [176]. These proteins interact with the kinase domain of JAKs, and inhibit signal transduction by competing with various signaling molecules (such as STATs) for the docking sites on the receptors. Via their SOCS box domain, SOCS proteins also interact with E3 ubiquitin ligases and thereby promote the ubiquitin-dependent degradation of their targets [176]. Normally, the expression of the SOCS proteins is under tight control, with robust induction by a wide spectrum of cytokines and growth factors to prevent the extracellular signals from over-firing and to ensure that the physiological responses are not excessive [176]. Thus, upon cytokine stimulation, the activated JAK/STAT3 signaling pathway promotes the expression of SOCS3, which serves as an important negative feedback mechanism to prevent over-activation of this pathway.

The homeostasis of STAT3 phosphorylation and activation is frequently disrupted in cancer cells due to the loss of SOCS expression [177]. In this regard, epigenetic silencing of *SOCS3* has been found in various types of cancer, including lung cancer, head and neck squamous cell carcinoma, hepatocellular carcinoma and Barrett-associated esophageal adenocarcinoma [177]. Experimental results have revealed that loss of SOCS3 indeed contributes to the activation of STAT3 in cancer cells, thereby promoting their proliferation, survival and motility [178-181]. SOCS1, another member of the SOCS family, is also frequently silenced by gene methylation, and this biochemical aberrancy has been shown to contribute to constitutive STAT3 activation in a wide range of cancer types [179, 182-185].

PTPs belong to a large family of proteins with >100 members, which is responsible for counteracting the effects of protein tyrosine kinases and maintaining the overall homeostasis of protein tyrosine phosphorylation. PTPs are known to dephosphorylate and thus inactivate the JAK/STAT3 signaling [186]. Similar to the SOCS proteins, many PTPs involved in the regulation of the JAK/STAT3 signaling are repressed or silenced in cancer cells. For example, SHP-1, a member of the tyrosine phosphatases highly expressed in normal lymphoid cells, is lost in many types of hematologic malignancies due to epigenetic silencing [184,187-189]. Loss of SHP-1 has been shown to directly contribute to the constitutive activation of STAT3 in these cancer types, including ALK-positive anaplastic large cell lymphoma, chronic myeloid leukemia and multiple myeloma, since gene transfection of *SHP1* in these cells can substantially decrease the level of STAT3 activation [184,187-189]. Interestingly, loss of SHP-1 in ALK-positive anaplastic large cell lymphoma is a direct consequence of the constitutive activation of STAT3 in these cells, as STAT3 plays a key role in promoting gene methylation and silencing of *SHP1* [188]. Thus, loss of SHP-1 and the constitutive activation of STAT3 form a vicious cycle in these lymphoma cells.

Other than the SOCS members and PTPs, PIAS3 (*i.e.* protein inhibitors of activated STAT3) is also known to inhibit STAT3 by reducing its DNA-binding and ability to regulate gene transcription. The expression of PIAS3 has been shown to be reduced in glioblastoma, and this finding correlates with an elevated level of STAT3 activation and increased cell proliferation [190]. Transfection of *PIAS3* into lung cancer cell lines can suppress cell proliferation and enhance the sensitivity of cells to chemotherapeutic drugs

[191]. In parallel with this concept, Kluge *et al.* found an inverse correlation between the expression levels of PIAS3 and pSTAT3 in lung squamous cell carcinomas [192].

1.3.3.2.2 Excessive stimulation of STAT3

Cancer cells and some of their surrounding inflammatory cells have been shown to produce and release various soluble factors (notably cytokines) into the tumor microenvironment, such that STAT3 in the cancer cell population is activated excessively and continuously. Cytokines involved in these autocrine or paracrine stimulatory pathways include IL-6, IL-10, IL-11, IL-21, IL-23, leukemia inhibitory factor and oncostatin [193]. Since STAT3 is a transcription factor known to upregulate many of these cytokines (such as IL-6 and IL-10), a vicious cycle of sustained STAT3 activation and excessive production of STAT3-stimulating cytokines often exists in tumors [137,193]. Previous studies have shown that stromal cells present in the tumor microenvironment are also participants of this vicious cycle. Multiple myeloma serves as an example in this regard. Specifically, IL-6–mediated STAT3 activation has been shown to promote the survival of myeloma cells via up-regulating the expression of several survival genes [194]; intriguingly, activation of STAT3 is observed in bone marrow stromal cells present in multiple myeloma, which produce IL-6 to sustain STAT3 activation in myeloma cells [195].

Constitutive activation of STAT3 in cancer cells also can be attributed to the expression of various oncogenic protein tyrosine kinases (PTKs). The oncogenic properties of these PTKs stem from the fact that they have

escaped the normal cellular control due to a variety of reasons, such as gain-of-function mutations, gene amplifications or chromosomal translocations. One well-known oncogenic PTK is Src, which is known to be over-active in cancer cells. Normally, the activation status of Src is increased by de-phosphorylation of Y527 and phosphorylation of Y416. In cancer cells, de-phosphorylation of Y527 can be due to the activity of tyrosine phosphatases (such as PTP1B), Y527F mutation or deletion of Y527 [196,197]. Phosphorylation of Y416, which correlates with Src activation and its malignant transforming ability, can be found in cancer cells [196,197]. Src has been shown to activate STAT3, and multiple studies have shown that the gene network regulated by STAT3-mediated transcription is required for v-src-induced cellular transformation [149,151,198].

STAT3 is also known to be highly activated in ALK-positive anaplastic large cell lymphoma by the oncogenic fusion protein, NPM-ALK, a constitutively active tyrosine kinase resulted from the specific chromosomal translocation that fuses the *anaplastic large cell lymphoma kinase* (*ALK*) gene on *2p23* to the *nucleophosmin* (*NPM*) gene on chromosome *5q35* [199,200]. In this type of lymphoma, NPM-ALK binds to, phosphorylate and activate STAT3, which has been shown to be central to the NPM-ALK–mediated tumorigenesis [201-204]. In one study, immortalized mouse embryonic fibroblasts with intact STAT3 expression were transformed by NPM-ALK, whereas *STAT3* gene knockout dramatically decreased the malignant transformation by NPM-ALK [201].

Gain-of-function mutations involving JAKs have been implicated in activating STAT3 in specific types of cancer. JAK2-V617F and other JAK mutants are known to activate STAT3 and contribute to the pathogenesis of chronic myeloproliferative neoplasms and leukemias [205-208]. Mutations in the kinase domain of the epidermal growth factor receptor also have been reported to sustain STAT3 activation by promoting IL-6 production in lung cancer cells [209]. In glioblastoma, a constitutively active mutant of epidermal growth factor receptor was found, and this mutant contributes to and sustains STAT3 activation by inducing a cytokine circuit involving IL-6 and leukemia inhibitory factor, which in turn activates gp130 in the neighboring cells that harbor wild-type epidermal growth factor receptor, leading to an enhanced growth of the entire tumor [210].

1.3.3.2.3 Positive feedback loops that sustain persistent STAT3 activation

As mentioned above, constitutive STAT3 activation and loss of SHP-1 in ALK-positive anaplastic large cell lymphoma have provided an example of a positive feedback loop. In this section, we will summarize the findings of a number of more recent studies focusing on the autocrine and/or paracrine IL-6/STAT3 stimulatory pathway that forms a positive feedback loop [211-214]. Using an inducible model of cellular transformation in mammary epithelial cells, Iliopoulos *et al.* has revealed a novel mechanism by which a transient inflammatory signal can initiate cellular transformation [211]. Specifically, using MCF-10A transfected with an inducible expression vector of *v-src*, the authors found that transient activation of v-src is sufficient to induce

transformation in these cells. In this system, STAT3 activated by v-src enhances the transcription of miR-21 and miR-181b-1, both of which lead to activation of NF-κB by targeting and inhibiting the expression of two tumor suppressors PTEN and CYLD. Through multiple pathways, activated NF-κB increases the production of IL-6, which in turn sustains the activation of STAT3 [211]. Interestingly, transient transfection of either of the two microRNA species in this circuit was sufficient to induce a stable transformed state, highlighting the importance of these two microRNA species in this transformation process [211].

Lee *et al.* revealed another positive feedback loop that confers STAT3 with a persistent activation property in cancer cells as well as the immune cells present in the tumor microenvironment [212]. In this scenario, STAT3 transcriptionally promotes the expression of a G protein-coupled receptor for the lysophospholipid sphingosine-1-phosphate, sphingosine-1-phosphate receptor-1, which in turn activates STAT3 by increasing IL-6 production and JAK2 tyrosine kinase activity [212]. This positive feedback loop was found in both tumor cells and tumor-associated stromal cells, and the IL-6 produced by these two types of cells mediates the crosstalk between them, and enables a persistent activation of STAT3 in both cell types. Blocking this positive feedback loop in either cell types was shown to decrease tumor growth and metastasis [212,213].

A few recent studies demonstrated other positive feedback loops that connect STAT3, gene regulation, metabolism, survival and proliferation in cancer cells [215]. In one study, pyruvate kinase M2 (PKM2), a protein that is known to be

essential for the Warburg effect and proliferation of cancer cells, was found to activate STAT3 via catalyzing its phosphorylation at Y705 [216,217]. In the initiation of a metabolic switch toward aerobic glycolysis similar to the Warburg effect, constitutively active STAT3 was found to promote HIF-1α transcription [218-220], which then directly increases the gene expression of PKM2 expression [221]. The PKM2—STAT3—HIF-1α positive feedback loop was shown to contribute to multiple malignant features of cancer. Similarly, STAT3 was shown to form a reciprocal regulatory loop with Polo-like kinase 1 (PLK1) to enhance the proliferation and survival of esophageal cancer cells [222]. In the context of *Helicobacter pylori*-associated gastric cancer, the existence of a positive feedback loop between STAT3 and COX-2 was also demonstrated [223].

1.3.3.2.4 Constitutively active somatic STAT3 mutations

Recently, somatic mutations in STAT3 were discovered in hepatocellular adenomas and many types of hematopoietic malignancies, such as T-cell large granular lymphocytic leukemia (T-cell LGL), chronic lymphoproliferative disorders of natural killer cells (CLPD-NKs), diffuse large B-cell lymphoma, and CD30+ T-cell lymphomas [224-230]. Specifically, Pilati *et al.* identified seven STAT3 mutations in 6/114 hepatocellular adenomas examined. Notably, all of these 6 tumors were inflammatory hepatocellular adenomas [224], suggesting the specificity of somatic STAT3 mutations for this type of hepatocellular tumor. Somatic STAT3 mutations have also been shown to be frequent in T-cell LGL and CLPD-NKs. Four independent studies have revealed somatic STAT3 mutations in T-cell LGL [225-228], and the reported

percentages of cases carrying STAT3 mutations were 4/36 (11%), 33/120 (28%), 31/77 (40%) and 40/55 (73%), respectively. Two independent studies in CLPD-NKs have described the finding of somatic STAT3 mutations occurring in 3/7 (43%) and 15/50 (30%) of the cases, respectively [226, 228]. It is notable that mutations in Y640 and D661 were shown to account for the vast majority of somatic mutations in the *STAT3* gene in both T-cell LGL and CLPD-NKs, representing about 80% of all mutations detected [225,226,228].

Intriguingly, most of the STAT3 mutations discovered (*e.g.* Y640F, D661H, D661V, D661Y, and N647I) reside in the SH2 domain that normally directs STAT3 dimerization, and many of these mutations were suggested to induce amino acid changes that confer higher hydrophobicity to the STAT3 SH2 dimerization surface, potentially facilitating phosphorylation of $STAT3^{Y705}$ and thus the activation of STAT3 [224,225]. Correlating with this concept, both the STAT3-Y640F and STAT3-D661V mutants were shown to increase the transcriptional activity of STAT3 in T-cell LGL, leading to the up-regulation of the downstream target genes of the STAT3 pathway including *IFNGR2*, *BCL2L1* and *JAK2* [225]. Moreover, Y640F, one of the most common STAT3 mutations, was shown to allow homodimerization of STAT3 independent of IL-6 or enhance the STAT3 homodimerization in response to IL-6 [224,225]. Recently, a M206K mutation that localizes in the coiled-coil domain of STAT3 was discovered in diffuse large B cell lymphoma, and this mutation was demonstrated to enhance both the $STAT3^{Y705}$ phosphorylation and its transcriptional activity [229]. Compared with cells harboring wild-type STAT3,

STAT3-M206K mutant cells were resistant to the JAK2 inhibitor TG101348, suggesting that this STAT3 mutant possesses constitutive activity [229].

1.3.3.3 The canonical STAT3 pathway in cancer

In the canonical pathway, the oncogenic function of STAT3 is dependent on its phosphorylation at Y705, and the subsequent dimerization and nuclear translocation [231]. As a transcription factor, STAT3 directly regulates the expression of a wide spectrum of genes, many of which play key roles in various aspects of oncogenesis **(Figure 1.4)**.

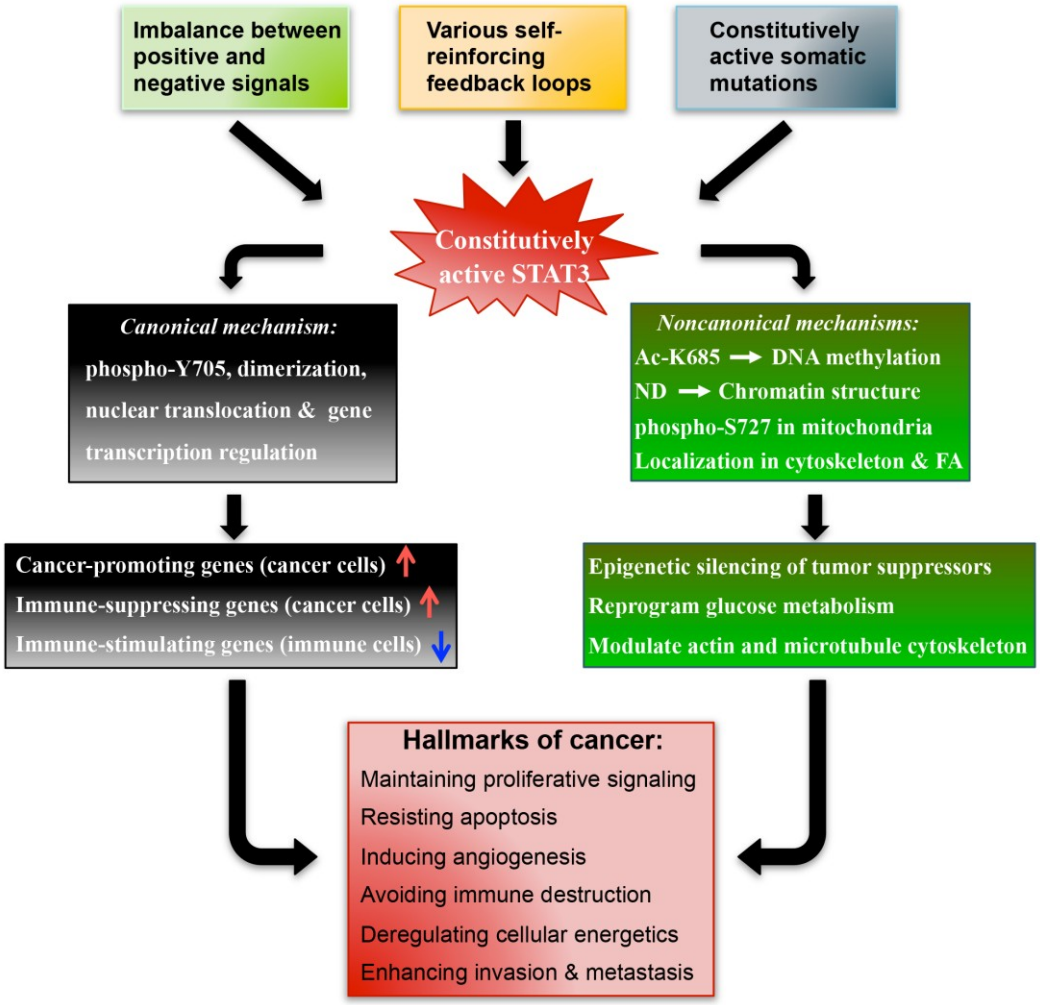

Figure 1.4 The upstream and downstream mechanisms underlying the pathobiological function of constitutively active STAT3 in cancer. Abbreviations: Ac, acetylation; ND: N-terminal domain; FA, focal adhesion.

1.3.3.3.1 Cell proliferation

It is well known that STAT3 increases the transcription and expression of multiple gene targets that are crucial in the regulation of cell cycle progression. These gene targets include *Cyclin D1*, *c-Myc*, *PLK-1* and *Pim1/2* [139, 222]. Thus, inhibition of STAT3 signaling using siRNAs or pharmacological agents can effectively reduce tumor growth by suppressing the expression of these cell-cycle facilitators [161,233]. A specific example is the observation that enforced expression of the STAT3-DN construct suppressed the proliferation of head and neck squamous cell carcinoma cells by lowering the expression of Cyclin D1 [233]. Zhang *et al.* also showed that siRNA-mediated STAT3 knockdown in esophageal squamous cell carcinoma cells repressed cell proliferation and tumor growth in mice by suppressing PLK1 expression [222].

1.3.3.3.2 Resistance to apoptosis

STAT3C has been shown to promote the survival of tumors cells in various models [136,139]. To achieve this, STAT3 regulates both the intrinsic and extrinsic apoptotic pathways. In many cancer cell types, STAT3 can transcriptionally increase the expression of various anti-apoptotic proteins involved in the intrinsic apoptotic pathway, such as survivin and the Bcl-2 family members (*e.g.* Bcl-xL, Bcl-2 and Mcl-1) [136,139]. STAT3 has been shown to cooperate with c-Jun to suppress the expression of FAS, a crucial mediator of the extrinsic apoptotic pathway; multiple studies have demonstrated that activated STAT3 protects cancer cells from FAS ligand–induced apoptosis and p53-dependent apoptosis [234-237].

1.3.3.3.3 Induction of angiogenesis

STAT3 has been shown to augment tumor angiogenesis in multiple cancer types, such as melanoma, pancreatic cancer, cervical cancer and renal carcinoma [238-243]. Mechanistic studies have revealed that STAT3 directly binds to the promoter region of the *VEGF* gene and promotes its transcription, thereby enhancing tumor growth and metastasis [238-240]. Consistent with these findings, a significant correlation between evidence of STAT3 activation and VEGF expression was observed in cell lines derived from breast cancer, head and neck carcinoma, melanoma and pancreatic cancer [238-240]. Furthermore, ectopic expression of STAT3C in B16 melanoma cells was found to promote the formation of capillaries in the xenografts established in nude mice [240]. The STAT3-VEGF circuit involves more than cancer cells within tumors. Using the inducible STAT3 knockout mouse model, a recent study has shown that STAT3 promotes the production of angiogenic factors (including VEGF and bFGF) in myeloid-derived suppressor cells and macrophages present in the tumor microenvironment, thereby stimulating endothelial cell migration and tumor angiogenesis [242]. Apart from being a stimulator of VEGF production, STAT3 also has been shown to directly mediate the pro-angiogenic activity of VEGF in microvascular endothelial cells [242,244,245]. For example, Yahata *et al.* found that VEGF stimulates STAT3 phosphorylation and nuclear translocation in human dermal microvascular endothelial cells, and inhibition of STAT3 using a dominant negative construct significantly impaired VEGF-induced migration and tube formation of these cells [244].

1.3.3.3.4 Promotion of invasion and metastasis

Previous studies have shown that STAT3 can promote invasiveness and the metastatic potential of cancer cells. In one study, transfection of *STAT3-DN* in pancreatic cancer cells suppressed tumor growth and liver metastasis in nude mice, whereas transfection of *STAT3C* enhanced tumor growth and liver metastasis [239]. STAT3C may exert these biological effects via several different mechanisms. First, STAT3 can trigger epithelial to mesenchymal transition (EMT) by upregulating several key EMT regulators such as Twist-1, Snail and ZEB-1 [246-249]. Second, STAT3 is known to increase the expression of various matrix metalloproteinases (MMPs), including MMP-1, MMP-2, MMP-7 and MMP-9, which facilitate cancer cell invasiveness by degrading various extracellular matrix proteins [150, 250-255]. Third, STAT3 can directly enhance the expression of focal adhesion molecules, such as integrin α6 and CTEN (C-terminal tensin-like) [151,256]. These observations are biologically significant, since over-expression of focal adhesion related proteins, which connect the cellular cytoskeleton to the extracellular matrix, has been linked to cancer metastasis [257,258]. Lastly, in a recent report, cytokines (*e.g.* IL-6 and IL-10) produced by tumors cells in a STAT3-dependent manner were shown to activate STAT3 in myeloid cells in the tumor microenvironment, resulting in sustained activation of STAT3 in these myeloid cells; these myeloid cells circulate to the lungs and promote the formation of pre-metastatic niche to support future cancer metastasis [213].

1.3.3.3.5 Evasion of anti-tumor immunity

The concept that STAT3 has a role in dampening the anti-tumor immune response came from the observation that tumor cell death induced by STAT3 blockade is associated with infiltration of various immune effector cells [259]. Several subsequent studies also have implicated STAT3 in the context of tumor immuno-surveillance [136]. For example, blocking STAT3 in macrophages has been shown to activate anti-tumor immune responses in a murine model of breast cancer [260]. Mechanistically, STAT3 signaling was shown to inhibit TH1-type inflammation after lipopolysaccharide stimulation by suppressing the production of specific cytokines and nitric oxide [261]. Furthermore, the STAT3 activity in tumor cells enhances the expression of several immune-suppressing soluble factors, such as IL-6, IL-10 and VEGF, all of which are known to prevent the maturation of dendritic cells [136,260]. STAT3 activation in immature dendritic cells has been shown to impair the expression of MHC class II molecules, CD80, CD86 and IL-12, thereby hindering their maturation and thus decreasing their ability to promote the anti-tumor function of CD8-positive T cells and natural killer cells [136].

1.3.3.3.6 STAT3 and cancer stem cells

In recent years, accumulating evidence suggests that STAT3 carries a critical role in promoting the self-renewal of cancer stem cells [153-157]. In one study, transfection of *STAT3C* in glioblastoma cells was found to increase the expression of several stem cell factors, such as Sox2, Oct4 and Nanog [154]. Using a large-scale loss-of-function screen, Marotta *et al.* identified 15 genes that are required for the proliferation of the breast cancer stem cell population characterized by the $CD44^{+}CD24^{-}$ immunophenotype, and five of these genes

facilitate STAT3 activation [155]. Further investigation indicated that the IL-6/JAK2/STAT3 pathway was preferentially active in $CD44^{+}CD24^{-}$ breast cancer stem cells, and inhibition of JAK2 decreased the number of cancer stem cell number and blocked the growth of xenografts in mice [155]. In glioblastoma, it has been shown that the stem cell factor EZH2 interacts with STAT3 and tri-methylates its K180 residue, thereby activates STAT3 and promotes tumorigenesis [156]. Importantly, the EZH2-STAT3 interaction preferentially occurs in the stem cell population, suggesting a specific role of these two factors in maintaining cancer stemness [156]. In another study, it was found that STAT3 activation by BMX (bone marrow X-linked), a non-receptor tyrosine kinase, is required for maintaining the self-renewal and tumorigenic potential of cancer stem cells in glioblastoma [154].

1.3.3.4 Non-canonical mechanisms

The non-canonical pathway comprises a number of biological functions of STAT3 that have been shown to be independent of its transcription activity or the phosphorylation of $STAT3^{Y705}$.

1.3.3.4.1 Gene silencing and regulation

Zhang *et al.* discovered that STAT3 interacts with DNA methyltransferase 1 (DNMT1) and histone deacetylase 1 (HDAC1), by which STAT3 facilitates gene methylation and silencing of *SHP-1* in malignant T lymphocytes; furthermore, blocking the expression of either DNMT1 or STAT3 using siRNA was found to induce DNA demethylation and re-expression of *SHP-1* in these cells [188]. In another study, it was revealed that K685-acetylated STAT3

cooperates with DNMT1 to silence several tumor suppressor genes, including *TP53, SHP-1, SOCS3* and *CDKN2A*, in melanomas; mutation of $STAT3^{K685}$ or treatment with resveratrol (a histone deacetylase activator) was found to diminish the tumor-promoting function of STAT3 in melanoma [262]. Yuan *et al.* demonstrated that histone acetyltransferase p300 is responsible for STAT3 acetylation at K685, and this process can be reversed by histone deacetylase 1 [263]. Recently, it also was shown that nuclear localized CD44 facilitates STAT3 acetylation on K685 residue [264].

Previous studies have provided multiple lines of evidence that STAT3 can exert oncogenic functions that are independent of the phosphorylation of its Y705 residue. First, un-phosphorylated STAT3 has been found to migrate to the nucleus with the help of importin-α3 [265]. Second, it has been shown that both un-phosphorylated STAT3 and STAT3-DN can interact with NFκB in the nucleus to drive the expression of multiple cancer-related genes, such as *RANTES, IL-6, IL-8, MET* and *MRAS* [266,267]. Third, in prostate cancer and chronic lymphocytic leukemia, phosphorylation of $STAT3^{Ser727}$ rather than $STAT3^{Y705}$ was found to be crucial for the nuclear translocation, DNA binding and the tumor-promoting function of STAT3. This finding correlates well with the observation that STAT3-DN does not interfere with the oncogenic function of STAT3 in these experimental models [268,269]. Recently, Timofeeva *et al.* showed that un-phosphorylated STAT3 binds to the regulatory region of several pro-apoptotic genes (such as *FOS, CHOP* and *NR4A2*) in tumor cells and prevents their expression by promoting a repressive chromatin structure [270]. Correlating with this concept, the authors were able to show that the

observed oncogenic effect of STAT3 was independent of its phosphorylation at Y705, whereas the N-terminal domain of STAT3 is indispensable, because the N-terminal domain was shown to be required for the dimerization of un-phosphorylated STAT3. In another study by the same group of researchers, it was found that un-phosphorylated STAT3 can bind to the interferon γ-activated sequence (GAS) either as dimers or as monomers, and it regulates gene expression via its binding to AT-rich DNA sequences and regulation of chromatin structure [271].

1.3.3.4.2 Mitochondrial STAT3

In 2009, two *Science* papers simultaneously reported the function of STAT3 present in the mitochondria [272,273]. Specifically, it was demonstrated that mitochondrial STAT3 controls cell respiration and metabolism by enhancing the activity of succinate oxidoreductase (complex II), ATP synthase (complex V) and lactate dehydrogenase, thereby sustaining the glycolytic and oxidative phosphorylation activities that are characteristic of cancer cells [273]. In one of these two papers, it was demonstrated that the phosphorylation of $STAT3^{S727}$ rather than $STAT3^{Y705}$ is required for the oncogenic role of mitochondrial STAT3 in the context of H-ras–induced transformation [272]. More recently, the significance of mitochondrial STAT3 also has been documented in breast cancer, in which it promotes tumor growth and metastasis by suppressing the generation of reactive oxygen species; again, this biological effect is dependent on phosphorylation of $STAT3^{S727}$ but not that of $STAT3^{Y705}$ [274].

1.3.3.4.3 STAT3 modulates cytoskeleton and focal adhesions

Results from multiple studies support the concept that STAT3 can modulate the cytoskeletal structures of the cells via multiple mechanisms. As mentioned above, STAT3 has been shown to regulate the migration and invasiveness of cancer cells by transcriptionally up-regulating the expression of focal adhesion-associated proteins [151,256]. Intriguingly, STAT3 also has been shown to directly localize in focal adhesion sites in ovarian cancer cells by interacting with multiple focal adhesion-associated molecules, such as focal adhesion kinase (FAK) and Paxillin [275,276]. In other studies, STAT3 was found to play an important role in regulating the assembly of cytoskeleton network, including actin and microtubule cytoskeleton, thereby promoting cell migration and invasion [277-279]. Specifically, gene transfer of wild-type *STAT3* was found to promote the rearrangement of actin stress fibers and microtubules, and facilitates the formation of lamellipodia in prostate cancer cells [277,278]; in the same studies, it was demonstrated that enforced expression of STAT3 can increase cell migration *in vitro*, and substantially enhance lung metastasis *in vivo* [277,278]. In other studies, STAT3 was shown to promote microtubule polymerization by interacting with and antagonizing the function of Stathmin, a tubulin-associated protein that modulates the polymerization of microtubules [280,281]. A recent study also has shown that depletion of STAT3 in gastric cancer cells impairs microtubule polymerization due to a disruption of the interaction between STAT3 and Stathmin; as a result, cell migration and invasion were decreased [279].

1.3.4 The tumor suppressor functions of STAT3

1.3.4.1 STAT3 can exert tumor suppressor effects

While the oncogenic effects of STAT3 have been well recognized, a relatively small number of studies published previously have shown that STAT3 carries tumor suppressor functions, a seemingly paradoxical notion. Importantly, some of these studies have proposed a novel concept that STAT3 can function as an oncoprotein or tumor suppressor in the same cells, and the decision is dependent on the genetic background and/or coexisting biochemical defects **(Figure 1.5)**. This section summarizes these experimental findings.

The first experimental evidence to support that STAT3 carries tumor suppressor functions comes from a study published in 2008 [282]. Using astrocytes derived from conditional STAT3 knockout mice, the authors found that the simultaneous deletion of STAT3 and shRNA knockdown of PTEN resulted in a dramatic increase in cell proliferation *in vitro* and tumor formation in SCID mice, whereas siRNA knockdown of PTEN alone (*i.e.* in the presence of normal STAT3 expression) resulted in significantly less tumorigenic effects in these cells. Furthermore, no significant tumor suppressor effect of STAT3 was observed in the presence of normal PTEN expression. In other words, in this experimental model, the tumor suppressor effects of STAT3 were revealed only in the absence of PTEN expression (**Figure 1.5**). Interestingly, in the same study using astrocytes harvested from the same conditional STAT3 knockout mice, the authors also found that transfection of EGFRvIII (epidermal growth factor receptor type III variant) in $STAT3^{+/+}$ astrocytes resulted in tumor formation in SCID mice, whereas the same treatment did not

result in any tumor formation in STAT3$^{-/-}$ astrocytes. Thus, the oncogenic effect of STAT3 was found to be dependent on the co-existence of EGFRvIII, which was shown to complex with STAT3 in the nuclei of these cells. Taken together, this study has demonstrated that STAT3 can function as a tumor suppressor as well as an oncoprotein, and the genetic background and/or coexisting biochemical defects of the cells play a key role in determining the functions of STAT3.

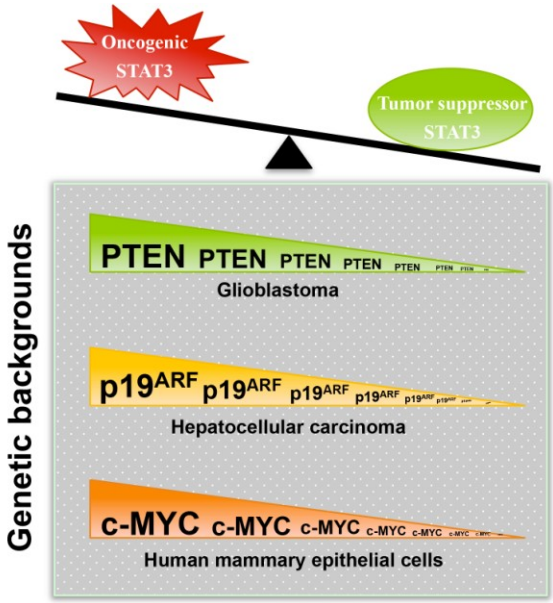

Figure 1.5. The genetic background determines whether STAT3 is oncogenic or tumor suppressive. Specifically, the expression status of PTEN, p19^{ARF}, or c-MYC in different types of cancers determines the opposing roles of STAT3. The details are described in the text.

Another report describing the tumor suppressor effects of STAT3 was published in 2011 [283]. Using ras-transformed mouse hepatocytes harvested from homozygous *p19^{ARF}* knockout mice, the authors found that transfection of *STAT3* or *STAT3C* significantly suppressed tumorigenecity in a SCID mouse xenograft model. In comparison, transfection of a double *STAT3* mutant in which both Y705 and S727 cannot be phosphorylated led to

significant tumor growth in SCID mice. In the same paper, the authors also found that cells transfected with the double *STAT3* mutant resulted in liver and lung metastasis after intravenous injection of the cells, while transfection with *STAT3* or *STAT3C* significantly decreased the metastatic potential of these hepatocytes. While the mechanisms underlying these observations require further investigations, these results have suggested the relevance of ras and/or $p19^{ARF}$ in regulating the tumor suppressor function of STAT3 (**Figure 1.5**).

In another study, the tumor suppressor function of STAT3 was revealed in the Apc(Min/+) mouse model of colorectal cancer [284]. In this model, the oncogenic driving force was provided by the *multiple intestinal neoplasia* (*Min*) gene, which is essentially the murine *Apc* (*adenomatous polyposis coli*) gene carrying a nonsense mutation at codon 850, leading to the production of a truncated and non-functional Apc protein. By crossing these animals with conditional STAT3 knockout mice, the authors were able to generate mice with which they assessed the impact of STAT3 knockout in the Apc(Min/+)-carrying intestinal epithelial cells. While deletion of STAT3 in the intestinal epithelial cells reduced the multiplicity of early adenoma formation (*i.e.* oncogenic role), ablation of STAT3 in the later stage of tumor progression significantly increased the invasiveness of the tumors and decreased the survival of the animals (*i.e.* tumor suppressor role).

The last example came from a recent study examining drug-induced liver carcinogenesis in conditional STAT3 knockout mice. It was found that the

hepatocytes with STAT3 expression had a significantly less tumor formation induced by chronic carbon tetrachloride, as compared to hepatocytes with STAT3 knockout. In contrast, hepatocytes with STAT3 expression were found to have a significantly higher tumor formation induced by diethylnitrosamine, as compared to hepatocytes with no STAT3 expression [285]. In other words, STAT3 can be either oncogenic or tumor suppressive, depending on the use of different carcinogens. As stated by the authors, the two carcinogens used in this study likely induce liver carcinogenesis through different mechanisms. Specifically, chronic carbon tetrachloride is believed to induce liver cancer by causing chronic liver injury, inflammation and fibrosis, whereas diethylnitrosamine is believed to induce liver cancer by promoting the formation of alkylated DNA adducts after being metabolically activated by cytochrome P450 enzymes in the liver [286]. As the author speculated, the tumor suppressor function of STAT3 in the carbon tetrachloride model correlates well with the fact STAT3 is known to play an important role in protecting liver against hepatocellular damage. In contrast, in the diethylnitrosamine model, the authors believed that the oncogenic effects of STAT3 are due to the fact that STAT3 can increase the expression of cyclin D1 and suppress the expression of p21. Thus, STAT3 can be a friend or foe, depending on the pathogenesis of specific types of cancer.

1.3.4.2 Mechanisms that mediate or regulate the tumor suppressor function of STAT3

Several recent studies have shed insights into how STAT3 might mediate tumor suppressor effects. In one study using thyroid cancer cell lines and an

SCID mouse xenograft model, Couto *et al.* found that siRNA knockdown of STAT3 resulted in significantly increased tumor growth, and this observation correlated with increased glucose consumption, lactate production, and expression of HIF-1α target genes in the tumor cells [287]. These findings suggest that one of the mechanisms by which STAT3 inhibits tumorigenesis is mediated by inhibiting aerobic glycolysis in the tumor cells.

Several proteins have also been implicated in regulating the function of STAT3 in cancer cells. In one study, STAT3C was found to suppress cell growth in $p53^{-/-}$ mouse embryonic fibroblasts transformed by c-Myc, but exert no appreciable effects on the same type of fibroblasts that were transformed by ras [288]. In another study, c-Myc was shown to function as a molecular switch to alter the function of oncostatin M-activated STAT3 in human mammary epithelial cells deficient in both p53 and p16 (**Figure 1.5**). Specifically, oncostatin M-STAT3 signaling was found to suppress c-Myc expression and tumorigenesis in human mammary epithelial cells that were deficient in both p53 and p16 [289]. In contrast, when c-Myc expression was restored by transfecting a constitutively active c-Myc construct into the cells, the cellular response to the oncostatin M-STAT3 signaling was switched from tumor suppressive to tumor promoting. Thus, in this particular cell context (*i.e.* deficiency in both p53 and p16), it appears that c-Myc is the dominant oncogenic protein, and STAT3 is a tumor suppressor.

In mice generated by crossing the Apc(Min/+) mice and conditional STAT3 knockout mice, Lee *et al.* found that that ablation of STAT3 significantly

increase the invasiveness of colorectal cancer [290], a finding that is in parallel to that reported by Musteanu *et al.* [284]. Furthermore, the authors found that STAT3 mediates the tumor suppressor effects by binding to GSK3β, which in turn promotes the phosphorylation and the degradation of Snail, a critical regulator of the EMT and cancer metastasis.

1.3.4.3 Clinical observations supporting the tumor suppressor role of STAT3

While the majority of studies evaluating the prognostic value of STAT3 and/or pSTAT3 have pointed to its oncogenic effects, a few studies have reported contradictory observations, with the expression of STAT3/pSTAT3 found to be 'paradoxically' associated with a better prognosis in various types of cancer, including those of the head and neck, salivary gland, breast, nasopharynx and rectum. For instance, high expression of pSTAT3 or nuclear STAT3 in head and neck cancer was found to be associated with a favorable clinical outcome; the progression free survival for patients carrying tumors with high expression of nuclear STAT3 was significantly longer than that of patients carrying tumors with relatively low STAT3 expression [291]. In another study including a large cohort of patients with salivary gland tumors, patients carrying tumors with strong nuclear pSTAT3 immunostaining were found to have a better clinical outcome compared with those carrying tumors with moderate or weak nuclear pSTAT3 staining; moreover, strong nuclear pSTAT3 also significantly correlated with a low histologic grade, as well as the absence of lymph node and distant metastases [292]. In breast cancer, two studies have documented that nuclear pSTAT3 expression significantly correlated with a favorable

clinical outcome, although this correlation was restricted to patients with low-grade tumors or node-negative tumors [293,294].

It is important to point out that the contradiction regarding the prognostic significance of STAT3 does not appear to be due to cell-type specificity. To illustrate this point, STAT3 was reported to be a marker of worse clinical outcome in head and neck cancer as well as breast cancer [150,295-298], the same types of cancer in which STAT3 was found to be associated with a better clinical outcome in other studies [291,292,294]. While these discrepancies may be partly attributed to the use of slightly different immunohistochemical methods and/or the inclusion of different patient cohorts, one may consider an alternative possibility, in light of the recent experimental data showing that the genetic background and/or coexisting biochemical defects can dictate whether STAT3 exert oncogenic or tumor suppressor effects in cancer cells. As mentioned in Section 1.3.4.1, the expression and/or functional status of PTEN, p53, $p19^{ARF}$ and c-myc have been implicated in influencing the function of STAT3 in various experimental models. With this new knowledge, it is perceivable that the studies of different cohorts of tumors that are biased toward specific molecular profiles will lead to different conclusions regarding the prognostic significance of STAT3.

1.3.5 STAT3β and the tumor suppressor effects of STAT3

1.3.5.1 STAT3β has biochemical and biological features different from STAT3α

The *STAT3* gene encodes two isoforms, STAT3α and STAT3β, which are generated by alternative splicing of exon 23. The relationship of these two isoforms and the initial characterization of STAT3β have been previously described [299]. Briefly, STAT3β is a result of the deletion of the first 50 nucleotides of exon 23, leading to a frame shift that introduces 7 amino acid residues followed by a stop codon. Thus, STAT3β is a truncated version of STAT3α, with the two isoforms sharing the identical amino acid sequence except for the 55 amino acids at the C-terminal of STAT3α that are replaced with a unique 7-amino-acid sequence in STAT3β. Consequently, STAT3β lacks the transactivation domain **(Figure 1.6)**.

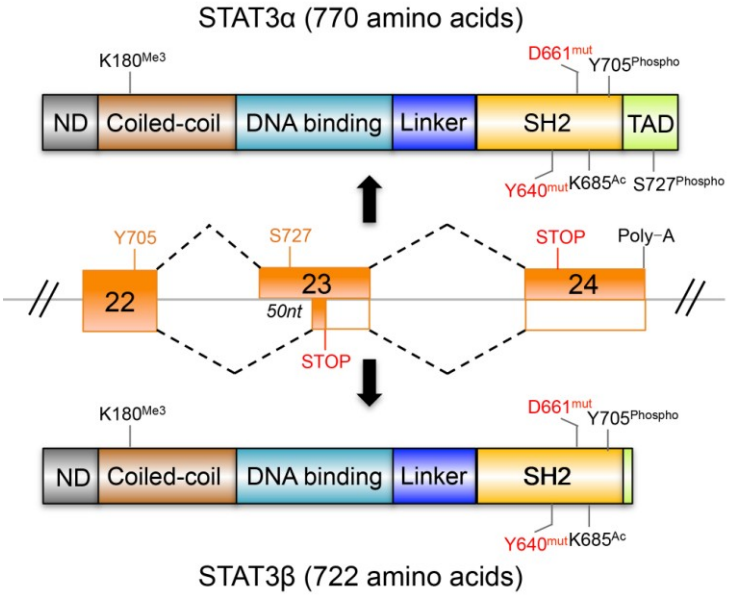

Figure 1.6. A schematic diagram showing the generation of STAT3α and STAT3β from primary STAT3 mRNA by alternative splicing, and the modification sites and somatic mutation sites in STAT3 that are relevant to cancer. Abbreviations: ND, N-terminal domain; SH2, Src homology 2; TAD, transactivation domain; Me3, trimethylation; mut, mutation; Phospho, phosphorylation; Ac, acetylation.

The expression STAT3β is found ubiquitously, but its level is lower than that of STAT3α [299,300]. Intriguingly, the ratio of the expression levels of STAT3α and STAT3β changes in response to physiologic changes or specific cytokine stimulations. For instance, the expression of STAT3β has been shown to dramatically increase in mouse hepatocytes in response to lipopolysaccharide-induced endotoxin shock [301]. The expression of STAT3β was also found to be increased in myeloid cells as they differentiate [302-304].

Previous studies have shown that STAT3α and STAT3β have significantly different biochemical and biological properties. Some of the early studies have showed that phosphorylated STAT3β^{Y705} (or pSTAT3β) has a much longer half-life and nuclear retention than phosphorylated STAT3α^{Y705} (or pSTAT3α) [305-307]. The difference in their biological behaviors was also highlighted in a study, in which STAT3β was found to have a higher DNA binding ability than STAT3α in COS-7 cells that had been serum starved [307]. Correlating with these observations, a subsequent study revealed that the negatively charged 55 amino acids present in the C-terminus of STAT3α confer a decreased stability of the STAT3α dimers, and this difference in the dimer stability between STAT3α and STAT3β is believed to be responsible for the longer half-life and nuclear retention of pSTAT3β [308]. Another study showed that the unique C-terminal 7-amino acid domain of STAT3β also contributes to the increased nuclear retention of STAT3β, since with the deletion of this domain was shown to decrease the nuclear retention time of STAT3β [305]. Moreover, compared with STAT3α, STAT3β showed an approximate of two-

fold decrease in intra-nuclear mobility, and this difference is more obvious under IL-6 stimulation [305].

1.3.5.2 The dominant negative role of STAT3β

Without the STAT3 transactivation domain, STAT3β is expected to be unable to activate promoters carrying the interferon/IL-6–responsive element. With this in mind, it was postulated that STAT3β may function as a dominant negative factor that can somewhat neutralize and/or regulate the biological effects of STAT3α. Experimental data supports this concept, as STAT3β was found to inhibit the transcription activity of full-length STAT3 or STAT3α [299]. In other studies, it has been demonstrated that STAT3β can abolish the transcriptional activation of several STAT3 downstream targets including *Cyclin D1*, *Bcl-xL* and *Mcl-1*, leading to inhibition of tumor growth and promotion of apoptosis [309-311]. While STAT3α was also found to act in cooperation with c-Jun to suppress the transcription of *Fas*, it was shown that STAT3β can counteract the transcription suppressive function of STAT3α in this context [234]. In the literature, we are able to find several studies in which STAT3β was used as an experimental tool to block STAT3 signaling [259,312,313].

1.3.5.3 STAT3β regulates a gene set that is distinct from that of STAT3α

In addition to its dominant negative role, STAT3β is believed to carry other functions, considering the fact that it possesses most of the important STAT3 functional domains including the activation domain (*i.e.* which carries the tyrosine 705 residue), the Src homology2 (SH2) domain that is responsible for

STAT3 dimerization and its binding to the receptor complex (*e.g.* JAKs), the coiled-coil domain that allows STAT3 to interact with other proteins, and the DNA binding domain. Accumulating evidence is in support of this concept. Schaefer *et al.* reported that STAT3β can cooperate with c-Jun to activate a promoter containing the IL-6 responsive element; interestingly, the nuclear extract from cells transfected with the *STAT3β* cDNA, but not that from cells transfected with the *STAT3α* cDNA, formed a complex with an oligonucleotide containing the STAT3 binding site [300]. In another study, STAT3β was found to compensate the function of STAT3; specifically, transfection of STAT3β effectively induced the expression of acute phase genes in STAT3-null hepatocytes challenged with lipopolysaccharide [314]. Furthermore, it has been demonstrated that STAT3β can rescue the embryonic lethality in STAT3-null mice, and high expression of endogenous STAT3β (compared to STAT3α expression) did not impair the activity of STAT3α in transgenic mice, either in embryos or in adult mice [315]. Another study showed that, compared with the wild-type mice, mice with specific STAT3β ablation were hypersensitive to lipopolysaccharide-induced inflammation, and these findings correlated with the dramatic alterations of the expression of lipopolysaccharide-responsive genes in the hepatocytes [301].

More recently, it has become evident that STAT3β has its own set of target genes that is distinct from that of STAT3α, and these genes include *LEDGF* (lens epithelium-derived growth factor), *PCAF* (p300/CBP-associated factor), CCNC (cyclin C), *PEX1* (peroxisomal biogenesis factor 1) and *STAT1β* [316]. In the same study, a novel agent called morpholino was also described;

specifically, morpholino was designed to modulate the STAT3 alternative splicing process such that STAT3β is favored at the expense of STAT3α. The shift from STAT3α to STAT3β was found to dramatically decreased tumor growth, which was shown to be mediated by STAT3β-specific downstream targets [316]. In another study, using STAT3-null murine embryonic fibroblasts with inducible expression of STAT3α or STAT3β, Ng *et al.* identified distinct gene sets modulated by STAT3α and STAT3β, respectively. Specifically, the authors identified 506 genes that are regulated by both STAT3α and STAT3β, with 651 STAT3α-specific target genes and 1331 STAT3β-specific target genes [306]. Taken together, there is strong evidence that STAT3β can function as an independent transcriptional regulator, despite the fact that it lacks the transactivation domain. In the absence of the transactivation domain, it is likely STAT3β relies on its interactions with other transcription co-factors, such as c-Jun, to regulate gene expression [300].

1.3.5.4. STAT3β regulates the phosphorylation dynamics of STAT3α

It was recently found that STAT3β can directly regulate STAT3α. In one study, STAT3β was found to upregulate and prolong the phosphorylation of STAT3α^{Y705} upon stimulation with oncostatin M in murine embryonic fibroblasts [306]. Specifically, in cells with only STAT3α expression, phosphorylation of STAT3α^{Y705} stimulated by oncostatin M was transient, reaching a peak at 15 minutes after the exposure to oncostatin M exposure and decreasing to an undetectable level at 60 minutes. In contrast, in the presence of STAT3β, phosphorylation of STAT3α^{Y705} was sustained at a high level for 120 minutes. Correlating with these findings, cells with STAT3β

expression had a prolonged nuclear retention of STAT3. In the same study, it was also demonstrated that an intact SH2 domain is required for the interaction between the two STAT3 isoforms and the cross-regulation of STAT3β on STAT3α.

1.3.5.5 Is STAT3β responsible for the tumor suppressor function of STAT3?

How are these findings related to the observation that STAT3 can function as a tumor suppressor? While the answer to this question needs further investigation, one may speculate that heterodimerization of pSTAT3α and pSTAT3β may sequester pSTAT3 away from its DNA target genes or interfere with the transcription activity of pSTAT3 due to the absence of the transactivation domain in STAT3β. Thus, in the presence of a high level of pSTAT3β, pSTAT3α becomes less available or effective in mediating gene transcription, despite the fact that its expression and nuclear retention are higher due to the stabilizing effect of pSTAT3β.

Correlating with these findings, STAT3β has been shown to play a tumor suppressor role in various types of cancer, including melanoma, breast cancer and lung cancer [234, 259,312,313,316,317]. For instance, transient *STAT3β* transfection in murine B16 melanoma cells induced cell cycle arrest as well as apoptosis [312]. Furthermore, electro-injection of *STAT3*β cDNA into established B16 melanoma xenografts in SCID mice induced apoptosis and suppressed tumor growth [259]. In another study, gene transfer of *STAT3β* was found to result in marked shrinkage of xenografts in SCID mice, whereas

siRNA knockdown of STAT3 resulted no significant effect on breast tumor growth [316]. Interestingly, in one study, apoptosis induced by STAT3β was found in *STAT3β*-transfected cells as well as the bystander non-transfected cells in the same tissue culture, due to the production of TRAIL (TNF-related apoptosis inducing ligand) induced by *STAT3β* transfection [312]. Moreover, it has been shown that transfection of *STAT3β* in a human melanoma cell line increases FAS expression and enhances apoptosis induced by FAS-ligand and UV irradiation [234]. A few years later, the same research team reported that STAT3β can effectively suppress the growth of human melanomas xenografted in nude mice by increasing the expression of TRAIL receptor 2, a pro-apoptotic factor expressed on the cell surface of the tumor cells [317].

1.3.6 Evaluation of STAT3 expression in patient samples

Since the late 90's when the potent oncogenic effects of STAT3α was demonstrated in various experimental models, there have been numerous published clinicopathologic studies showing a significant correlation between a high expression level of STAT3 and/or pSTAT3 (typically shown using immunohistochemistry applied to archival tissues) and a worse clinical outcome and/or adverse pathologic features. Nevertheless, as mentioned in Section 1.3.5, a few clinicopathologic studies had pointed to the opposite conclusion. While some of these discrepancies may be theoretically attributed to differences in the immunohistochemical methods and/or interpretation, we believe that this explanation is not sufficient, since these experimental protocols have been extensively published. Another possibility is that the discrepancies among published studies are related to cell-type specificity,

such that STAT3 is oncogenic in one type of cancer whereas it is a tumor suppressor in another. We do not favor this argument, since there are a good number of examples in which studies of the same types of cancer came up to different conclusions (Section 1.3.5).

While we summarized all the existing data regarding STAT3β, we came to realize that virtually all published clinicopathologic studies pertaining the prognostic value of STAT3/pSTAT3 did not differentiate the two STAT3 isoforms. Considering the concept that STAT3 can be an oncoprotein or a tumor suppressor (as described in Section 1.3.4), and that STAT3β functions as a dominant negative factor for STAT3α (as described in Section 1.3.5), it is highly possible that the expression of STAT3 and/pSTAT3 in tumor samples may correlate with the clinical outcome in either direction, depending on the genetic background of the tumor cells and/or the coexisting biochemical defects present in these cells, and whether the tumor suppressor effects of STAT3β overcomes the oncogenic effects of STAT3α. Thus, a high expression level of pSTAT3 detectable by immunohistochemistry does not necessarily correlate with the transcriptional activity of STAT3, which is believed to be an important determinant of the oncogenic effects of STAT3. In other words, accurate evaluation of the biological and clinical significance of STAT3 in human tumor samples will require some understanding of the relevant coexisting biochemical defects (*e.g.* c-myc, PTEN and $p14^{ARF}$) as well as the simultaneous evaluation of STAT3α and STAT3β. From a technical perspective, the detection of the two STAT3 isoforms in tumor samples is currently feasible only by analyzing fresh tissues using western

blots, with which STAT3α and STAT3β can be differentiated from each other based on the difference in their molecular weights (*i.e.* with STAT3β being the faster-migrating isoform). Immunohistochemistry, which has been used in the vast majority of clinicopathologic studies of STAT3 in the past, is only useful if antibodies specific for STAT3α or STAT3β (and their phosphorylated counterparts) are available. To our knowledge, most if not all commercially available anti-STAT3 or anti-pSTAT3 antibodies are not isoform-specific. We are aware of a small number of reports describing antibodies that recognize STAT3β but not STAT3α, although these antibodies are not widely available and/or extensively characterized.

1.4 Cancer stem cells (CSCs)

1.4.1 Overview

Mounting evidence has demonstrated that not every cell within a bulk tumor is the same and has the capacity to initiate a tumor, only a tiny fraction of cells possess the ability to start a tumor, and these rare cells are regarded as cancer stem cells (CSCs) [318,319]. CSCs have similar properties as normal stem cells, having the ability to self-renew to maintain the CSCs population, and to differentiate into the non-CSCs that constitute the vast majority cells within a bulk tumor [320]. Since 1997 when the first evidence of CSCs was discovered in leukemia [321], CSCs have been identified and characterized in various cancers, such as brain, breast, colon, ovary, pancreas, prostate, and skin carcinomas [322].

CSCs can be identified and isolated using several approaches, including labeling CSCs with specific cell surface markers [323-325], side population identification using hoechst 33342 dye efflux assay [326], and tumorshpere formation assay under special culture conditions. Currently, various cell surface markers for CSCs have been identified, for instance, both $CD44^{+}CD24^{-/Low}$ and $ALDH^{+}$ have been used as markers for breast cancer CSCs [323], $CD133^{+}$ has been used as a marker for both colon and brain CSCs [324,325]. Moreover, side population cells have also been proven effective in the isolation of CSCs from multiple cancers, such as ESCC, breast cancer, and colon cancer. The principal of side population idetification using hoechst 33342 dye efflux assay is that CSCs have a higher ability to transport/efflux the incorporated dye out of the cells using ATP-binding cassette transporters, which have been shown to be expressed in a higher level in CSCs compared with non-CSCs [326]. Thus, the hoechst-negative cells can be isolated using flow cytometry. Lastly, tumorsphere formation assay is performed by culturing cells in a serum-free medium that contains specific growth factors, and this assay has been demonstrated to be efficient to enrich and maintain undifferentiated mammary epithelial cells as well as CSCs from both breast and other cancer cell lines [327,328].

1.4.2 Key proteins for the stemness of CSCs

The stem cell factors that are preferentially enriched in embryonic stem cells compared with differentiated cells include transcription factors such as Nanog, Oct3/4, MYC and Sox2, and epigenetic regulators that modulate histone modification, such as polycomb group proteins BMI1, EZH2 and SUZ12. The

self-renewal and differentiation ability of CSCs are traits that are possessed by normal stem cells [329]. In keeping with this, it has been demonstrated that these stem cell factors are overexpressed in CSCs compared with non-CSCs. For example, EZH2 and its regulated H3K27me3 (methylation of lysine 4 on histone H3) has been shown to be consistently higher in CSCs in both breast and pancreatic cancers, and knockdown of EZH2 led to the decrease of the population of CSCs [330]. BMI1 has been shown to be preferentially expressed in the CSCs from breast and head and neck carcinomas as well as leukemia [331-333], and BMI1-deficient leukemia cells were unable to induce disease following transplantation in mice. Sox2, a well-studied stem cell factor, has been shown to be involved in the biology of CSCs in skin squamous cell carcinoma, as cancer cells from Sox2-knockin mice were greatly enriched in CSCs that were able to give rise to tumors upon serial transplantations, while conditional ablation of Sox2 in pre-existing tumors decreased the tumorigenic capability of cancer cells upon transplantation into immunodeficient mice [334]. The potent function of MYC in CSCs has been reported in skin cancer [335]. In this study, it was demonstrated that single transfection of MYC was able to reactivate the embryonic stem cell programs; importantly, MYC enriched the proportion of CSCs by 150-fold in keratinocytes transformed by Ras and IκBα, enabling tumor initiation and propagation with as few as 500 cells [335].

1.4.3 Key pathways for the stemness of CSCs

To maintain stemness, CSCs have been shown to hijack several developmental signaling pathways that are important in the biology of normal stem cells, including the Wnt, Notch and Hedgehog signaling pathways [336].

Notch signaling pathway plays an important role in development by modulating stem cell fate, cell cycle progression as well as differentiation. Four Notch receptors (Notch1-4) and five ligands (Delta-like protein 1-3, and Jagged 1 and 2) have been discovered in mammalian cells. Upon ligand binding, the transmembrane Notch precursor proteins are consecutively cleaved twice by by ADAM protease and γ-secretase, and the intracellular domain of the Notch receptor is translocated to the nucleus to regulate gene transcription. The important role played by the Notch pathway in CSCs is supported by these findings. For instance, blockade of Notch 4 signaling in both primary breast tumor cells and cell lines decreased the proportion of $CD44^{+}/CD24^{low}$ cells as well as the tumorigenic potential [337]. The role of Notch 4 in stemness is also evidenced by its specific expression in the basal stem cells in the breast [338]. In brain cancers, a higher expression of the components of the Notch pathway has been found in $CD133^{+}$ brain CSCs compared with $CD133^{-}$ cells, and inhibition of this pathway using either siRNAs targeting Notch or using γ-secretase inhibitors decreased both the neurosphere formation and tumor formation in mice xenografts [339,340].

The Wnt signaling pathway includes the canonical pathway where β-catenin is the central mediator by regulating gene transcription in the nucleus, and the non-canonical pathway where a β-catenin-independent mechanism is involved. Although the role of the non-canonical pathway in CSCs is still elusive, the canonical pathway has been shown to facilitate the tumor initiating properties of colon and breast CSCs. In colon cancer, although the

activation of the Wnt canonical pathway is a key driver in the initiation and malignant progression of this disease, the nuclear expression of β-catenin was found to be heterogeneous within a tumor, leading to the hypothesis that this pathway may be involved in the stemness of colon CSCs. Indeed, it was reported that high responsiveness of cancer cells to a Wnt reporter (*i.e.* TOP-GFP reporter that measures the activity of the canonical Wnt pathway) correlated with the CD133 CSC maker expression, and were more tumorigenic *in vivo* [341]. In breast cancer, the expression of multiple Wnt pathway components, such as β-catenin, Wnt1, LEF1 and TCF4, were markedly elevated in the CSCs enriched mammospheres compared with cells grown in monolayers [342]. Beside, the expression of LEF1, a critical regulator of the canonical Wnt pathway, showed a remarkable correlation with the breast CSC marker ALDH1 in both mouse and human breast tumors. Importantly, blockade of the Wnt pathway using a small-molecular inhibitor CWP232228 preferentially inhibited the growth of breast CSCs [342].

The Hedgehog (Hh) pathway is comprised of three ligands (*i.e.* Sonic Hh, Desert Hh, and Indian Hh), two membrane receptors (*i.e.* Patched 1 and 2), a G protein coupled receptor and signal transducer Smoothened, and three downstream effectors (GLI1, GLI2 and GLI3 transcription factors). The binding of the ligands determines the activation status of the GLI transcription factors, which regulate a variety of target genes involved in proliferation, migration and differentiation [343-345]. In breast cancer, compared with the non-CSCs, the $CD44^{+}/CD24^{low}$ CSCs as well as breast cancer side population cells have been shown to have a higher activation status of the Hh pathway [343]. In

support of the important role of the Hh pathway in the initiation of breast cancer or breast CSCs, enforced expression of GLI1 in mouse mammary glands was capable to drive tumor formation [344]. In brain cancer, the Hh pathway was found to regulate the expression of multiple stem cell factors such as Nanog, Oct4, Sox2 and BMI1, thereby regulating the stemness of $CD133^+$ glioma CSCs [345].

1.4.4 Cancer stem cells in ESCC

Our understanding of the tumor heterogeneity of ESCC remains elusive. To date, only a few studies have attempted to label and isolate CSC-like cells in ESCC based on the expression status of certain markers, including $p75^{NTR}$, CD44, CD90, and ALDH1A1 [359-363], or based on the activity of ATP-binding cassette transporters [364-365]. The CSC-like ESCC cells identified by these studies were shown to be more tumorigenic and/or more chemoresistant. For instance, Huang, et al. reavealed that the CSC-like ESCC cells identified based on the activity of ATP-binding cassette transporters were found to possess approxiamately 100 times higher tumor-initiating capacity in NOD/SCID mice, as compared with the non-CSC-like ESCC cells [364]. Other studies found that the CD90+, ALDH1A1+ or CD44+ CSC-like ESCC cells were also significantly higher tumorigenic than the counterpart non-CSC-like cells [360, 361, 363]. To our knowledge, only four of these studies have employed mice xenografts to show that the CSC-like ESCC cells (*i.e.* CD44+, CD90+, or ALDH1A1+ cells) possess higher tumor initiating capacities than the non-CSC-like cells [360, 361, 363, 364], while the rest only used *in vitro* assays to compare the tumorigenicity of the two cell

populations [359, 362, 365]. None of these studies have elucidated the mechanisms underlying how these CSC-like cells are generated, largely due to the limitations of their models.

1.4.5 Reactive oxygen species (ROS) in CSCs

Reactive oxygen species (ROS) are a group of radical and non-radical oxygen species mainly generated by the partial reduction of oxygen in the process of endogenous mitochondrial oxidative metabolism, and ROS can also be produced from interactions with exogenous materials such as environmental agents and pharmaceuticals [346,347]. Although the oxidative stress induced by excessive levels of ROS are cytotoxic due to the oxidative damage on cellular macromolecules, mild levels of ROS has been shown to activate survival and proliferation pathways, such as the MAPK signaling pathway and the PI3K-AKT signaling pathway [346,347]. The balance of cellular ROS is tightly regulated by a wide spectrum of antioxidant proteins/componds involved in the redox mechanism, such as glutathione S-transferase, NADPH quinone oxidoreductase-1, copper/zinc superoxide dismutase [346,347].

Recent studies have shown that normal stem cells and cancer stem cells harbor a low-level of ROS via maintaining a high expression of certain antioxidants, including glutamate-cysteine ligase and glutathione synthetase [348,349]. An increase in the level of ROS has been shown to decrease the lifespan and the repopulating capability of hematopoietic stem cells *in vivo.* On the contrary, treatment with antioxidant N-acetyl-L-cystein was able to extend the lifespan of these stem cells in serial transplantation experiments in mice [350]. The negative correlation between ROS levels and stemness is further supported by another study, which shows that a lower intracellular

ROS can be promoted by the stem cell factor MYC to facilitate tumorigenesis [351]. Moreover, a recent study discovered that the CSC marker CD44, in particular the CD44v isoform, interacts and stabilizes xCT, a subunit of a glutamate-cystine transporter, to promote the uptake of cystine for the synthesis of the master antioxidant glutathione [349]. The negative role played by ROS has been challenged by a recent study, which provide evidence to show that ROS stimulates self-renewal of neural stem cells [352].

1.5 Thesis overview

1.5.1 Rationale

ESCC is one of the leading causes of cancer-related deaths worldwide, characterized by its aggressive features, such as highly invasive and metastatic, and a low 5-year survival rate (~14%) [1-4]. However, the mechanisms underlying the aggressiveness of ESCC remain poorly understood. To this end, we explored from different perspectives the molecular mechanisms behind the pathobiology of ESCC, aiming to reveal important prognostic markers and potential therapeutic targets.

1) miRNAs have been shown to play critical roles in virtually all stages of tumor progression, such as tumor initiation, angiogenesis, invasion, metastasis and chemoresistance. We previously used microarrays to obtain the expression profile of miRNAs [353], and 33 upregulated miRNAs and 40 downregulated miRNAs were revealed in ESCC tumors compared with adjacent non-tumorous esophageal tissues. However, how miRNAs are involved in the pathobiology of ESCC remained unclear. 2) The oncogenic potential of STAT3 has been well documented in various cancers, including

ESCC. However, accumulating evidence from both experimental and clinical studies has suggested that STAT3 may also carry a tumor suppressor role in specific contexts [354], and the regulation of these opposing effects is elusive. STAT3β, one of the two STAT3 isoforms that has been shown to be dominant-negative factor of STAT3, is largely neglected in the vast majority of studies in cancer biology. 3) Cancer stem cells (CSCs) have been shown to play a key role the initiation and chemoresistance of various cancers [322,355]. These features of CSCs contribute to treatment failure and cancer recurrence, which is one of the most lethal events for cancer patients. However, our understanding of the molecular basis of the origin of CSCs remains limited, especially in ESCC. Using a lentiviral SRR2 (Sox2 Regulatory Region 2) reporter expressing both GFP and luciferase under the control of SRR2 that contains consensus binding sites of multiple stem cell factors and oncogenic transcription factors, our previous studies in breast cancer has successfully identified and purified two distinct subsets of cells [356,357]. These subsets of cells were shown to possess different stem cell-like properties [356,357]. Sox2 has been shown to play an important role in ESCC cancer stem cells and the initiation of ESCC [358].

1.5.2 Hypotheses

Based on the background information described above, we hypothesized that aberrant loss of tumor suppressors including miRNAs and STAT3β, and gain of oncoproteins/stem cell factors contribute to the aggressive traits of ESCC, including stemness, chemoresistance and invasiveness. Specifically, this general hypothesis is divided into three sub-hypotheses: 1) Loss of miR-200b

promotes the pathobiology of ESCC by enhancing the expression of tumor-associated proteins and the activation of oncogenic pathways; 2) STAT3β is a tumor suppressor in ESCC, and a key determining factor that determines the opposing roles of STAT3 as an oncoprotein and a tumor suppressor; and 3) SRR2 reporter can be used to identify CSC-like cell subpopulations as well as the driving forces (*i.e.* oncoproteins and stem cell factors) of the CSC-like features in ESCC, providing an ideal model to further our understanding of the pathobiology of ESCC.

1.5.3 Objectives

Corresponding to the three hypotheses mentioned above, I developed three objectives:

1) **In Chapter 2,** I aimed to investigate how the deregulated miRNAs in ESCC revealed by our previous study [353] contribute to the pathobiology of ESCC. I focused on miR-200b, a miRNA that had been shown to one of the master regulators of EMT, a process that plays a key role in the invasion and metastasis of tumors. I comprehensively studied the role of miR-200b in ESCC from various perspectives, such as assessing its expression status and clinical significance in ESCC patient samples, investigating the biological function both *in vitro* and *in vivo,* and searching the downstream target genes and downstream signaling pathways.

2) **In Chapter 3**, I aimed to evaluate the prognostic significance of STAT3α and STAT3β in ESCC patients, the biological function of STAT3β in the stemness, tumorigenicity, chemoresistance both *in vitro* and *in vivo*, the interplay between STAT3α and STAT3β in ESCC cells, and how the interplay

between STAT3α and STAT3β can affect the prognostic value of STAT3 in patients.

3) **In Chapter 4**, I aimed to use the SRR2 reporter to identify and isolate subpopulations of ESCC cells that possess distinctive CSC-like properties. Using this cell model that GFP and luciferase are used as readouts, I investigated whether the stem-like features can be acquired (using GFP/luciferase as an indicator) by ESCC cells under certain conditions, such as the stimulation of ROS. I also studied what are the possible molecular mechanisms that promote the stem-like properties of ESCC cells. I also determined how the CSC-like features contribute to the aggressiveness such as chemoresistance of ESCC cells, as well as the clinical significance of the key proteins that contribute to CSC-like features of ESCC cells.

1.6 References

1. Ferlay J, Shin HR, Bray F, et al. Estimates of worldwide burden of cancer in 2008: GLOBOCAN 2008. Int J Cancer 2010;127:2893-917.
2. Jemal A, Bray F, Center MM, et al. Global cancer statistics. CA Cancer J Clin 2011;61:69-90.
3. Enzinger PC, Mayer RJ. Esophageal cancer. N Engl J Med 2003;349:2241-2252.
4. Ries LAG, Eisner MP, Kosary C, et al. eds. SEER cancer statistics review, 1973-1999. Bethesda, Md.: National Cancer Institute, 2002.
5. Ke L. Mortality and incidence trends from esophagus cancer in selected geographic areas of China circa 1970-90. Int J Cancer. 2002;102:271-274.

6. Ke L, Yu P, Zhang ZX. Novel epidemiologic evidence for the association between fermented fish sauce and esophageal cancer in South China. Int J Cancer 2002;99:424-426.
7. Tang WR, Chen ZJ, Lin K, et al. Development of esophageal cancer in Chaoshan region, China: association with environmental, genetic and cultural factors. Int J Hyg Environ Health 2015;218:12-18.
8. Wang LD, Zhou FY, Li XM, et al. Genome-wide association study of esophageal squamous cell carcinoma in Chinese subjects identifies susceptibility loci at PLCE1 and C20orf54. Nat Genet 2010;42:759-63.
9. Wu C, Kraft P, Zhai K, et al. Genome-wide association analyses of esophageal squamous cell carcinoma in Chinese identify multiple susceptibility loci and gene-environment interactions. Nat Genet 2012;44:1090-7.
10. Song Y, Li L, Ou Y, et al. Identification of genomic alterations in oesophageal squamous cell cancer. Nature 2014;509(7498):91-5.
11. Gao YB, Chen ZL, Li JG, et al. Genetic landscape of esophageal squamous cell carcinoma. Nat Genet 2014;46:1097-102.
12. Lin DC, Hao JJ, Nagata Y, et al. Genomic and molecular characterization of esophageal squamous cell carcinoma. Nat Genet 2014;46:467-73.
13. Bartel DP. MicroRNAs: genomics, biogenesis, mechanism, and function. Cell 2004; 116: 281–297.
14. Inui M, Martello G, Piccolo S. MicroRNA control of signal transduction. Nat Rev Mol Cell Biol 2010; 11: 252-63.
15. Forman JJ, Coller HA. The code within the code: microRNAs target coding regions. Cell Cycle 2010; 9: 1533-41.

16. Reczko M, Maragkakis M, Alexiou P, et al. Functional microRNA targets in protein coding sequences. Bioinformatics 2012; 28: 771-6.
17. Lee I, Ajay SS, Yook JI, et al. New class of microRNA targets containing simultaneous 5'-UTR and 3'-UTR interaction sites. Genome Res 2009; 19: 1175-83.
18. Ørom UA, Nielsen FC, Lund AH. MicroRNA-10a Binds the 5′UTR of Ribosomal Protein mRNAs and Enhances Their Translation. Mol Cell 2008; 30: 460-71.
19. Kloosterman WP, Plasterk RH. The diverse functions of microRNAs in animal development and disease. Dev Cell 2006; 11: 441-50.
20. Leung AK, Sharp PA. microRNAs: a safeguard against turmoil? Cell 2007; 130: 581-5.
21. Iorio MV, Croce CM. MicroRNA dysregulation in cancer: diagnostics, monitoring and therapeutics. A comprehensive review. EMBO Mol Med 2012; 4: 143-59.
22. Dews M, Homayouni A, Yu D, et al. Augmentation of tumor angiogenesis by a Myc-activated microRNA cluster. Nat Genet 2006; 38: 1060-5.
23. He L, He XY, Lim LP, et al. A microRNA component of the p53 tumour suppressor network. Nature 2007; 447: 1130-34.
24. Esteller M. Epigenetics in Cancer. N Engl J Med 2008; 358: 1148-59.
25. Gosden RG, Feinberg AP. Genetics and epigenetics--nature's pen-and-pencil set. N Engl J Med 2007; 356: 731-3.
26. Ganesan A, Nolan L, Crabb SJ, et al. Epigenetic therapy: histone acetylation, DNA methylation and anti-cancer drug discovery. Curr Cancer Drug Targets 2009; 9: 963-81.

27. Zheng H, Wu H. Enhancement on the predictive power of the prediction model for human genomic DNA methylation. International Conference on Bioinformatics and Computational Biology (BIOCOMP), 2011.
28. Christman JK. 5-Azacytidine and 5-aza-2'-deoxycytidine as inhibitors of DNA methylation: mechanistic studies and their implications for cancer therapy. Oncogene 2002; 21: 5483-95.
29. Stresemann C, Lyko F. Modes of action of the DNA methyltransferase inhibitors azacytidine and decitabine. Int J Cancer 2008; 123: 8-13.
30. Yeh CC, Deng YT, Sha DY, et al. Suberoylanilide hydroxamic acid sensitizes human oral cancer cells to TRAIL-induced apoptosis through increase DR5 expression. Mol Cancer Ther 2009; 8: 2718-25.
31. Butler LM, Liapis V, Bouralexis S, et al. The histone deacetylase inhibitor, suberoylanilide hydroxamic acid, overcomes resistance of human breast cancer cells to Apo2L/TRAIL. Int J Cancer 2006; 119: 944-54.
32. Elmén J, Lindow M, Schütz S, et al. LNA-mediated microRNA silencing in non-human primates. Nature 2008; 452: 896-9.
33. Ma L, Reinhardt F, Pan E, et al. Therapeutic silencing of miR-10b inhibits metastasis in a mouse mammary tumor model. Nat Biotechnol 2010; 28: 341-7.
34. Burk U, Schubert J, Wellner U, et al. A reciprocal repression between ZEB1 and members of the miR-200 family promotes EMT and invasion in cancer cells. EMBO Rep 2008; 9: 582-9.
35. Bracken CP, Gregory PA, Kolesnikoff N, et al. A double-negative feedback loop between ZEB1-SIP1 and the microRNA-200 family regulates epithelial-mesenchymal transition. Cancer Res 2008; 68: 7846-

54.

36. Gregory PA, Bert AG, Paterson EL, et al. The miR-200 family and miR-205 regulate epithelial to mesenchymal transition by targeting ZEB1 and SIP1. Nat Cell Biol 2008; 10: 593-601.
37. Korpal M, Lee ES, Hu G, et al. The miR-200 family inhibits epithelial-mesenchymal transition and cancer cell migration by direct targeting of E-cadherin transcriptional repressors ZEB1 and ZEB2. J Biol Chem 2008; 283: 14910-4.
38. Park SM, Gaur AB, Lengyel E, et al. The miR-200 family determines the epithelial phenotype of cancer cells by targeting the E-cadherin repressors ZEB1 and ZEB2. Genes Dev 2008; 22: 894-907.
39. Shimono Y, Zabala M, Cho RW, et al. Downregulation of miRNA-200c links breast cancer stem cells with normal stem cells. Cell 2009; 138: 592-603.
40. Wellner U, Schubert J, Burk UC, et al. The EMT-activator ZEB1 promotes tumorigenicity by repressing stemness-inhibiting microRNAs. Nat Cell Biol 2009; 11: 1487-95.
41. Iliopoulos D, Lindahl-Allen M, Polytarchou C, et al. Loss of miR-200 inhibition of SUZ12 leads to polycomb-mediated repression required for the formation and maintenance of cancer stem cells. Mol Cell 2010; 39: 761-72.
42. Iliopoulos D, Polytarchou C, Hatziapostolou M, et al. MicroRNAs differentially regulated by Akt isoforms control EMT and stem cell renewal in cancer cells. Sci Signal 2009; 2: ra62.
43. Chan YC, Khanna S, Roy S, et al. miR-200b targets ETS1 and is down-

regulated by hypoxia to induce angiogenic response of endothelial cells. J Biol Chem 2011; 286: 2047-56

44. Choi YC, Yoon S, Jeong Y, et al. Regulation of Vascular Endothelial Growth Factor Signaling by miR-200b. Mol Cells 2011; 32: 77-82.
45. Roybal JD, Zang Y, Ahn YH, et al. miR-200 Inhibits lung adenocarcinoma cell invasion and metastasis by targeting FLT1/VEGFR1. Mol Cancer Res 2011; 9: 25-35.
46. Chan YC, Roy S, Khanna S, et al. Downregulation of endothelial microRNA-200b supports cutaneous wound angiogenesis by desilencing GATA binding protein 2 and vascular endothelial growth factor receptor 2. Arterioscler Thromb Vasc Biol 2012; 32: 1372-82.
47. McArthur K, Feng B, Wu Y, et al. MicroRNA-200b regulates vascular endothelial growth factor-mediated alterations in diabetic retinopathy. Diabetes 2011; 60: 1314-23.
48. Adam L, Zhong M, Choi W, et al. miR-200 expression regulates epithelial-to-mesenchymal transition in bladder cancer cells and reverses resistance to epidermal growth factor receptor therapy. Clin Cancer Res 2009; 15: 5060-72.
49. Cochrane DR, Spoelstra NS, Howe EN, et al. MicroRNA-200c mitigates invasiveness and restores sensitivity to microtubule-targeting chemotherapeutic agents. Mol Cancer Ther 2009; 8: 1055-66.
50. Li Y, VandenBoom TG 2nd, Kong D, et al. Up-regulation of miR-200 and let-7 by natural agents leads to the reversal of epithelial-to-mesenchymal transition in gemcitabine-resistant pancreatic cancer cells. Cancer Res 2009; 69: 6704-12.

51. Cochrane DR, Howe EN, Spoelstra NS, et al. Loss of miR-200c: A Marker of Aggressiveness and Chemoresistance in Female Reproductive Cancers. J Oncol 2010; 2010: 821717.
52. Tryndyak VP, Beland FA, Pogribny IP. E-cadherin transcriptional down-regulation by epigenetic and microRNA-200 family alterations is related to mesenchymal and drug-resistant phenotypes in human breast cancer cells. Int J Cancer 2010; 126: 2575-83.
53. van Jaarsveld MT, Helleman J, Berns EM, et al. MicroRNAs in ovarian cancer biology and therapy resistance. Int J Biochem Cell Biol 2010; 42: 1282-90.
54. Rui W, Bing F, Hai-Zhu S, et al. Identification of microRNA profiles in docetaxel-resistant human non-small cell lung carcinoma cells (SPC-A1). J Cell Mol Med 2010; 14: 206-14.
55. Wu XM, Shao XQ, Meng XX, et al. Genome-wide analysis of microRNA and mRNA expression signatures in hydroxycamptothecin-resistant gastric cancer cells. Acta Pharmacol Sin 2011; 32: 259-69.
56. Feng B, Wang R, Song HZ, et al. MicroRNA-200b reverses chemoresistance of docetaxel-resistant human lung adenocarcinoma cells by targeting E2F3. Cancer 2012; 118: 3365-76.
57. Korpal M, Ell BJ, Buffa FM, et al. Direct targeting of Sec23a by miR-200s influences cancer cell secretome and promotes metastatic colonization. Nat Med 2011; 17: 1101-8.
58. Dykxhoorn DM, Wu Y, Xie H, et al. miR-200 enhances mouse breast cancer cell colonization to form distant metastases. PLoS One 2009; 4: e7181.

59. Wicha MS, Liu S, Dontu G. Cancer Stem Cells: An Old Idea—A Paradigm Shift. Cancer Res 2006; 66: 1883-90.

60. Reya T, Morrison SJ, Clarke MF, et al. Stem cells, cancer, and cancer stem cells. Nature 2001; 414: 105-11.

61. Molofsky AV, He S, Bydon M, et al. Bmi-1 promotes neural stem cell self-renewal and neural development but not mouse growth and survival by repressing the p16Ink4a and p19Arf senescence pathways. Genes Dev 2005; 19: 1432-7.

62. Park IK, Qian D, Kiel M, et al. Bmi-1 is required for maintenance of adult self-renewing haematopoietic stem cells. Nature 2003; 423: 302-5.

63. Pietersen AM, Evers B, Prasad AA, et al. Bmi1 regulates stem cells and proliferation and differentiation of committed cells in mammary epithelium. Curr Biol 2008; 18: 1094-9.

64. Boyer LA, Plath K, Zeitlinger J, et al. Polycomb complexes repress developmental regulators in murine embryonic stem cells. Nature 2006; 441: 349–353.

65. Lee TI, Jenner RG, Boyer LA, et al. Control of developmental regulators by Polycomb in human embryonic stem cells. Cell 2006; 125: 301–313.

66. Squazzo SL, O'Geen H, Komashko VM, et al. SUZ12 binds to silenced regions of the genome in a cell-type-specific manner. Genome Res 2006; 6: 890–900.

67. Zhong X, Li Y, Peng F, et al. Identification of tumorigenic retinal stem-like cells in human solid retinoblastomas. Int J Cancer 2007; 121: 2125–2131.

68. Bracken AP, and Helin K. Polycomb group proteins: navigators of lineage pathways led astray in cancer. Nat Rev Cancer 2009; 9: 773–784.

69. Hoenerhoff MJ, Chu I, Barkan D, et al. BMI1 cooperates with H-RAS to induce an aggressive breast cancer phenotype with brain metastases. Oncogene 2009; 28: 3022–3032.

70. Thiery JP, Sleeman JP. Complex networks orchestrate epithelial-mesenchymal transitions. Nat Rev Mol Cell Biol 2006; 7: 131–142.

71. Huber MA, Kraut N, Beug H. Molecular requirements for epithelial–mesenchymal transition during tumor progression. Curr Opin Cell Biol 2005; 17: 548–558.

72. Thiery JP. Epithelial-mesenchymal transitions in development and pathologies. Curr Opin Cell Biol 2003; 15: 740–746.

73. Brabletz T, Jung A, Spaderna S, et al. Migrating cancer stem cells — an integrated concept of malignant tumor progression. Nat Rev Cancer 2005; 5: 744-9.

74. Gotzmann J, Huber H, Thallinger C, et al. Hepatocytes convert to a fibroblastoid phenotype through the cooperation of TGF-beta1 and Ha-Ras: Steps towards invasiveness. J Cell Sci 2002; 115: 1189-1202.

75. Baumgart E, Cohen MS, Silva NB, et al. Identification and prognostic significance of an epithelial-mesenchymal transition expression profile in human bladder tumors. Clin Cancer Res 2007; 13: 1685-94.

76. Brabletz S, Brabletz T. The ZEB/miR-200 feedback loop—a motor of cellular plasticity in development and cancer? EMBO Rep 2010; 11: 670-7.

77. Liu YN, Yin JJ, Abou-Kheir W, et al. MiR-1 and miR-200 inhibit EMT via SLUG-dependent and tumorigenesis via SLUG-independent mechanisms. Oncogene 2012; 32: 296-306.

78. Sun L, Yao Y, Liu B, et al. MiR-200b and miR-15b regulate chemotherapy-induced epithelial-mesenchymal transition in human tongue cancer cells by targeting BMI1. Oncogene 2012; 31: 432-45.
79. Eades G, Yao Y, Yang M, et al. miR-200a regulates SIRT1 expression and epithelial to mesenchymal transition (EMT)-like transformation in mammary epithelial cells. J Biol Chem 2011; 286: 25992-6002.
80. Olson P, Lu J, Zhang H, et al. MicroRNA dynamics in the stages of tumorigenesis correlate with hallmark capabilities of cancer. Genes Dev 2009; 23: 2152-65.
81. Gibbons DL, Lin W, Creighton CJ, et al. Contextual extracellular cues promote tumor cell EMT and metastasis by regulating miR-200 family expression. Genes Dev 2009; 23: 2140-51.
82. Vallejo DM, Caparros E, Dominguez M. Targeting Notch signalling by the conserved miR-8/200 microRNA family in development and cancer cells. EMBO J 2011; 30: 756-69.
83. Brabletz S, Bajdak K, Meidhof S, et al. The ZEB1/miR-200 feedback loop controls Notch signalling in cancer cells. EMBO J 2011; 30: 770-82.
84. Yang Y, Ahn YH, Gibbons DL, et al. The Notch ligand Jagged2 promotes lung adenocarcinoma metastasis through a miR-200-dependent pathway in mice. J Clin Invest 2011; 121: 1373-85.
85. Polyak K, Weinberg RA. Transitions between epithelial and mesenchymal states: acquisition of malignant and stem cell traits. Nat Rev Cancer 2009; 9: 265e73.
86. Yates CC, Shepard CR, Stolz DB, et al. Co-culturing human prostate carcinoma cells with hepatocytes leads to increased expression of E-

cadherin. Br J Cancer 2007; 96: 1246e52.

87. Kowalski PJ, Rubin MA, Kleer CG. E-cadherin expression in primary carcinomas of the breast and its distant metastases. Breast Cancer Res 2003; 5: R217e22.
88. Hur K, Toiyama Y, Takahashi M, et al. MicroRNA-200c modulates epithelial-to-mesenchymal transition (EMT) in human colorectal cancer metastasis. Gut Published Online First: 10 July 2012. Available from: http://gut.bmj.com/content/early/2012/07/09/gutjnl-2011-301846.
89. Gravgaard KH, Lyng MB, Laenkholm AV, et al. The miRNA-200 family and miRNA-9 exhibit differential expression in primary versus corresponding metastatic tissue in breast cancer. Breast Cancer Res Treat 2012; 134: 207-17.
90. Sabbah M, Emami S, Redeuilh G, et al. Molecular signature and therapeutic perspective of the epithelialto-mesenchymal transitions in epithelial cancers. Drug Resist Updat 2008; 11: 123–51.
91. Fuchs BC, Fujii T, Dorfman JD, et al. Epithelial-to-mesenchymal transition and integrin-linked kinase mediate sensitivity to epidermal growth factor receptor inhibition in human hepatoma cells. Cancer Res 2008; 68: 2391-9.
92. Leskelä S, Leandro-García LJ, Mendiola M, et al. The miR-200 family controls beta-tubulin III expression and is associated with paclitaxel-based treatment response and progression-free survival in ovarian cancer patients. Endocr Relat Cancer 2010; 18: 85-95.
93. Pogribny IP, Filkowski JN, Tryndyak VP, et al. Alterations of microRNAs and their targets are associated with acquired resistance of MCF-7

breast cancer cells to cisplatin. Int J Cancer 2010; 127: 1785-94.

94. Kovalchuk O, Filkowski J, Meservy J, et al. Involvement of microRNA-451 in resistance of the MCF-7 breast cancer cells to chemotherapeutic drug doxorubicin. Mol Cancer Ther 2008; 7: 2152-9.
95. Ali S, Ahmad A, Banerjee S, et al. Gemcitabine sensitivity can be induced in pancreatic cancer cells through modulation of miR-200 and miR-21 expression by curcumin or its analogue CDF. Cancer Res 2010; 70: 3606-17.
96. Bao B, Ali S, Kong D, et al. Anti-tumor activity of a novel compound-CDF is mediated by regulating miR-21, miR-200, and PTEN in pancreatic cancer. PLoS One 2011; 6: e17850.
97. Soubani O, Ali AS, Logna F, et al. Re-expression of miR-200 by novel approaches regulates the expression of PTEN and MT1-MMP in pancreatic cancer. Carcinogenesis 2012; 33: 1563-71.
98. Liao CH, Sang S, Ho CT, et al. Garcinol modulates tyrosine phosphorylation of FAK and subsequently induces apoptosis through down-regulation of Src, ERK, and Akt survival signaling in human colon cancer cells. J Cell Biochem 2005; 96: 155-69.
99. Ahmad A, Wang Z, Ali R, et al. Apoptosis-inducing effect of garcinol is mediated by NF-kappaB signaling in breast cancer cells. J Cell Biochem 2010; 109: 1134-41.
100. Prasad S, Ravindran J, Sung B, et al. Garcinol potentiates TRAIL-induced apoptosis through modulation of death receptors and antiapoptotic proteins. Mol Cancer Ther 2010; 9: 856-68.
101. Ahmad A, Sarkar SH, Bitar B, et al. Garcinol regulates EMT and Wnt

signaling pathways in vitro and in vivo leading to anticancer activity against breast cancer cells. Mol Cancer Ther 2012; 11: 2193-201.

102. Schliekelman MJ, Gibbons DL, Faca VM, et al. Targets of the tumor suppressor miR-200 in regulation of the epithelial-mesenchymal transition in cancer. Cancer Res 2011; 71: 7670-82.
103. Ebert MS, Neilson JR, Sharp PA. MicroRNA sponges: competitive inhibitors of small RNAs in mammalian cells. Nat Methods 2007; 4: 721-6.
104. Akinc A, Zumbuehl A, Goldberg M, et al. A combinatorial library of lipid-like materials for delivery of RNAi therapeutics. Nat Biotechnol 2008; 26: 561-9.
105. Arima Y, Hayashi H, Sasaki M, et al. Induction of ZEB proteins by inactivation of RB protein is key determinant of mesenchymal phenotype of breast cancer. J Biol Chem 2012; 287: 7896-906.
106. Gregory PA, Bracken CP, Smith E, et al. An autocrine TGF-beta/ZEB/miR-200 signaling network regulates establishment and maintenance of epithelial-mesenchymal transition. Mol Biol Cell 2011; 22: 1686-98.
107. Ahmad A, Aboukameel A, Kong D, et al. Phosphoglucose isomerase/autocrine motility factor mediates epithelial-mesenchymal transition regulated by miR-200 in breast cancer cells. Cancer Res 2011; 71: 3400-9.
108. Howe EN, Cochrane DR, Richer JK. Targets of miR-200c mediate suppression of cell motility and anoikis resistance. Breast Cancer Res 2011; 13: R45.
109. Uhlmann S, Zhang JD, Schwäger A, et al. miR-200bc/429 cluster targets

PLCgamma1 and differentially regulates proliferation and EGF-driven invasion than miR-200a/141 in breast cancer. Oncogene 2010; 29: 4297-306.

110. Sossey-Alaoui K, Bialkowska K, Plow EF. The miR200 family of microRNAs regulates WAVE3-dependent cancer cell invasion. J Biol Chem 2009; 284: 33019-29.
111. Jurmeister S, Baumann M, Balwierz A, et al. MicroRNA-200c represses migration and invasion of breast cancer cells by targeting actin-regulatory proteins FHOD1 and PPM1F. Mol Cell Biol 2012; 32: 633-51.
112. Tellez CS, Juri DE, Do K, et al. EMT and stem cell-like properties associated with miR-205 and miR-200 epigenetic silencing are early manifestations during carcinogen-induced transformation of human lung epithelial cells. Cancer Res 2011; 71: 3087-97.
113. Wang Z, Zhao Y, Smith E, et al. Reversal and prevention of arsenic-induced human bronchial epithelial cell malignant transformation by microRNA-200b. Toxicol Sci 2011; 121: 110-22.
114. Hung CS, Liu HH, Liu JJ, et al. MicroRNA-200a and -200b Mediated Hepatocellular Carcinoma Cell Migration Through the Epithelial to Mesenchymal Transition Markers. Ann Surg Oncol 2012 Aug 7. Available from: http://link.springer.com/article/10.1245%2Fs10434-012-2482-4.
115. Zhang Z, Liu ZB, Ren WM, et al. The miR-200 family regulates the epithelial-mesenchymal transition induced by EGF/EGFR in anaplastic thyroid cancer cells. Int J Mol Med 2012; 30: 856-62.
116. Braun J, Hoang-Vu C, Dralle H, et al. Downregulation of microRNAs directs the EMT and invasive potential of anaplastic thyroid carcinomas.

Oncogene 2010; 29: 4237-44.

117. Ono H, Imoto I, Kozaki K, et al. SIX1 promotes epithelial-mesenchymal transition in colorectal cancer through ZEB1 activation. Oncogene 2012; 314923-34.

118. Kong D, Banerjee S, Ahmad A, et al. Epithelial to mesenchymal transition is mechanistically linked with stem cell signatures in prostate cancer cells. PLoS One 2010; 5: e12445.

119. Kong D, Li Y, Wang Z, et al. miR-200 regulates PDGF-D-mediated epithelial-mesenchymal transition, adhesion, and invasion of prostate cancer cells. Stem Cells 2009; 27: 1712-21.

120. Kurashige J, Kamohara H, Watanabe M, et al. MicroRNA-200b Regulates Cell Proliferation, Invasion, and Migration by Directly Targeting ZEB2 in Gastric Carcinoma. Ann Surg Oncol 2012; 19 Suppl 3: 656-64.

121. Shinozaki A, Sakatani T, Ushiku T, et al. Downregulation of microRNA-200 in EBV-associated gastric carcinoma. Cancer Res 2010; 70: 4719-27.

122. Du Y, Xu Y, Ding L, et al. Down-regulation of miR-141 in gastric cancer and its involvement in cell growth. J Gastroenterol 2009; 44: 556-61.

123. Su J, Zhang A, Shi Z, et al. MicroRNA-200a suppresses the Wnt/β-catenin signaling pathway by interacting with β-catenin. Int J Oncol 2012; 40: 1162-70.

124. Cai J, Liu X, Cheng J, et al. MicroRNA-200 is commonly repressed in conjunctival MALT lymphoma, and targets cyclin E2. Graefes Arch Clin Exp Ophthalmol 2012; 250: 523-31.

125. Mateescu B, Batista L, Cardon M, et al. miR-141 and miR-200a act on ovarian tumorigenesis by controlling oxidative stress response. Nat Med 2011; 17: 1627-35.

126. Chen J, Wang L, Matyunina LV, et al. Overexpression of miR-429 induces mesenchymal-to-epithelial transition (MET) in metastatic ovarian cancer cells. Gynecol Oncol 2011; 121: 200-5.

127. Bendoraite A, Knouf EC, Garg KS, et al. Regulation of miR-200 family microRNAs and ZEB transcription factors in ovarian cancer: evidence supporting a mesothelial-to-epithelial transition. Gynecol Oncol 2010; 116: 117-25.

128. Wiklund ED, Bramsen JB, Hulf T, et al. Coordinated epigenetic repression of the miR-200 family and miR-205 in invasive bladder cancer. Int J Cancer 2011; 128: 1327-34.

129. Xia H, Ng SS, Jiang S, et al. miR-200a-mediated downregulation of ZEB2 and CTNNB1 differentially inhibits nasopharyngeal carcinoma cell growth, migration and invasion. Biochem Biophys Res Commun 2010; 391: 535-41.

130. Lo WL, Yu CC, Chiou GY, et al. MicroRNA-200c attenuates tumour growth and metastasis of presumptive head and neck squamous cell carcinoma stem cells. J Pathol 2011; 223: 482-95.

131. Saydam O, Shen Y, Würdinger T, et al. Downregulated microRNA-200a in meningiomas promotes tumor growth by reducing E-cadherin and activating the Wnt/beta-catenin signaling pathway. Mol Cell Biol 2009; 29: 5923-40.

132. Hamano R, Miyata H, Yamasaki M, et al. Overexpression of miR-200c

induces chemoresistance in esophageal cancers mediated through activation of the Akt signaling pathway. Clin Cancer Res 2011; 17: 3029-38.

133. Elson-Schwab I, Lorentzen A, Marshall CJ. MicroRNA-200 family members differentially regulate morphological plasticity and mode of melanoma cell invasion. PLoS One 2010; 5. pii: e13176.
134. Kent OA, Mullendore M, Wentzel EA, et al. A resource for analysis of microRNA expression and function in pancreatic ductal adenocarcinoma cells. Cancer Biol Ther 2009; 8: 2013-24.
135. Mees ST, Mardin WA, Wendel C, et al. EP300--a miRNA-regulated metastasis suppressor gene in ductal adenocarcinomas of the pancreas. Int J Cancer 2010; 126: 114-24.
136. Yu, H.; Kortylewski, M.; Pardoll, D., Crosstalk between cancer and immune cells: Role of stat3 in the tumour microenvironment. Nat Rev Immunol 2007, 7, 41-51.
137. Yu, H.; Jove, R., The stats of cancer--new molecular targets come of age. Nature reviews. Cancer 2004, 4, 97-105.
138. Yue, P.; Turkson, J., Targeting stat3 in cancer: How successful are we? Expert opinion on investigational drugs 2009, 18, 45-56.
139. Sara Pensa, G.R., Daniela Boselli, Francesco Novelli, and Valeria Poli, Stat1 and stat3 in tumorigenesis: Two sides of the same coin? Landes Bioscience: Austin, TX, USA, 2009.
140. Sellier, H.; Rebillard, A.; Guette, C.; Barre, B.; Coqueret, O., How should we define stat3 as an oncogene and as a potential target for therapy? Jak-Stat 2013, 2, e24716.

141. Levy, D.E.; Lee, C.K., What does stat3 do? The Journal of clinical investigation 2002, 109, 1143-1148.

142. Akira, S., Roles of stat3 defined by tissue-specific gene targeting. Oncogene 2000, 19, 2607-2611.

143. Akira, S., Functional roles of stat family proteins: Lessons from knockout mice. Stem Cells 1999, 17, 138-146.

144. Takeda, K.; Noguchi, K.; Shi, W.; Tanaka, T.; Matsumoto, M.; Yoshida, N.; Kishimoto, T.; Akira, S., Targeted disruption of the mouse stat3 gene leads to early embryonic lethality. Proceedings of the National Academy of Sciences of the United States of America 1997, 94, 3801-3804.

145. Sano, S.; Itami, S.; Takeda, K.; Tarutani, M.; Yamaguchi, Y.; Miura, H.; Yoshikawa, K.; Akira, S.; Takeda, J., Keratinocyte-specific ablation of stat3 exhibits impaired skin remodeling, but does not affect skin morphogenesis. The EMBO journal 1999, 18, 4657-4668.

146. Chapman, R.S.; Lourenco, P.C.; Tonner, E.; Flint, D.J.; Selbert, S.; Takeda, K.; Akira, S.; Clarke, A.R.; Watson, C.J., Suppression of epithelial apoptosis and delayed mammary gland involution in mice with a conditional knockout of stat3. Genes & development 1999, 13, 2604-2616.

147. Sano, S.; Takahama, Y.; Sugawara, T.; Kosaka, H.; Itami, S.; Yoshikawa, K.; Miyazaki, J.; van Ewijk, W.; Takeda, J., Stat3 in thymic epithelial cells is essential for postnatal maintenance of thymic architecture and thymocyte survival. Immunity 2001, 15, 261-273.

148. Takeda, K.; Kaisho, T.; Yoshida, N.; Takeda, J.; Kishimoto, T.; Akira, S., Stat3 activation is responsible for il-6-dependent t cell proliferation

through preventing apoptosis: Generation and characterization of t cell-specific stat3-deficient mice. J Immunol 1998, 161, 4652-4660.

149. Bromberg, J.F.; Wrzeszczynska, M.H.; Devgan, G.; Zhao, Y.; Pestell, R.G.; Albanese, C.; Darnell, J.E., Jr., Stat3 as an oncogene. Cell 1999, 98, 295-303.

150. Dechow, T.N.; Pedranzini, L.; Leitch, A.; Leslie, K.; Gerald, W.L.; Linkov, I.; Bromberg, J.F., Requirement of matrix metalloproteinase-9 for the transformation of human mammary epithelial cells by stat3-c. Proceedings of the National Academy of Sciences of the United States of America 2004, 101, 10602-10607.

151. Azare, J.; Leslie, K.; Al-Ahmadie, H.; Gerald, W.; Weinreb, P.H.; Violette, S.M.; Bromberg, J., Constitutively activated stat3 induces tumorigenesis and enhances cell motility of prostate epithelial cells through integrin beta 6. Molecular and cellular biology 2007, 27, 4444-4453.

152. Kortylewski, M.; Yu, H., Stat3 as a potential target for cancer immunotherapy. J Immunother 2007, 30, 131-139.

153. Sherry, M.M.; Reeves, A.; Wu, J.K.; Cochran, B.H., Stat3 is required for proliferation and maintenance of multipotency in glioblastoma stem cells. Stem Cells 2009, 27, 2383-2392.

154. Guryanova, O.A.; Wu, Q.; Cheng, L.; Lathia, J.D.; Huang, Z.; Yang, J.; MacSwords, J.; Eyler, C.E.; McLendon, R.E.; Heddleston, J.M., et al., Nonreceptor tyrosine kinase bmx maintains self-renewal and tumorigenic potential of glioblastoma stem cells by activating stat3. Cancer cell 2011, 19, 498-511.

155. Marotta, L.L.; Almendro, V.; Marusyk, A.; Shipitsin, M.; Schemme, J.;

Walker, S.R.; Bloushtain-Qimron, N.; Kim, J.J.; Choudhury, S.A.; Maruyama, R., et al., The jak2/stat3 signaling pathway is required for growth of cd44(+)cd24(-) stem cell-like breast cancer cells in human tumors. The Journal of clinical investigation 2011, 121, 2723-2735.

156. Kim, E.; Kim, M.; Woo, D.H.; Shin, Y.; Shin, J.; Chang, N.; Oh, Y.T.; Kim, H.; Rheey, J.; Nakano, I., et al., Phosphorylation of ezh2 activates stat3 signaling via stat3 methylation and promotes tumorigenicity of glioblastoma stem-like cells. Cancer cell 2013, 23, 839-852.
157. Liu, K.; Jiang, M.; Lu, Y.; Chen, H.; Sun, J.; Wu, S.; Ku, W.Y.; Nakagawa, H.; Kita, Y.; Natsugoe, S., et al., Sox2 cooperates with inflammation-mediated stat3 activation in the malignant transformation of foregut basal progenitor cells. Cell stem cell 2013, 12, 304-315.
158. Kaptein, A.; Paillard, V.; Saunders, M., Dominant negative stat3 mutant inhibits interleukin-6-induced jak-stat signal transduction. The Journal of biological chemistry 1996, 271, 5961-5964.
159. Chen, C.L.; Cen, L.; Kohout, J.; Hutzen, B.; Chan, C.; Hsieh, F.C.; Loy, A.; Huang, V.; Cheng, G.; Lin, J., Signal transducer and activator of transcription 3 activation is associated with bladder cancer cell growth and survival. Molecular cancer 2008, 7, 78.
160. Rivat, C.; De Wever, O.; Bruyneel, E.; Mareel, M.; Gespach, C.; Attoub, S., Disruption of stat3 signaling leads to tumor cell invasion through alterations of homotypic cell-cell adhesion complexes. Oncogene 2004, 23, 3317-3327.
161. Wang, X.; Crowe, P.J.; Goldstein, D.; Yang, J.L., Stat3 inhibition, a novel approach to enhancing targeted therapy in human cancers (review).

International journal of oncology 2012, 41, 1181-1191.

162. Bromberg, J., Stat proteins and oncogenesis. The Journal of clinical investigation 2002, 109, 1139-1142.
163. Xiong, H.; Du, W.; Wang, J.L.; Wang, Y.C.; Tang, J.T.; Hong, J.; Fang, J.Y., Constitutive activation of stat3 is predictive of poor prognosis in human gastric cancer. J Mol Med (Berl) 2012, 90, 1037-1046.
164. Kusaba, T.; Nakayama, T.; Yamazumi, K.; Yakata, Y.; Yoshizaki, A.; Inoue, K.; Nagayasu, T.; Sekine, I., Activation of stat3 is a marker of poor prognosis in human colorectal cancer. Oncology reports 2006, 15, 1445-1451.
165. Huang, X.; Meng, B.; Iqbal, J.; Ding, B.B.; Perry, A.M.; Cao, W.; Smith, L.M.; Bi, C.; Jiang, C.; Greiner, T.C., et al., Activation of the stat3 signaling pathway is associated with poor survival in diffuse large b-cell lymphoma treated with r-chop. Journal of clinical oncology : official journal of the American Society of Clinical Oncology 2013, 31, 4520-4528.
166. Takemoto, S.; Ushijima, K.; Kawano, K.; Yamaguchi, T.; Terada, A.; Fujiyoshi, N.; Nishio, S.; Tsuda, N.; Ijichi, M.; Kakuma, T., et al., Expression of activated signal transducer and activator of transcription-3 predicts poor prognosis in cervical squamous-cell carcinoma. British journal of cancer 2009, 101, 967-972.
167. Schoppmann, S.F.; Jesch, B.; Friedrich, J.; Jomrich, G.; Maroske, F.; Birner, P., Phosphorylation of signal transducer and activator of transcription 3 (stat3) correlates with her-2 status, carbonic anhydrase 9 expression and prognosis in esophageal cancer. Clinical & experimental

metastasis 2012, 29, 615-624.

168. You, Z.; Xu, D.; Ji, J.; Guo, W.; Zhu, W.; He, J., Jak/stat signal pathway activation promotes progression and survival of human oesophageal squamous cell carcinoma. Clinical & translational oncology : official publication of the Federation of Spanish Oncology Societies and of the National Cancer Institute of Mexico 2012, 14, 143-149.
169. Macha, M.A.; Matta, A.; Kaur, J.; Chauhan, S.S.; Thakar, A.; Shukla, N.K.; Gupta, S.D.; Ralhan, R., Prognostic significance of nuclear pstat3 in oral cancer. Head & neck 2011, 33, 482-489.
170. Shah, N.G.; Trivedi, T.I.; Tankshali, R.A.; Goswami, J.V.; Jetly, D.H.; Shukla, S.N.; Shah, P.M.; Verma, R.J., Prognostic significance of molecular markers in oral squamous cell carcinoma: A multivariate analysis. Head & neck 2009, 31, 1544-1556.
171. Li, C.; Wang, Z.; Liu, Y.; Wang, P.; Zhang, R., Stat3 expression correlates with prognosis of thymic epithelial tumors. Journal of cardiothoracic surgery 2013, 8, 92.
172. Auernhammer, C.J.; Bousquet, C.; Melmed, S., Autoregulation of pituitary corticotroph socs-3 expression: Characterization of the murine socs-3 promoter. Proceedings of the National Academy of Sciences of the United States of America 1999, 96, 6964-6969.
173. Yoshimura, A.; Naka, T.; Kubo, M., Socs proteins, cytokine signalling and immune regulation. Nat Rev Immunol 2007, 7, 454-465.
174. Ostman, A.; Hellberg, C.; Bohmer, F.D., Protein-tyrosine phosphatases and cancer. Nature reviews. Cancer 2006, 6, 307-320.
175. Julien, S.G.; Dube, N.; Hardy, S.; Tremblay, M.L., Inside the human

cancer tyrosine phosphatome. Nature reviews. Cancer 2011, 11, 35-49.

176. Anna C. Barry, L.A.O.S.a.A.C.W., Suppressors of cytokine signaling: Functions in normal biology and roles in disease. Landes Bioscience: Austin, TX, USA, 2009.

177. Inagaki-Ohara, K.; Kondo, T.; Ito, M.; Yoshimura, A., Socs, inflammation, and cancer. Jak-Stat 2013, 2, e24053.

178. Weber, A.; Hengge, U.R.; Bardenheuer, W.; Tischoff, I.; Sommerer, F.; Markwarth, A.; Dietz, A.; Wittekind, C.; Tannapfel, A., Socs-3 is frequently methylated in head and neck squamous cell carcinoma and its precursor lesions and causes growth inhibition. Oncogene 2005, 24, 6699-6708.

179. Tischoff, I.; Hengge, U.R.; Vieth, M.; Ell, C.; Stolte, M.; Weber, A.; Schmidt, W.E.; Tannapfel, A., Methylation of socs-3 and socs-1 in the carcinogenesis of barrett's adenocarcinoma. Gut 2007, 56, 1047-1053.

180. Niwa, Y.; Kanda, H.; Shikauchi, Y.; Saiura, A.; Matsubara, K.; Kitagawa, T.; Yamamoto, J.; Kubo, T.; Yoshikawa, H., Methylation silencing of socs-3 promotes cell growth and migration by enhancing jak/stat and fak signalings in human hepatocellular carcinoma. Oncogene 2005, 24, 6406-6417.

181. He, B.; You, L.; Uematsu, K.; Zang, K.; Xu, Z.; Lee, A.Y.; Costello, J.F.; McCormick, F.; Jablons, D.M., Socs-3 is frequently silenced by hypermethylation and suppresses cell growth in human lung cancer. Proceedings of the National Academy of Sciences of the United States of America 2003, 100, 14133-14138.

182. Yoshikawa, H.; Matsubara, K.; Qian, G.S.; Jackson, P.; Groopman, J.D.;

Manning, J.E.; Harris, C.C.; Herman, J.G., Socs-1, a negative regulator of the jak/stat pathway, is silenced by methylation in human hepatocellular carcinoma and shows growth-suppression activity. Nature genetics 2001, 28, 29-35.

183. Galm, O.; Yoshikawa, H.; Esteller, M.; Osieka, R.; Herman, J.G., Socs-1, a negative regulator of cytokine signaling, is frequently silenced by methylation in multiple myeloma. Blood 2003, 101, 2784-2788.
184. Chim, C.S.; Fung, T.K.; Cheung, W.C.; Liang, R.; Kwong, Y.L., Socs1 and shp1 hypermethylation in multiple myeloma: Implications for epigenetic activation of the jak/stat pathway. Blood 2004, 103, 4630-4635.
185. To, K.F.; Chan, M.W.; Leung, W.K.; Ng, E.K.; Yu, J.; Bai, A.H.; Lo, A.W.; Chu, S.H.; Tong, J.H.; Lo, K.W., et al., Constitutional activation of il-6-mediated jak/stat pathway through hypermethylation of socs-1 in human gastric cancer cell line. British journal of cancer 2004, 91, 1335-1341.
186. Alonso, A.; Sasin, J.; Bottini, N.; Friedberg, I.; Osterman, A.; Godzik, A.; Hunter, T.; Dixon, J.; Mustelin, T., Protein tyrosine phosphatases in the human genome. Cell 2004, 117, 699-711.
187. Oka, T.; Ouchida, M.; Koyama, M.; Ogama, Y.; Takada, S.; Nakatani, Y.; Tanaka, T.; Yoshino, T.; Hayashi, K.; Ohara, N., et al., Gene silencing of the tyrosine phosphatase shp1 gene by aberrant methylation in leukemias/lymphomas. Cancer research 2002, 62, 6390-6394.
188. Zhang, Q.; Wang, H.Y.; Marzec, M.; Raghunath, P.N.; Nagasawa, T.; Wasik, M.A., Stat3- and DNA methyltransferase 1-mediated epigenetic silencing of shp-1 tyrosine phosphatase tumor suppressor gene in

malignant t lymphocytes. Proceedings of the National Academy of Sciences of the United States of America 2005, 102, 6948-6953.

189. Zhang, Q.; Raghunath, P.N.; Vonderheid, E.; Odum, N.; Wasik, M.A., Lack of phosphotyrosine phosphatase shp-1 expression in malignant t-cell lymphoma cells results from methylation of the shp-1 promoter. The American journal of pathology 2000, 157, 1137-1146.
190. Brantley, E.C.; Nabors, L.B.; Gillespie, G.Y.; Choi, Y.H.; Palmer, C.A.; Harrison, K.; Roarty, K.; Benveniste, E.N., Loss of protein inhibitors of activated stat-3 expression in glioblastoma multiforme tumors: Implications for stat-3 activation and gene expression. Clinical cancer research : an official journal of the American Association for Cancer Research 2008, 14, 4694-4704.
191. Ogata, Y.; Osaki, T.; Naka, T.; Iwahori, K.; Furukawa, M.; Nagatomo, I.; Kijima, T.; Kumagai, T.; Yoshida, M.; Tachibana, I., et al., Overexpression of pias3 suppresses cell growth and restores the drug sensitivity of human lung cancer cells in association with pi3-k/akt inactivation. Neoplasia 2006, 8, 817-825.
192. Kluge, A.; Dabir, S.; Vlassenbroeck, I.; Eisenberg, R.; Dowlati, A., Protein inhibitor of activated stat3 expression in lung cancer. Molecular oncology 2011, 5, 256-264.
193. Yu, H.; Pardoll, D.; Jove, R., Stats in cancer inflammation and immunity: A leading role for stat3. Nature reviews. Cancer 2009, 9, 798-809.
194. Catlett-Falcone, R.; Landowski, T.H.; Oshiro, M.M.; Turkson, J.; Levitzki, A.; Savino, R.; Ciliberto, G.; Moscinski, L.; Fernandez-Luna, J.L.; Nunez, G., et al., Constitutive activation of stat3 signaling confers resistance to

apoptosis in human u266 myeloma cells. Immunity 1999, 10, 105-115.

195. Shain, K.H.; Yarde, D.N.; Meads, M.B.; Huang, M.; Jove, R.; Hazlehurst, L.A.; Dalton, W.S., Beta1 integrin adhesion enhances il-6-mediated stat3 signaling in myeloma cells: Implications for microenvironment influence on tumor survival and proliferation. Cancer research 2009, 69, 1009-1015.
196. Frame, M.C., Src in cancer: Deregulation and consequences for cell behaviour. Biochimica et biophysica acta 2002, 1602, 114-130.
197. Alvarez, R.H.; Kantarjian, H.M.; Cortes, J.E., The role of src in solid and hematologic malignancies: Development of new-generation src inhibitors. Cancer 2006, 107, 1918-1929.
198. Turkson, J.; Bowman, T.; Garcia, R.; Caldenhoven, E.; De Groot, R.P.; Jove, R., Stat3 activation by src induces specific gene regulation and is required for cell transformation. Molecular and cellular biology 1998, 18, 2545-2552.
199. Morris, S.W.; Kirstein, M.N.; Valentine, M.B.; Dittmer, K.G.; Shapiro, D.N.; Saltman, D.L.; Look, A.T., Fusion of a kinase gene, alk, to a nucleolar protein gene, npm, in non-hodgkin's lymphoma. Science 1994, 263, 1281-1284.
200. Shiota, M.; Fujimoto, J.; Semba, T.; Satoh, H.; Yamamoto, T.; Mori, S., Hyperphosphorylation of a novel 80 kda protein-tyrosine kinase similar to ltk in a human ki-1 lymphoma cell line, ams3. Oncogene 1994, 9, 1567-1574.
201. Chiarle, R.; Simmons, W.J.; Cai, H.; Dhall, G.; Zamo, A.; Raz, R.; Karras, J.G.; Levy, D.E.; Inghirami, G., Stat3 is required for alk-mediated

lymphomagenesis and provides a possible therapeutic target. Nature medicine 2005, 11, 623-629.

202. Zamo, A.; Chiarle, R.; Piva, R.; Howes, J.; Fan, Y.; Chilosi, M.; Levy, D.E.; Inghirami, G., Anaplastic lymphoma kinase (alk) activates stat3 and protects hematopoietic cells from cell death. Oncogene 2002, 21, 1038-1047.
203. Zhang, Q.; Raghunath, P.N.; Xue, L.; Majewski, M.; Carpentieri, D.F.; Odum, N.; Morris, S.; Skorski, T.; Wasik, M.A., Multilevel dysregulation of stat3 activation in anaplastic lymphoma kinase-positive t/null-cell lymphoma. J Immunol 2002, 168, 466-474.
204. Lai, R.; Ingham, R.J., The pathobiology of the oncogenic tyrosine kinase npm-alk: A brief update. Therapeutic advances in hematology 2013, 4, 119-131.
205. Gabler, K.; Behrmann, I.; Haan, C., Jak2 mutants (e.G., jak2v617f) and their importance as drug targets in myeloproliferative neoplasms. Jak-Stat 2013, 2, e25025.
206. Oku, S.; Takenaka, K.; Kuriyama, T.; Shide, K.; Kumano, T.; Kikushige, Y.; Urata, S.; Yamauchi, T.; Iwamoto, C.; Shimoda, H.K., et al., Jak2 v617f uses distinct signalling pathways to induce cell proliferation and neutrophil activation. British journal of haematology 2010, 150, 334-344.
207. Quintas-Cardama, A.; Vaddi, K.; Liu, P.; Manshouri, T.; Li, J.; Scherle, P.A.; Caulder, E.; Wen, X.; Li, Y.; Waeltz, P., et al., Preclinical characterization of the selective jak1/2 inhibitor incb018424: Therapeutic implications for the treatment of myeloproliferative neoplasms. Blood 2010, 115, 3109-3117.

208. Mughal, T.I.; Girnius, S.; Rosen, S.T.; Kumar, S.; Wiestner, A.; Abdel-Wahab, O.; Kiladjian, J.J.; Wilson, W.H.; Van Etten, R.A., Emerging therapeutic paradigms to target the dysregulated janus kinase/signal transducer and activator of transcription pathway in hematological malignancies. Leukemia & lymphoma 2014.

209. Gao, S.P.; Mark, K.G.; Leslie, K.; Pao, W.; Motoi, N.; Gerald, W.L.; Travis, W.D.; Bornmann, W.; Veach, D.; Clarkson, B., et al., Mutations in the egfr kinase domain mediate stat3 activation via il-6 production in human lung adenocarcinomas. The Journal of clinical investigation 2007, 117, 3846-3856.

210. Inda, M.M.; Bonavia, R.; Mukasa, A.; Narita, Y.; Sah, D.W.; Vandenberg, S.; Brennan, C.; Johns, T.G.; Bachoo, R.; Hadwiger, P., et al., Tumor heterogeneity is an active process maintained by a mutant egfr-induced cytokine circuit in glioblastoma. Genes & development 2010, 24, 1731-1745.

211. Iliopoulos, D.; Jaeger, S.A.; Hirsch, H.A.; Bulyk, M.L.; Struhl, K., Stat3 activation of mir-21 and mir-181b-1 via pten and cyld are part of the epigenetic switch linking inflammation to cancer. Molecular cell 2010, 39, 493-506.

212. Lee, H.; Deng, J.; Kujawski, M.; Yang, C.; Liu, Y.; Herrmann, A.; Kortylewski, M.; Horne, D.; Somlo, G.; Forman, S., et al., Stat3-induced s1pr1 expression is crucial for persistent stat3 activation in tumors. Nature medicine 2010, 16, 1421-1428.

213. Deng, J.; Liu, Y.; Lee, H.; Herrmann, A.; Zhang, W.; Zhang, C.; Shen, S.; Priceman, S.J.; Kujawski, M.; Pal, S.K., et al., S1pr1-stat3 signaling is

crucial for myeloid cell colonization at future metastatic sites. Cancer cell 2012, 21, 642-654.

214. Chang, Q.; Bournazou, E.; Sansone, P.; Berishaj, M.; Gao, S.P.; Daly, L.; Wels, J.; Theilen, T.; Granitto, S.; Zhang, X., et al., The il-6/jak/stat3 feed-forward loop drives tumorigenesis and metastasis. Neoplasia 2013, 15, 848-862.

215. Demaria, M.; Poli, V., Pkm2, stat3 and hif-1alpha: The warburg's vicious circle. Jak-Stat 2012, 1, 194-196.

216. Semenova, G.; Chernoff, J., Pkm2 enters the morpheein academy. Molecular cell 2012, 45, 583-584.

217. Christofk, H.R.; Vander Heiden, M.G.; Harris, M.H.; Ramanathan, A.; Gerszten, R.E.; Wei, R.; Fleming, M.D.; Schreiber, S.L.; Cantley, L.C., The m2 splice isoform of pyruvate kinase is important for cancer metabolism and tumour growth. Nature 2008, 452, 230-233.

218. Demaria, M.; Giorgi, C.; Lebiedzinska, M.; Esposito, G.; D'Angeli, L.; Bartoli, A.; Gough, D.J.; Turkson, J.; Levy, D.E.; Watson, C.J., et al., A stat3-mediated metabolic switch is involved in tumour transformation and stat3 addiction. Aging 2010, 2, 823-842.

219. Demaria, M.; Poli, V., From the nucleus to the mitochondria and back: The odyssey of a multitask stat3. Cell Cycle 2011, 10, 3221-3222.

220. Marzec, M.; Liu, X.; Wong, W.; Yang, Y.; Pasha, T.; Kantekure, K.; Zhang, P.; Woetmann, A.; Cheng, M.; Odum, N., et al., Oncogenic kinase npm/alk induces expression of hif1alpha mrna. Oncogene 2011, 30, 1372-1378.

221. Luo, W.; Hu, H.; Chang, R.; Zhong, J.; Knabel, M.; O'Meally, R.; Cole,

R.N.; Pandey, A.; Semenza, G.L., Pyruvate kinase m2 is a phd3-stimulated coactivator for hypoxia-inducible factor 1. Cell 2011, 145, 732-744.

222. Zhang, Y.; Du, X.L.; Wang, C.J.; Lin, D.C.; Ruan, X.; Feng, Y.B.; Huo, Y.Q.; Peng, H.; Cui, J.L.; Zhang, T.T., et al., Reciprocal activation between plk1 and stat3 contributes to survival and proliferation of esophageal cancer cells. Gastroenterology 2012, 142, 521-530 e523.
223. Xiong, H.; Du, W.; Sun, T.T.; Lin, Y.W.; Wang, J.L.; Hong, J.; Fang, J.Y., A positive feedback loop between stat3 and cyclooxygenase-2 gene may contribute to helicobacter pylori-associated human gastric tumorigenesis. International journal of cancer. Journal international du cancer 2013.
224. Pilati, C.; Amessou, M.; Bihl, M.P.; Balabaud, C.; Nhieu, J.T.; Paradis, V.; Nault, J.C.; Izard, T.; Bioulac-Sage, P.; Couchy, G., et al., Somatic mutations activating stat3 in human inflammatory hepatocellular adenomas. The Journal of experimental medicine 2011, 208, 1359-1366.
225. Koskela, H.L.; Eldfors, S.; Ellonen, P.; van Adrichem, A.J.; Kuusanmaki, H.; Andersson, E.I.; Lagstrom, S.; Clemente, M.J.; Olson, T.; Jalkanen, S.E., et al., Somatic stat3 mutations in large granular lymphocytic leukemia. The New England journal of medicine 2012, 366, 1905-1913.
226. Jerez, A.; Clemente, M.J.; Makishima, H.; Koskela, H.; Leblanc, F.; Peng Ng, K.; Olson, T.; Przychodzen, B.; Afable, M.; Gomez-Segui, I., et al., Stat3 mutations unify the pathogenesis of chronic lymphoproliferative disorders of nk cells and t-cell large granular lymphocyte leukemia. Blood 2012, 120, 3048-3057.
227. Ohgami, R.S.; Ma, L.; Merker, J.D.; Martinez, B.; Zehnder, J.L.; Arber,

D.A., Stat3 mutations are frequent in cd30+ t-cell lymphomas and t-cell large granular lymphocytic leukemia. Leukemia 2013, 27, 2244-2247.

228. Fasan, A.; Kern, W.; Grossmann, V.; Haferlach, C.; Haferlach, T.; Schnittger, S., Stat3 mutations are highly specific for large granular lymphocytic leukemia. Leukemia 2013, 27, 1598-1600.

229. Hu, G.; Witzig, T.E.; Gupta, M., A novel missense (m206k) stat3 mutation in diffuse large b cell lymphoma deregulates stat3 signaling. PloS one 2013, 8, e67851.

230. Couronne, L.; Scourzic, L.; Pilati, C.; Della Valle, V.; Duffourd, Y.; Solary, E.; Vainchenker, W.; Merlio, J.P.; Beylot-Barry, M.; Damm, F., et al., Stat3 mutations identified in human hematologic neoplasms induce myeloid malignancies in a mouse bone marrow transplantation model. Haematologica 2013, 98, 1748-1752.

231. Levy, D.E.; Darnell, J.E., Jr., Stats: Transcriptional control and biological impact. Nature reviews. Molecular cell biology 2002, 3, 651-662.

232. Jing, N.; Tweardy, D.J., Targeting stat3 in cancer therapy. Anti-cancer drugs 2005, 16, 601-607.

233. Masuda, M.; Suzui, M.; Yasumatu, R.; Nakashima, T.; Kuratomi, Y.; Azuma, K.; Tomita, K.; Komiyama, S.; Weinstein, I.B., Constitutive activation of signal transducers and activators of transcription 3 correlates with cyclin d1 overexpression and may provide a novel prognostic marker in head and neck squamous cell carcinoma. Cancer research 2002, 62, 3351-3355.

234. Ivanov, V.N.; Bhoumik, A.; Krasilnikov, M.; Raz, R.; Owen-Schaub, L.B.; Levy, D.; Horvath, C.M.; Ronai, Z., Cooperation between stat3 and c-jun

suppresses fas transcription. Molecular cell 2001, 7, 517-528.

235. Ivanov, V.N.; Krasilnikov, M.; Ronai, Z., Regulation of fas expression by stat3 and c-jun is mediated by phosphatidylinositol 3-kinase-akt signaling. The Journal of biological chemistry 2002, 277, 4932-4944.

236. Kunigal, S.; Lakka, S.S.; Sodadasu, P.K.; Estes, N.; Rao, J.S., Stat3-sirna induces fas-mediated apoptosis in vitro and in vivo in breast cancer. International journal of oncology 2009, 34, 1209-1220.

237. Niu, G.; Wright, K.L.; Ma, Y.; Wright, G.M.; Huang, M.; Irby, R.; Briggs, J.; Karras, J.; Cress, W.D.; Pardoll, D., et al., Role of stat3 in regulating p53 expression and function. Molecular and cellular biology 2005, 25, 7432-7440.

238. Wei, L.H.; Kuo, M.L.; Chen, C.A.; Chou, C.H.; Lai, K.B.; Lee, C.N.; Hsieh, C.Y., Interleukin-6 promotes cervical tumor growth by vegf-dependent angiogenesis via a stat3 pathway. Oncogene 2003, 22, 1517-1527.

239. Wei, D.; Le, X.; Zheng, L.; Wang, L.; Frey, J.A.; Gao, A.C.; Peng, Z.; Huang, S.; Xiong, H.Q.; Abbruzzese, J.L., et al., Stat3 activation regulates the expression of vascular endothelial growth factor and human pancreatic cancer angiogenesis and metastasis. Oncogene 2003, 22, 319-329.

240. Niu, G.; Wright, K.L.; Huang, M.; Song, L.; Haura, E.; Turkson, J.; Zhang, S.; Wang, T.; Sinibaldi, D.; Coppola, D., et al., Constitutive stat3 activity up-regulates vegf expression and tumor angiogenesis. Oncogene 2002, 21, 2000-2008.

241. Xu, Q.; Briggs, J.; Park, S.; Niu, G.; Kortylewski, M.; Zhang, S.; Gritsko, T.; Turkson, J.; Kay, H.; Semenza, G.L., et al., Targeting stat3 blocks

both hif-1 and vegf expression induced by multiple oncogenic growth signaling pathways. Oncogene 2005, 24, 5552-5560.

242. Kujawski, M.; Kortylewski, M.; Lee, H.; Herrmann, A.; Kay, H.; Yu, H., Stat3 mediates myeloid cell-dependent tumor angiogenesis in mice. The Journal of clinical investigation 2008, 118, 3367-3377.

243. Jung, J.E.; Kim, H.S.; Lee, C.S, et al. Caffeic acid and its synthetic derivative cadpe suppress tumor angiogenesis by blocking stat3-mediated vegf expression in human renal carcinoma cells. Carcinogenesis 2007, 28, 1780-1787.

244. Yahata, Y.; Shirakata, Y.; Tokumaru, S, et al. Nuclear translocation of phosphorylated stat3 is essential for vascular endothelial growth factor-induced human dermal microvascular endothelial cell migration and tube formation. The Journal of biological chemistry 2003, 278, 40026-40031.

245. Bartoli, M.; Platt, D.; Lemtalsi, T.; Gu, X.; Brooks, S.E.; Marrero, M.B.; Caldwell, R.B., Vegf differentially activates stat3 in microvascular endothelial cells. FASEB journal : official publication of the Federation of American Societies for Experimental Biology 2003, 17, 1562-1564.

246. Yadav, A.; Kumar, B.; Datta, J.; Teknos, T.N.; Kumar, P., Il-6 promotes head and neck tumor metastasis by inducing epithelial-mesenchymal transition via the jak-stat3-snail signaling pathway. Molecular cancer research : MCR 2011, 9, 1658-1667.

247. Lo, H.W.; Hsu, S.C.; Xia, W, et al. Epidermal growth factor receptor cooperates with signal transducer and activator of transcription 3 to induce epithelial-mesenchymal transition in cancer cells via up-regulation of twist gene expression. Cancer research 2007, 67, 9066-9076.

248. Guo, L.; Chen, C.; Shi, M, et al. Stat3-coordinated lin-28-let-7-hmga2 and mir-200-zeb1 circuits initiate and maintain oncostatin m-driven epithelial-mesenchymal transition. Oncogene 2013, 32, 5272-5282.

249. Xiong, H.; Hong, J.; Du, W, et al., Roles of stat3 and zeb1 proteins in e-cadherin down-regulation and human colorectal cancer epithelial-mesenchymal transition. The Journal of biological chemistry 2012, 287, 5819-5832.

250. Itoh, M.; Murata, T.; Suzuki, T.; Shindoh, M.; Nakajima, K.; Imai, K.; Yoshida, K., Requirement of stat3 activation for maximal collagenase-1 (mmp-1) induction by epidermal growth factor and malignant characteristics in t24 bladder cancer cells. Oncogene 2006, 25, 1195-1204.

251. Song, Y.; Qian, L.; Song, S, et al., Fra-1 and stat3 synergistically regulate activation of human mmp-9 gene. Molecular immunology 2008, 45, 137-143.

252. Tsareva, S.A.; Moriggl, R.; Corvinus, F.M.; Wiederanders, B.; Schutz, A.; Kovacic, B.; Friedrich, K., Signal transducer and activator of transcription 3 activation promotes invasive growth of colon carcinomas through matrix metalloproteinase induction. Neoplasia 2007, 9, 279-291.

253. Xie, T.X.; Wei, D.; Liu, M, et al. Stat3 activation regulates the expression of matrix metalloproteinase-2 and tumor invasion and metastasis. Oncogene 2004, 23, 3550-3560.

254. Fukuda, A.; Wang, S.C.; Morris, J.P.t, et al. Stat3 and mmp7 contribute to pancreatic ductal adenocarcinoma initiation and progression. Cancer cell 2011, 19, 441-455.

255. Li, H.; Huang, C.; Huang, K.; Wu, W.; Jiang, T.; Cao, J.; Feng, Z.; Qiu, Z., Stat3 knockdown reduces pancreatic cancer cell invasiveness and matrix metalloproteinase-7 expression in nude mice. PloS one 2011, 6, e25941.

256. Barbieri, I.; Pensa, S.; Pannellini, T, et al. Constitutively active stat3 enhances neu-mediated migration and metastasis in mammary tumors via upregulation of cten. Cancer research 2010, 70, 2558-2567.

257. McLean, G.W.; Carragher, N.O.; Avizienyte, E.; Evans, J.; Brunton, V.G.; Frame, M.C., The role of focal-adhesion kinase in cancer - a new therapeutic opportunity. Nature reviews. Cancer 2005, 5, 505-515.

258. Nagano, M.; Hoshino, D.; Koshikawa, N.; Akizawa, T.; Seiki, M., Turnover of focal adhesions and cancer cell migration. International journal of cell biology 2012, 2012, 310616.

259. Niu, G.; Heller, R.; Catlett-Falcone, R, et al. Gene therapy with dominant-negative stat3 suppresses growth of the murine melanoma b16 tumor in vivo. Cancer research 1999, 59, 5059-5063.

260. Sun, Z.; Yao, Z.; Liu, S.; Tang, H.; Yan, X., An oligonucleotide decoy for stat3 activates the immune response of macrophages to breast cancer. Immunobiology 2006, 211, 199-209.

261. Takeda, K.; Clausen, B.E.; Kaisho, T.; Tsujimura, T.; Terada, N.; Forster, I.; Akira, S., Enhanced th1 activity and development of chronic enterocolitis in mice devoid of stat3 in macrophages and neutrophils. Immunity 1999, 10, 39-49.

262. Lee H, Zhang P, Herrmann A, et al. Acetylated stat3 is crucial for methylation of tumor-suppressor gene promoters and inhibition by resveratrol results in demethylation. Proceedings of the National

Academy of Sciences of the USA 2012, 109, 7765-7769.

263. Yuan, Z.L.; Guan, Y.J.; Chatterjee, D.; Chin, Y.E., Stat3 dimerization regulated by reversible acetylation of a single lysine residue. Science 2005, 307, 269-273.

264. Lee, J.L.; Wang, M.J.; Chen, J.Y., Acetylation and activation of stat3 mediated by nuclear translocation of cd44. The Journal of cell biology 2009, 185, 949-957.

265. Liu, L.; McBride, K.M.; Reich, N.C., Stat3 nuclear import is independent of tyrosine phosphorylation and mediated by importin-alpha3. Proceedings of the National Academy of Sciences of the United States of America 2005, 102, 8150-8155.

266. Yang, J.; Chatterjee-Kishore, M.; Staugaitis, S.M, et al. Novel roles of unphosphorylated stat3 in oncogenesis and transcriptional regulation. Cancer research 2005, 65, 939-947.

267. Yang, J.; Liao, X.; Agarwal, M.K.; Barnes, L.; Auron, P.E.; Stark, G.R., Unphosphorylated stat3 accumulates in response to il-6 and activates transcription by binding to nfkappab. Genes & development 2007, 21, 1396-1408.

268. Hazan-Halevy, I.; Harris, D.; Liu, Z, et al. Stat3 is constitutively phosphorylated on serine 727 residues, binds DNA, and activates transcription in cll cells. Blood 2010, 115, 2852-2863.

269. Qin, H.R.; Kim, H.J.; Kim, J.Y, et al. Activation of signal transducer and activator of transcription 3 through a phosphomimetic serine 727 promotes prostate tumorigenesis independent of tyrosine 705 phosphorylation. Cancer research 2008, 68, 7736-7741.

270. Timofeeva, O.A.; Tarasova, N.I.; Zhang, X, et al. Stat3 suppresses transcription of proapoptotic genes in cancer cells with the involvement of its n-terminal domain. Proceedings of the National Academy of Sciences of the United States of America 2013, 110, 1267-1272.

271. Timofeeva, O.A.; Chasovskikh, S.; Lonskaya, I, et al. Mechanisms of unphosphorylated stat3 transcription factor binding to DNA. The Journal of biological chemistry 2012, 287, 14192-14200.

272. Gough, D.J.; Corlett, A.; Schlessinger, K.; Wegrzyn, J.; Larner, A.C.; Levy, D.E., Mitochondrial stat3 supports ras-dependent oncogenic transformation. Science 2009, 324, 1713-1716.

273. Wegrzyn, J.; Potla, R.; Chwae, Y.J.; Sepuri, N.B.; Zhang, Q.; Koeck, T.; Derecka, M.; Szczepanek, K.; Szelag, M.; Gornicka, A., et al., Function of mitochondrial stat3 in cellular respiration. Science 2009, 323, 793-797.

274. Zhang, Q.; Raje, V.; Yakovlev, V.A, et al. Mitochondrial localized stat3 promotes breast cancer growth via phosphorylation of serine 727. The Journal of biological chemistry 2013, 288, 31280-31288.

275. Badgwell, D.B.; Lu, Z.; Le, K, et al., The tumor-suppressor gene arhi (diras3) suppresses ovarian cancer cell migration through inhibition of the stat3 and fak/rho signaling pathways. Oncogene 2012, 31, 68-79.

276. Silver, D.L.; Naora, H.; Liu, J.; Cheng, W.; Montell, D.J., Activated signal transducer and activator of transcription (stat) 3: Localization in focal adhesions and function in ovarian cancer cell motility. Cancer research 2004, 64, 3550-3558.

277. Abdulghani, J.; Gu, L.; Dagvadorj, A, et al. Stat3 promotes metastatic progression of prostate cancer. The American journal of pathology 2008,

172, 1717-1728.

278. Gu, L.; Dagvadorj, A.; Lutz, J, et al., Transcription factor stat3 stimulates metastatic behavior of human prostate cancer cells in vivo, whereas stat5b has a preferential role in the promotion of prostate cancer cell viability and tumor growth. The American journal of pathology 2010, 176, 1959-1972.
279. Wei, Z.; Jiang, X.; Qiao, H, et al. Stat3 interacts with skp2/p27/p21 pathway to regulate the motility and invasion of gastric cancer cells. Cellular signalling 2013, 25, 931-938.
280. Ng, D.C.; Lin, B.H.; Lim, C.P, et al. Stat3 regulates microtubules by antagonizing the depolymerization activity of stathmin. The Journal of cell biology 2006, 172, 245-257.
281. Verma, N.K.; Dourlat, J.; Davies, A.M, et al. Stat3-stathmin interactions control microtubule dynamics in migrating t-cells. The Journal of biological chemistry 2009, 284, 12349-12362.
282. de la Iglesia, N.; Konopka, G.; Puram, S.V, et al. Identification of a pten-regulated stat3 brain tumor suppressor pathway. Genes & development 2008, 22, 449-462.
283. Schneller, D.; Machat, G.; Sousek, A, et al. P19(arf) /p14(arf) controls oncogenic functions of signal transducer and activator of transcription 3 in hepatocellular carcinoma. Hepatology 2011, 54, 164-172.
284. Musteanu, M.; Blaas, L.; Mair, M, et al. Stat3 is a negative regulator of intestinal tumor progression in apc(min) mice. Gastroenterology 2010, 138, 1003-1011 e1001-1005.
285. Wang, H.; Lafdil, F.; Wang, L, et al. Hepatoprotective versus oncogenic

functions of stat3 in liver tumorigenesis. The American journal of pathology 2011, 179, 714-724.

286. Verna, L.; Whysner, J.; Williams, G.M., N-nitrosodiethylamine mechanistic data and risk assessment: Bioactivation, DNA-adduct formation, mutagenicity, and tumor initiation. Pharmacology & therapeutics 1996, 71, 57-81.

287. Couto, J.P.; Daly, L.; Almeida, A, et al., Stat3 negatively regulates thyroid tumorigenesis. Proceedings of the National Academy of Sciences of the United States of America 2012, 109, E2361-2370.

288. Ecker, A.; Simma, O.; Hoelbl, A.; Kenner, L.; Beug, H.; Moriggl, R.; Sexl, V., The dark and the bright side of stat3: Proto-oncogene and tumor-suppressor. Front Biosci (Landmark Ed) 2009, 14, 2944-2958.

289. Kan, C.E.; Cipriano, R.; Jackson, M.W., C-myc functions as a molecular switch to alter the response of human mammary epithelial cells to oncostatin m. Cancer research 2011, 71, 6930-6939.

290. Lee, J.; Kim, J.C.; Lee, S.E, et al. Signal transducer and activator of transcription 3 (stat3) protein suppresses adenoma-to-carcinoma transition in apcmin/+ mice via regulation of snail-1 (snai) protein stability. The Journal of biological chemistry 2012, 287, 18182-18189.

291. Pectasides, E.; Egloff, A.M.; Sasaki, C, et al., Nuclear localization of signal transducer and activator of transcription 3 in head and neck squamous cell carcinoma is associated with a better prognosis. Clinical cancer research : an official journal of the American Association for Cancer Research 2010, 16, 2427-2434.

292. Ettl, T.; Stiegler, C.; Zeitler, K, et al. Egfr, her2, survivin, and loss of

pstat3 characterize high-grade malignancy in salivary gland cancer with impact on prognosis. Human pathology 2012, 43, 921-931.

293. Dolled-Filhart, M.; Camp, R.L.; Kowalski, D.P, et al. Tissue microarray analysis of signal transducers and activators of transcription 3 (stat3) and phospho-stat3 (Y705) in node-negative breast cancer shows nuclear localization is associated with a better prognosis. Clinical cancer research : an official journal of the American Association for Cancer Research 2003, 9, 594-600.
294. Sato, T.; Neilson, L.M.; Peck, A.R, et al. Signal transducer and activator of transcription-3 and breast cancer prognosis. American journal of cancer research 2011, 1, 347-355.
295. Lai, S.Y.; Johnson, F.M., Defining the role of the jak-stat pathway in head and neck and thoracic malignancies: Implications for future therapeutic approaches. Drug resistance updates : reviews and commentaries in antimicrobial and anticancer chemotherapy 2010, 13, 67-78.
296. Leeman, R.J.; Lui, V.W.; Grandis, J.R., Stat3 as a therapeutic target in head and neck cancer. Expert opinion on biological therapy 2006, 6, 231-241.
297. Song, J.I.; Grandis, J.R., Stat signaling in head and neck cancer. Oncogene 2000, 19, 2489-2495.
298. Gritsko, T.; Williams, A.; Turkson, J, et al., Persistent activation of stat3 signaling induces survivin gene expression and confers resistance to apoptosis in human breast cancer cells. Clinical cancer research : an official journal of the American Association for Cancer Research 2006, 12, 11-19.

299. Caldenhoven, E.; van Dijk, T.B.; Solari, R, et al. Stat3beta, a splice variant of transcription factor stat3, is a dominant negative regulator of transcription. The Journal of biological chemistry 1996, 271, 13221-13227.

300. Schaefer, T.S.; Sanders, L.K.; Nathans, D., Cooperative transcriptional activity of jun and stat3 beta, a short form of stat3. Proceedings of the National Academy of Sciences of the United States of America 1995, 92, 9097-9101.

301. Yoo, J.Y.; Huso, D.L.; Nathans, D.; Desiderio, S., Specific ablation of stat3beta distorts the pattern of stat3-responsive gene expression and impairs recovery from endotoxic shock. Cell 2002, 108, 331-344.

302. Biethahn, S.; Alves, F.; Wilde, S.; Hiddemann, W.; Spiekermann, K., Expression of granulocyte colony-stimulating factor- and granulocyte-macrophage colony-stimulating factor-associated signal transduction proteins of the jak/stat pathway in normal granulopoiesis and in blast cells of acute myelogenous leukemia. Experimental hematology 1999, 27, 885-894.

303. Chakraborty, A.; White, S.M.; Schaefer, T.S.; Ball, E.D.; Dyer, K.F.; Tweardy, D.J., Granulocyte colony-stimulating factor activation of stat3 alpha and stat3 beta in immature normal and leukemic human myeloid cells. Blood 1996, 88, 2442-2449.

304. Hevehan, D.L.; Miller, W.M.; Papoutsakis, E.T., Differential expression and phosphorylation of distinct stat3 proteins during granulocytic differentiation. Blood 2002, 99, 1627-1637.

305. Huang, Y.; Qiu, J.; Dong, S, et al. Stat3 isoforms, alpha and beta,

demonstrate distinct intracellular dynamics with prolonged nuclear retention of stat3beta mapping to its unique c-terminal end. The Journal of biological chemistry 2007, 282, 34958-34967.

306. Ng, I.H.; Ng, D.C.; Jans, D.A.; Bogoyevitch, M.A., Selective stat3-alpha or -beta expression reveals spliceform-specific phosphorylation kinetics, nuclear retention and distinct gene expression outcomes. The Biochemical journal 2012, 447, 125-136.
307. Schaefer, T.S.; Sanders, L.K.; Park, O.K.; Nathans, D., Functional differences between stat3alpha and stat3beta. Molecular and cellular biology 1997, 17, 5307-5316.
308. Park, O.K.; Schaefer, L.K.; Wang, W.; Schaefer, T.S., Dimer stability as a determinant of differential DNA binding activity of stat3 isoforms. The Journal of biological chemistry 2000, 275, 32244-32249.
309. Epling-Burnette, P.K.; Liu, J.H.; Catlett-Falcone, R.; et al., Inhibition of stat3 signaling leads to apoptosis of leukemic large granular lymphocytes and decreased mcl-1 expression. The Journal of clinical investigation 2001, 107, 351-362.
310. Karni, R.; Jove, R.; Levitzki, A., Inhibition of pp60c-src reduces bcl-xl expression and reverses the transformed phenotype of cells overexpressing egf and her-2 receptors. Oncogene 1999, 18, 4654-4662.
311. Sinibaldi, D.; Wharton, W.; Turkson, J, et al. Induction of p21waf1/cip1 and cyclin d1 expression by the src oncoprotein in mouse fibroblasts: Role of activated stat3 signaling. Oncogene 2000, 19, 5419-5427.
312. Niu, G.; Shain, K.H.; Huang, M, et al. Overexpression of a dominant-negative signal transducer and activator of transcription 3 variant in

tumor cells leads to production of soluble factors that induce apoptosis and cell cycle arrest. Cancer research 2001, 61, 3276-3280.

313. Xu, G.; Zhang, C.; Zhang, J., Dominant negative stat3 suppresses the growth and invasion capability of human lung cancer cells. Molecular medicine reports 2009, 2, 819-824.

314. Alonzi, T.; Maritano, D.; Gorgoni, B, et al. Essential role of stat3 in the control of the acute-phase response as revealed by inducible gene inactivation [correction of activation] in the liver. Molecular and cellular biology 2001, 21, 1621-1632.

315. Maritano, D.; Sugrue, M.L.; Tininini, S, et al. The stat3 isoforms alpha and beta have unique and specific functions. Nature immunology 2004, 5, 401-409.

316. Zammarchi, F.; de Stanchina, E.; Bournazou, E, et al. Antitumorigenic potential of stat3 alternative splicing modulation. Proceedings of the National Academy of Sciences of the United States of America 2011, 108, 17779-17784.

317. Ivanov, V.N.; Zhou, H.; Partridge, M.A.; Hei, T.K., Inhibition of ataxia telangiectasia mutated kinase activity enhances trail-mediated apoptosis in human melanoma cells. Cancer research 2009, 69, 3510-3519.

318. Reya T, Morrison SJ, Clarke MF, et al. Stem cells, cancer, and cancer stem cells. Nature 2001;414(6859):105-11.

319. Kreso A, van Galen P, Pedley NM, et al. Self-renewal as a therapeutic target in human colorectal cancer. Nat Med 2014;20(1):29-36.

320. Gupta PB, Chaffer CL, Weinberg RA. Cancer stem cells: mirage or reality? Nat Med 2009;15(9):1010-2.

321. Bonnet D, Dick JE. Human acute myeloid leukemia is organized as a hierarchy that originates from a primitive hematopoietic cell. Nat Med 1997;3(7):730-7.

322. Ailles LE, Weissman IL. Cancer stem cells in solid tumors. Curr Opin Biotechnol 2007;18(5):460-6.

323. Al-Hajj M, Wicha MS, Benito-Hernandez A, et al. Prospective identification of tumorigenic breast cancer cells. Proc Natl Acad Sci U S A 2003;100(7):3983-8.

324. Singh SK, Hawkins C, Clarke ID, et al. Identification of human brain tumour initiating cells. Nature 2004;432(7015):396-401.

325. O'Brien CA, Pollett A, Gallinger S, et al. A human colon cancer cell capable of initiating tumour growth in immunodeficient mice. Nature 2007;445(7123):106-10.

326. Golebiewska A, Brons NH, Bjerkvig R, et al. Critical appraisal of the side population assay in stem cell and cancer stem cell research. Cell Stem Cell 2011;8(2):136-47.

327. Dontu G, Abdallah WM, Foley JM, et al. In vitro propagation and transcriptional profiling of human mammary stem/progenitor cells. Genes Dev 2003;17(10):1253-70.

328. Ponti D, Costa A, Zaffaroni N, et al. Isolation and in vitro propagation of tumorigenic breast cancer cells with stem/progenitor cell properties. Cancer Res 2005;65(13):5506-11.

329. Ben-Porath I, Thomson MW, Carey VJ, et al. An embryonic stem cell-like gene expression signature in poorly differentiated aggressive human tumors. Nat Genet 2008;40(5):499-507.

330. van Vlerken LE, Kiefer CM, Morehouse C, et al. EZH2 is required for breast and pancreatic cancer stem cell maintenance and can be used as a functional cancer stem cell reporter. Stem Cells Transl Med 2013;2(1):43-52.

331. Liu S, Dontu G, Mantle ID, et al. Hedgehog signaling and Bmi-1 regulate self-renewal of normal and malignant human mammary stem cells. Cancer Res 2006;66(12):6063-71.

332. Prince ME, Sivanandan R, Kaczorowski A, et al. Identification of a subpopulation of cells with cancer stem cell properties in head and neck squamous cell carcinoma. Proc Natl Acad Sci U S A 2007;104(3):973-8.

333. Lessard J, Sauvageau G. Bmi-1 determines the proliferative capacity of normal and leukaemic stem cells. Nature 2003;423(6937):255-60.

334. Boumahdi S, Driessens G2, Lapouge G2, et al. SOX2 controls tumour initiation and cancer stem-cell functions in squamous-cell carcinoma. Nature 2014;511(7508):246-50.

335. Wong DJ, Liu H, Ridky TW, et al. Module map of stem cell genes guides creation of epithelial cancer stem cells. Cell Stem Cell 2008;2(4):333-44.

336. Karamboulas C, Ailles L. Developmental signaling pathways in cancer stem cells of solid tumors. Biochim Biophys Acta 2013;1830(2):2481-95.

337. Harrison H, Farnie G, Howell SJ, et al. Regulation of breast cancer stem cell activity by signaling through the Notch4 receptor. Cancer Res 2010;70(2):709-18.

338. Raouf A, Zhao Y, To K, et al. Transcriptome analysis of the normal human mammary cell commitment and differentiation process. Cell Stem Cell 2008;3(1):109-18.

339. Ulasov IV, Nandi S, Dey M, et al. Inhibition of Sonic hedgehog and Notch pathways enhances sensitivity of CD133(+) glioma stem cells to temozolomide therapy. Mol Med 2011;17(1-2):103-12.
340. Fan X, Khaki L, Zhu TS, et al. NOTCH pathway blockade depletes CD133-positive glioblastoma cells and inhibits growth of tumor neurospheres and xenografts. Stem Cells 2010;28(1):5-16.
341. Vermeulen L, De Sousa E Melo F, van der Heijden M, et al. Wnt activity defines colon cancer stem cells and is regulated by the microenvironment. Nat Cell Biol 2010;12(5):468-76.
342. Jang GB, Hong IS, Kim RJ, et al. Wnt/β-Catenin Small-Molecule Inhibitor CWP232228 Preferentially Inhibits the Growth of Breast Cancer Stem-like Cells. Cancer Res 2015;75(8):1691-702.
343. Tanaka H, Nakamura M, Kameda C, et al. The Hedgehog signaling pathway plays an essential role in maintaining the CD44+CD24-/low subpopulation and the side population of breast cancer cells. Anticancer Res 2009;29(6):2147-57.
344. Fiaschi M, Rozell B, Bergström A, et al. Development of mammary tumors by conditional expression of GLI1. Cancer Res 2009;69(11):4810-7.
345. Clement V, Sanchez P, de Tribolet N, et al. HEDGEHOG-GLI1 signaling regulates human glioma growth, cancer stem cell self-renewal, and tumorigenicity. Curr Biol 2007;17(2):165-72.
346. Ray PD, Huang BW, Tsuji Y. Reactive oxygen species (ROS) homeostasis and redox regulation in cellular signaling. Cell Signal 2012;24(5):981-90.

347. Klaunig JE, Kamendulis LM, Hocevar BA. Oxidative stress and oxidative damage in carcinogenesis. Toxicol Pathol 2010;38(1):96-109.

348. Diehn M, Cho RW, Lobo NA, et al. Association of reactive oxygen species levels and radioresistance in cancer stem cells. Nature 2009;458(7239):780-3.

349. Ishimoto T, Nagano O, Yae T, et al. CD44 variant regulates redox status in cancer cells by stabilizing the xCT subunit of system xc(-) and thereby promotes tumor growth. Cancer Cell 2011;19(3):387-400.

350. Ito K, Hirao A, Arai F, et al. Reactive oxygen species act through p38 MAPK to limit the lifespan of hematopoietic stem cells. Nat Med 2006;12(4):446-51.

351. DeNicola GM, Karreth FA, Humpton TJ, et al. Oncogene-induced Nrf2 transcription promotes ROS detoxification and tumorigenesis. Nature 2011;475(7354):106-9.

352. Le Belle JE, Orozco NM, Paucar AA, et al. Proliferative neural stem cells have high endogenous ROS levels that regulate self-renewal and neurogenesis in a PI3K/Akt-dependant manner. Cell Stem Cell 2011;8(1):59-71.

353. Wu BL, Xu LY, Du ZP, Liao LD, Zhang HF, Huang Q, et al. MiRNA profile in esophageal squamous cell carcinoma: downregulation of miR-143 and miR-145. World J Gastroenterol 2011;17:79-88.

354. Zhang HF, Lai R. STAT3 in Cancer-Friend or Foe? Cancers (Basel). 2014;6:1408-1440.

355. Abdullah LN, Chow EK. Mechanisms of chemoresistance in cancer stem cells. Clin Transl Med 2013;2(1):3.

356. Wu F, Zhang J, Wang P, et al. Identification of two novel phenotypically distinct breast cancer cell subsets based on Sox2 transcription activity. Cell Signal 2012;24(11):1989-98.

357. Jung K, Gupta N, Wang P, et al. Triple negative breast cancers comprise a highly tumorigenic cell subpopulation detectable by its high responsiveness to a Sox2 regulatory region 2 (SRR2) reporter. Oncotarget 2015;6(12):10366-73.

358. Liu K, Jiang M, Lu Y, et al. Sox2 cooperates with inflammation-mediated Stat3 activation in the malignant transformation of foregut basal progenitor cells. Cell Stem Cell 2013;12(3):304-15.

359. Okumura T, Shimada Y, Imamura M, et al. Neurotrophin receptor p75(NTR) characterizes human esophageal keratinocyte stem cells in vitro. Oncogene 2003;22(26):4017-26.

360. Zhao JS, Li WJ, Ge D, Zhang PJ, Li JJ, Lu CL, et al. Tumor initiating cells in esophageal squamous cell carcinomas express high levels of CD44. PLoS One 2011;6:e21419.

361. Tang KH, Dai YD, Tong M, et al. A CD90(+) tumor-initiating cell population with an aggressive signature and metastatic capacity in esophageal cancer. Cancer Res 2013;73(7):2322-32.

362. Almanaa TN, Geusz ME, Jamasbi RJ. A new method for identifying stem-like cells in esophageal cancer cell lines. J Cancer 2013;4(7):536-48.

363. Yang L, Ren Y, Yu X, et al. ALDH1A1 defines invasive cancer stem-like cells and predicts poor prognosis in patients with esophageal squamous cell carcinoma. Mod Pathol 2014;27(5):775-83.

364. Huang D, Gao Q, Guo L, et al. Isolation and identification of cancer stem-like cells in esophageal carcinoma cell lines. Stem Cells Dev. 2009;18(3):465-73.

365. Li H, Gao Q, Guo L, et al. The PTEN/PI3K/Akt pathway regulates stem-like cells in primary esophageal carcinoma cells. Cancer Biol Ther 2011;11(11):950-8.

Chapter 2

miR-200b suppresses invasiveness and modulates the cytoskeletal and adhesive machinery in esophageal squamous cell carcinoma cells via targeting Kindlin-2

This chapter has been modified from the following publications:

1. Zhang HF, Zhang K, Liao LD, Li LY, Du ZP, Wu BL, Wu JY, Xu XE, Zeng FM, Chen B, Cao HH, Zhu MX, Dai LH, Long L, Wu ZY, Lai R, Xu LY, Li EM. miR-200b suppresses invasiveness and modulates the cytoskeletal and adhesive machinery in esophageal squamous cell carcinoma cells via targeting Kindlin-2. *Carcinogenesis* 2014; 35:292–301.

2. **Zhang HF**, Alshareef A, Wu CS, Li S, Jiao JW, Cao HH, Lai R, Xu LY, Li EM. Loss of miR-200b promotes invasion via activating the Kindlin-2/Integrin β1/AKT pathway in esophageal squamous cell carcinoma: an E-cadherin-independent mechanism. Oncotarget. 2015 Aug 20. [Epub ahead of print].

For the first publication, Zhang HF is the first author of the paper and performed all the experiments described herein except for the following: Zhang K and Li LY performed mass spectrometry shown in Figure 2.3 and Table 2.5. Liao LD performed real-time PCR to assess the expression of miR-200 in patient samples shown in Figure 2.1B. Du ZP, Wu BL helped with the preliminary optimization of the micoRNA transfection protocol. Wu JY, Xu XE, Chen B, Cao HH, Zhu MX and Wu ZY performed the surgical resection and

process of patient samples, as well as patient follow up. Zeng FM helped with the preparation of certain confocal microscopy slides (no data acquisition). Dai LH and Long L performed site-directed mutagenesis of the pGL3-Kindlin-2 reporter and the luciferase analysis shown in Figure 2D. Li EM, Xu LY and Lai R supervised the whole project.

For the second publication, Zhang HF is the first author of the paper and performed all the experiments described herein except for the following: Alshareef A prepared the 5-aza-dC reagent and helped perform the experiment shown in Figure 2.12F, and he also provided critical help in the preperation of the manuscript. Wu CS prepared the LY294002 reagent and helped performed the experiment shown in Figure 2.12B. Cao HH performed the E-cadherin immunohistochemistry shown in Figure 2.12A. Li S performed the experiment shown in Figure 2.12C. Jiao JW performed the analysis shown in Figure 2.14A and B. Li EM, Xu LY and Lai R supervised the whole project.

2.1 Abstract

To further our understanding of the pathobiology of ESCC, we previously performed miRNA profiling that revealed downregulation of miR-200b in ESCC. Using quantitative qRT-PCR applied to 88 patient samples, we confirmed that ESCC tumors expressed significantly lower levels of miR-200b compared to the respective adjacent benign tissues, and downregulation of miR-200b significantly correlated with shortened survival, lymph node metastasis and advanced clinical stage. Quantitative mass spectrometry identified 57 putative miR-200b targets, including Kindlin-2, previously implicated in the regulation of tumor invasiveness and actin cytoskeleton in other cell types. Furthermore, transfection of miR-200b mimic or knockdown of Kindlin-2 in ESCC cells decreased cell protrusion and focal adhesion formation, reduced cell spreading and invasiveness/migration. Enforced expression of Kindlin-2 largely abrogated the inhibitory effects of miR-200b on ESCC cell invasiveness. Mechanistic studies revealed that Rho-family GTPases and focal adhesion kinase mediated the biological effects of the miR-200b—Kindlin-2 axis in ESCC cells. Lastly, we revealed that the Kindlin-2-Integrin β1-AKT axis also mediated the invasiveness suppressive function of miR-200b in ESCC. To conclude, loss of miR-200b, a frequent biochemical defect in ESCC, correlates with aggressive clinical features. The tumor suppressor effects of miR-200b may be due to its suppression of Kindlin-2, a novel target of miR-200b that modulates actin cytoskeleton, focal adhesion formation and the migratory/invasiveness properties of ESCC.

2.2 Introduction

Esophageal cancer represents the sixth leading cause of cancer deaths and the eighth most common type of cancer worldwide (1,2). Despite the use of multimodal treatments such as radical surgery, chemotherapy, and radiotherapy, the 5-year overall survival rate of patients with ESCC remains less than 14% (2-4). A poor survival rate in ESCC patients is highly associated with a frequent local invasion and distant metastasis, and more than 50 percent of patients have either unresectable cancer or radiographically visible metastases at diagnosis (2,5). However, our understanding of the molecular mechanisms that regulate local invasiveness and metastatic potential of ESCC remain incomplete. To improve the overall outcome for patients with ESCC, it is important to understand the molecular mechanisms underlying these processes, thereby useful biomarkers and novel therapeutic targets can be discovered.

Over the past few years, miRNAs have been recognized as critical regulators of cancer invasion and metastasis, either as promoters or as suppressors (6-8). Deregulation of miRNAs in cancer may result in aberrant expression of proteins that regulate cancer cell invasiveness, such as cytoskeletal regulatory proteins, cell adhesion molecules or proteins regulating epithelial-to-mesenchymal transition (9). Recently, the miR-200 family was identified as potent suppressors of epithelial-to-mesenchymal transition by directly targeting the E-cadherin transcriptional repressors ZEB1 and ZEB2, thereby suppressing tumor invasion and/or metastasis (10-14). The miR-200 family is

comprised of 5 members that are encoded within two clusters: the miR-200b-200a-429 cluster (miR-200b cluster) located on chr1p36 and the miR-200c-141 cluster located on chr12p13. Our previous investigation using miRNA profiling has revealed that the miR-200b cluster members are consistently downregulated in ESCC (15). However, our knowledge about the exact roles played by the miR-200 family in ESCC and the underlying molecular mechanisms remain relatively unclear.

In this study, we firstly confirmed that the miR-200b cluster members are frequently downregulated in ESCC, and this abnormality significantly correlates with a poor prognosis and unfavorable clinicopathological features in ESCC patients. Our *in vitro* studies suggest that miR-200b strongly represses the invasiveness and modulates the cytoskeletal and adhesive machinery in ESCC cells. Mass spectrometry studies allowed us to discover Kindlin-2 as an important mediator of the tumor suppressor functions of miR-200b. Moreover, we found an inverse correlation between the expression levels of ZEB1/2 and miR-200b in both ESCC cell lines and surgically resected ESCC specimens. High expression levels of ZEB1 and ZEB2 were also associated with a shorter overall survival in ESCC patients. Besides, we revealed that DNA methylation of the *E-cadherin* gene blocked its transcriptional regulation by the miR-200b-ZEB1 axis, and E-cadherin is not necessarily a mediator of the function of miR-200b in ESCC. We identified AKT as an important mediator of the miR-200b-Kindlin-2-Integrin β1 axis in

the regulation of ESCC invasiveness, highlighting an additional mechanism underlying the tumor suppressor function of miR-200b in ESCC.

2.3 Materials and Methods

2.3.1 Clinical samples

Human ESCC samples and adjacent non-tumorous esophageal epithelial tissues were collected between Oct. 2007 and Dec. 2008 directly after surgical resection at the Department of Tumor Surgery of Shantou Central Hospital, China. The cases were selected based on a clear pathological diagnosis, follow-up data, and had not received previous local or systemic treatment. The histological characterization and clinicopathological staging of the samples were performed in accordance with the 7th edition of American Joint Committee on Cancer Tumor-Nodes-Metastasis staging system (16). Detailed clinical information of the ESCC patients is described in **Table 2.1**. The study was approved by the ethical committee of the Central Hospital of Shantou City and the ethical committee of Shantou University Medical College, and written informed consent was obtained from all surgical patients to use resected samples for research.

2.3.2 Human ESCC cell lines

KYSE510, KYSE180, KYSE150, KYSE70 and TE3 human ESCC cell lines were kindly provided by Dr. Ming-Zhou Guo, Department of Gastroenterology & Hepatology, Chinese PLA General Hospital, Beijing, China. EC109 and EC9706 were obtained from Chinese Academy of Medical Sciences, Beijing,

China. The ESCC cell lines used in this study were cultured according to the methods described below: KYSE510, KYSE180, KYSE150, KYSE70 and TE3 cells were cultured in RPMI-1640 medium supplemented with 10% fetal bovine serum. EC109 and EC9706 cells were maintained in DMEM medium plus 10% newborn calf serum.

Table 2.1 Clinicopathological characteristics of patients

Clinical parameters	No. of patients (n = 88)
Gender	
Male	68
Female	20
Age	
≤50	23
＞50	65
Tumor size	
≤3cm	27
＞3cm	61
Histologic grade	
G1	21
G2	56
G3	11
G4	0
Invasive depth	
Tis	0
T1	7
T2	18
T3	63
T4	0
Lymph node metastasis	
N0	54
N1	23
N2	7
N3	4
TNM classification	
0	0
IA + IB	2
IIA + IIB	58
IIIA + IIIB + IIIC	28
IV	0

2.3.3 *In vitro* invasion and migration assays

Cell invasion, migration assays were performed as described below: 48h after transfection with 10nM miR-200b mimic or 200nM anti-200b or their corresponding negative control RNA, cells were starved for 24h and 1×10^5

starved cells were seeded into transwells (BD Biosciences, San Jose, CA, USA) with 8μm-pore size membranes coated with or without Matrigel (for invasion and migration assays, respectively). After 48h, cells within the transwells were removed and migrated/invaded cells on the bottom of the transwells were stained with crystal violet. Photos of migrated/invaded cells on the transwell membrane were taken under 200X magnification, and the numbers of migratory/invaded cells were counted from at least five different fields.

2.3.4 *In Vivo* Tumor Invasion Assay

EC109 cells transfected with 20nM miR-200b mimic or negative control RNA (denoted as EC109-NC and EC109-200b) were trypsinized and suspended in PBS. 50μl cell suspensions containing 1×10^6 cells were injected into the left footpads of 5-week-old male BALB/c nu/nu mice (n=10 per group). After 23 days, the mice were sacrificed. The invasive length was measured from the injection site in the footpad to the furthest visible invasion site. The width and height of the invasive area were also measured using a vernier caliper. Tumor local invasion area was measured by multiplying the length, width, and height. The primary tumors in the footpad and the invasive tumors in the inner thigh muscles were excised and embedded in paraffin after fixation in 10% formaldehyde/PBS. Subsequently, the tissue sections were stained with haematoxylin-eosin and examined for the existence of invasive carcinoma. E-cadherin and vimentin expression was analyzed in the primary tumors by immunohistochemistry. The animal experiments were performed in

accordance with the Institutional Animal Care and Use Committee of Shantou University.

2.3.5 Chemical Treatment

Both demethylation agent 5-Aza-2'-deoxycytidine (5-Aza-dC) and PI3K inhibitor LY294002 were purchased from Sigma-Aldrich (St. Louis, MO, USA). 5-aza-dC was dissolved in acetic acid, while LY294002 was dissolved in DMSO. For 5-aza-dC treatment, cells were cultured in medium containing different concentrations of this chemical for 72h before RNA extraction or cell lysate collection. The culture medium was changed every 24 h with corresponding concentrations of 5-aza-dC. For LY294002 treatment, cells were incubated with medium containing different concentrations of this chemical for 24h before cell lysate harvest or biological function study.

2.3.6 RNA isolation and quantitative real-time PCR

Total RNA was extracted with TRIzol reagent (Invitrogen, Carlsbad, CA, USA). For the real-time PCR of miR-200a, miR-200b, miR-429 and RNU6B (U6, endogenous control), TaqMan MicroRNA Assay kits (Applied Biosystems, Carlsbad, CA, USA) were used and real-time PCR reaction was carried out using ABI 7500 fast real-time PCR system (Applied Biosystems) as described before (15). For the real-time PCR or RT-PCR of ZEB1, ZEB2, E-cadherin, vimentin and GAPDH, cDNA was synthesized with the Reverse Transcription System (Promega, Madison, WI, USA). The sequences of the primers are described in **Table 2.2**.

Table 2.2 Primers for RT-PCR and real-time PCR

Primer Name	Application	Primer Sequence
ZEB1-F	real-time PCR	TTCAAACCCATAGTGGTTGCT
ZEB1-R	real-time PCR	TGGGAGACACCAAACCAACTG
ZEB2-F	real-time PCR	CAAGAGGCGCAAACAAGC
ZEB2-R	real-time PCR	GGTTGGCAATACCGTCATCC
E-cadherin-F	RT-PCR	CACACGGGGCGAGTGCCAAC
E-cadherin-R	RT-PCR	GCGGCCCCTTCACAGTCACA
vimentin-F	RT-PCR	GATGCCCTTAAAGGAACCAATGAG
vimentin-R	RT-PCR	GGCGGCCAATAGTGTCTTGGTAG
GAPDH-F	RT-PCR	GGCGGCCAATAGTGTCTTGGTAG
GAPDH-R	RT-PCR	GAAGATGGTGATGGGATTTC

2.3.7 Vector construction and site-directed mutagenesis

The coding region of Kindlin-2 was amplified and cloned (*BamHI* & *XhoI*) into the eukaryotic expression vector pcDNA3.1 (Invitrogen) to generate pcDNA3.1-Kindlin-2 expression vector. To construct the Luciferase reporter vector, the 3'UTR of *FERMT2, CDK2, CFL2, HMOX1, PAF, PAK2, RALB* and *RDX* containing the putative miR-200b binding site(s) were amplified and cloned (XbaI & FseI) into pGL3-Control vector (Promega). All the primers used for gene cloning are described in **Table 2.3** For site-directed mutagenesis, Fast Mutagenesis System (TransGen Biotech, Beijing, China) was used, and the experiment was performed according to the manufacturer's instructions. Primers for mutagenesis are listed in **Table 2.3**.

Table 2.3 Primers used for gene cloning and mutagenesis

Primers	Primer Sequence (5' - 3')
Primers used for the cloning of pGL3-Control-3'UTR luciferase reporter vectors	
CDK2-F	TCTAGACCTAATCTCACCCTCTCCTC
CDK2-R	GGCCGGCCTACGGCAAATCTAACGTGTAG
CFL2-F	TCTAGAAGTGCCATCTGGATCTTAAG
CFL2-R	GGCCGGCCAACACATCTCAACAGCTTTAC
FERMT2-F	TCTAGAAAGCTGTTTGTTATATGCTGC
FERMT2-R	GGCCGGCCTAAAAGTTTTGCTTTTATTTA
HMOX1-F	TCTAGACTCTTGGCTGGCTTCCTTACC
HMOX1-R	GGCCGGCCACAGTGCCGTTAAACACCTCC
PAF-F	TCTAGACCAATTAGCTTTGTTGAACAGG
PAF-R	GGCCGGCCCAATCTCGGCTCACTGCAAG
PAK2-F	TCTAGATTCCTGGGTTCAAGCAATTC
PAK2-R	GGCCGGCCTCTTTGCCAGAGTGTTCAATC
RALB-F	TCTAGAAAGCCAGCTGCTCCTAAGGAC
RALB-R	GGCCGGCCAGTCAGATCATAATTTCTACC
RDX-F	TCTAGATTCGGTTATAGCTTACTGAAG
RDX-R	GGCCGGCCTTGAAGGCATGAGCTTTTG
Primers used for the cloning of pcDNA3.1-Kindlin-2 expression vector	
Kind2-F	GGATCCATGGCTCTGGACGGGATAAGGATG
Kind2-R	CTCGAGCAGTATTCCTATTCACACCCAACC
Primers used for mutagenesis	
Mutant1-F	CCATATTGTATTACACTTTTA**CGC**TTCACCAGCATAATCACTGTCTGCC
Mutant1-R	**GCG**TAAAAGTGTAATACAATATGGTGTAAAAATAAAAACACGAGACAAT
Mutant2-F	GAGGGAGAGGTGGATTACCA**CGC**TTGTTCAATAATCCATGGTTC
Mutant2-R	**GCG**TGGTAATCCACCTCTCCCTCGCACCCTTTTGGGCTATG

Note: Underlined sequences are mutant sites

2.3.8 Oligonucleotide transfection

Syn-hsa-miR-200b miScript miRNA Mimic, Anti-hsa-miR-200b miScript miRNA Inhibitor, Kindlin-2 siRNA and their corresponding negative control RNAs were all purchased from Qiagen (Hilden, Germany). The sequence of Kinlin-2 siRNA is 5'-CTGGTGGAGAAACTCGATGTA-3'. Oligonucleotide alone transfection was performed with Hiperfect reagents (Qiagen) and co-transfection of Oligonucleotide and vectors were performed with Attractene reagents (Qiagen).

2.3.9 Luciferase reporter assay

The firefly luciferase construct was co-transfected with a control Renilla luciferase vector into EC109 cells in the presence of either miR-200b mimic or anti-200b or corresponding negative control RNA. After 48h, luciferase activity was measured using the Dual-Luciferase Reporter Assay System (Promega). Data are presented as ratios between firefly and Renilla fluorescence activities. The experiments were performed independently in triplicate.

2.3.10 Western blot and Rho GTPase activation assay

Proteins were separated on SDS–PAGE and transferred to PVDF membrane (Millipore). The membranes were blocked with 5% non-fat milk and incubated with antibodies against Kindlin-2 (Millipore, St Charles, MO, USA), pFAK(Tyr397) (Invitrogen), FAK (BD Transduction Laboratories), E-cadherin (Santa Cruz Biotechnology, Santa Cruz, CA, USA), vimentin (Dako, Carpinteria, CA, USA), $pAKT^{S473}$ (Cell Signaling, Danvers, MA, USA), AKT

(Cell Signaling), and β-actin (Sigma). The proteins were detected with Western Blot Luminol Reagent (Santa Cruz).

The pull-down of the GTP-bound form of Rho-family GTPases was performed using RhoA and Cdc42/Rac1 activation assay kits (Cytoskeleton, Denver, CO, USA) in accordance with the manufacturer's instructions. Protein quantitative analysis was performed by Western-blot analysis using antibodies against RhoA, Cdc42 and Rac1 provided within the kits.

2.3.11 Immunohistochemistry

Paraffin embedded tissue blocks were cut into 4 μm sections and processed for Immunohistochemistry with a protocol described previously (17). Antibodies against Kindlin-2 (Millipore), E-cadherin (1:1, Zhongshan Golden Bridge Biotechnology, Beijing, China), and vimentin (Carpinteria, CA) were used. Scoring was classified into 4 grades: no reactivity scored 0, faint reactivity scored 1, moderate reactivity scored 2, and strong reactivity scored 3.

2.3.12 Flow Cytometry

The expression of active and total Integrin β1 was determined by flow cytometry. Briefly, cells were gently dissociated with 0.05% trypsin and 0.02% EDTA, washed in medium containing 1% BSA, counted and diluted in PBS. 5μl antibody against active Integrin β1 (HUTS-4-FITC, Millipore) and 2.5μl antibody against total Integrin β1 (Santa Cruz Biotechnology) was added to

95µl PBS containing 5×10^5 cells for the detection of active Integrin β1 and total Integrin β1, respectively. These cells were incubated for 30min at room temperature. No antibody was added in the negative control cells. The cells incubated with antibody against total Integrin β1 were then incubated with FITC-conjugated secondary antibody (goat-anti-mouse, Santa Cruz Biotechnology) for 30min on ice. Then, all the samples were washed in cold PBS and analyzed by flow cytometry. Data were analyzed using the Flow Jo software.

2.3.13 Immunofluorescence

Cells transfected with miR-200b mimic, Kindlin-2 siRNA or their corresponding negative control RNA were seeded on fibronectin coated (2µg/cm^2) coverslips and allowed to adhere for 1h or 12h and then fixed with 4% paraformaldehyde. Subsequently, cells were incubated with antibodies against Paxillin (1:50, BD Transduction Laboratories) or Kindlin-2 (1:200, Millipore). Acti-stain 555 phalloidin was applied with together with donkey anti-mouse secondary antibody conjugated to DyLight 488 (1:200, Jackson) and nuclei were counterstained with 4',6-diamidino-2-phenylindole (DAPI). The cover slips were examined under Olympus 20X/0.5 lens by FV-1000 laser-scanning confocal microscope consisting of an Olympus IX81 microscope and a FV1000 scan head with integrated TIRF module. Images were acquired using FV10-ASW software (Olympus, Tokyo, Japan). Cell spreading area was measured with the NIH software ImageJ (http://rsbweb.nih.gov/ij/index.html). For each treatment, at least three different fields were analyzed.

2.3.14 SILAC (stable isotope labeling with amino acids in cell culture) coupled to mass spectrometry

SILAC labeling, cell lysates preparation and SDS-PAGE: EC109 cells were grown in 1640 medium containing 0.46mM "light" ($^{12}C_6$)-lysine or "heavy" ($^{13}C_6$)-lysine supplemented with 10% (v/v) dialyzed FBS (Pierce SILAC Protein Quantitation Kit, Pierce, Rockford, IL, USA). After culturing for 7 passages, the cells were seeded into 6-well plates, the ''light'' labeled cells were mock transfected with 10nM negative control RNA and the "heavy" labeled cells were transfected with 10nM miR-200b mimic. At 48h post-transfection, the cells were trypsinized and washed with ice-cold PBS before evaluating cell concentrations. Then, cells were combined at a ratio of 1:1 (1×10^6 each) and splited with Laemmli buffer (Bio-Rad, Philadelphia, PA, USA). The lysates were resolved in a 12% SDS-PAGE gel and visualized by colloidal Coomassie staining (Invitrogen). Gel bands of interest were excised into 10 sections and subjected to in-gel digestion respectively. Briefly, the gel bands were sliced into small pieces (~1 mm^3) and destained with 25 mM ammonium bicarbonate in ethanol/water (50:50, v/v). The destained gel pieces were washed in an acidic buffer (acetic acid/ethanol/water, 10:50:40, v/v/v) three times for 1 h each time, and in water two times for 20 min each time. The gel pieces were dehydrated in acetonitrile (Thermo Fisher, Lafayette, CO, USA) and dried in a SpeedVac (Thermo Fisher). 200ng of porcine modified trypsin (Promega) in 50 mM ammonium bicarbonate was added to the dried gels and incubated overnight at 37℃. Tryptic peptides were sequentially extracted from the gel pieces with 50% acetonitrile

(acetonitrile/water/TFA, 50:45:5, v/v/v) and 75% acetonitrile (acetonitrile/water/TFA, 75:24:1, v/v/v). The peptide extracts were pooled and dried in a SpeedVac. Every mixture of peptides was desalted using a µ-C18 ZipTip (Millipore) respectively before HPLC/MS/MS analysis.

Nano-HPLC/mass spectrometric analysis and protein sequencing alignment: This experiment was performed in a single run. The tryptic digests were injected into a Nano-LC system (Eksigent Technologies), and analyzed by an LTQ-Orbitrap Velos mass spectrometer (Thermo Fisher). Briefly, each tryptic digest was dissolved in 10 µL of HPLC buffer A (0.1% (v/v) formic acid in water), and 2 µL was injected into a Nano-LC system. Peptides were separated on a homemade capillary HPLC column (100-mm length×75-µm inner diameter) containing Jupiter C12 resin (4-µm particle size, 90-Å pore diameter, Phenomenex) with a 2-hr HPLC-gradient from 5 to 90% HPLC buffer B (0.1% formic acid in acetonitrile) at a flow rate of 200 nL/min and electrosprayed directly into the mass spectrometer using a nanospray source. The LTQ-orbitrap Velos mass spectrometer was operated in a data-dependent mode with resolution R = 60,000 at m/z 400. Full scan MS spectra from m/z 300–2000 were acquired in the Orbitrap. The twenty most intense ions were sequentially isolated in the linear ion trap and subjected to collision-activated dissociation (CAD) with a normalized energy of 35%. The exclusion duration for the data-dependant scan was 36 sec, the repeat count was 2, and the exclusion window was set at +/-2 Da. AGC settings were 1E6 for full scan Orbitrap analysis, 1E4 for MSn scaning ion trap and 6E4 for MSn scan in

Orbitrap. Signal threshold for CID acquisition was set at 5000. The resulting MS/MS data were searched against the IPI human protein sequence database using Mascot search engine (v2.2) and Maxquant software (v1.0.13.13) with an overall false discovery rate (FDR) for peptides of less than 1%. Trypsin was specified as the proteolytic enzyme, and up to 4 missed cleavage sites per peptide were allowed. Oxidation of methionine and lysine-$^{13}C_6$ were fixed as variable modifications. Charge states of +1, +2, or +3 were considered for parent ions. The quantification was performed using Maxquant software (v1.0.13.13) tool.

2.3.15 Statistical analysis

All statistical analyses were performed using the SPSS V.13.0 statistical software package. The Wilcoxon signed-rank test was used to compare the expression levels of miR-200b cluster members between ESCC tissues and their paired non-tumorous tissues. To evaluate significant differences between two independent groups of samples, Student's *t*-test or Mann-Whitney *U* test were used. Survival curves were plotted using the Kaplan-Meier method and compared using the log-rank test, and X-tile software was used for the selection of optimal cutpoints before analysis (18). The $\chi 2$ test or Fisher's exact test was used to analyze the association of miR-200b-200a-429 expression and clinical-pathological parameters, and the same cutpoints were used as in the survival analysis. Differences were considered significant when the *P* value was less than 0.05.

2.4. Results

2.4.1 Decreased expression of the miR-200b cluster correlates with unfavorable outcomes in ESCC patients

Our previous studies using miRNA profiling applied to 3 cases of ESCC revealed a downregulation of the miR-200b-200a-429 cluster in ESCC, as compared to adjacent benign esophageal tissues (15). In the present study, we aimed to confirm these findings using real-time PCR applied to 88 pairs of ESCC and the adjacent benign esophageal tissues. As illustrated in **Figure 2.1A**, the three miR-200b cluster members (namely, miR-200b, miR-200a and miR-429) are clustered within a short segment of chromosome 1. Using Wilcoxon signed-rank test, we confirmed that the expression levels of the miR-200b cluster members were significantly lower in ESCC when compared to the adjacent benign esophageal tissues **(Figure 2.1B**, $P<0.05$**)**. We also found that the expression levels of these three miRNAs significantly correlated with each other in ESCC **(Figure 2.1C**, $P<0.001$**)**.

Kaplan-Meier analysis was performed to compare the prognosis of patients carrying tumors with different expression levels of the three miR-200b cluster members. As shown in **Figure 2.1D**, ESCC patients carrying tumors expressing low levels of the miR-200b cluster members had a significantly shorter survival, as compared to patients carrying tumors with high expression levels of these miRNAs ($P<0.05$). We also revealed that a relatively low expression of miR-200b and miR-429 significantly correlated with lymph node metastasis **(Figure 2.1E and Table 2.3)**. Moreover, low expression of miR-

200b also significantly correlated with advanced clinical stage **(Table 2.4**, *P*=0.020). Given that miR-200b showed the highest correlation with the clinical outcomes of ESCC patients, we examined miR-200b expression in a panel of ESCC cell lines (n=7), and the data showed that miR-200b was expressed at a relatively low level, compared to benign esophageal tissues **(Figure 2.1F)**.

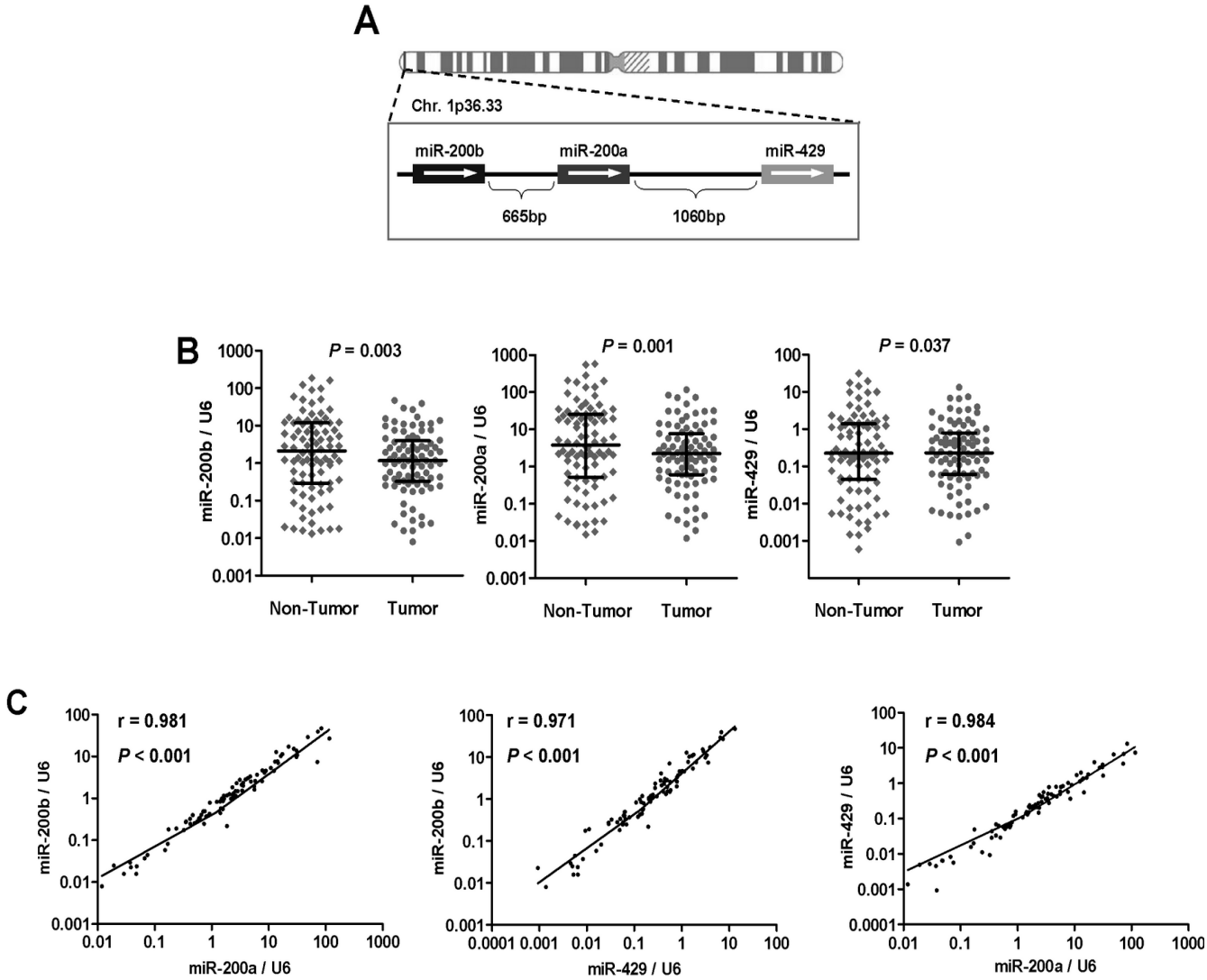

Figure 2.1 Expression status of the miR-200b cluster in ESCC specimens and their clinical significance. (**A**) A schematic representation of the localization of the miR-200b cluster members within the genome. (**B**) The expression levels of the miR-200b cluster members were examined by Taqman real-time PCR in 88 cases of ESCC specimens (Tumor) and adjacent non-tumor esophageal epithelial tissues (Non-Tumor). U6 was used as an endogenous control. Data are presented as median ± interquartile range, and Wilcoxon signed-rank test was used in statistical analysis. (**C**) The expression levels of the three miR-200b cluster members in ESCC were compared with each other (n=88). Pearson's correlation analysis was performed. **(Continued on the next page)**

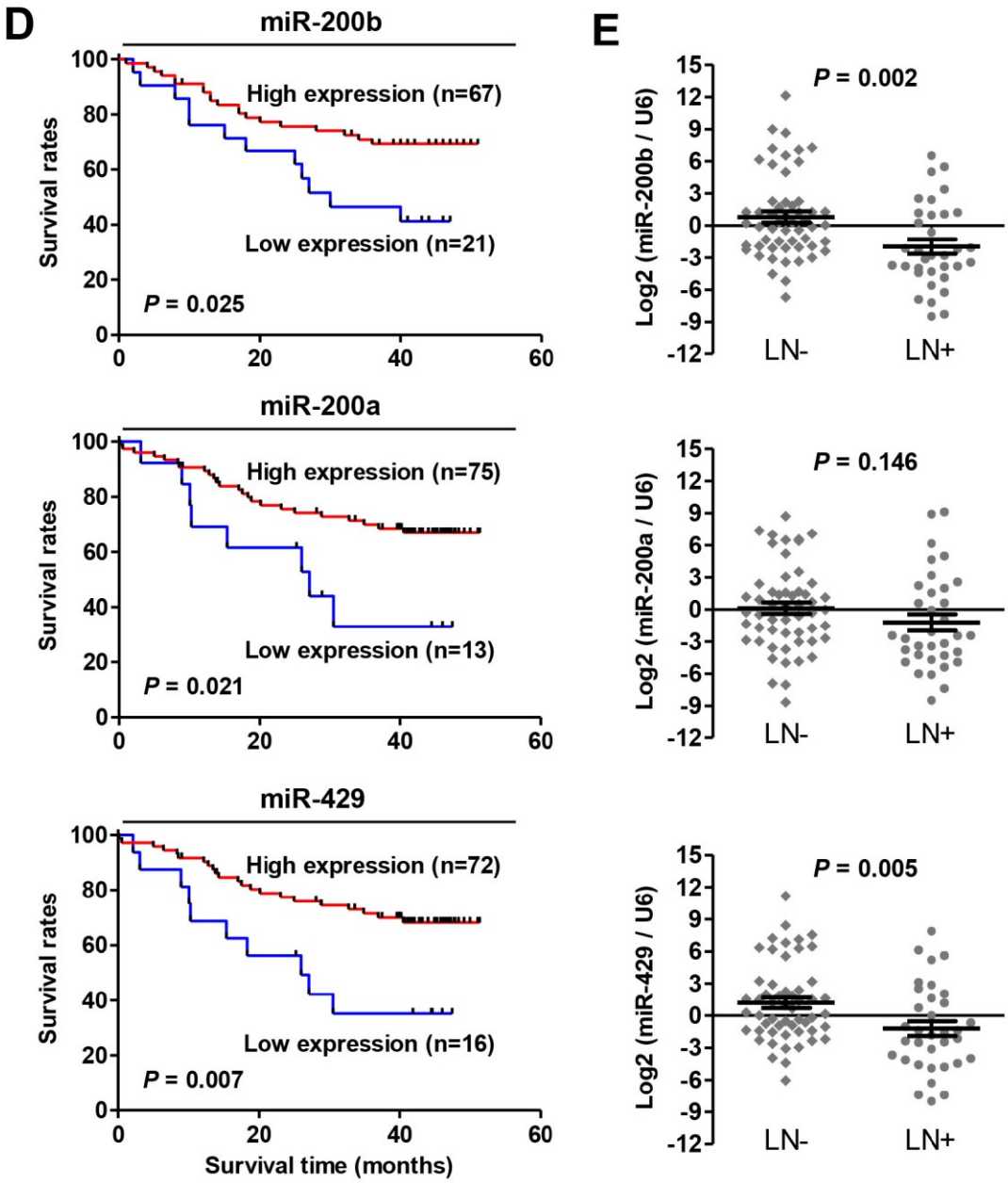

Figure 2.1D-E (**D**) Kaplan-Meier survival curves for ESCC patients were plotted on miRNA expression levels, and survival difference was analyzed by log-rank test. The optimal cutpoint values for the survival analysis were generated using X-tile software (18). (**E**) The expression levels of the miR-200b cluster members were compared between tumors with (LN+, n=34) and without lymph node metastasis (LN-, n=54). Data are plotted as mean ± SEM.

(Continued on the next page)

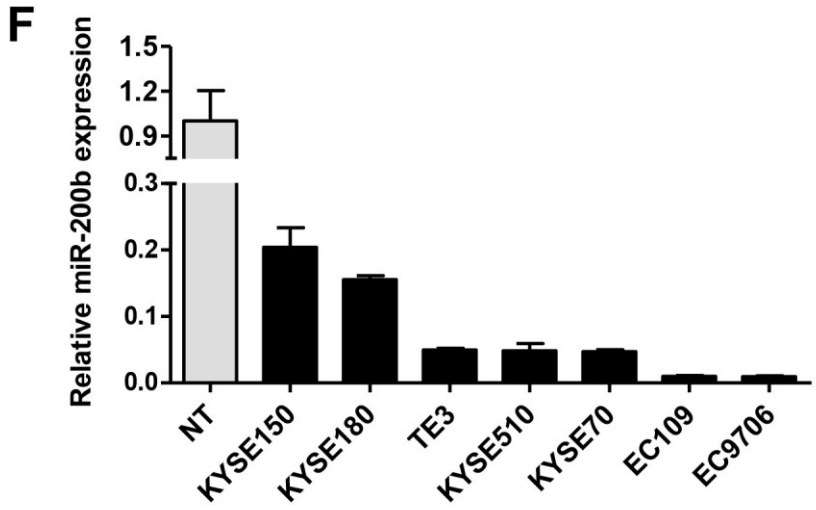

Figure 2.1F Expression levels of miR-200b in a panel of seven ESCC cell lines were detected by Taqman real-time PCR. The mean expression level of miR-200b in non-tumorous esophageal epithelial tissues (NT) from the 88-patient cohort was used as the normal control, extreme values outside of the normal distribution were excluded.

Table 2.4 Correlation of the miR-200b-200a-429 cluster expression with clinicopathological features of 88 ESCC patients

Parameters	miR-200b (%)		*P*	miR-200a (%)		*P*	miR-429 (%)		*P*
	Low	High		Low	High		Low	High	
Gender									
Female	3 (14.3%)	17 (25.4%)	0.380	2 (15.4%)	18 (24.0%)	0.724	2 (12.5%)	18 (25.0%)	0.345
Male	18 (85.7%)	50 (74.6%)		11 (84.6%)	57 (76.0%)		14 (87.5%)	54 (75.0%)	
Age									
<56	13 (61.9%)	31 (46.3%)	0.211	8 (61.5%)	36 (48.0%)	0.367	10 (62.5%)	34 (47.2%)	0.269
≥56	8 (38.1%)	36 (53.7%)		5 (38.5%)	39 (52.0%)		6 (37.5%)	38 (52.8%)	
Differentiation									
Well	5 (23.8%)	16 (23.9%)	0.935	3 (23.1%)	18 (24.0%)	0.908	4 (25.0%)	17 (23.6%)	0.552
Moderate	13 (61.9%)	43 (64.2%)		8 (61.5%)	48 (64.0%)		9 (56.2%)	47 (65.3%)	
Poor	3 (14.3%)	8 (11.9%)		2 (15.4%)	9 (12.0%)		3 (18.8%)	8 (11.1%)	
Tumor size									
<3cm	5 (23.8%)	22 (32.8%)	0.434	2 (15.4%)	25 (33.3%)	0.329	3 (18.8%)	24 (33.3%)	0.371
≥3cm	16 (76.2%)	45 (67.2%)		11 (84.6%)	50 (66.7%)		13 (81.2%)	48 (66.7%)	
Infiltration degree									
T1 + T2	7 (33.3%)	18 (26.9%)	0.566	6 (46.2%)	19 (25.3%)	0.124	5 (31.2%)	20 (27.8%)	0.781
T3	14 (67.6%)	49 (73.1%)		7 (53.8%)	56 (74.7%)		11 (68.8%)	52 (72.2%)	
Lymph node									
N0	7 (33.3%)	47 (70.1%)	**0.002**	5 (38.5%)	49 (65.3%)	0.066	6 (37.5%)	48 (66.7%)	**0.030**
N1 + N2 + N3	14 (67.6%)	20 (29.9%)		8 (61.5%)	26 (34.7%)		10 (62.5%)	24 (33.3%)	
TNM classification									
I + II	10 (47.6%)	50 (74.6%)	**0.020**	7 (53.8%)	53 (70.7%)	0.229	8 (50.0%)	52 (72.2%)	0.084
III + IV	11 (52.4%)	17 (25.4%)		6 (46.2%)	22 (29.3%)		8 (50.0%)	20 (27.8%)	

2.4.2 Identification of miR-200b targets using quantitative mass spectrometry

To further define the mechanism by which miR-200b exerts its tumor suppressor effects, we performed a quantitative proteomics study comparing EC109 cells (a cell line that expressed a low level of miR-200b) transfected with miR-200b mimic or NC. The experimental approach was based on SILAC (stable isotope labeling with amino acids in cell culture) coupled to mass spectrometry; schematic outline of this study is shown in **Figure 2.2A**. The labeling efficiency test data showed that > 95% of newly synthesized proteins were labeled with Lysine-$^{13}C_6$ before miR-200b mimic transfection **(Figure 2.3)**. A total of 2174 proteins were identified, and the majority of these 2174 proteins had an H/L ratio between 0.9 and 1.1 **(**data not shown**)**, which is consistent with the previous report that ectopic expression of miRNAs only causes moderate changes in the overall protein synthesis (19). 309 of these 2174 proteins were considered probable candidates since they had an H/L ratio ≤ 0.9 **(Table 2.5)**. Of these 309 downregulated proteins, 57 overlapped with the gene lists generated by the *in silico* prediction using the "TargetScan" algorithm that revealed 3414 potential miR-200b targets based on their potential miR-200b binding site(s) on their 3' untranslated regions (3'UTRs) **(Figure 2.2B and Table 2.5)**. Notably, 4/57 genes have been previously published to be direct targets of miR-200, including *MARCKS, CFL2, TUBB3* and *MATR3* (7,20-22), and 2/57 were shown to be putative targets that can be downregulated by miR-200, including *CRTAP* and *SERPINH1* (7).

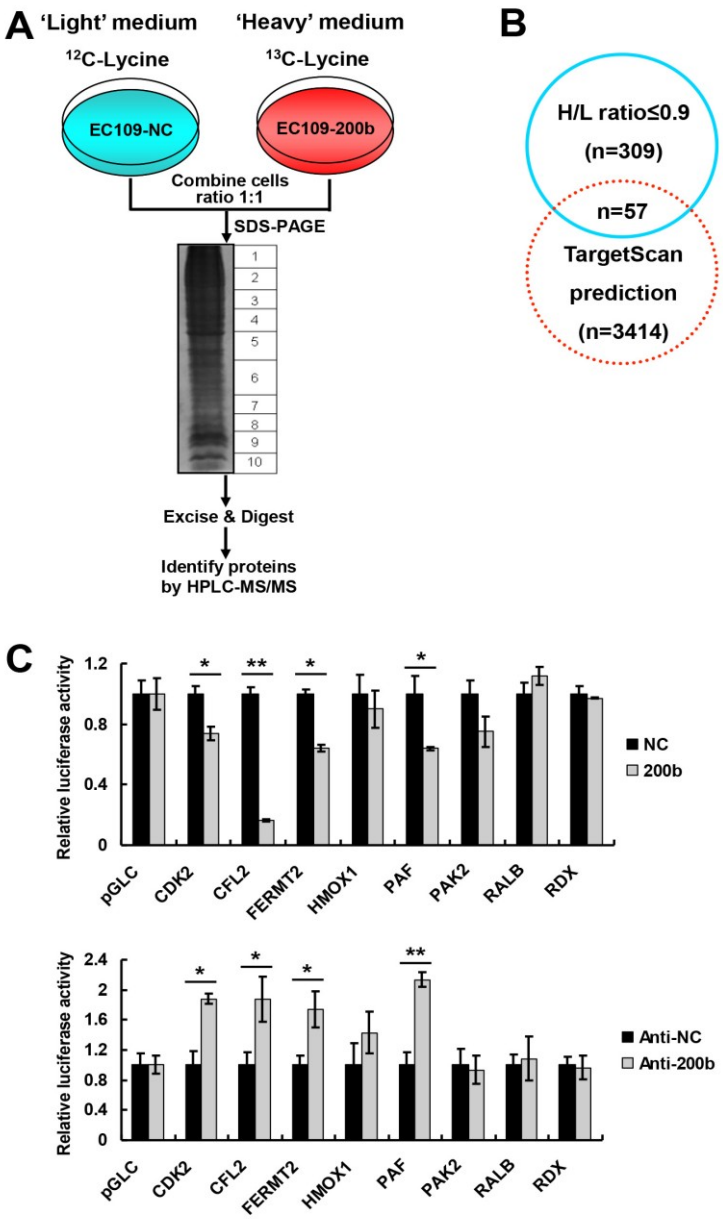

Figure 2.2 Identification of miR-200b targets by SILAC (stable isotope labeling with amino acids in cell culture) coupled to mass spectrometry proteomics study. (**A**) Schematic outline of the SILAC proteomics study. Details are described in "Materials and Methods". (**B**) Screening of the putative target genes of miR-200b. The 309 proteins identified by the proteomics study with H/L ratios ≤ 0.9 were selected as candidates and overlapped with the 3414 potential miR-200b targets predicted by the "TargetScan" algorithm. 57 overlapping genes were identified by this analysis. (**C**) Dual luciferase reporter assays in EC109 cells testing eight miR-200b putative target genes (n=3, **P*<0.05, ***P*<0.01, Student's *t*-test). **(Continued on the next page)**

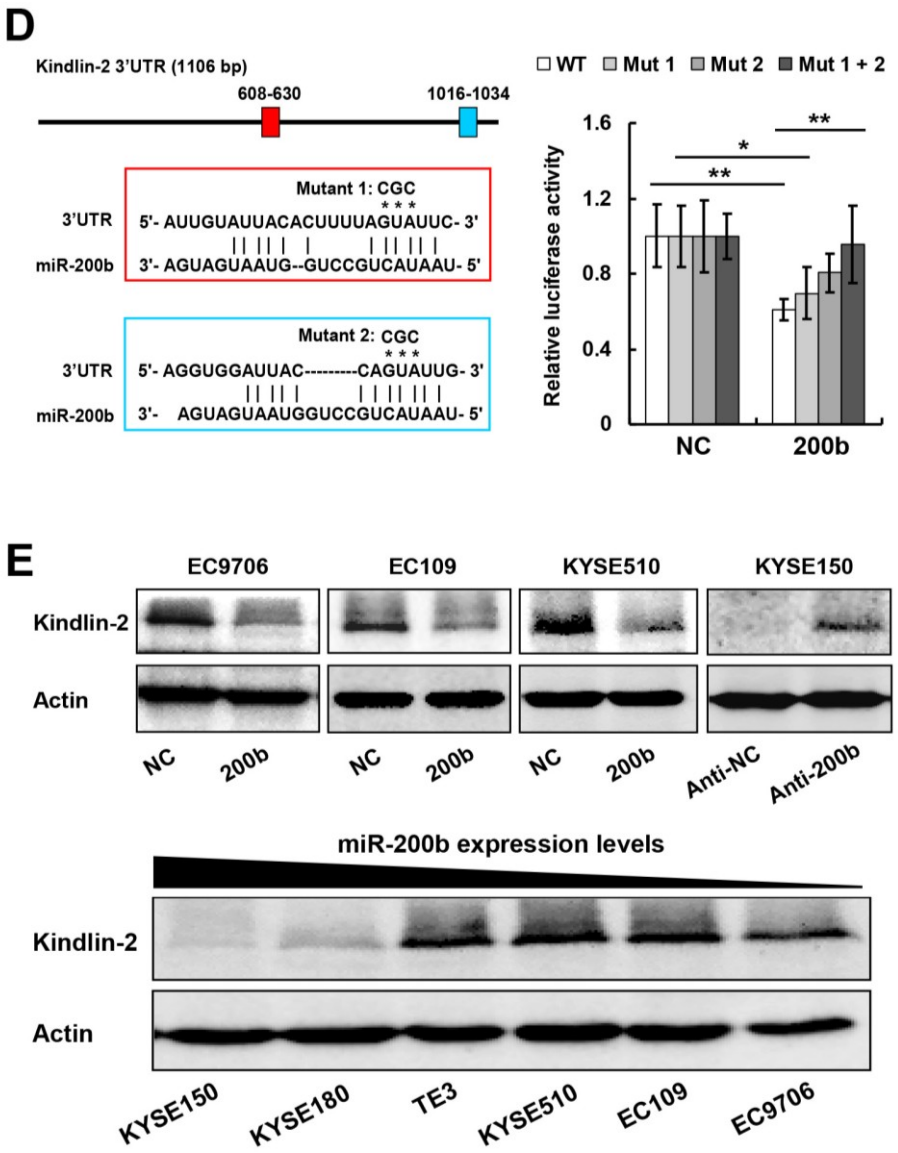

Figure 2.2C-E (**C**) Dual luciferase reporter assays in EC109 cells testing eight miR-200b putative target genes (**D**) Left panel: Schematic illustration of the two potential miR-200b binding sites on the 3'UTR of Kindlin-2 encoding mRNA, asterisks indicate the mutated sites of the putative miR-200b binding region. Right panel: Dual luciferase reporter assays in EC109 cells testing the influence of miR-200b mimic or NC on the luciferase activity mediated by reporter constructs harboring either wild-type (WT) or mutant (Mut) Kindlin-2 3'UTR (**E**) The effects of miR-200b mimic or inhibitor transfection on Kindlin-2 protein expression were examined by Western-blot (top panel). The expression levels of Kindlin-2 in six ESCC cell lines were examined by Western-blot (bottom panel). (n=3, **P*<0.05, ***P*<0.01, Student's *t*-test).

(Continued on the next page)

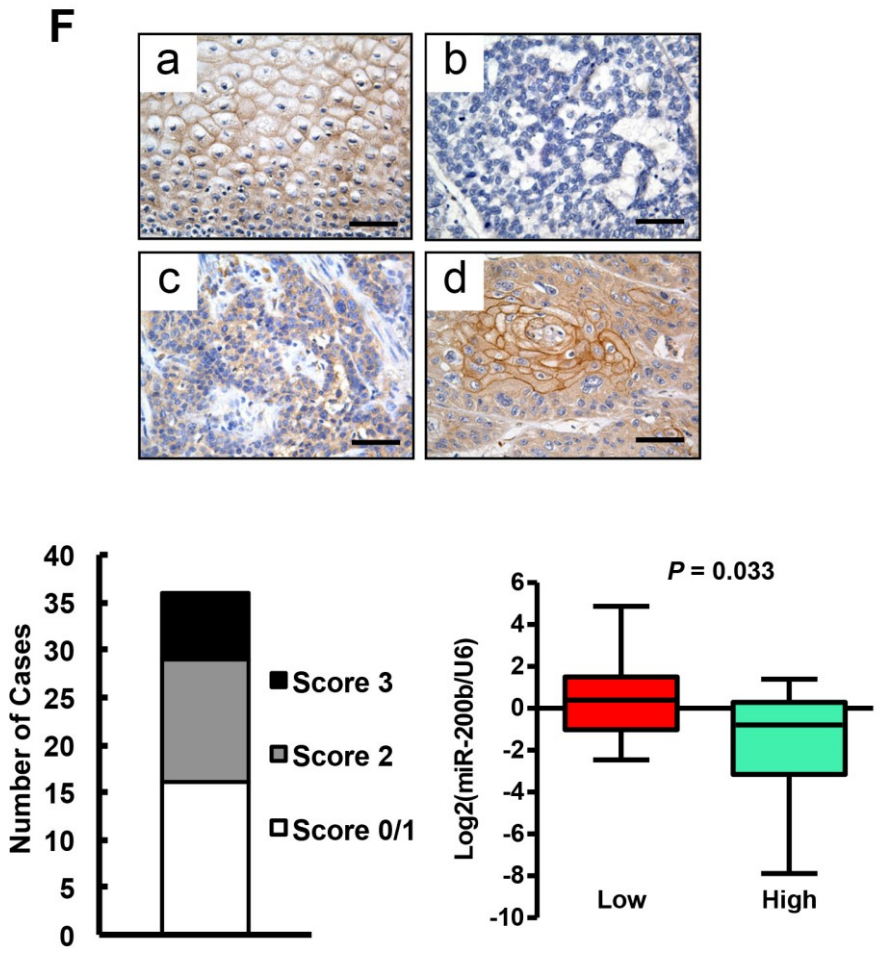

Figure 2.2F (**F**) Kindlin-2 expression was detected by immunohistochemistry in non-tumor esophageal tissues (a) and 36 cases of ESCC specimens (b-d). Upper panel: representative images show different staining intensities of Kindlin-2. Scale bars: 50μm. Lower panel: proportions of ESCC specimens with different Kindlin-2 staining intensities are shown, and the correlation between miR-200b expression level and Kindlin-2 protein expression level was analysed. Box plots describe the relative expression of miR-200b in ESCC tissues with low or high expression of Kindlin-2. Low indicates IHC scores of 0 and 1; high indicates IHC scores of 2 and 3. Statistical analysis was performed with Student's *t*-test.

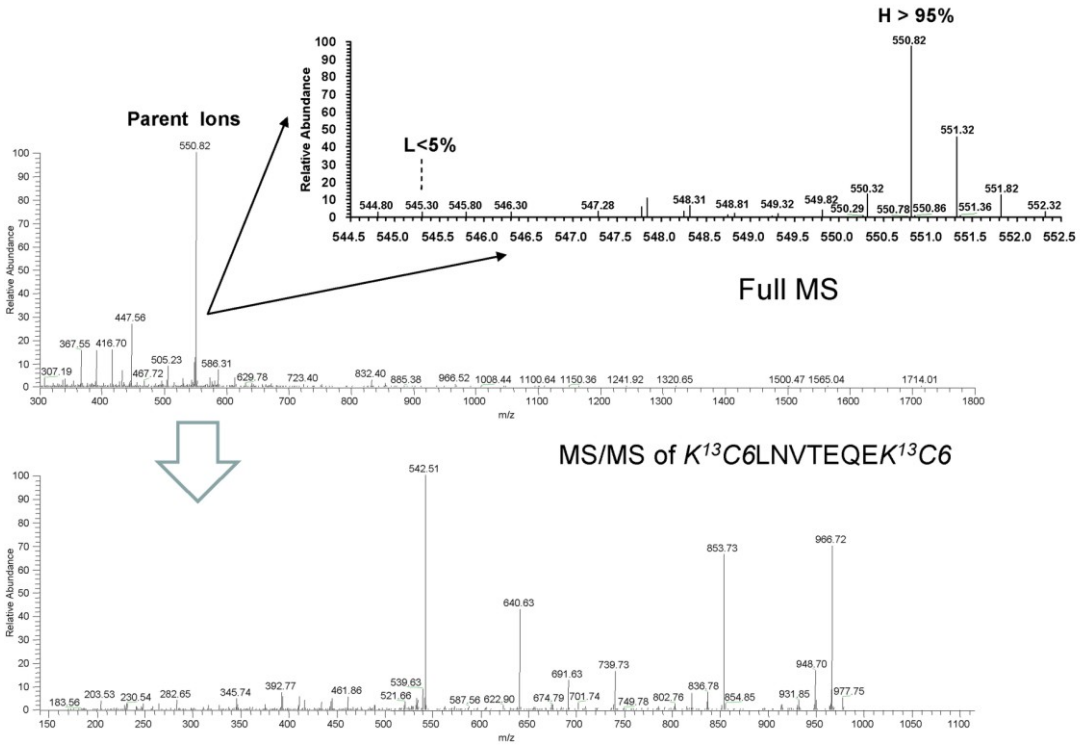

Figure 2.3 SILAC labeling efficiency analysis by Nano-LC/MS/MS. Over 95% proteins are present in the heavy state $^{13}C_6$-lysine after seven doublings to allow the incorporation of the heavy amino acid (Lysine-$^{13}C_6$) using SILAC method.

Table 2.5 Putative miR-200b targets identified by SILAC proteomics study

Gene Name	H/L Ratio	Gene Name	H/L Ratio	Gene Name	H/L Ratio
DCUN1D4	0.49	TRIO	0.82	ATP2A2	0.88
PFDN4	0.67	DNAJC15	0.82	IPO8	0.88
HMOX1	0.69	C5orf33	0.82	SWAP70	0.88
CRTAP	0.71	BCAP29	0.83	MRPS35	0.89
TIMP2	0.72	PPP2R1B	0.83	TXNDC5	0.89
MARCKS	0.73	FERMT2	0.83	RDX	0.89
CFL2	0.74	PMPCB	0.83	WDR82	0.89
LAMC1	0.74	ABHD10	0.84	MATR3	0.89
FGF2	0.76	FUNDC1	0.84	GCSH	0.89
MCFD2	0.78	CUL4A	0.85	PAK2	0.89
UACA	0.78	CD59	0.85	ERBB4	0.89
TUBB3	0.78	NDUFS4	0.85	ISOC1	0.89
CUGBP2	0.78	C12orf5	0.86	GSTM3	0.90
UBE2K	0.79	RCN1	0.87	RAB18	0.90
RHOT1	0.79	KIAA0101	0.87	SUPT4H1	0.90
SERPINH1	0.79	EHD1	0.87	SPCS2	0.90
GMFB	0.80	EHD3	0.87	SASH1	0.90
XRN2	0.81	CDK2	0.87	RALB	0.90
FREQ	0.81	ACTR1A	0.87	CNN3	0.90

Of the remaining 51 potential targets of miR-200b, we performed validation studies. We identified seven potential targets that have been implicated in tumorigenesis or malignant progression in other cancer types, including *CDK2*, *FERMT2* (encodes Kindlin-2 protein), *HMOX1*, *PAF* (*KIAA0101*), *PAK2*, *RALB* and *RDX* (23-30). *CFL2*, which was previously shown to be a miR-200b target gene (7), served as the positive control in our subsequent validation analysis. Our experimental approach was to clone the 3'UTRs of these eight candidates into a luciferase reporter vector, as detailed in Materials and Methods. By performing bidirectional screening using miR-200b mimic and miR-200b inhibitor, our studies allowed us to validate three novel miR-200b targets, including CDK2, PAF and Kindlin-2 **(Figure 2.2C)**. The luciferase

reporters containing the 3'UTR of the other four putative miR-200b targets were shown not to respond accordingly to the manipulation of miR-200b expression levels, probably due to the fact that their protein expression were regulated by miR-200b through indirect mechanisms other than direct binding of miR-200b to their 3'UTR.

2.4.3 Kindlin-2 is a novel target of miR-200b in ESCC cells

Among the three newly identified miR-200b targets, Kindlin-2 was previously shown to promote cancer cell migration and invasiveness (23,24). Our following observations support the concept that Kindlin-2 is indeed a target of miR-200b in ESCC. First, *in silico* prediction revealed two potential binding sites of miR-200b on Kindlin-2 3'UTR, and simultaneous mutation of both potential binding sites abolished the suppression of miR-200b mimic on the luciferase activity **(Figure 2.2D)**. Second, an inverse correlation between the expression of Kindlin-2 and miR-200b can be observed in a panel of six ESCC cell lines **(Figure 2.1F and Figure 2.2E).** Third, to test whether miR-200b indeed regulates the protein expression of Kindlin-2, three cell lines (*i.e.* EC9706, EC109 and KYSE510) that expressed the lowest level of miR-200b and the highest level of Kindlin-2 were chosen to transfect with miR-200b mimic, while KYSE150 cells that had the highest expression of miR-200b and the lowest expression of Kindlin-2 was transfected with miR-200b inhibitor. As shown in Figure 2E, transfection of miR-200b mimic reduced Kindlin-2 expression in all three ESCC cell lines tested, and inhibition of endogenous miR-200b in KYSE150 cells increased Kindlin-2 expression. Lastly, we found a significant inverse correlation between Kindlin-2 protein expression (by

immunohistochemistry) and miR-200b levels (by qRT-PCR) in ESCC samples **(Figure 2.2F**, *P*=0.033**)**.

2.4.4 miR-200b and Kindlin-2 regulate invasiveness and migratory function in ESCC

Transfection of miR-200b mimic into three ESCC cell lines (EC9706, EC109 and KYSE510, **Figure 2.4A**), all of which had a low level of miR-200b expression, induced a significant decrease in their cell migration and invasiveness **(Figure 2.4B and C)**. Accordingly, when we inhibited miR-200b using an inhibitor in KYSE150 **(Figure 2.4A)**, an ESCC cell line that expressed miR-200b at the highest level among all ESCC cell lines examined, we found a significant increase in cell migration and invasiveness **(Figure 2.4B and C)**. To determine whether Kindlin-2 is a mediator of the biological function of miR-200b, two representative cell lines with low miR-200b expression and high Kindlin-2 expression (*i.e.* EC109 and KYSE510) were used as cell models in our subsequent biological analyses. As shown in **Figure 2.4D and E**, siRNA knockdown of Kindlin-2 reduced ESCC cell invasiveness in both EC109 and KYSE510 cells. Furthermore, enforced expression of Kindlin-2 in both EC109 and KYSE510 cells largely restored the invasiveness that was suppressed by miR-200b **(Figure 2.4F and G)**.

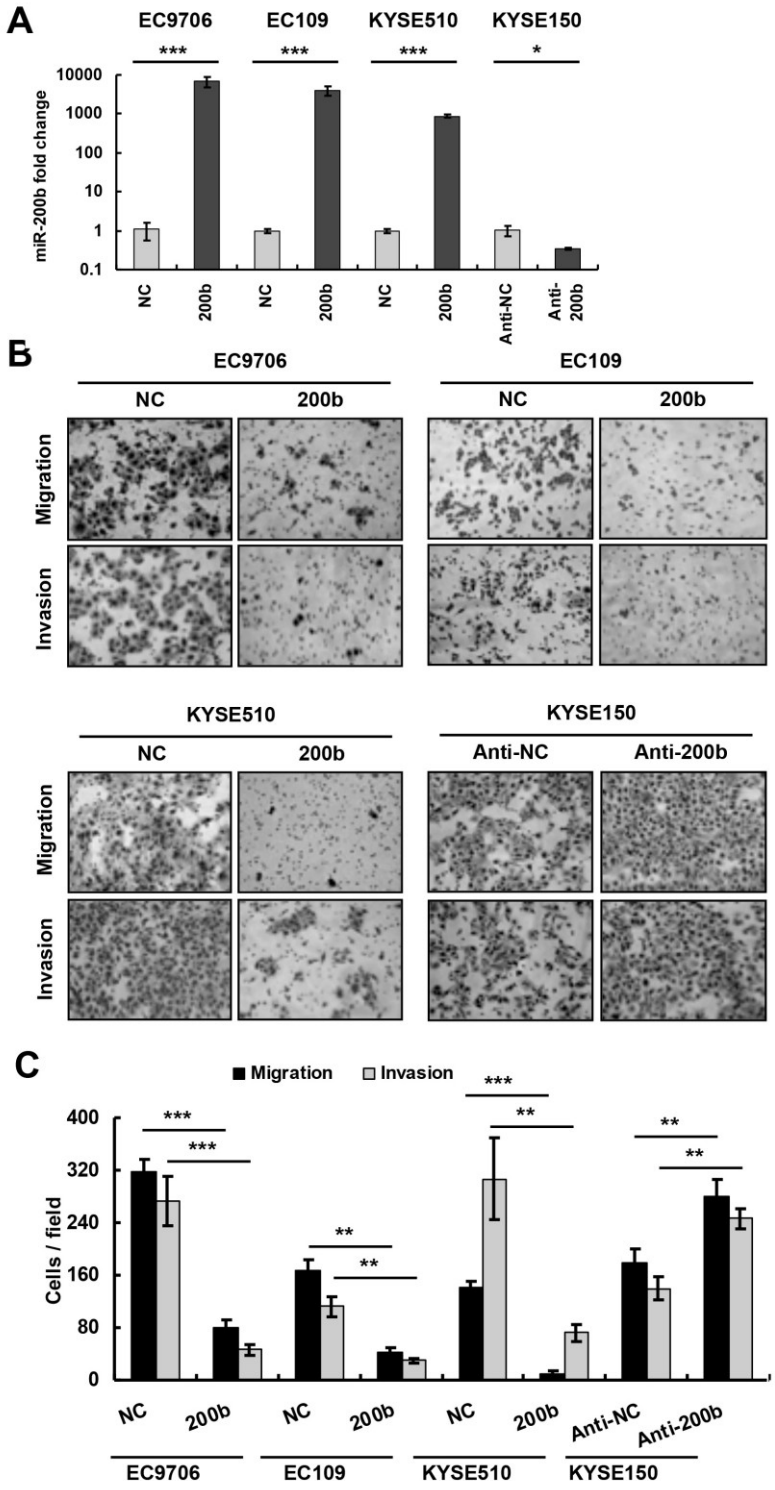

Figure 2.4 Kindlin-2 is an important mediator of the biological function of miR-200b in suppressing ESCC cell migration and invasiveness. (**A**) 48h after transfection, miR-200b expression was detected by Taqman real-time PCR (n=3, **P*<0.05, ****P*<0.001, Student's *t*-test). (**B** and **C**) Cell migration and invasiveness were determined using transwell migration/invasion assays (n=3, ***P*<0.01, ****P*<0.001, Student's *t*-test). **(Continued on the next page)**

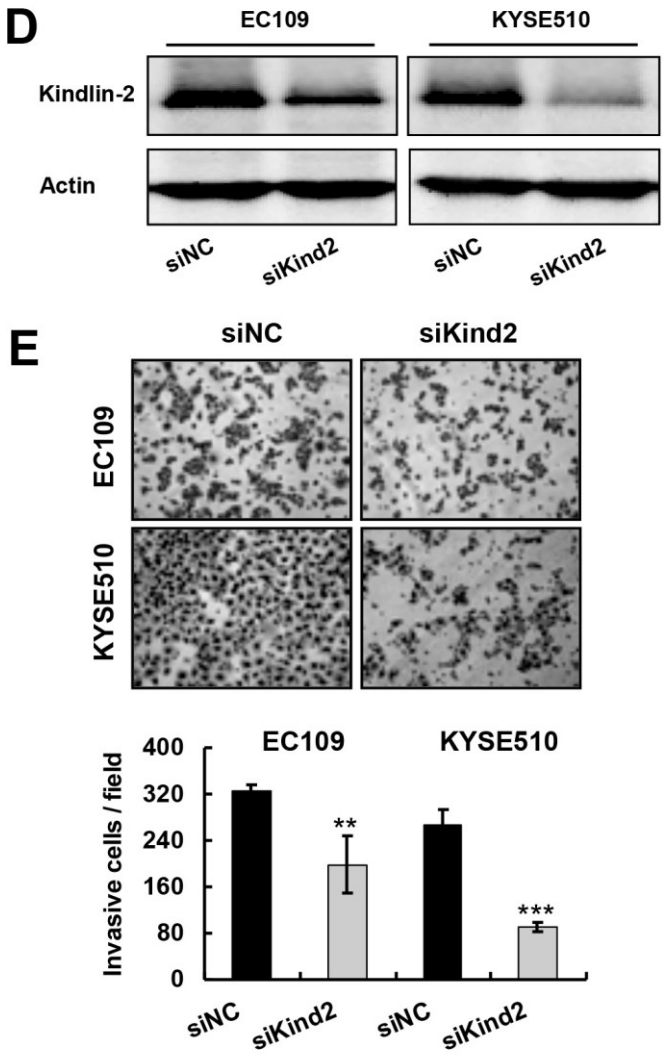

Figure 2.4D-E (**D**) siRNA mediated knockdown of Kindlin-2 was examined by Western-blot. Actin was used as an internal control. (**E**) The impact of Kindlin-2 knockdown on ESCC cell invasiveness was determined using transwell invasion assay as described above (n=3, ***P*<0.01, ****P*<0.001, Student's *t*-test). **(Continued on the next page)**

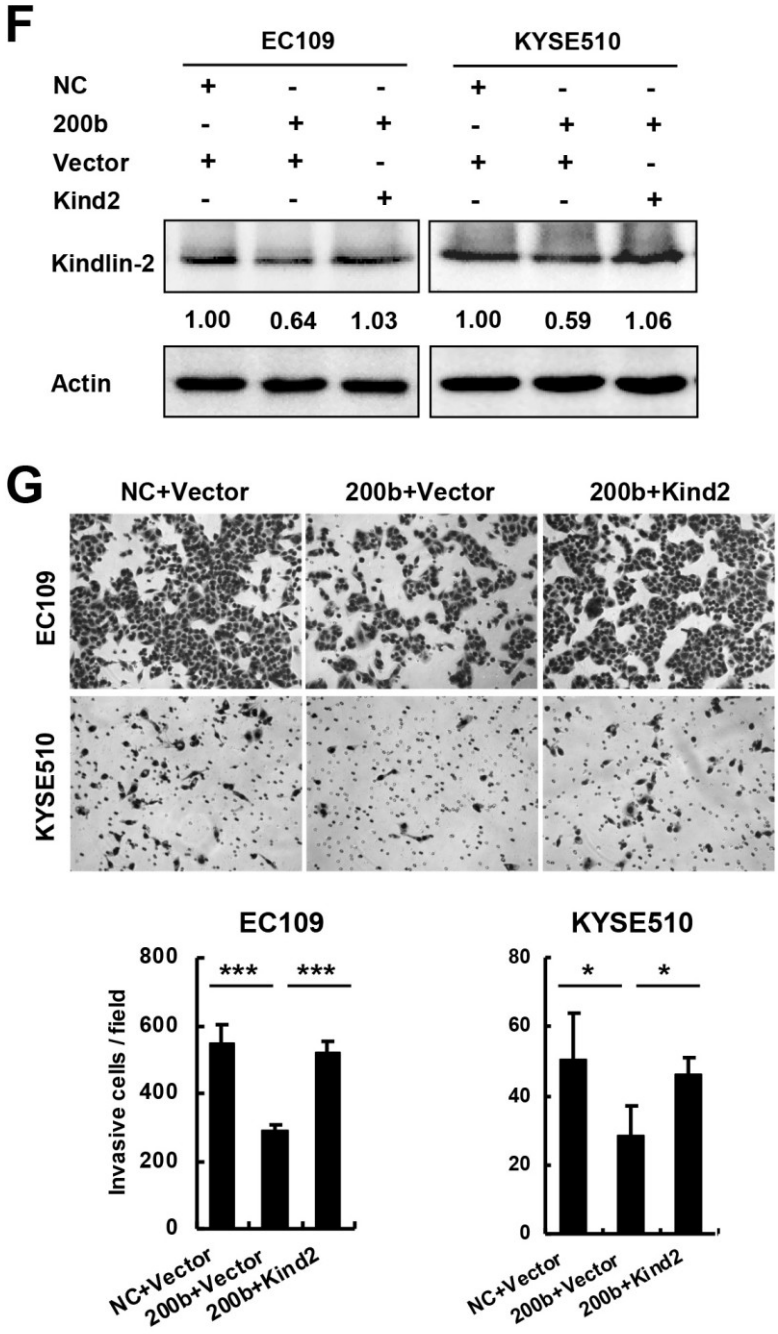

Figure 2.4F-G (**F**) 48h after the transfection of the indicated reagents, Kindlin-2 expression was examined by Western-blot, and Actin was used as an internal control. Vector: pcDNA3.1, Kind2: pcDNA3.1-Kindlin-2. The results shown are representatives of three repeated experiments. (**G**) Enforced expression of Kindlin-2 largely restored cell invasiveness that was suppressed by miR-200b (n=3, **P*<0.05, ****P*<0.001, Student's *t*-test).

2.4.5 Both miR-200b and Kindlin-2 regulate actin cytoskeleton and focal adhesion formation in ESCC cells

Previous studies have shown that Kindlin-2 regulates cell–extracellular matrix interaction, cytoskeletal structure, focal adhesion (FA) formation and cell spreading (31-33). Based on these observations, we hypothesized that miR-200b may regulate these biological functions via its downregulation of Kindlin-2. This hypothesis was supported by multiple experimental observations. First, after transfection of miR-200b mimic into two ESCC cell lines that express a low level of miR-200b (*i.e*. EC109 and KYSE510), cell spreading and protrusion formation, two key features dictated by actin cytoskeleton (34-36), were substantially inhibited **(Figure 2.5A)**. Second, confocal microscopy analysis showed that enforced expression of miR-200b mimic markedly suppressed actin cytoskeleton reorganization, as evidenced by decreased formation of stress fibers and filopodia protrusions in EC109 cells, and diminished podosomes in KYSE510 cells **(Figure 2.5B and C)**. Third, miR-200b mimic repressed the formation of large mature FAs in both cell lines, as revealed by confocal microscopy **(Figure 2.5B and C)**. Finally, quantitative analysis showed that the cell spreading areas were dramatically reduced as miR-200b mimic transfection in both cell lines **(Figure 2.5D)**. As shown in **Figure 2.6A-D**, siRNA knockdown of Kindlin-2 in EC109 and KYSE510 largely mimicked the biological effects of transfection of miR-200b mimic, *i.e.* reduced cell spreading area, decreased stress fibers and FA formation.

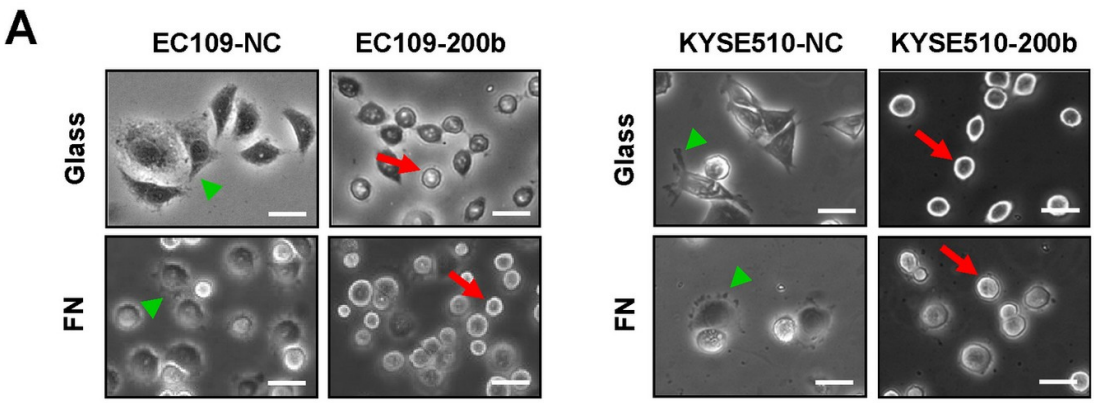

Figure 2.5 miR-200b represses ESCC cell spreading and focal adhesion formation. (**A**) The influence of miR-200b mimic transfection on ESCC cell morphology. Cells were seeded on glass slides (for 24h) or fibronectin-coated glass slides (for 1h). Arrowheads indicate cells with protrusions, and arrows indicate rounded cells with no visible protrusions. Scale bars: 30μm. **(Continued on the next page)**

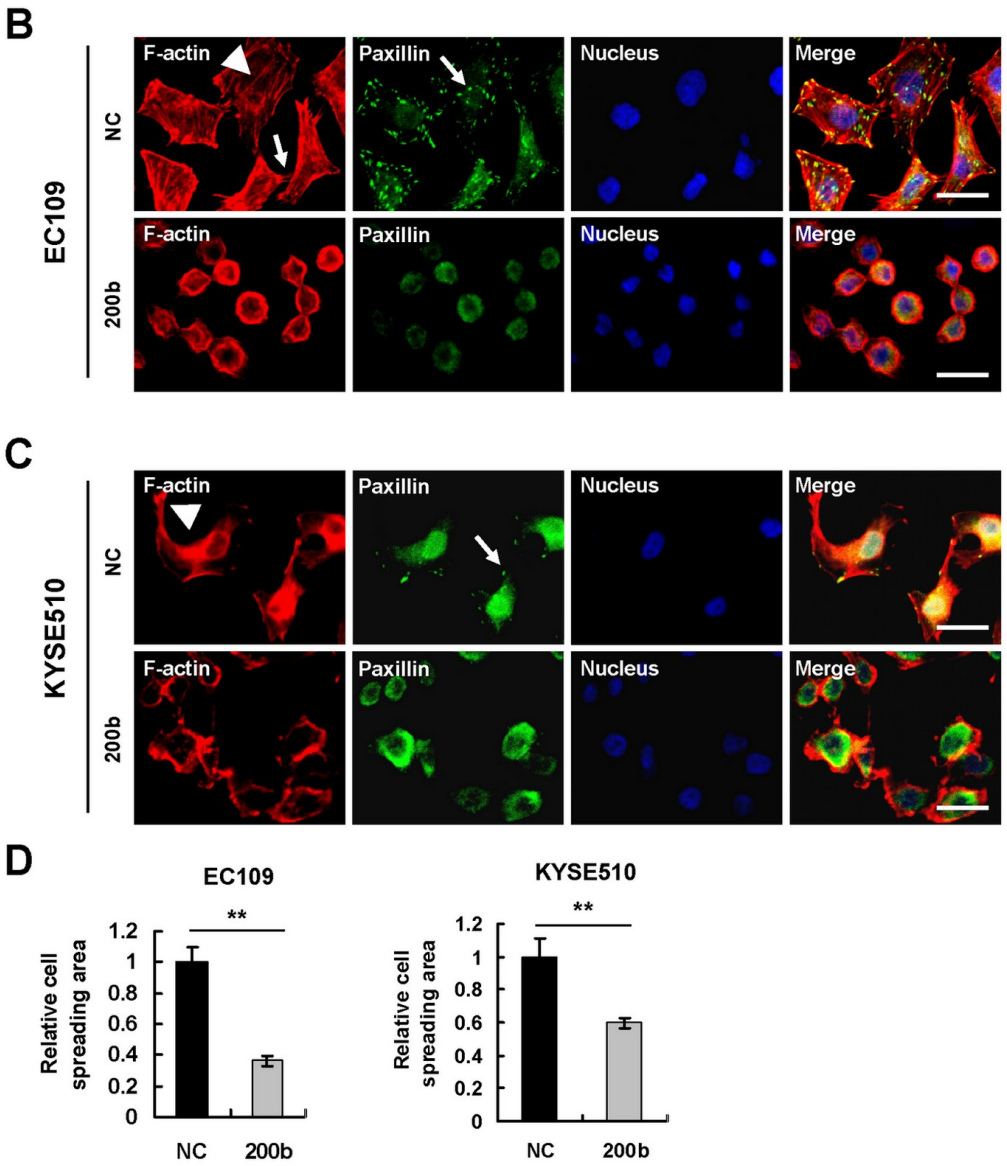

Figure 2.5B-D (**B** and **C**) The impact of miR-200b mimic transfection on actin cytoskeleton structure and focal adhesion formation was analyzed by confocal microscopy. Actin cytoskeleton and focal adhesions were visualized by phalloidin staining (red) and paxillin labeling (green), respectively. For EC109 cells, stress fibers and filopodia are respectively noted by arrowheads and arrows in the F-actin fields; arrows in the paxillin field indicate focal adhesions. For KYSE510 cells, arrowheads in the F-actin field indicate large podosomes, and arrows in the paxillin field indicate focal adhesions. Scale bars: 20μm. (**D**) miR-200b diminished cell spreading area in both EC109 and KYSE510 cells. Cell spreading area was measured with the software Image J, cells from at least three different fields were analyzed (**P<0.01, Student's t-test).

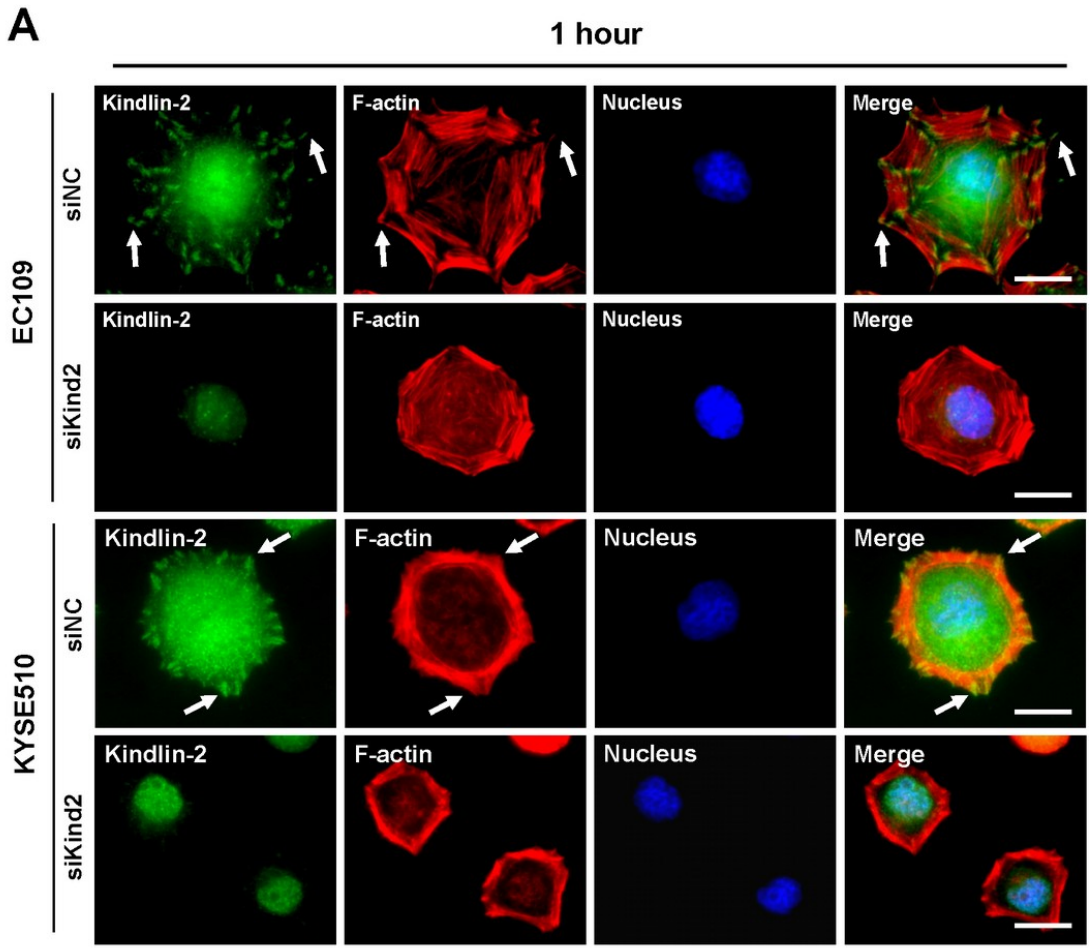

Figure 2.6 Kindlin-2 knockdown suppresses cell spreading and focal adhesion formation in ESCC cells. (**A**) After siNC or siKindlin-2 transfection, cells were seeded on fibronectin-coated slides and allowed to adhere for 1h before the detection of Kindlin-2 and F-actin cytoskeleton by immunofluorescence. Arrows indicate the colocalization of Kindlin-2 and cell spreading edges (marked with F-actin staining) in siNC transfected cells. Scale bars: 10μm Scale bars: 20μm. **(Continued on the next page)**

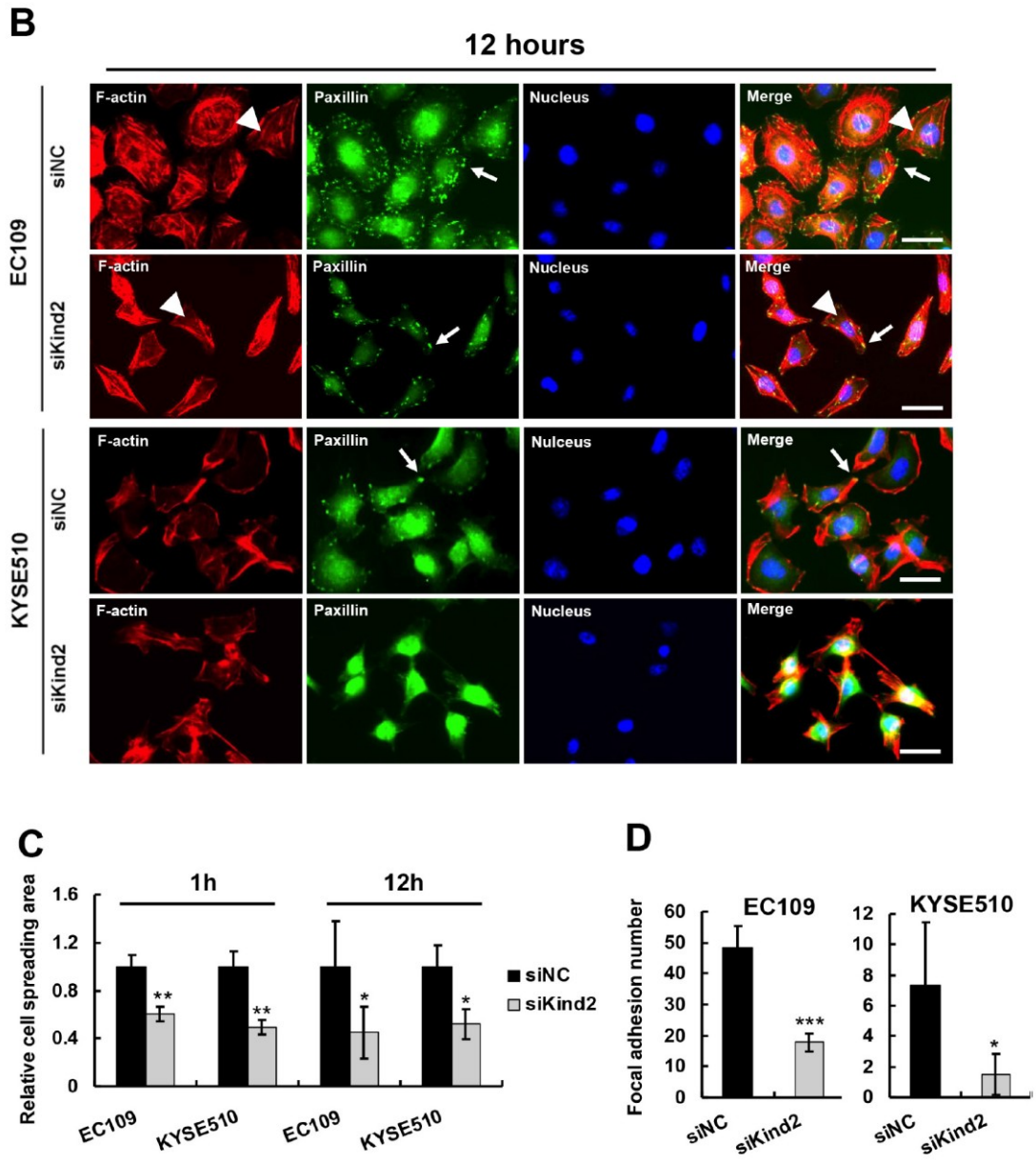

Figure 2.6B-D (B) After siNC or siKindlin-2 transfection, cells were allowed to adhere for 12h on fibronectin-coated slides. Focal adhesions and F-actin cytoskeleton were examined by immunofluorescence. Arrowheads indicate stress fibers and arrows indicate focal adhesions as detected by paxillin staining. (**C**) Cell spreading area was measured with the software ImageJ after adhesion for 1h or 12h on fibronectin-coated slides, cells from at least three different fields were analyzed. (**D**) After adhesion for 12h on fibronectin-coated slides, the average focal adhesion number was compared between siNC and siKind2 transfected cells, cells from at least three different fields were analyzed (*P<0.05, **P<0.01, ***P<0.001, Student's t-test).

2.4.6 Both miR-200b and Kindlin-2 regulate the activity of the Rho-family GTPases

Since members of the Rho-family GTPases have been demonstrated as master regulators of actin cytoskeleton reorganization (37), we speculated that miR-200b might have influenced the cytoskeletal structure by regulating Rho-family GTPases. In support of this concept, transfection with miR-200b mimic significantly repressed the expression levels of GTP-bound Cdc42 and RhoA in both EC109 and KYSE510 cells, suggesting a decreased activity of these Rho-family GTPases **(Figure 2.7A)**. However, the active form of another member of Rho-family GTPases, Rac1, was undetectable in both EC109 and KYSE510 cells **(Figure 2.8)**. As shown in **Figure 2.7B**, Kindlin-2 knockdown produced similar biological effects as miR-200b mimic transfection in both EC109 and KYSE510 cells.

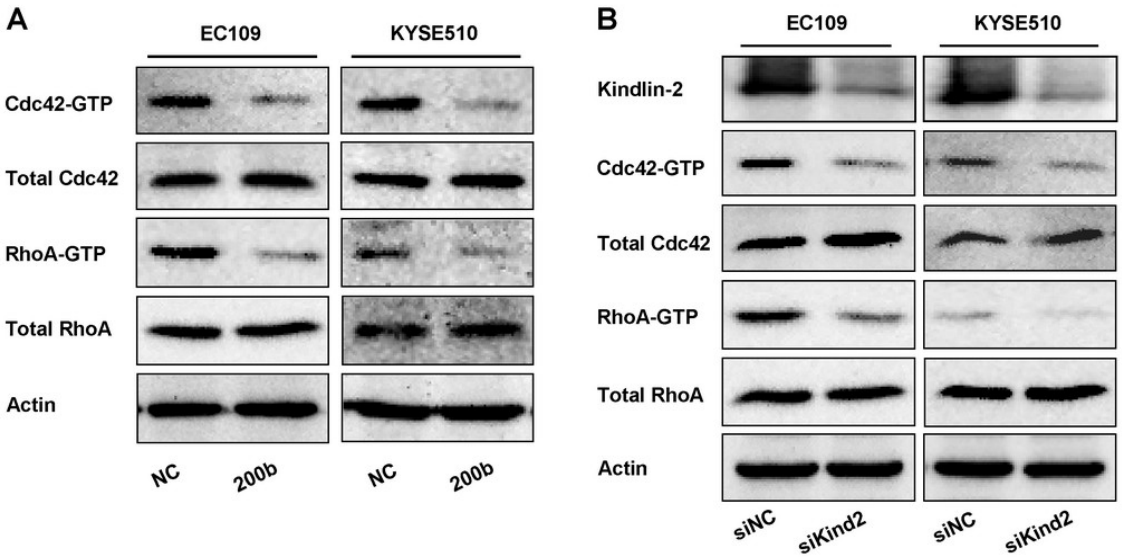

Figure 2.7 Kindlin-2 is an important mediator of miR-200b in modulating the activity of the Rho-family GTPases and FAK. (**A** and **B**) 48 hours after miR-200b mimic transfection (A) or Kindlin-2 knockdown (B), GTP-bound (active) forms of Cdc42 and RhoA were pulled down and detected by Western-blot. Total Cdc42 and RhoA expression from equal amounts of input lysates was detected, and Actin was used as an internal control. **(Continued on the next page)**

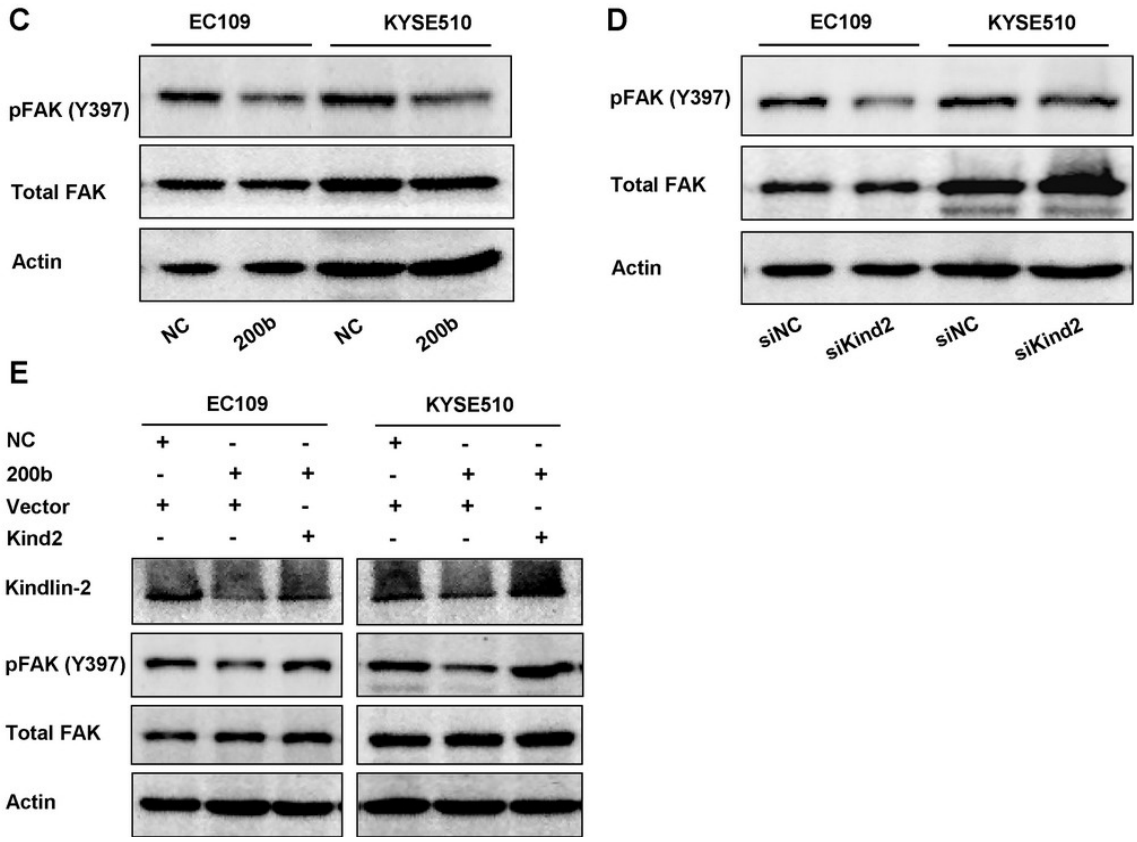

Figure 2.7C-E (**C** and **D**) 48 hours after miR-200b mimic transfection or Kindlin-2 knockdown, phosphorylated FAK on Tyrosine397, *i.e.* pFAK(Y397), and total FAK was detected by Western-blot. Actin was used as an internal control. (**E**) 48h after the transfection of the indicated reagents, the indicated proteins were examined by Western-blot, and Actin was used as an internal control. Vector: pcDNA3.1, Kind2: pcDNA3.1-Kindlin-2.

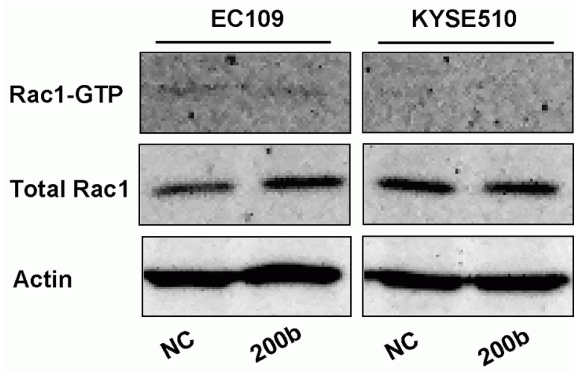

Figure 2.8 The impact of miR-200b on the activation of Rac1. GTP-bound (active form) Rac1 was pulled down after miR-200b mimic or NC transfection in EC109 and KYSE510 cells, active form of Rac1 and total Rac1 and were detected by Western blot.

2.4.7 Both miR-200b and Kindlin-2 regulate the expression of pFAK (Y397)

Since focal adhesion kinase (FAK) has been shown to play a crucial role in the regulation of the formation and turnover of focal adhesions (38,39) as well as cell spreading (40, 41), we examined the biological impact of miR-200b on FAK phosphorylation. As shown in **Figure 2.7C**, transfection of miR-200b mimic inhibited the phosphorylation of FAK on Tyrosine397 in both EC109 and KYSE510 cells. To determine whether Kindlin-2 plays a role in mediating the biological effects of miR-200b in the modulation of FAK activation, we inhibited Kindlin-2 expression using siRNA. As shown in **Figure 2.7D**, knockdown of Kindlin-2 by siRNA also decreased the expression of pFAK(Y397). In contrast, enforced expression of Kindlin-2 markedly restored pFAK(Y397) expression that was suppressed by miR-200b mimic transfection

(Figure 2.7E). Collectively, these findings suggest that Kindlin-2 is an important mediator of the biological functions of miR-200b in ESCC cells.

2.4.8 miR-200b suppresses ESCC tumor invasion *in vivo*

The data presented above show that miR-200b impairs ESCC cell migration and invasion *in vitro.* Then, we asked if miR-200b also affects the tumor invasiveness of ESCC *in vivo*. To this end, EC109 cells were transfected with either a miR-200b mimic or negative control RNA, and these cells were injected into the left footpads of mice. As shown in **Figure 2.8A**, enforced expression of miR-200b significantly reduced the local invasion area compared with the negative control (P=0.024). Notably, invasive tumor nodules were found in the unilateral thigh region in a higher proportion of mice in the negative control group (6/10) compared to the miR-200b-transfected group (2/9) (**Figure 2.8A-C**), even though the difference does not reach statistical significance (P=0.17). As shown in **Figure 2.8D-E**, despite the inhibitory effect of miR-200b in the tumor invasion of ESCC, the expression of neither E-cadherin nor vimentin was appreciably altered by the miR-200b mimic in the xenografts.

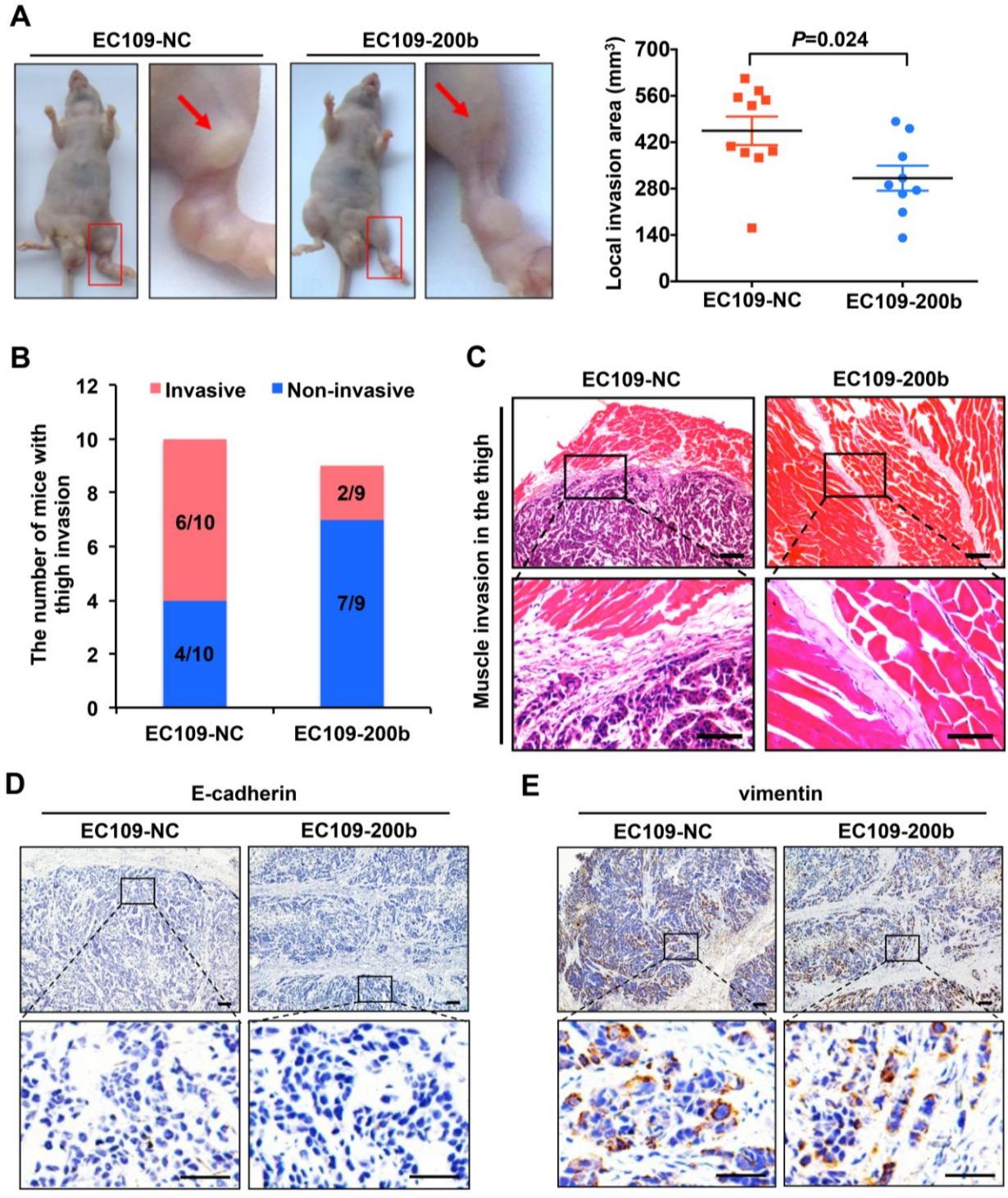

Figure 2.9 miR-200b suppresses ESCC tumor invasion *in vivo*. (**A**) Left panel: representative mice showing the impact of miR-200b on ESCC tumor invasion *in vivo*. Note that the invasion sites on the thigh were magnified, and the arrows indicate the invaded tumor nodules. Right panel: the local invasion areas of tumors formed by EC109-NC and EC109-200b cells were compared. Data are presented as mean ± SD. Student's *t* test was used in the statistical

analysis. (**B**) The proportions of mice that developed invasive tumors in the thigh region were compared. n=10 for NC transfected group, and n=9 for miR-200b transfected group. (**C**) Representative H&E staining showing the invaded tumor nodules within the muscle of the thigh area. Upper panel scale bars: 100μm; lower panel scale bars: 50μm. (**D-E**) Immunostaining of E-cadherin and vimentin in EC109-NC and EC109-200b tumor xenografts dissected from the mice. Upper panel scale bars: 100μm; lower panel scale bars: 50μm.

2.4.9 The miR-200b-ZEB1/2-E-cadherin axis in ESCC cells

We then asked if the tumor suppressor effects are mediated via the ZEB/E-cadherin axis. As shown in **Figure 2.10A-B**, the expression of miR-200b was substantially decreased in 6/7 ESCC cell lines as compared to an immortalized esophageal cell line (P<0.01), and a low expression of miR-200b was associated with a high expression of ZEB1/2 mRNA in this panel of cell lines (P<0.05). Enforced expression of miR-200b in EC109, a miR-200-low cell line, dramatically decreased the expression of ZEB1/2 in these cells (**Figure 2.10C**). Furthermore, in the cohort of 88 ESCC tumor samples, we found a significant inverse correlation between the expression levels of ZEB1/2 and that of miR-200b (P=0.01) (**Figure 2.10D**). Importantly, a high expression of ZEB2 significantly correlated with a shorter overall survival (P=0.034), although the correlation between ZEB1 and survival just fell short of statistical significance (P=0.078) (**Figure 2.10E**). Nonetheless, although transfection of the miR-200b mimic induced dramatic morphological changes in EC109 and EC9706 cells (**Figure 2.11A**), it did not increase the protein expression of E-cadherin, and only slightly increased its mRNA (**Figure 2.11B)**.

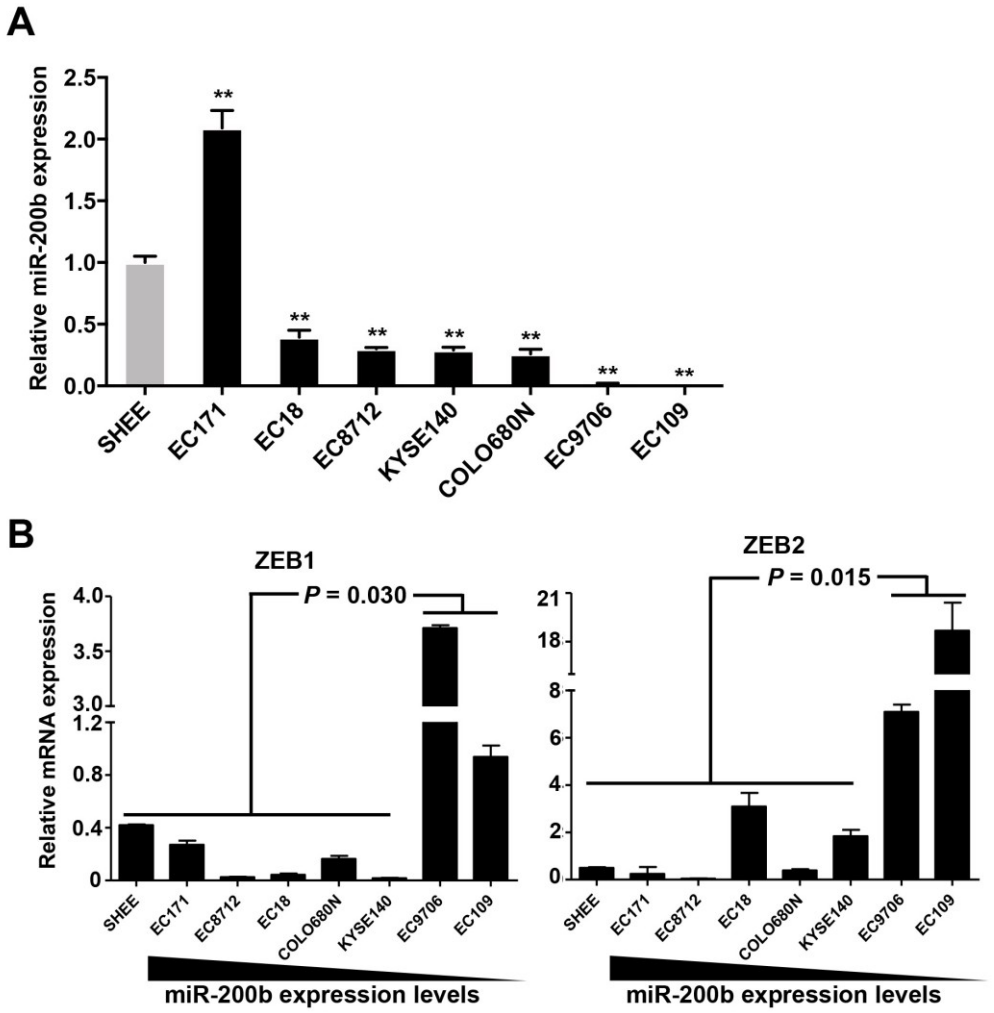

Figure 2.10 The miR-200b-ZEB1/2 axis in ESCC cell lines and patient tumors. (**A-B**) The expression of miR-200b and ZEB1/2 were determined using real-time PCR in a panel of cell lines. SHEE, an immortalized cell line was used as a normal control. Data are presented as mean ± SD (n=3, ***P*<0.01, Student's *t* test). **(Continued on the next page)**

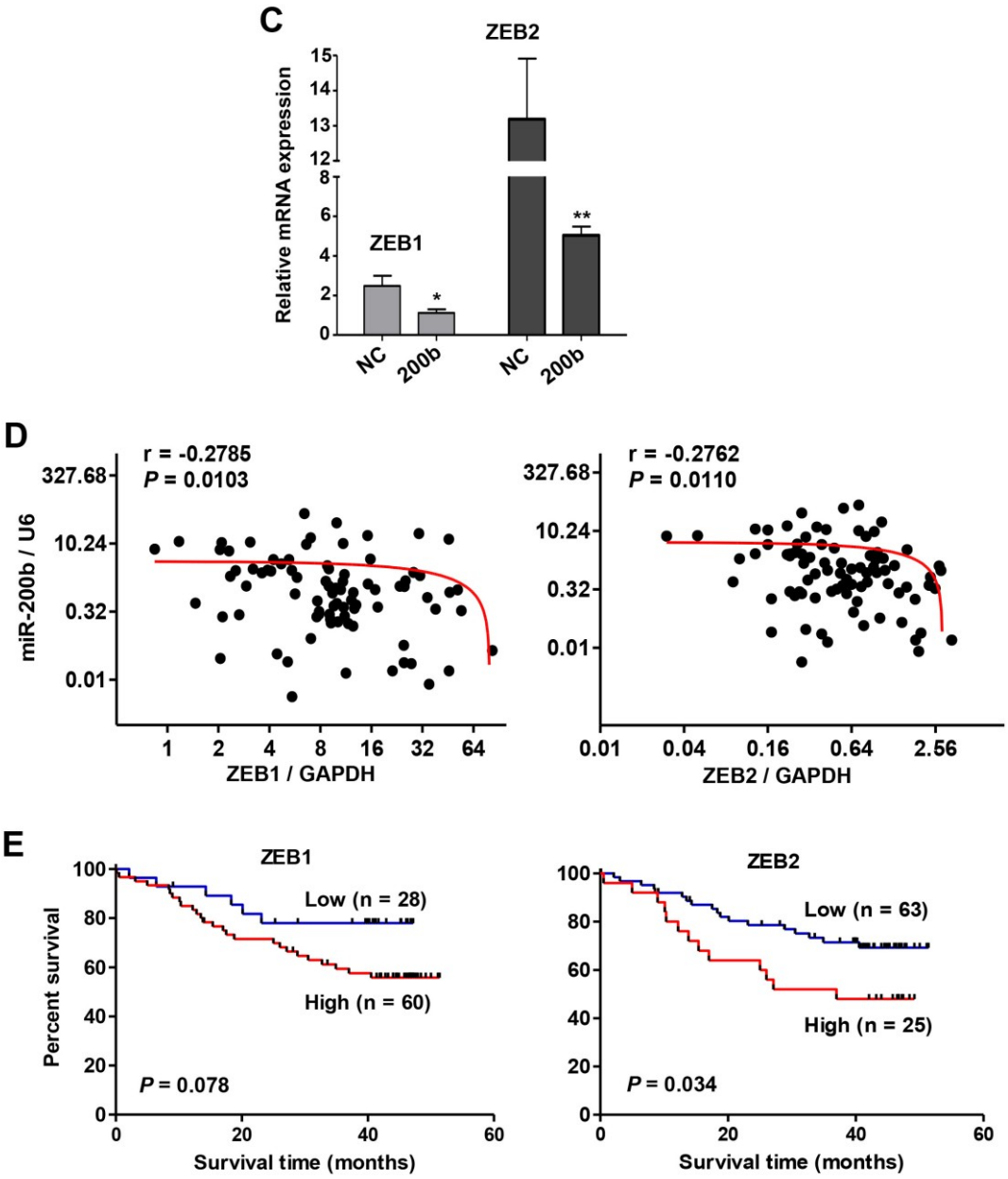

Figure 2.10C-E (**C**) In EC109 cells, the influence of the enforced expression of miR-200b on the expression of ZEB1/2 mRNA was determined using real-time PCR (n=3, **P*<0.05, ***P*<0.01, Student's *t* test). (**D**) The correlation between the expression levels of miR-200b and ZEB1/2 mRNA in ESCC samples were analyzed using Spearman's rank correlation analysis (n=88). U6 and GAPDH were used as loading controls for the detection of miR-200 and ZEB1/2, respectively. (**E**) The association of ZEB1 and ZEB2 expression with the overall survival of ESCC patients was analyzed using Kaplan-Meier survival analysis, and log-rank test was used in the statistical analysis.

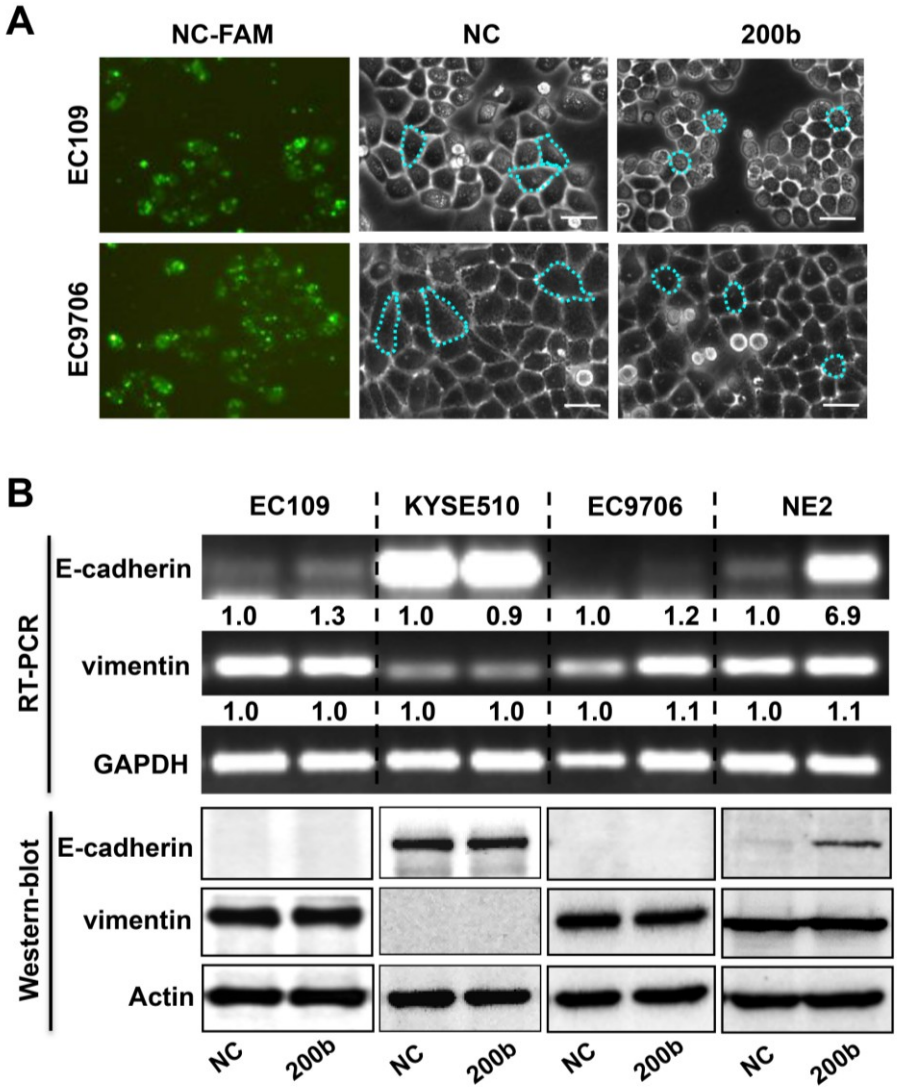

Figure 2.11 miR-200b suppresses ESCC cell invasiveness without altering E-cadherin protein expression. (**A**) EC109 and EC9706 cells were transfected with either a miR-200b mimic or negative control RNA (NC). In parallel, transfection of a fluorescein amidite-labeled NC was used as a positive control to evaluate the transfection efficiency. Dashed lines were used to note the morphological changes. (**B**) RT-PCR and Western-blot assays were performed to determine the impact of miR-200b mimic transfection on the expression of E-cadherin and vimentin in ESCC cell lines (EC109, KYSE510 and EC9706) and an immortalized esophageal cell line NE2.

Using immunohistochemistry applied to 37 cases of ESCC tumor samples, we found no significant correlation between the E-cadherin and miR-200b or ZEB1/2 (**Figure 2.12A-B**). These results were further confirmed by Western blot analysis (**Figure 2.12C-D**). This lack of correlation between E-cadherin and miR-200b or ZEB1/2 is probably due to the fact that most ESCC tumors did not express E-cadherin, which has been reported to be frequently silenced via gene methylation in ESCC [72]. In keeping with this concept, treatment of ESCC cell lines with 5-aza-dC restored the expression of E-cadherin which was under the regulatory control of the miR-200b-ZEB1/2 axis (**Figure 2.12E-F**). Furthermore, in an immortalized esophageal epithelial cell line NE2, in which the loss of E-cadherin has been shown to be unassociated with DNA hypermethylation [73], miR-200b mimic transfection could effectively induce E-cadherin expression (**Figure 2.11B**). Overall, these data suggests that an E- cadherin-independent mechanism may mediate the tumor suppressive effects of miR-200b in ESCC.

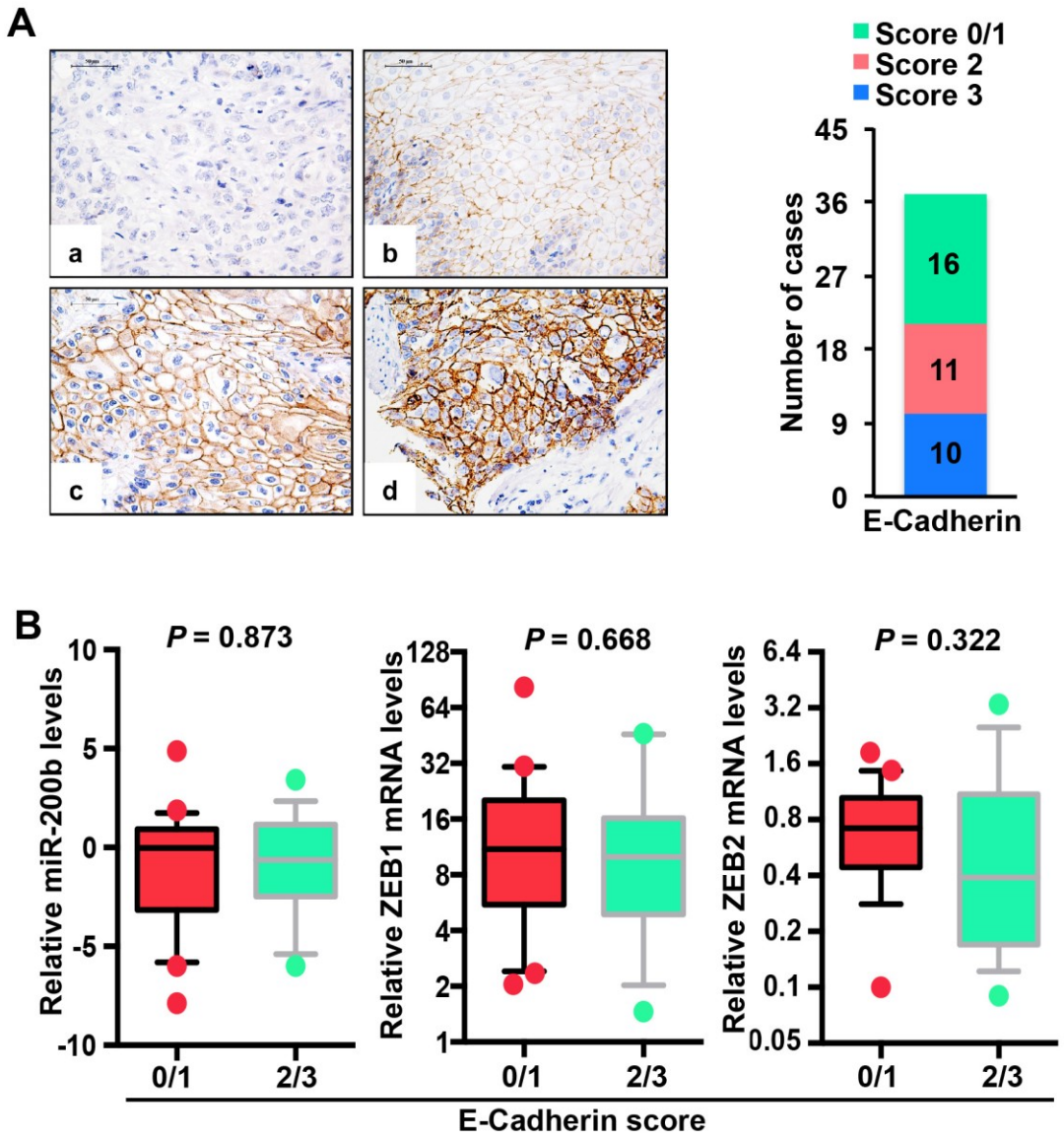

Figure 2.12 The expression levels of E-cadherin do not correlate with miR-200b or ZEB1/2 in ESCC tumors. (**A**) The expression of E-cadherin was detected using immunohistochemistry in 37 cases of ESCC specimens. Left panel: representative images show: (a) negative staining, score 0; (b) weak staining, score 1; (c) moderate staining, score 2; (d) strong staining, score 3. Right panel: the proportion of tumors displaying different E-cadherin staining intensities. (**B**) The expression of miR-200b and ZEB1/2 were compared between ESCC tumors with different staining intensities of E-cadherin. Box plots are presented as 10-90 percentile. Statistical analysis was performed using Student's *t* test and Mann-Whitney *U* test for miR-200b and ZEB1/2, respectively (n=37). **(Continued on the next page)**

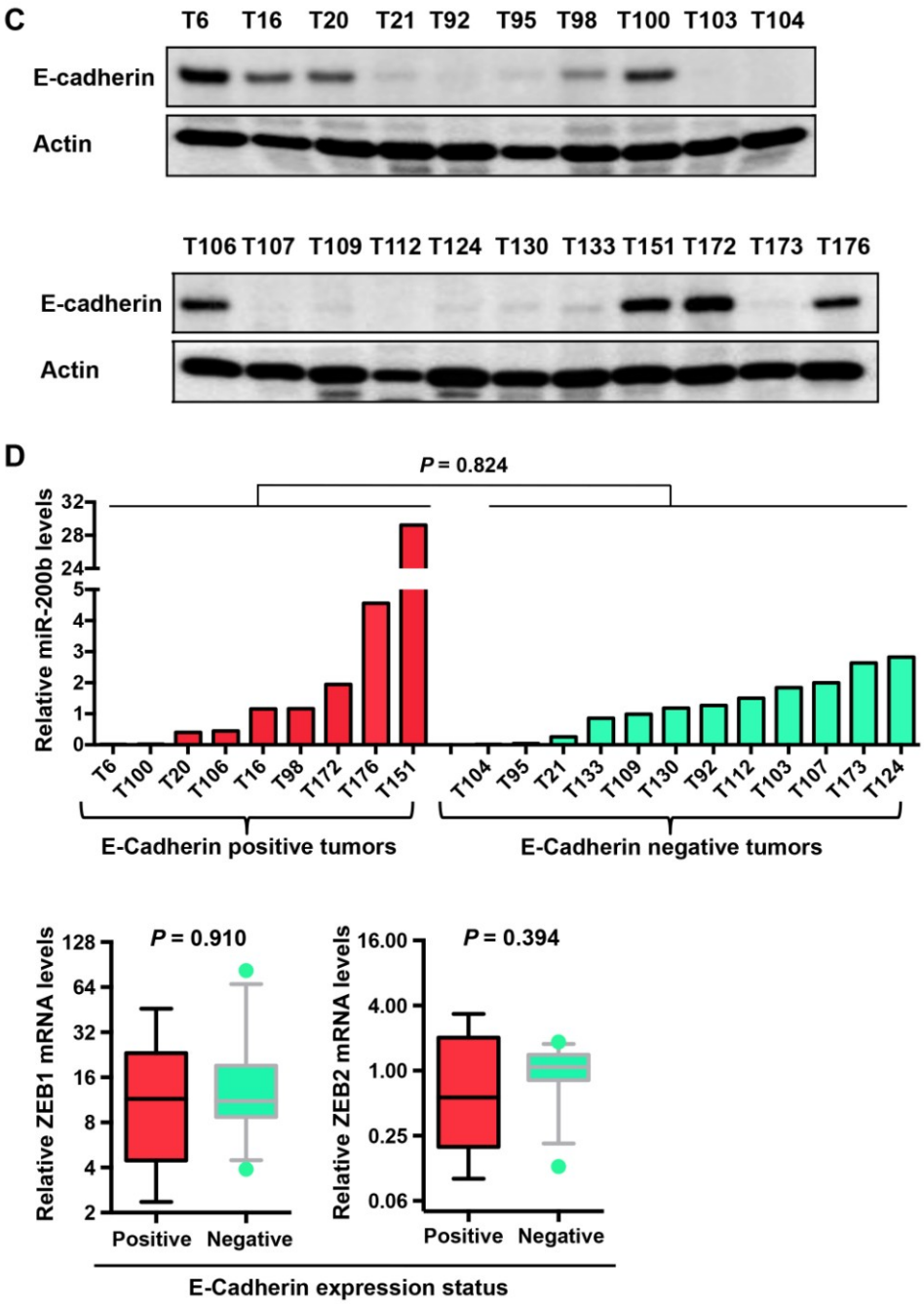

Figure 2.12C-D (**C**) Western-blot was performed to determine E-cadherin expression in 22 cases of frozen tumors randomly chosen from the 37 cases of ESCC tumors described in (A). Actin was used as a loading control. (**D**) The expression of miR-200b and ZEB1/2 were compared between ESCC tumors with different expression levels of E-cadherin as determined by Western-blot shown in (C). Statistical analysis was performed using Student's *t* test and Mann-Whitney *U* test for miR-200b and ZEB1/2, respectively. Box plots are presented as 10-90 percentile. **(Continued on the next page)**

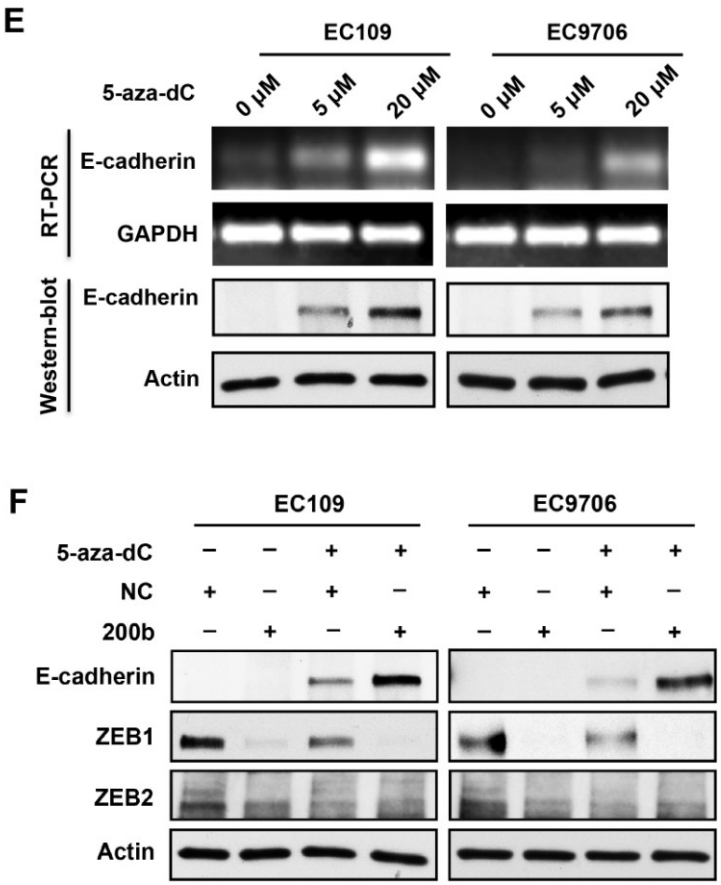

Figure 2.12E-F (E) RT-PCR and Western-blot assays were performed to determine the impact of 5-aza-dC treatment (72h) on the expression of E-cadherin and vimentin in EC109 and EC9706 cells. GAPDH and Actin were used as loading controls for RT-PCR and Western-blot, respectively. (F) Western-blot was performed to determine the impact of 5-aza-dC treatment and/or miR-200b mimic transfection on the expression of E-cadherin. Actin was used as a loading control.

2.4.10 The modulation of the of the PI3K-AKT pathway mediates the biological effect of miR-200b

It has been reported that the PI3K pathway plays an important role in modulating actin cytoskeleton and cell morphology [74,75], we assessed whether the phenotypic changes caused by miR-200b was linked to the PI3K pathway. As shown in **Figure 2.13A**, enforced expression of miR-200b decreased the expression of $pAKT^{Ser473}$ (pAKT), a key downstream mediator of the PI3K pathway, in both EC109 and EC9706 cells. In comparison, miR-200b inhibition in KYSE150, an ESCC cell line that expressed a relatively high level of miR-200b, substantially increased pAKT. Then, we assessed whether inhibition of the PI3K pathway using LY294002 can mimic the biological function of miR-200b in ESCC cells. As shown in **Figure 2.13B-C**, LY294002 induced cell rounding and inhibition of invasiveness in a dose-dependent manner in both EC109 and EC9706 cells. Moreover, the morphological changes and invasiveness enhanced by miR-200b inhibition in KYSE150 cells were dramatically retarded by LY294002 treatment (**Figure 2.13D**). Furthermore, as shown in **Figure 2.13E**, enforced expression of a constitutively active form of AKT, *i.e.* myristoylated AKT (myr-AKT) significantly restored invasiveness that was suppressed by miR-200b in both EC109 and EC9706 cells ($P<0.05$).

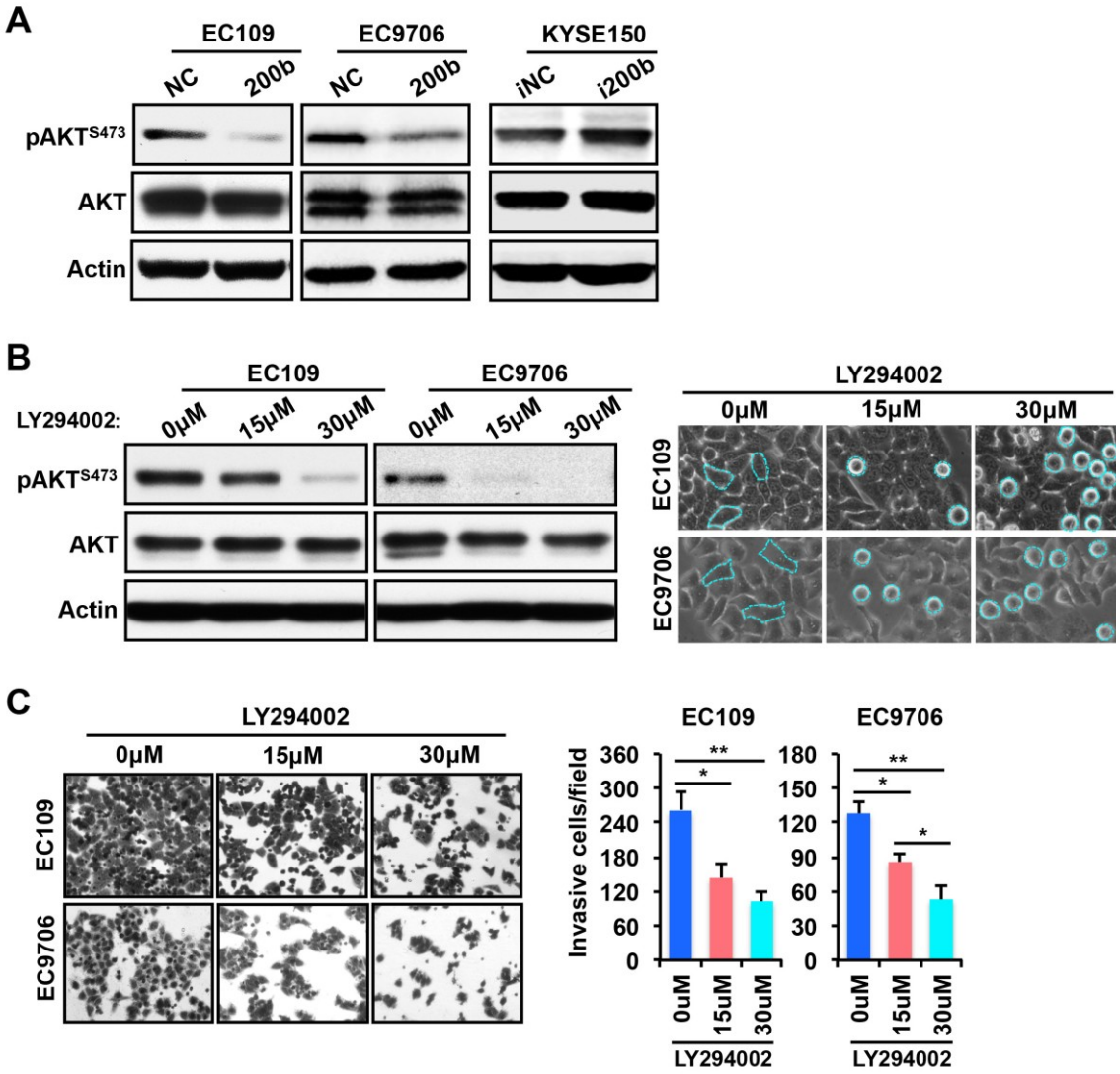

Figure 2.13 The Kindlin-2-Integrin β1-AKT cascade mediates the biological effect of miR-200b in suppressing ESCC cell invasiveness. (**A**) The effects of miR-200b mimic (200b) or miR-200b inhibitor (i200b) transfection on the expression of pAKT^{Ser473} (pAKT^{S473}) was determined by Western-blot. Actin was used as a loading control. (**B**) Left panel: the inhibitor effect of the PI3K inhibitor LY294002 on the expression of pAKT^{S473} was determined by Western-blot. Actin was used as a loading control. Right panel: The impact of LY294002 on cell morphology. Dashed lines were used to note the morphological changes. (**C**) The impact of LY294002 on cell invasiveness was detected using transwell invasiveness assays. Data are presented as mean ± SD (n=3, **P*<0.05, ***P*<0.01, Student's *t* test). **(Continued on the next page)**

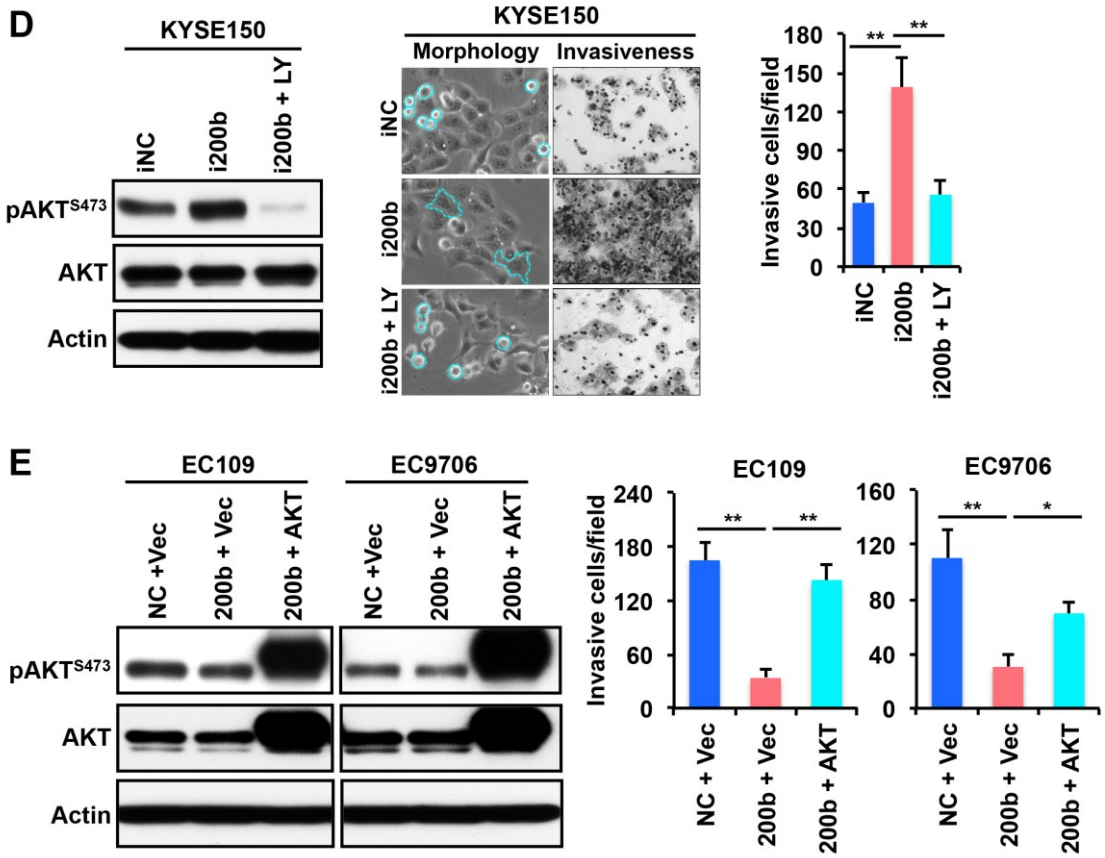

Figure 2.13D-E (D) LY294002 (LY) suppresses the biological effects of miR-200b inhibitor (i200b) in KYSE150 cells. Data are presented as mean ± SD (n=5, ***P*<0.01, Student's *t* test). (E) A constitutively active form of AKT, myristoylated AKT (myr-AKT), restored cell invasiveness that was suppressed by miR-200b mimic transfection. Data are presented as mean ± SD (n=3, ***P*<0.01, Student's *t* test). **(Continued on the next page)**

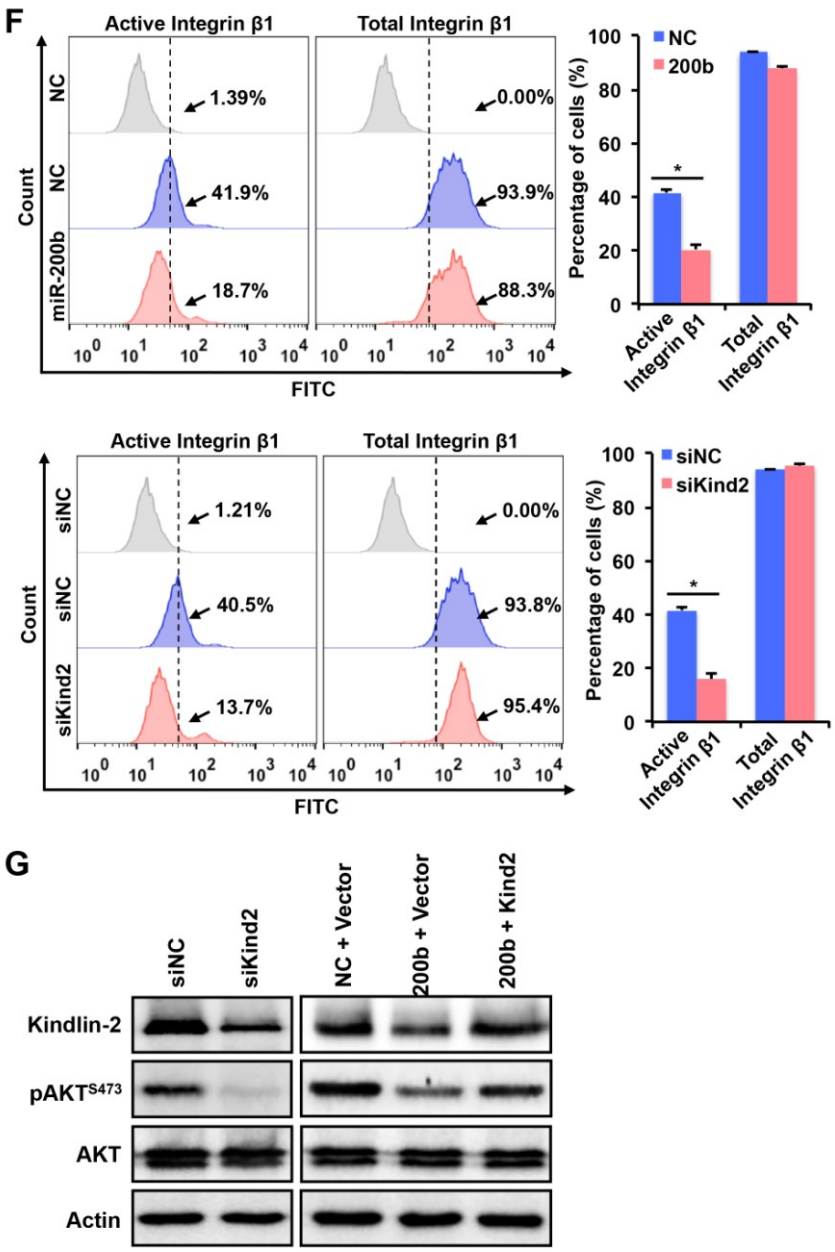

Figure 2.13F-G (**F**) In EC109 cells, flow cytometry was performed to assess the effects of enforced expression of miR-200b and Kindlin-2 knockdown on the expression of active/total Integrin β1. The grey graphs indicate negative control staining. Data are presented as mean ± SD. **P*<0.05, Student's *t* test (n=3). (**G**) In EC109 cells, Western-blot was performed to determine the expression of Kindlin-2 and pAKT^{S473} upon transfection. Actin was used as a loading control.

2.4.11 The Kindlin-2-Integrin β1-AKT axis

The mechanism underlying the suppression of the PI3K pathway by miR-200b remains unclear in ESCC. Since Kindlin-2, a target of miR-200b [68], is one of the key molecules mediating the inside-out activation of Integrin β1 [78,79], and Integrin β1 has been shown to play important roles in the activation of the PI3K-AKT pathway [74-77], we hypothesized that the miR-200b-Kindlin-2 axis modulates the Integrin β1-PI3K-AKT pathway. First, as shown in **Figure 2.13F**, both enforced expression of miR-200b and Kindlin-2 knockdown significantly decreased the percentage of cells with active Integrin β1, detected by flow cytometry. Second, as shown in **Figure 2.13G**, knockdown of Kindlin-2 dramatically decreased the expression of pAKT, and re-expression of Kindlin-2 restored the pAKT expression that was suppressed by miR-200b mimic transfection. Moreover, data form the GSEA (Gene Set Enrichment Analysis) [80,81] showed that Kindlin-2 expression was positively correlated with the activation of the Integrin signaling pathway and the PI3K-AKT signaling pathway in two independent cohorts of ESCC patients (both $P<0.01$, n=20 and n=53, respectively) (**Figure 2.14A-B**). Specifically, up-regulated target genes in both signaling pathways tend to be more enriched in tumors that expressed higher levels of Kindlin-2 in both cohorts of ESCC patients. Collectively, these data suggest that miR-200b suppresses the Integrin β1-AKT pathway via targeting Kindlin-2, which may mediate the role of miR-200b in mitigating ESCC cell invasiveness.

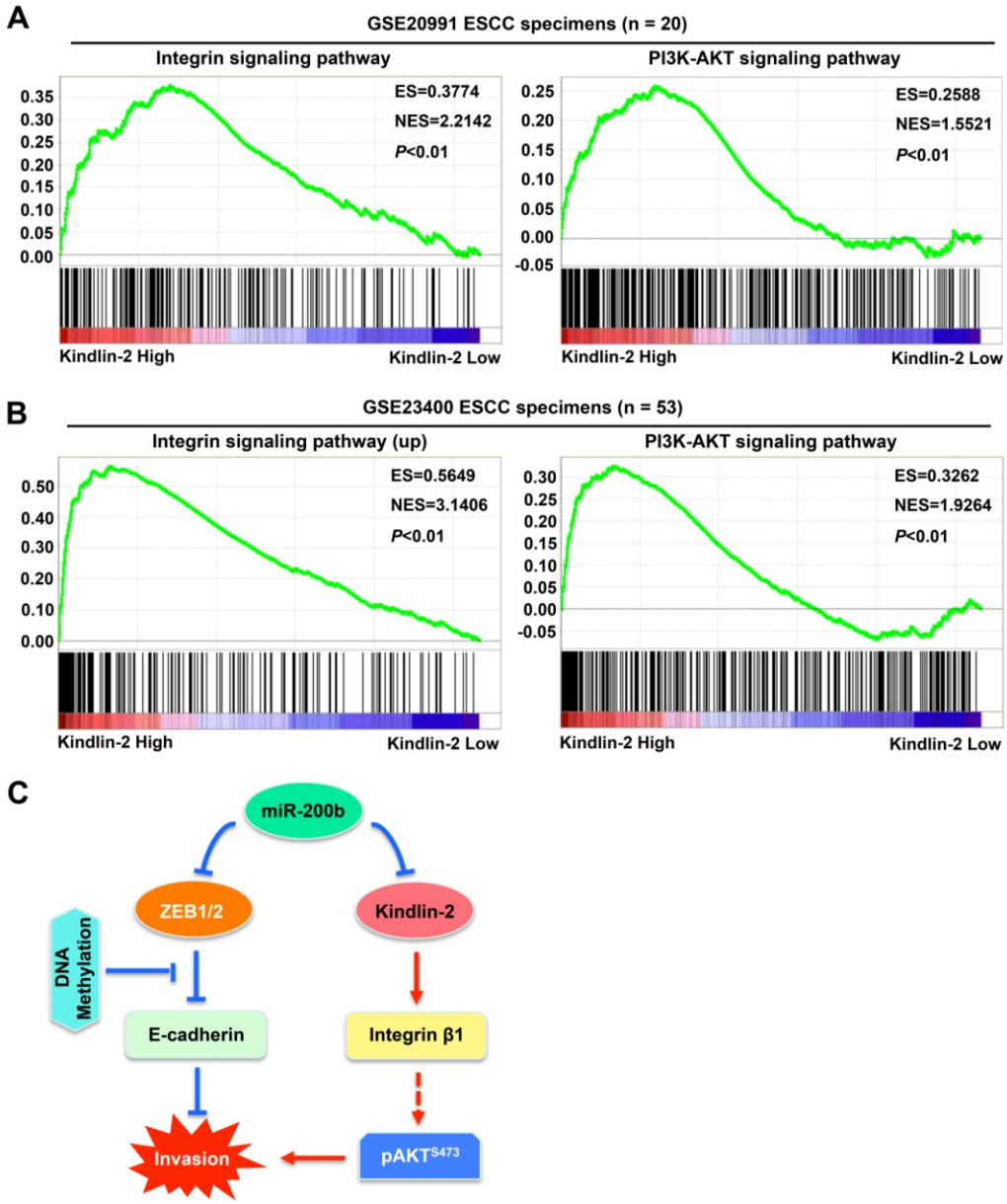

Figure 2.14 Correlation between Kindlin-2 and the Integrin signaling pathway and the PI3K-AKT signaling pathway in ESCC tumors. (A-B) GSEA (Gene Set Enrichment Analysis) was performed to analysis the correlation between Kindlin-2 and the Integrin signaling pathway and the PI3K-AKT signaling pathway in two independent sets of published ESCC patient gene profiles (NCBI/GEO/GSE20991, n=20; and NCBI/GEO/GSE23400, n=53). (C) A schematic model showing the possible mechanisms underlying the invasiveness-suppressing role of miR-200b in ESCC. Note that arrows indicate stimulation effects, whereas blunt arrows indicate inhibitory effects.

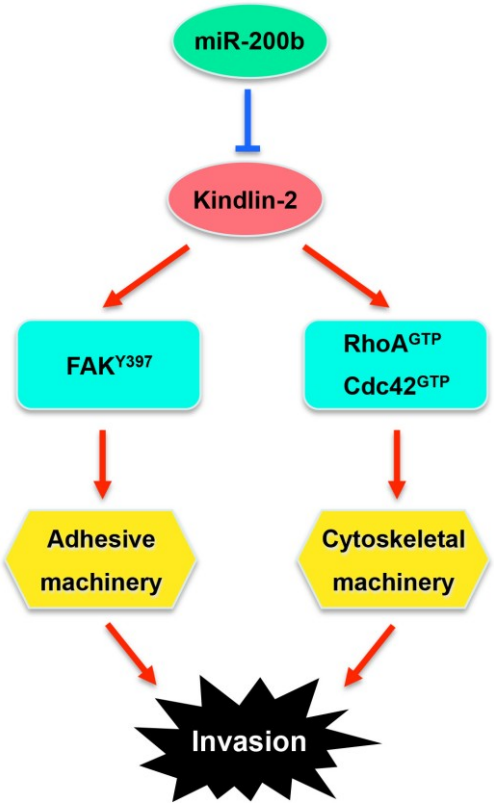

Figure 2.15 miR-200b suppresses ESCC cell invasion by modulating the adhesive and cytoskeletal machinery via targeting Kindlin-2. Note that arrows indicate stimulation effects, whereas blunt arrows indicate inhibitory effects.

2.5 Discussion

During the past few years, mounting evidence has demonstrated that loss of the miR-200 family promotes tumor initiation by modulating the stemness of cancer stem cells (42-44), and enhances tumor malignant progression by regulating epithelial-to-mesenchymal transition and modulating the tumor microenvironment that favors metastasis (10-14,45). However, our understanding about the clinical significance and the biological role of the miR-200 family in ESCC is rather limited. In keeping with the previous concepts, we found that low expression of the members of the miR-200b-200a-429 cluster significantly correlate with short patient survival and

aggressive phenotypes, the first study that confirms the clinical significance of the miR-200b cluster in ESCC.

While we have presented compelling evidence that the miR-200b cluster is decreased in ESCC and has associated features suggesting tumor suppressor functions, it has been reported that miR-200c is overexpressed in ESCC, and high expression of miR-200c confers chemoresistance in ESCC cells (16). Correlating with these, the expression of the miR-200c and the miR-200b cluster are oppositely altered in ESCC, probably due to the fact that chr1p36 containing the miR-200b cluster is often deleted in ESCC (46), whereas chr12p13 containing the miR-200c-141 cluster is frequently amplified in ESCC (46,47).

Kindlin-2 is a FERM domain containing protein, which has been shown to modulate cell shape by linking the cytoskeleton with the cell-extracellular matrix adhesions (31-33). Importantly, Kindlin-2 belongs to the Kindlin protein family, which is one of the only two known families of proteins that mediate the inside-out activation of Integrin signaling pathways (48). Currently, the importance of Kindlin-2 in tumor malignant progression has been recognized; Kindlin-2 was shown to highly expressed in the invasive front of tumors and its overexpression promotes cell migration/invasion (23,24). However, the expression and the biological significance of Kindlin-2 are not clear in ESCC. In this study, we are the first to identify that Kindlin-2 expression is modulated by miR-200b in ESCC cells, and our data suggest that Kindlin-2 is an important mediator of the biological functions of miR-200b in ESCC.

Knockdown of Kindlin-2 phenocopied the suppressor functions of miR-200b in ESCC cell migration/invasiveness, whereas enforced expression of Kindlin-2 reversed the phenotypic effects of miR-200b. A latest report has shown that Kindlin-2 promotes breast cancer invasion by repressing the expression of miR-200b through an epigenetic mechanism (49), suggesting that Kindlin-2 and miR-200 may form a reciprocal feedback loop to regulate tumor progression. Further studies are required to validate this mechanism in ESCC.

We also showed that Kindlin-2 mediated the biological effects of miR-200b on the modulation of cytoskeleton assembly and FA formation, two key processes that regulate cell migratory/invasive properties (35-39). Specifically, the dynamic assembly of cytoskeleton regulates cell invasiveness/migration by governing the formation of various migratory organelles, such as stress fibers, lamellipodia, filopodia, invadopodia and podosomes (50). The formation and turnover of FAs, cell–substratum contact sites that link integrins to the actin cytoskeleton, not only transmit extracellular signals into cells but also facilitate cells to migrate (38,39). We found that both enforced expression of miR-200b and Kindlin-2 knockdown suppressed the formation of migratory organelles like stress fibers and filopodia/podosomes, and inhibited FA formation. Our data also revealed that the miR-200b—Kindlin-2 axis exerts its biological functions via modulating the activity of Rho-family GTPases and FAK, which are well-recognized key regulators of actin cytoskeleton structure and FA formation and turnover, respectively (37-39). Thus, our findings suggest that by targeting Kindlin-2, miR-200b is likely to regulate ESCC cell migration and invasion via modulating the cytoskeletal and adhesive

machinery (**Figure 2.15**). Notably, this mechanism may correlate with our clinical observations that the loss of miR-200b in ESCC tumors is associated with lymph node metastasis, advanced clinical stage and short survival.

The dynamic assembly of actin cytoskeleton directly modulates cell morphology and migration/invasion by powering the formation of various migratory/invasive organelles, such as stress fibers, lamellipodia, filopodia and invadopodia [88]. It has been well-recognized that these cytoskeletal and morphological changes can be linked to the EMT process [91]. Nevertheless, cancer cell invasion can also be driven by cytoskeletal reorganization independent of EMT [60]. The data presented in this study is in support of this concept. In E-cadherin-negative ESCC cells, such as EC109 and EC9706 used in this study, although the connection between miR-200b and E-cadherin was disrupted, it did not impair the function this miRNA in regulating ESCC cell morphology and invasiveness. In addition, in E-cadherin-positive but highly invasive ESCC cells such as KYSE510, miR-200b could still suppress invasiveness and alter cell morphology, but the expression of E-cadherin was not further enhanced (**Figure 2.11B**). Therefore, compared with E-cadherin, a low expression status of miR-200b could potentially be used as a better indicator of strong cell invasiveness in ESCC, although we are aware that the link between miR-200b and E-cadherin is likely to be intact in a certain proportion of ESCC cells/tumors.

In support of our findings, multiple recent studies have also provided evidence supporting the EMT-independent but cytoskeleton-dependent role of miR-200

in suppressing tumor invasion and metastasis. In breast cancer cells, miR-200 was shown to target cytoskeleton remodeling proteins, such as WASF3, Moesin, FHOD1, PPM1F, WIPF1 and CFL2, which were found to be functional mediators of these miRNAs in invasion and/or metastasis [65-67, 92]. Notably, different from the case in ESCC, miR-200 was shown to impact both the classic ZEB1/2-EMT pathway and the cytoskeleton reorganization process. These two mechanisms were shown to be independent, since siRNA knockdown of the cytoskeleton remodeling proteins, such as WASF3, FHOD1 and PPM1F, did not significantly alter the expression of E-cadherin [55,56], and knockdown of ZEB1/2 did not alter the cytoskeleton features either [66].

Integrins are a family of cell adhesion receptors comprising 18α and 8β subunits that form over 24 heterodimers, which have been shown to play crucial roles in the initiation, progression and metastasis of solid tumors [94,95]. Integrin β1 is one of the most important members that can potentially form 12 Integrin receptors, which has been shown to play important roles in promoting cytoskeleton remodeling, cell morphology, and cell motility/invasiveness [74,94,95]. The activation of Integrins are bidirectional, including the outside-in activation (activated by extracellular matrix components such as collagens and fibronectins) and the inside-out activation (activated by focal adhesion proteins such as Talins and Kindlins) [78,79]. Our previous study has identified Kindlin-2, a significant prognostic marker in ESCC [86], as a target and mediator of the function of miR-200b in ESCC [68]. In this study, we revealed that miR-200b inhibits the inside-out activation of Integrin β1 via targeting Kindlin-2. Moreover, this finding also further

deciphered the mechanism behind the role of miR-200b in the regulation of CDC42, RhoA and FAK, which can transmit signals downstream of Integrin β1 to promote cancer cell morphological changes and invasiveness [94,95]. Moreover, in keeping with the findings that the PI3K-AKT pathway is one of the key mediators of the biological function of Integrin β1 [74-77], the present study demonstrates that pAKT mediates the biological function of the miR-200b downstream of the Kindlin-2-Integrin β1 cascade in the regulation of cell morphology and invasiveness in ESCC (**Figure 2.14C**).

Notably, Kindlin-2 knockdown did not perfectly mimic the effects of miR-200b on cell morphology or the assembly of the cytoskeletal machinery **(Figures 2.5 and 2.6)**, suggesting that other cytoskeleton-regulatory molecules targeted by miR-200b may function synergistically with Kindlin-2 to mediate the role of miR-200b in ESCC cells. Indeed, miR-200b has been shown to target genes associated with actin cytoskeleton remodeling, such as *WAVE3* and *MARCKS* (20,51). Moreover, the list of proteins down-regulated by miR-200b may contain proteins that could also mediate the biological function of miR-200b similar to that of Kindlin-2 but do not possess miR-200b binding site within the 3'UTR of their encoding mRNA, in those cases, their expression is probably regulated by miR-200b through indirect mechanisms (*e.g.* modulated by direct miR-200b targets or by signaling pathways that could be altered by miR-200b).

To conclude, our data suggest that the miR-200-ZEB1/2 axis contributes to the pathobiology of ESCC, which can serve as prognostic markers in ESCC

patients. DNA methylation of *E-cadherin* gene may disrupt the link between the miR-200b-ZEB1/2 axis and E-cadherin in ESCC, but miR-200b can suppress invasiveness via targeting the Kindlin-2-Integrin β1-AKT cascade, which modulates the cytoskeletal and adhesive machinery. Our findings also suggest that miR-200b and its targets may serve as promising prognostic markers for ESCC and therapeutic targets for ESCC invasion intervention.

2.6 References

1. Parkin,D.M. *et al.* (2005) Global cancer statistics, 2002. *CA Cancer J. Clin.,* **55,** 74-108.
2. Enzinger,P.C. *et al.* (2003) Esophageal cancer. *N. Engl. J. Med.,* **349,** 2241-2252.
3. McCann,J. (1999) Esophageal Cancers: Changing Character, Increasing Incidence. *J. Natl. Cancer Inst.,* **91,** 497-498.
4. Ries,L.A. *et al.* (2002) SEER cancer statistics review, 1973-1999, National Cancer Institute. Bethesda, MD.
5. Kimura,H. *et al.* (1999) Number of lymph node metastases influences survival in patients with thoracic esophageal carcinoma: therapeutic value of radiation treatment for recurrence. *Dis. Esophagus,* **12,** 205-208.
6. Valastyan,S. *et al.* (2009) A pleiotropically acting microRNA, miR-31, inhibits breast cancer metastasis. *Cell,* **137,** 1032-1046.
7. Korpal,M. *et al.* (2011) Direct targeting of Sec23a by miR-200s influences cancer cell secretome and promotes metastatic colonization. *Nat. Med.,* **17,** 1101-1108.
8. Zhang,L. *et al.* (2013) Epigenetic activation of the MiR-200 family

contributes to H19-mediated metastasis suppression in hepatocellular carcinoma. *Carcinogenesis,* **34,** 577-586.

9. Valastyan,S. *et al.* (2011) Roles for microRNAs in the regulation of cell adhesion molecules. *J. Cell Sci.,* **124,** 999-1006.
10. Bracken,C.P. *et al.* (2008) A double-negative feedback loop between ZEB1-SIP1 and the microRNA-200 family regulates epithelial-mesenchymal transition. *Cancer Res.,* **68,** 7846-7854.
11. Korpal,M. *et al.* (2008) The miR-200 family inhibits epithelial-mesenchymal transition and cancer cell migration by direct targeting of E-cadherin transcriptional repressors ZEB1 and ZEB2. *J. Biol. Chem.,* **283,** 14910-14914.
12. Park,S.M. *et al.* (2008) The miR-200 family determines the epithelial phenotype of cancer cells by targeting the E-cadherin repressors ZEB1 and ZEB2. *Genes Dev.,* **22,** 894-907.
13. Burk,U. *et al.* (2008) A reciprocal repression between ZEB1 and members of the miR-200 family promotes EMT and invasion in cancer cells. *EMBO Rep.,* **9,** 582-589.
14. Gibbons,D.L. *et al.* (2009) Contextual extracellular cues promote tumor cell EMT and metastasis by regulating miR-200 family expression. *Genes Dev.,* **23,** 2140-2151.
15. Wu,B.L. *et al.* (2011) MiRNA profile in esophageal squamous cell carcinoma: downregulation of miR-143 and miR-145. *World J .Gastroenterol.,* **17,** 79-88.
16. Edge SB, Compton CC. The American Joint Committee on Cancer: the 7th edition of the AJCC cancer staging manual and the future of TNM. *Ann*

Surg Oncol., 2010;**17,**1471-1474.

17. Fang,W.K, *et al.* (2010) Reduced membranous and ectopic cytoplasmic expression of DSC2 in esophageal squamous cell carcinoma: an independent prognostic factor. *Human Pathology,* **41,** 1456-465.
18. Camp,R.L. *et al.* (2004) X-tile: a new bio-informatics tool for biomarker assessment and outcome-based cut-point optimization. *Clin. Cancer Res.,* **10,** 7252-7259.
19. Selbach,M. *et al.* (2008) Widespread changes in protein synthesis induced by microRNAs. *Nature,* **455,** 58-63.
20. Elson-Schwab,I. *et al.* (2010) MicroRNA-200 family members differentially regulate morphological plasticity and mode of melanoma cell invasion. *PLoS One,* **5,** e13176.
21. Cochrane,D.R. *et al.* (2009) MicroRNA-200c mitigates invasiveness and restores sensitivity to microtubule-targeting chemotherapeutic agents. *Mol. Cancer Ther.,* **8,** 1055-1066.
22. Bimpaki,E.I. *et al.* (2010) MicroRNA signature in massive macronodular adrenocortical disease and implications for adrenocortical tumourigenesis. *Clin Endocrinol (Oxf).,* **72,** 744-751.
23. An,Z. *et al.* (2010) Kindlin-2 is expressed in malignant mesothelioma and is required for tumor cell adhesion and migration. *Int. J. Cancer,* **127,** 1999-2008.
24. Yu,Y. *et al.* (2012) Kindlin 2 forms a transcriptional complex with β-catenin and TCF4 to enhance Wnt signalling. *EMBO Rep.,* **13,** 750-758.
25. Shapiro,G.I. (2006) Cyclin-dependent kinase pathways as targets for cancer treatment. *J. Clin. Oncol.,* **24,** 1770-1783.

26. Gueron,G. *et al.* (2009) Critical Role of Endogenous Heme Oxygenase 1 as a Tuner of the Invasive Potential of Prostate Cancer Cells. *Mol. Cancer Res.,* **7,** 1745-1755.
27. Yu,P. *et al.* (2001) p15(PAF), a novel PCNA associated factor with increased expression in tumor tissues. *Oncogene,* **20,** 484-489.
28. Li,T. *et al.* (2011) P21-activated protein kinase (PAK2)-mediated c-Jun phosphorylation at 5 threonine sites promotes cell transformation. *Carcinogenesis,* **32,** 659-666.
29. Bodemann,B.O. *et al.* (2008) Ral GTPases and cancer: linchpin support of the tumorigenic platform. *Nat. Rev. Cancer,* **8,** 133-140.
30. Valderrama,F. *et al.* (2012) Radixin regulates cell migration and cell-cell adhesion through Rac1. *J. Cell Sci.,* **125,** 3310-3319.
31. Tu,Y. *et al.* (2003) Migfilin and Mig-2 link focal adhesions to filamin and the actin cytoskeleton and function in cell shape modulation. *Cell,* **113,** 37-47.
32. He,Y. *et al.* (2011) Role of kindlin-2 in fibroblast functions: implications for wound healing. *J. Invest. Dermatol.,* **131,** 245-256.
33. Bandyopadhyay,A. *et al.* (2012) Functional differences between kindlin-1 and kindlin-2 in keratinocytes. *J. Cell. Sci.,* **125,** 2172-2184.
34. Mooney,D.J. *et al.* (1995) Cytoskeletal filament assembly and the control of cell spreading and function by extracellular matrix. *J. Cell Sci.,* **108,** 2311-2320.
35. Small,J.V. *et al.* (2005) The comings and goings of actin: coupling protrusion and retraction in cell motility. *Curr. Opin. Cell Biol.,* **17,** 517-523.
36. Mattila,P.K. *et al.* (2008) Filopodia: molecular architecture and cellular functions. *Nat. Rev. Mol. Cell Biol.,* **9,** 446-454.

37. Hall,A. *et al.* (1998) Rho GTPases and the actin cytoskeleton. *Science,* **279,** 509–514.

38. Webb,D.J. *et al.* (2003) Illuminating adhesion complexes in migrating cells: moving toward a bright future. *Curr. Opin. Cell Biol.,* **15,** 614-620.

39. Mitra,S.K. *et al.* (2006) Integrin-regulated FAK-Src signaling in normal and cancer cells. *Curr. Opin. Cell Biol.,* **18,** 516-523.

40. Schlaepfer,D.D. *et al.* (1999) Signaling through focal adhesion kinase. *Prog. Biophys. Mol. Biol.,* **71,** 435-478.

41. Zhang,X. *et al.* (2008) Talin depletion reveals independence of initial cell spreading from integrin activation and traction. *Nat. Cell Biol.,* **10,** 1062-1068.

42. Shimono,Y. *et al.* (2009) Downregulation of miRNA-200c links breast cancer stem cells with normal stem cells. *Cell,* **138,** 592-603.

43. Wellner,U. *et al.* (2009) The EMT-activator ZEB1 promotes tumorigenicity by repressing stemness-inhibiting microRNAs. *Nat. Cell Biol.,* **11,** 1487-1495.

44. Iliopoulos,D. *et al.* (2010) Loss of miR-200 inhibition of Suz12 leads to polycomb-mediated repression required for the formation and maintenance of cancer stem cells. *Mol. Cell,* **39,** 761-772.

45. Schliekelman,M.J. *et al.* (2011) Targets of the tumor suppressor miR-200 in regulation of the epithelial-mesenchymal transition in cancer. *Cancer Res.,* **71,** 7670-7682.

46. Qin,Y.R. *et al.* (2008) Comparative genomic hybridization analysis of genetic aberrations associated with development of esophageal squamous cell carcinoma in Henan, China. *World J. Gastroenterol.,* **14,** 1828-1835.

47. Carneiro,A. *et al.* (2008) Prognostic impact of array-based genomic profiles in esophageal squamous cell cancer. *BMC Cancer,* **8,** 98.

48. Karaköse,E. *et al.* (2010) The kindlins at a glance. *J. Cell Sci.,* **123,** 2353-2356.

49. Yu,Y. *et al.* (2013) Kindlin 2 promotes breast cancer invasion via epigenetic silencing of the microRNA200 gene family. Int J Cancer 2013;133(6):1368-79.

50. Yamaguchi,H. *et al.* (2007) Regulation of the actin cytoskeleton in cancer cell migration and invasion. *Biochim. Biophys. Acta,* **1773,** 642-652.

51. Sossey-Alaoui,K. *et al.* (2009) The miR200 family of microRNAs regulates WAVE3-dependent cancer cell invasion. *J. Biol. Chem.* **284,** 33019-33029.

52. Ferlay J, Shin HR, Bray F, *et al*. Estimates of worldwide burden of cancer in 2008: GLOBOCAN 2008. Int J Cancer 2010;127:2893-917.

53. Jemal A, Bray F, Center MM, *et al*. Global cancer statistics. CA Cancer J Clin 2011;61:69-90.

54. Enzinger PC, Mayer RJ. Esophageal cancer. N Engl J Med 2003;349:2241-2252.

55. McCann, J. Esophageal Cancers: Changing Character, Increasing Incidence. J. Natl. Cancer Inst 1999;91:497-498.

56. Ries LAG, Eisner MP, Kosary CL, *et al*. SEER Cancer Statistics Review, 1973-1999. Bethesda, MD: National Cancer Institute, 2002.

57. Kimura H, Konishi K, Arakawa H, *et al*. Number of lymph node metastases influences survival in patients with thoracic esophageal carcinoma: therapeutic value of radiation treatment for recurrence. Dis Esophagus 1999;12:205-208.

58. Thiery JP, Acloque H, Huang RY, *et al*. Epithelial-mesenchymal transitions in development and disease. Cell 2009;139:871-90.

59. Vanharanta S, Massagué J. Origins of metastatic traits. Cancer Cell 2013;24:410-21.

60. Wicki A, Lehembre F, Wick N, *et al*. Tumor invasion in the absence of epithelial-mesenchymal transition: podoplanin-mediated remodeling of the actin cytoskeleton. Cancer Cell 2006;9:261-72.

61. Cheung KJ, Gabrielson E, Werb Z, *et al*. Collective invasion in breast cancer requires a conserved basal epithelial program. Cell 2013;155:1639-51.

62. Dykxhoorn DM, Wu Y, Xie H, *et al*. miR-200 enhances mouse breast cancer cell colonization to form distant metastases. PLoS One 2009;4:e7181.

63. Le MT, Hamar P, Guo C, *et al*. miR-200-containing extracellular vesicles promote breast cancer cell metastasis. J Clin Invest 2014;124:5109-5128.

64. Zhang HF, Xu LY, Li EM. A family of pleiotropically acting microRNAs in cancer progression, miR-200: potential cancer therapeutic targets. Curr Pharm Des 2014;20:1896-1903.

65. Sossey-Alaoui K, Bialkowska K, Plow EF. The miR200 family of microRNAs regulates WAVE3-dependent cancer cell invasion. J Biol Chem 2009;284:33019-33029.

66. Jurmeister S, Baumann M, Balwierz A, *et al*. MicroRNA-200c represses migration and invasion of breast cancer cells by targeting actin-regulatory proteins FHOD1 and PPM1F. Mol Cell Biol 2012;32:633-651.

67. Bracken CP, Li X, Wright JA, *et al*. Genome-wide identification of miR-200

targets reveals a regulatory network controlling cell invasion. EMBO J 2014;33:2040-2056.

68. Zhang HF, Zhang K, Liao LD, *et al*. miR-200b suppresses invasiveness and modulates the cytoskeletal and adhesive machinery in esophageal squamous cell carcinoma cells via targeting Kindlin-2. Carcinogenesis 2014;35:292-301.
69. Wu BL, Xu LY, Du ZP, Liao LD, Zhang HF, Huang Q, *et al*. MiRNA profile in esophageal squamous cell carcinoma: downregulation of miR-143 and miR-145. World J Gastroenterol 2011;17:79-88.
70. Fang WK, Liao LD, Li LY, *et al*. Down-regulated desmocollin-2 promotes cell aggressiveness through redistributing adherens junctions and activating beta-catenin signalling in oesophageal squamous cell carcinoma. J Pathol 2013;231:257-70.
71. Fang WK, Gu W, Li EM, *et al*. Reduced membranous and ectopic cytoplasmic expression of DSC2 in esophageal squamous cell carcinoma: an independent prognostic factor. Human Pathology 2010;41:1456-1465.
72. Takeno S, Noguchi T, Fumoto S, *et al*. E-cadherin expression in patients with esophageal squamous cell carcinoma: promoter hypermethylation, Snail overexpression, and clinicopathologic implications. Am J Clin Pathol 2004;122:78-84.
73. Cheung PY, Deng W, Man C, *et al*. Genetic alterations in a telomerase-immortalized human esophageal epithelial cell line: implications for carcinogenesis. Cancer Lett 2010;293:41-51.
74. Keely PJ, Westwick JK, Whitehead IP, *et al*. Cdc42 and Rac1 induce integrin-mediated cell motility and invasiveness through PI(3)K. Nature

1997;390:632-636.

75. Qian Y, Zhong X, Flynn DC, *et al*. ILK mediates actin filament rearrangements and cell migration and invasion through PI3K/Akt/Rac1 signaling. Oncogene 2005;24:3154-65.
76. Pankov R, Cukierman E, Clark K, *et al*. Specific beta1 integrin site selectively regulates Akt/protein kinase B signaling via local activation of protein phosphatase 2A. J Biol Chem 2003;278:18671-18681.
77. Velling T, Nilsson S, Stefansson A, *et al*. beta1-Integrins induce phosphorylation of Akt on serine 473 independently of focal adhesion kinase and Src family kinases. EMBO Rep 2004;5:901-905.
78. Montanez E, Ussar S, Schifferer M, *et al*. Kindlin-2 controls bidirectional signaling of integrins. Genes Dev 2008;22:1325-1330.
79. Karaköse E, Schiller HB, Fässler R. The kindlins at a glance. J Cell Sci 2010;123:2353-2356.
80. Subramanian A, Tamayo P, Mootha VK, *et al*. Gene set enrichment analysis: a knowledge-based approach for interpreting genome-wide expression profiles. Proc Natl Acad Sci U S A 2005;102:15545-15550.
81. Mootha VK, Lindgren CM, Eriksson KF, *et al*. PGC-1alpha-responsive genes involved in oxidative phosphorylation are coordinately downregulated in human diabetes. Nat Genet 2003;34:267-273.
82. Shimono Y, Zabala M, Cho RW, *et al*. Downregulation of miRNA-200c links breast cancer stem cells with normal stem cells. Cell 2009; 138: 592-603.
83. Wellner U, Schubert J, Burk UC, *et al*. The EMT-activator ZEB1 promotes tumorigenicity by repressing stemness-inhibiting microRNAs. Nat Cell Biol

2009; 11:1487-1495.

84. Iliopoulos D, Lindahl-Allen M, Polytarchou C, *et al*. Loss of miR-200 inhibition of SUZ12 leads to polycomb-mediated repression required for the formation and maintenance of cancer stem cells. Mol Cell 2010; 39:761-772.

85. Lu YX, Yuan L, Xue XL, *et al*. Regulation of colorectal carcinoma stemness, growth, and metastasis by an miR-200c-Sox2-negative feedback loop mechanism. Clin Cancer Res 2014;20:2631-2642.

86. Liu YN, Yin JJ, Abou-Kheir W, *et al*. MiR-1 and miR-200 inhibit EMT via SLUG-dependent and tumorigenesis via SLUG-independent mechanisms. Oncogene 2012; 32:296-306.

87. Park SM, Gaur AB, Lengyel E, *et al*. The miR-200 family determines the epithelial phenotype of cancer cells by targeting the E-cadherin repressors ZEB1 and ZEB2. Genes Dev 2008;22:894-907.

88. Gregory PA, Bert AG, Paterson EL, *et al*. The miR-200 family and miR-205 regulate epithelial to mesenchymal transition by targeting ZEB1 and SIP1. Nat Cell Biol 2008;10:593-601.

89. Feng B, Wang R, Chen LB. Review of miR-200b and cancer chemosensitivity. Biomed Pharmacother 2012;66:397-402.

90. Yamaguchi H, Condeelis J. Regulation of the actin cytoskeleton in cancer cell migration and invasion. Biochim Biophys Acta 2007;1773:642-652.

91. Yilmaz M, Christofori G. EMT, the cytoskeleton, and cancer cell invasion. Cancer Metastasis Rev 2009;28:15-33.

92. Li X, Roslan S, Johnstone CN, *et al*. MiR-200 can repress breast cancer metastasis through ZEB1-independent but moesin-dependent pathways.

Oncogene 2014;33:4077-4088.

93. Howe EN, Cochrane DR, Richer JK. Targets of miR-200c mediate suppression of cell motility and anoikis resistance. Breast Cancer Res 2011;13:R45.

94. Desgrosellier JS, Cheresh DA. Integrins in cancer: biological implications and therapeutic opportunities. Nat Rev Cancer 2010;10:9-22.

95. Barkan D, Chambers AF. β1-integrin: a potential therapeutic target in the battle against cancer recurrence. Clin Cancer Res 2011;17:7219-7223.

96. Cao HH, Zhang SY, Shen JH, *et al*. A three-protein signature and clinical outcome in esophageal squamous cell carcinoma. Oncotarget 2015;6:5435-5448.

Chapter 3

The opposing function of STAT3 as an oncoprotein and tumor suppressor is dictated by the expression status of STAT3β in esophageal squamous cell carcinoma

This chapter has been modified from the publication:

Zhang HF, Chen Y, Wu CS, Wu ZY, Tweardy DJ, Alshareef A, Liao LD, Xue YJ, Wu JY, Chen B, Xu XE, Gopal K, Gupta N, Li EM, Xu LY, Lai R. The interplay between STAT3α and STAT3β dictates the dual role of STAT3 in esophageal squamous cell carcinoma. Clin Cancer Res 2015. (Accepted).

Zhang HF is the first author of the paper and performed all the experiments described herein except for the following: Chen Y, Wu CS, Alshareef A and Liao LD performed the animal study shown in Figure 3.4. Tweardy DJ prepared and provided the STAT3β antibody used in the experiments shown in Figure 3.1A. Wu ZY, Xue YJ, Wu JY, Chen B and Xu XE performed the surgical resection and process of patient samples, as well as patient follow up. Gopal K and Gupta N provided assitance in the critical review of the paper. Lai R, Li EM and Xu LY supervised the whole project.

3.1 Abstract

While the oncogenic role of STAT3 is well established, recent reports have described its tumor suppressor roles in various cancers. We hypothesized that the interplay between the two STAT3 isoforms, STAT3α and STAT3β, may be the key determinant of the opposing roles of STAT3 in cancer biology. In esophageal squamous cell carcinoma (ESCC) cells, we found that although STAT3β substantially increased the tyrosine^{705}-phosphorylation, nuclear translocation and DNA-binding of STAT3α, it significantly decreased the transcription activity of STAT3 and its tumorigenic potential. STAT3β also decreased the cancer stem cell population, the tumorsphere forming capacity, and markedly sensitized ESCC cells to 5-flurouracil and cisplatin both *in vitro* and *in vivo*. In ESCC patients, decreased expression of STAT3β in the tumor was significantly associated with a shorter overall survival and recurrence-free survival in those who received radio-chemotherapy. Mechanistically, we found that the STAT3β-induced increase in pSTAT3α^{Y705} was attributed to the decreased binding and dephosphorylation of STAT3α by PTP-MEG2, a protein tyrosine phosphatase. Moreover, the expression of STAT3β and pSTAT3α^{Y705} was positively correlated in ESCC tumors, and associated with a longer survival in ESCC patients. Importantly, the prognostic value of pSTAT3α^{Y705} was dependent on the expression status of STAT3β. These findings gain insights into the emerging controversial roles of STAT3 in cancer, and suggest that STAT3β is a tumor suppressor in ESCC, by interfering with the oncogenic effects of STAT3α. STAT3 can be both oncogenic and tumor suppressive, and the interplay between STAT3α and STAT3β is the key determining factor.

3.2 Introduction

STAT3, a member of the STAT family of transcription factors, is responsible for the signal transduction of a host of extracellular stimuli such as the IL-6 family cytokines and various growth factors (1-3). Upon these stimulations, phosphorylation of $STAT3^{Y705}$ is essential for the subsequent dimerization, nuclear translocation and activation of STAT3 (1-3). The oncogenic potential of STAT3 has been well documented; specifically, the constitutively activated STAT3 mutant (commonly labeled STAT3C) can effectively induce malignant transformation (4), and many human cancers harbor constitutively active STAT3 (1-3). Nevertheless, accumulating evidence from both experimental and clinical studies has suggested that STAT3 may also carry a tumor suppressor role in specific contexts (5-14). For instance, in a mouse model of intestine adenoma, tissue specific *STAT3* gene knockout was found to enhance tumor invasion and promote tumor progression (5-6). STAT3 expression was found to be reduced in the majority of skin squamous cell carcinomas compared with adjacent non-malignant tissues (8). Moreover, nuclear-STAT3 or $pSTAT3^{Y705}$ was shown to correlate with a better prognosis in multiple cancers, such as head and neck squamous cell carcinoma, salivary gland cancer, low-grade or node-negative breast cancer, colorectal cancer and nasopharyngeal carcinoma (9-14).

In a recent review article, we have speculated that the molecular basis of how STAT3 can function as a tumor suppressor and oncoprotein may be related to the existence of two STAT3 isoforms, STAT3α and STAT3β (3). STAT3β, a truncated form of the full-length STAT3α, is generated by alternative splicing

of exon 23 (15-17). STAT3β is identical to STAT3α with the exception of 55 amino acids at the C-terminal of STAT3α that are replaced by a unique 7-amino-acid sequence of STAT3β (15-17). Importantly, compared with STAT3α, STAT3β lacks the C-terminal transcription activation domain. A relatively small number of previous publications have suggested that STAT3β is a tumor suppressor (18-22). For instance, it has been reported that STAT3β induces cell-cycle arrest and apoptosis in melanoma cells (18-21). A study published in 1996 using COS-1 cells (a monkey kidney cell line) suggested that the tumor suppressor effects of STAT3β may be related to its heterodimerization with STAT3α, thereby inhibiting the transactivation activity of STAT3α (16). Nonetheless, the biological and clinical significance of STAT3β in human cancers has not been extensively examined. Whether STAT3β can indeed inhibit STAT3α in human cancer cells has not been extensively tested or established. To our knowledge, virtually all previously published clinical studies examining the prognostic significance of STAT3 in cancers did not examine the relative expression and contributions of the two STAT3 isoforms separately.

Esophageal squamous cell carcinoma (ESCC) is one of the most deadly cancers worldwide, representing the fifth leading cause of cancer-related death in males and the eighth in females (23). Aberrant activation of STAT3 has been shown to promote tumorigenesis in this type of cancer (24-26). Using ESCC as a study model, we examined the interaction between STAT3α and STAT3β in detail, with the hope that the generated data can provide insights into the tumor suppressor role of STAT3β and the molecular

mechanism underlying the dual role of STAT3 in cancers. Our data show that STAT3β is a key regulator of the signaling and oncogenic effects of STAT3α. Our findings support the concept that the relative expression levels of STAT3α and STAT3β as well as their interactions dictate whether STAT3 is tumor suppressive or oncogenic in a specific setting.

3.3 Materials and Methods

3.3.1 Clinical samples

Human ESCC tumors and adjacent non-tumorous esophageal epithelial tissues were collected directly after surgical resection between Jan. 2000 and Dec. 2006, at the Department of Tumor Surgery of Shantou Central Hospital (Shantou, China). The cases were selected based on a clear pathological diagnosis, follow-up data, and had not received local or systemic treatment before surgery. The frozen tissues, including both the case-paired adjacent non-cancerous esophageal epithelial tissues and the tumor samples that were used for the western blot analysis, were rigorously resected by pathologists to ensure that only the epithelium of the normal esophagus was included in the non-cancerous tissues, and that no benign tissues were included in tumor samples. The histological characterization and clinicopathological staging of the samples were performed in accordance with the 7th edition of American Joint Committee on Cancer Tumor-Nodes-Metastasis staging system (27). Detailed clinical information of the ESCC patients is described in **Table 3.1**. The study was approved by the ethical committee of the Central Hospital of Shantou City and the ethical committee of Shantou University Medical College,

and written informed consent was obtained from all surgical patients to use resected samples for research.

Table 3.1 Characteristics of ESCC patients

Clinical parameters	Total patient number (n=286)	
	Patient number	Percentage
Gender		
Male	223	78%
Female	63	22%
Age		
≤58 years	149	52%
>58 years	137	48%
Tumor Size		
<3cm	63	22%
3-5cm	135	47%
>5cm	88	31%
Histological grade		
G1	47	16%
G2	217	76%
G3	22	8%
Primary tumor		
Tis	0	0%
T1	10	4%
T2	45	16%
T3	230	80%
T4	1	1%
Lymph node metastasis		
N0	145	51%
N1	76	27%
N2	48	17%
N3	17	6%
TNM clasification		
I	22	8%
IIA	66	23%
IIB	70	25%
IIIA	69	24%
IIIB	41	14%
IIIC	18	6%
IV	0	0%

3.3.2 Human ESCC cell lines

EC109 human ESCC cell line was obtained from Chinese Academy of Medical Sciences, Beijing, China. KYSE150 human ESCC cell line was kindly provided by Dr. Ming-Zhou Guo, Chinese PLA General Hospital, Beijing, China. KYSE150 cells were cultured in RPMI-1640 medium supplemented with 10% fetal bovine serum, while EC109 cells were maintained in (Dulbecco's Modified Eagle's medium) DMEM medium plus 10% fetal bovine serum. All the stable cell clones derived from these cells were cultured in the same type of medium that was used for the parental cell line.

3.3.3 DNA constructs

pXJ40-STAT3α-Flag, pXJ40-STAT3β-Flag and their corresponding Y705F mutant constructs were gifts of Dr. MA Bogoyevitch, University of Melbourne, Victoria, Australia. For the construction of the *STAT3β* gene Tetracycline-off (TetOff) vector, the coding region of *STAT3β* coupled with the Flag coding sequence were subcloned into the *MluI* and *SalI* sites of the pTRE2hyg vector (Clontech). The primers are: 5'- CGACGCGTATGGATTACAAG-GATGACGACGATAAG-3' (Foward), and 5'-ACGCGTCGACTTATTTCCAAACTGCAT-CAATGAA-3' (Reverse). The STAT3-specific luciferase reporter plasmid pLucTKS3 that contains seven copies of STAT3 consensus binding sequence (TTCCCGAA) was donated by Dr. J Turkson, University of Central Florida College of Medicine, Orlando, FL. The pRL-TK Renilla luciferase internal control vector was purchased from Promega.

3.3.4 Plasmid and small interfering RNA (siRNA) transfection

Plasmids and siRNAs were transfected using Lipofectamine 2000 (Invitrogen) and Lipofectamine RNAiMAX (Invitrogen) respectively. For plasmid and siRNA co-transfection, only Lipofectamine 2000 was used. STAT3 siRNA smart pool and the negative control scrambled RNA were purchased from Dharmacon. A final concentration of 30nM siRNA was used in all STAT3 knockdown experiments.

3.3.5 Stable cell clone generation

The generation of the *STAT3β* and *STAT3C* Tetracycline-off stable cell clones was performed according to the protocol provided by the manufacturer of the Tetracycline-off system (Clontech, Mountain View, CA, USA). Briefly, the EC109 and KYSE150 cells were firstly transfected with the pTet-Off vector that expresses tetracycline-controlled transactivator (tTA), stable cell clones were selected by exposure to 400μg/ml geneticin (Invitrogen). Then, these stable clones were transfected with the pTRE2hyg-*STAT3β* or pTRE2hyg-*STAT3C* vectors to select the double stable cell clones by exposure to 400μg/ml hygromycin B (Invitrogen).

3.3.6 Clonogenic assay

For chemoresistance assay, cells were pretreated with 50 μg/ml 5-flurouracil (Sigma) or 4μM Cisplatin (Hospira, Saint-Laurent, QC, Canada) for 24h, and then cells were plated at a number of 10,000 cells/well in 12-well plates and cultured in media without chemotherapeutic agents. After 2-3 weeks, the cells were fixed with cold absolute methanol and stained with 1% crystal violet

(Sigma). For cells that were not treated with chemotherapeutic agents, 200 cells/well were seeded into 12-well plates, after which the cells were cultured under normal conditions as described above for about 10 days before methanol fixation and crystal violet staining.

3.3.7 Cell proliferation assay

24h after plasmid or siRNA transfection, cells were treated with 50 μg/ml 5-flurouracil or 4μM Cisplatin for 24h before being trypsinized and plated into 48-well plates at a concentration of 15,000 cells/well. Cells were then cultured in media containing no chemotherapeutic agents. At the indicated times, cell viability was measured using the CellTiter 96AQueous One Solution Cell Proliferation Assay (Promega), also known as MTS assay, according to the manufacturer's protocol. Absorbance at 490nm was measured using a microplate reader (BMG Labtech, Ortenberg, Germany).

3.3.8 Tumorsphere formation assay

After trypsinization, single-cell suspensions were obtained by filtering the cells using a 40μm Cell Strainer (BD). Then, cells were counted and 500 cells were plated into ultra-low attachment surface 6-well plates (Corning, Santa Clara, CA, USA) and cultured in medium described in previous studies (25). Tumorspheres containing more than ten cells were counted 6 days after seeding.

3.3.9 Animal study

1×10^6 KYSE150-TetOff-STAT3β cells pretreated with/without 100ng/ml

doxycycline (Dox) were injected subcutaneously into the flank of male nude mice that were 8-week old. The Dox+ group mice were treated with Dox by adding Dox in drinking water at a concentration of 100ng/ml, whereas no Dox was added for the Dox- group mice. Eight days after tumor cell injection when the xenograft tumors were palpable, Cisplatin (2mg/kg body weight, Calbiochem, Millipore) or 5-FU (20mg/kg body weight, Sigma) were injected intraperitoneally every three days. Tumor volumes were measured every three days. 23 days after tumor cell injection, the mice were euthanized, and the tumors were surgically resected. H&E staining and immunohistochemical detection of pan Cytokeratin (ZM-0069, ZSGB-BIO, Beijing, China) were used to identify the xenografted tumor cells in mice. The expression of Flag and pSTAT3α^{Y705} were detected by immunohistochemistry using antibodies against Flag (Sigma; F3165) and pSTAT3α^{Y705} (Cell Signaling; #9145), respectively.

3.3.10 Flow cytometry analysis

Cell apoptosis was determined by the propidium iodide and Annexin V double staining assay. Briefly, cells were gently dissociated with trypsin and stained with propidium iodide and Annexin V using the Annexin V-FITC Apoptosis Detection Kit I (BD Biosciences) according to the manufacturer's instructions. For side population cell identification, a previously described method was used (25). For CD44 detection, cells were gently dissociated with trypsin and stained with APC-conjugated CD44 antibody (BD pharmingen, 1:25) or the Mouse IgG2b, κ isotope control antibody (BD pharmingen, 1:25), and flow

cytometry analysis was performed. All the flow cytometry data were analyzed using the Flow Jo software.

3.3.11 Luciferase reporter assay

In 48-well plates, ESCC cells were transfected with 200ng pLucTKS3 firefly luciferase construct (STAT3 reporter) and 4ng control Renilla luciferase vector pRL-TK along with other plasmids, and the cells were treated with/without 10ng/ml oncostatin M. 48h after transfection, luciferase activity was measured using the Dual-Luciferase Reporter Assay System (Promega) according to the manufacturer's instructions. Data are presented as ratios between firefly and Renilla luminescence activities.

3.3.12 Western blot

Frozen ESCC samples and adjacent non-tumorous esophageal epithelial tissues were homogenized and lysed with RIPA buffer (Cell Signaling) supplemented with protease inhibitors (Calbiochem, San Diego, CA, USA) and phosphatase inhibitors (Calbiochem). Whole cell lysates were prepared using RIPA buffer (Cell Signaling), and cytoplasmic/nuclear fractionations were prepared using NE-PER Nuclear and Cytoplasmic Extraction Kit (Pierce, Rockford, IL, USA). Protein concentration was determined using BCA Protein Assay Kit (Pierce). Proteins were separated on 10% SDS-PAGE and transferred to PVDF membrane (Millipore). The membranes were blocked in 5% non-fat milk and incubated with antibodies against pSTAT3^{Y705} (Cell Signaling; #9145), STAT3 (Cell Signaling; #4904), STAT3α (Cell Signaling; #8768), Flag (Sigma; F3165), β-Actin (Santa Cruz; sc-47778), α-Tubulin (Cell Signaling;

#9099), HDAC1 (Cell Signaling; #2062), PTP-MEG2 (Santa Cruz; sc-32671) and Fascin (DAKO; M3567). Next, the blots were washed, incubated with Anti-Rabbit IgG, HRP-linked Antibody (Cell Signaling; #7074) or Anti-mouse IgG, HRP-linked Antibody (Cell Signaling; #7076) and detected with ECL Western Blotting Substrate (Pierce).

3.3.13 Co-immunoprecipitation

Cells were washed in cold PBS and lysed using Cell Lytic Buffer M (Sigma) supplemented with protease inhibitors and phosphatase inhibitors. After 30min incubation on ice, the lysates were centrifuged at 15,000 ×g for 15 min. Protein concentrations were evaluated using BCA assay (Pierce), and 700µg of the supernatant diluted in 500µl Cell Lytic Buffer M was used for the subsequent co-immunoprecipitation assay. Four micrograms of the Flag antibody or the PTP-MEG2 antibody was used in each reaction, whereas 5µl STAT3α antibody was added in each reaction. These reaction tubes were rotated overnight at 4°C. No antibody was added in the negative control reaction. Then, 35µl of Protein G Plus/Protein A-Agarose suspension beads slurry (Calbiochem) was added, and allowed to incubate on a rotator for 6h at 4°C. The beads were then washed four times with cold PBS, and the final wash was performed using cold Cell Lytic Buffer M. The proteins were finally eluted from the beads in 50µl SDS protein loading buffer by boiling for 5min at 100°C. The samples were then subjected to SDS-PAGE and Western blot analysis.

3.3.14 STAT3 DNA-binding assay

300μg nuclear protein prepared using the NE-PER Nuclear and Cytoplasmic Extraction Kit was reconstituted in 500μl nuclear buffer, and was incubated with 3pmol of the STAT3 probe linked with biotin (Integrated DNA Technologies, Coralville, IA, USA) for 20min by rotating at room temperature. The sequence of the STAT3 probe is 5'-GATCCTTCTGGGAATTCCTAGA-3' (the underlined sequence is the STAT3 consensus binding motif). No probe was added in the negative control reaction. Then, 75μl streptoadvidin beads (Fisher Scientific) were added to each sample, and the samples were incubated overnight by rotating at 4°C. The next day, the samples were washed three times with cold PBS and centrifuged 5min at 2,500×g. Then, 50μl loading dye was added to the pellet beads which was boiled 100°C at for 5min, centrifuged at 16,000×g for 10min to obtain the supernatant. Western-blot assay was performed to detect the proteins.

3.3.15 Chromatin immunoprecipitation assay

The EZ-ChIP chromatin immunoprecipitation kit (Millipore) was used for this assay, and the experiments were performed according to the manufacturer's instructions. Briefly, 48h after the transfection in EC109 cells with wild-type STAT3β-Flag, mutant STAT3β-Y705F-Flag, or empty vector, 1×10^7 cells were treated with 1% formaldehyde to cross-link proteins to DNA, and the cell lysates were sonicated to shear the DNA into lengths between 200bp and 1000bp. The sheared DNA fragments were immunoprecipitated with antibodies against STAT3α (Cell Signaling, 1:50), Flag (Sigma, 1:50) or mouse IgG provided by the chromatin immunoprecipitation kit. The primers used for the PCR amplification of the *PLK1* promoter region containing the

STAT3 binding sites were: Primer 1, forward: 5'-GACAGCTTCGTTGCATCATGG-3'; reverse: 5'-CTGCGGTTCACTTGCGCCTCC-3'; Primer 2, forward: 5'-GCGTCCGTGTCAATCAGGTT-3'; reverse: 5'-CCTGCAGTCACTG-CAGCACTC-3'.

3.3.16 Immunohistochemistry

Paraffin embedded tissue blocks were constructed into tissue microarrays with a thickness of 4µm, duplicate sections were used for each sample. A recently published monoclonal antibody against STAT3β (clone E9E7) (28), a gift from Dr. David J. Tweardy, was used. For the scoring of STAT3β, the staining intensity was classified into 4 grades: negative staining was scored 0, weak staining was scored 1, moderate staining was scored 2, and strong staining was scored 3. The final score was calculated as the average of the duplicate samples.

3.3.17 Confocal microscopy

Cells transfected with the indicated plasmids were seeded on coverslips and allowed to grow for 24h under normal conditions or stimulated with oncostatin M (10ng/ml) after 20h starvation before being fixed with 4% paraformaldehyde (for 10min at room temperature). After washing with PBS, the cells were permeabilized in 0.2% Triton X-100 in PBS containing 3% BSA (w/v) and 10mM HEPES. Then, the cells were washed in PBS and blocked with 3% BSA (w/v) in PBS for 1h at room temperature. After rinsing the slides with PBS, the cells were incubated at room temperature for 1h with antibodies,

diluted in the blocking buffer, against pSTAT3^{Y705} (1:100; Cell Signaling, #9145) or STAT3α (1:200; Cell Signaling, #8768) plus Flag (1:1500; Sigma, F3165) or PTP-MEG2 (1:100; Santa Cruz, sc-32671). Then, the slides were washed in PBS and applied 45min with Alexa Fluor488 Goat Anti-Mouse Antibody (1:500; Molecular probes, A-11001, Eugene, OR, USA) and/or Alexa Fluor594 Goat Anti-Rabbit Antibody (1:500; Molecular probes, A-11037) that were diluted in PBS. Finally, the slides were mounted in ProLong Gold Antifade Mountant with DAPI that counterstains the nuclei. The cells were visualized with a Zeiss LSM510 confocal microscope at the Core Cell Imaging Facility, Cross Cancer Institute, University of Alberta.

3.3.18 Statistical analysis

The statistical analyses were performed using either the SPSS V.13.0 statistical software package or the Graphpad Prism6. To determine the differences between two independent groups of samples, Student's *t* test was used. Survival curves were plotted using the Kaplan-Meier method and compared using the log-rank test. The *χ2* test or Fisher's exact test was used to analyze the correlation between the expression of STAT3β and STAT3α/pSTAT3α^{Y705}, and the association of the expression status of various STAT3 markers and the clinical-pathological parameters. Differences were considered significant when the *P* value was less than 0.05.

3.4 Results

3.4.1 High STAT3β expression correlates with a favorable prognosis in ESCC patients

To our knowledge, the prognostic significance of STAT3β in human cancers has never been assessed. Using immunohistochemistry and a STAT3β-specific monoclonal antibody (28), we surveyed STAT3β expression in a cohort of 286 ESCC tumors. As shown in **Figure 3.1A**, 28 (9.8%) tumors expressed high levels of STAT3β, whereas 128 (44.8%) and 130 (45.5%) tumors expressed negative/weak and moderate STAT3β levels, respectively (**Figure 3.1B**). Benign epithelia adjacent to the tumors strongly expressed STAT3β in the supra-basal layer but negative in the basal layer (**Figure 3.1A**). Kaplan-Meier analysis revealed that moderate/strong expression of STAT3β significantly correlated with a longer overall survival (*P*=0.0009) and recurrence-free survival (*P*=0.0001) (**Figure 3.1C**). Moreover, among the 95 ESCC patients who received radio-chemotherapy, patients with tumors expressing moderate/strong STAT3β had a significantly longer overall survival (*P*=0.005) and recurrence-free survival (*P*=0.006), as compared to those with tumors expressing negative/weak levels of STAT3β (**Figure 3.1C**). Furthermore, as shown in **Table 3.2**, tumors with moderate/strong STAT3β expression were significantly less likely to have lymph node metastasis (*P*<0.001) and correlated with a low clinical stage (*P*<0.001). Multivariate Cox regression analysis revealed that moderate/strong expression of STAT3β is a significant independent protective factor for both overall survival (Hazard ratio=0.711, 95% confidence interval=0.511-0.990, *P*=0.043) and recurrence-free survival (Hazard ratio=0.708, 95% confidence interval =0.515-0.974, *P*=0.034) (**Table 3.3**).

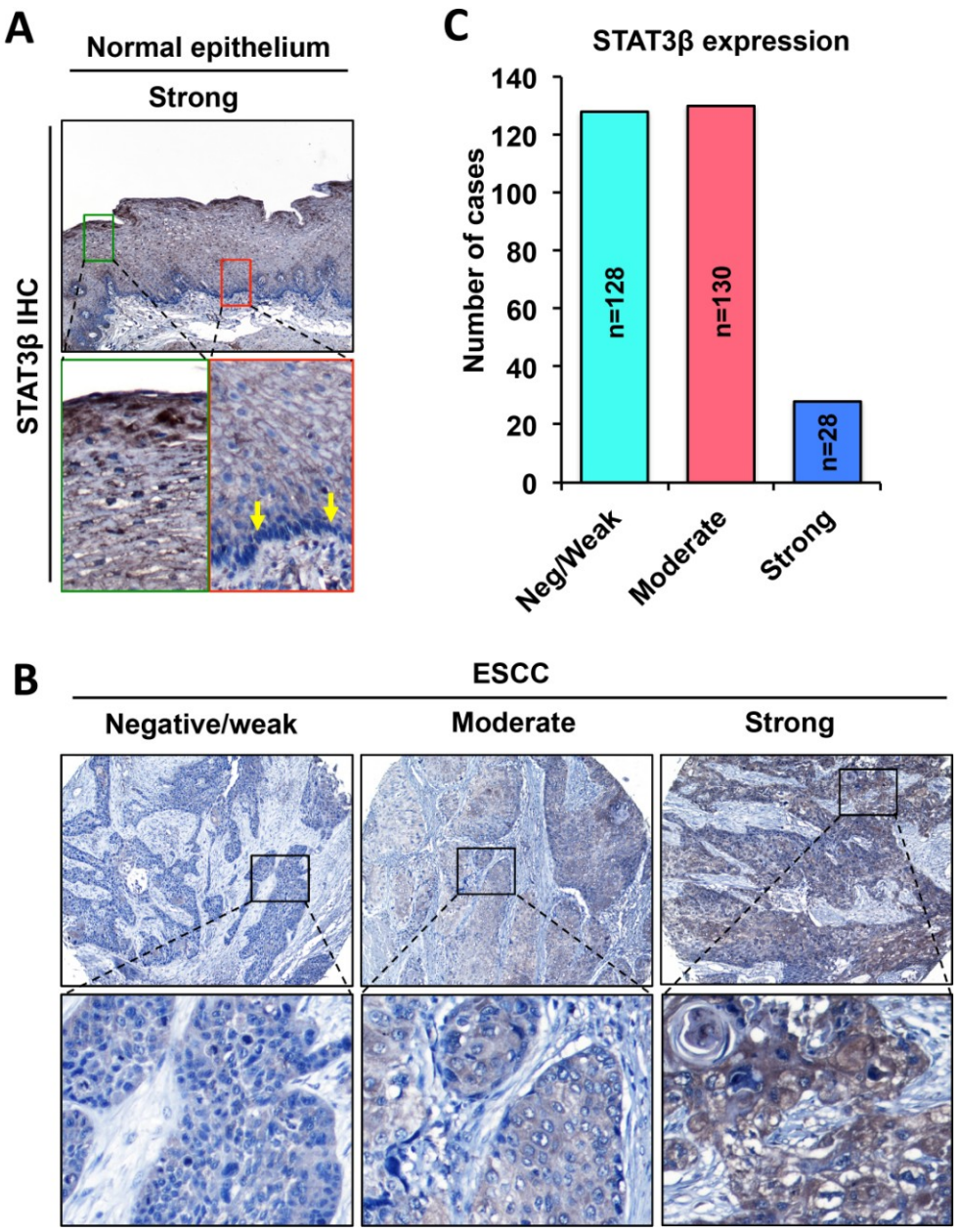

Figure 3.1 The expression and prognostic significance of STAT3β in ESCC. (***A-B***) Immunohistochemistry was performed to detect the expression of STAT3β in normal esophageal epithelial tissues and ESCC tumor samples. Representative cases of tissues showing different staining intensities of STAT3β were shown. The three ESCC cases shown from left to right represent negative/weak (Neg/Weak), moderate (Mod) and strong STAT3β staining, respectively. (***C***) The distribution of ESCC cases that show different expression levels of STAT3β as detected by Immunohistochemistry. **(Continued on the next page)**

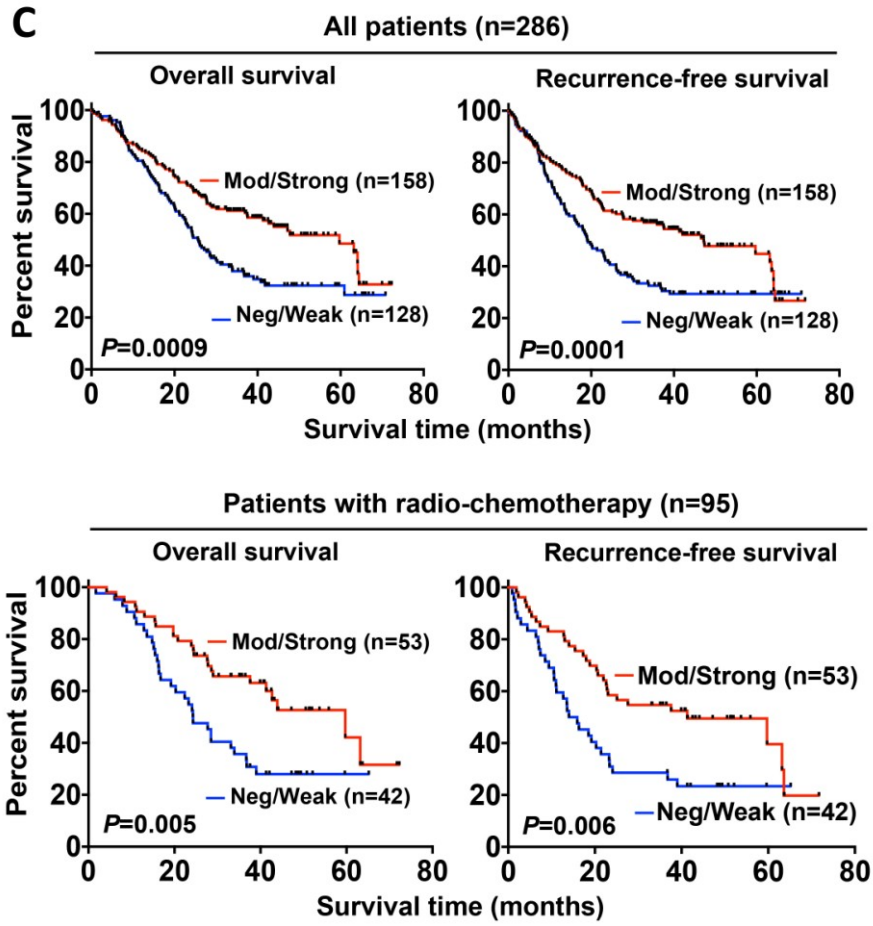

Figure 3.1C Kaplan-Meier survival analysis was used to evaluate the prognostic value of STAT3β in ESCC patients, and log-rank test was used in the statistical analysis.

Table 3.2 Correlation among clinicopathological parameters and the expression of STAT3β in ESCC patients (n=286)

Parameters	Patient number	STAT3β expression		*P*
		Negative/Weak	Strong	
Gender				
Male	223	100 (45%)	123 (55%)	
Female	63	28 (44%)	35(56%)	1.000
Age				
<58 years	149	66 (44%)	83 (56%)	
≥58 years	137	62 (45%)	75 (55%)	0.906
Histological grade				
G1	47	18 (38%)	29 (62%)	
G2 + G3	239	110 (46%)	129 (54%)	0.342
Primary tumor				
T1 + T2	55	21 (38%)	34 (62%)	
T3 + T4	231	107 (46%)	124 (54%)	0.294
Tumor size				
⩽5cm	198	92 (47%)	106 (53%)	
＞5cm	88	36 (41%)	52 (59%)	0.440
Lymph node				
Negative	145	48 (33%)	97 (67%)	
Positive	141	80 (57%)	61 (43%)	***<0.001***
TNM stage				
I + IIA + IIB	158	52 (33%)	106 (67%)	
IIIA + IIIB + IIIC + IV	128	76 (59%)	52 (41%)	***<0.001***

Table 3.3 Multivariate Cox regression analysis for patient survival (n=286)

Variables	Overall survival		Recurrence-free survival	
	HR (95% CI)	*P*	HR (95% CI)	*P*
STAT3β				
Mod/strong vs Neg/weak	0.711 (0.511 - 0.990)	***0.043****	0.708 (0.515 - 0.974)	***0.034****
Tumor size				
>5cm vs ≤5cm	1.294 (0.927 - 1.808)	0.130	1.41 (1.014-1.957)	***0.041****
Histological grade				
G2 + G3 vs G1	1.252 (0.801 - 1.95)	0.325	1.292 (0.835 -2.001)	0.249
Primary tumor				
T3 + T4 vs T1 + T2	1.297 (0.832 - 2.020)	0.252	1.032 (0.677 - 1.572)	0.883
Lymph node				
N1 + N2 + N3 vs N0	1.972 (1.403 - 2.770)	***0.001*****	1.953 (1.412 - 2.703)	***0.001*****

3.4.2 STAT3β sensitizes ESCC cells to chemotherapy *in vitro*

The prognostic significance of STAT3β suggests that STAT3β is a tumor suppressor in ESCC. To delineate the mechanism, we employed EC109 and KYSE150 cells that had been stably transfected with *STAT3β* cloned in a conditional expression vector (*i.e.* the tetracycline-off system), and these cells were labeled EC109-STAT3β-TetOff and KYSE150-STAT3β-TetOff, respectively. As shown in **Figure 3.2A-D**, enforced expression of STAT3β (*i.e.* no doxycycline treatment) in EC109 cells significantly decreased the clonogenic capacity and increased their sensitivity to 5-flurouracil (5-FU) and cisplatin in a STAT3β dose-dependent manner ($P<0.05$). Similar observations were made with KYSE150-STAT3β-TetOff cells (**Figure 3.2E**). To determine whether the tumor suppressor function of STAT3β was mediated via antagonizing the oncogenic function of STAT3α, the relative expression of STAT3α and STAT3β were modulated using STAT3 siRNA and doxycycline, respectively, in the same two cell lines. As shown in **Figure 3.2F-H,** high expression of STAT3β (*i.e.* no doxycycline treatment) markedly enhanced the chemosensitivity of ESCC cells to 5-FU and cisplatin, which was comparable to the effects of STAT3α knockdown.

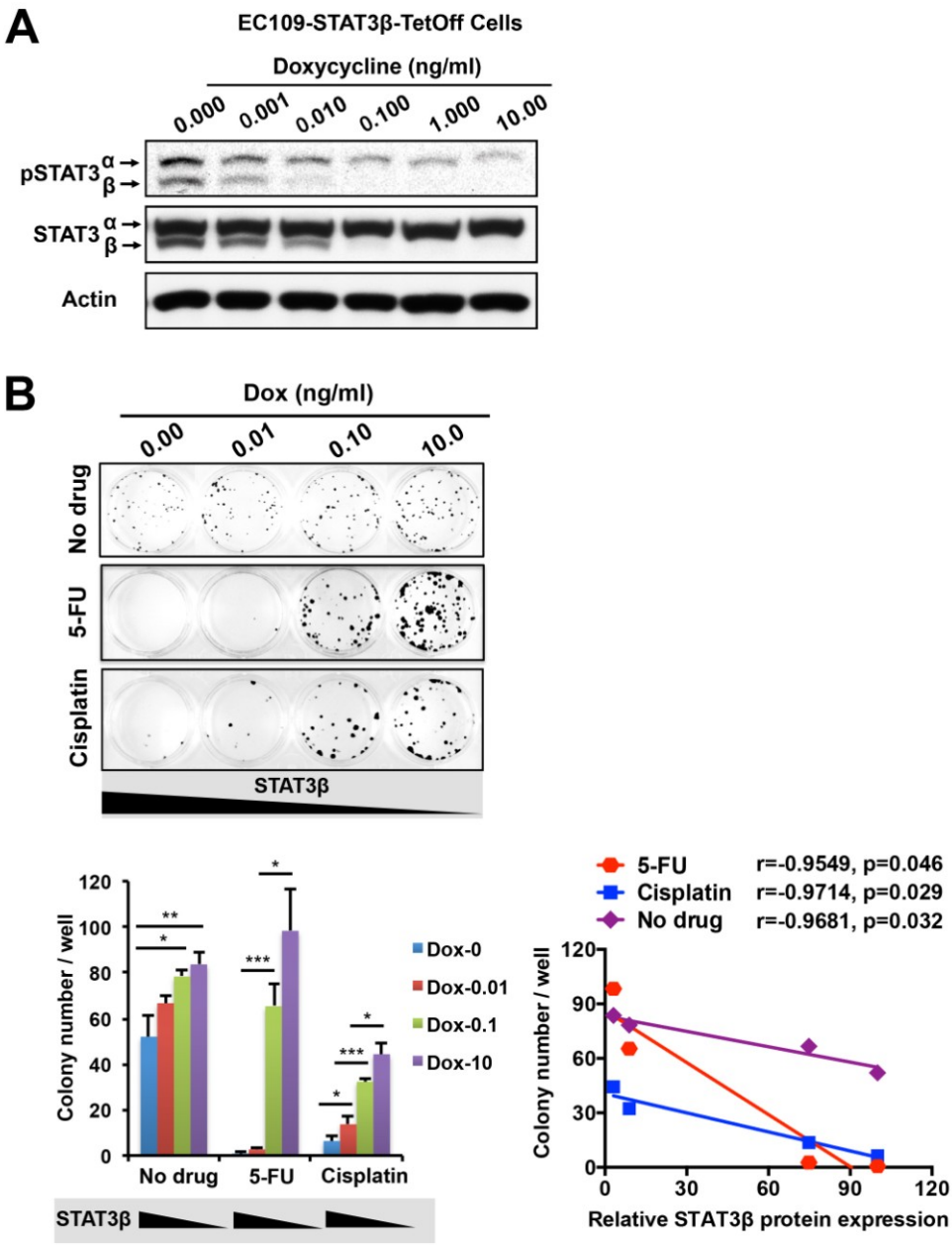

Figure 3.2 STAT3β suppresses the chemoresistance and stem-like properties of ESCC cells. (A) Doxycycline (Dox) was used to control STAT3β expression in EC109-STAT3β-TetOff cells. (B) The function of STAT3β in chemoresistance was determined using clonogenic assay, and the correlation between STAT3β and chemoresistance was analyzed (n=4, Pearson correlation). **(Continued on the next page)**

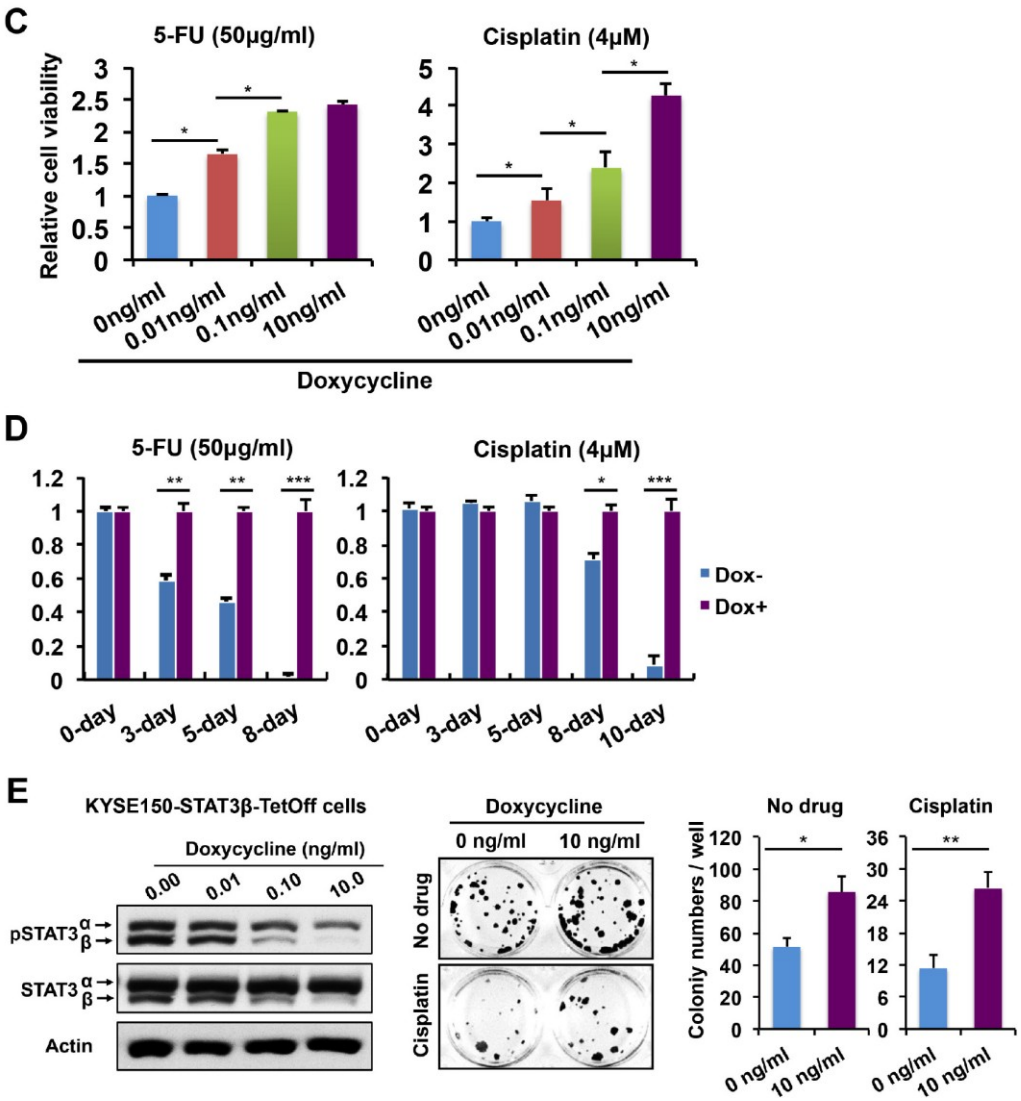

Figure 3.2C-E (**C**) EC109-STAT3β-TetOff cells treated with different concentrations of doxycycline were exposed to 50μg/ml 5-fluorouracil or 4μM cisplatin for 4 days and 5 days, respectively. Cell viability was measured using MTS assay. Data are presented as the mean ± SD (n=3). (**D**) EC109-STAT3β-TetOff cells that were treated with/without doxycycline (Dox+ or Dox-) were exposed to 50μg/ml 5-fluorouracil or 4μM cisplatin for 24h, then cell viability was measured on the indicated times. Data are presented as the mean ± SD (n=3). (**E**) KYSE150-STAT3β-TetOff cells treated with different doses of Doxycycline, Western blot and clonogenic assay was performed. **P*<0.05, ***P*<0.01, Student's *t* test (n=3). **(Continued on the next page)**

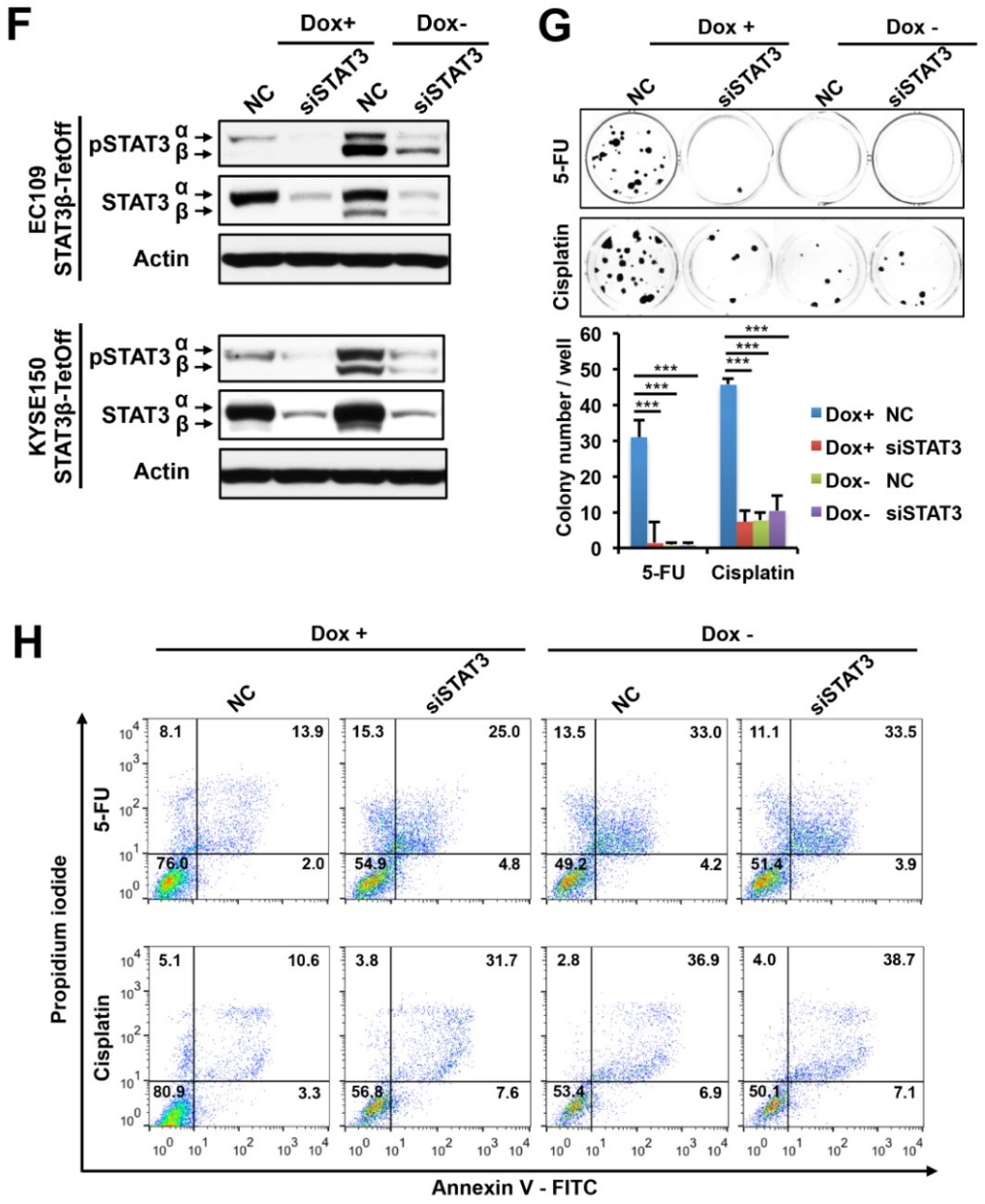

Figure 3.2F-H Protein expression was determined by western blots (**F**), and chemoresistance was assessed using clonogenic assay (n=3) (**G**) and Propidium iodide and Annexin V double staining (n=3) (**H**).

3.4.3 STAT3β decreases the cancer stem cell population and sensitizes ESCC cells to chemotherapy *in vitro*

Since extensive studies have linked cancer stem cells to chemoresistance (29), we therefore determined the impact of STAT3β on the cancer stem cell population of ESCC cells. As shown in **Figure 3.3A**, cells with enforced expression of STAT3β (no doxycycline treatment) or STAT3α knockdown formed approximately 2-fold less tumorspheres compared with the negative controls (P<0.01). Furthermore, the number of cells per tumorsphere was significantly decreased (~3.5 fold) in response to either treatment (P<0.001) (**Figure 3.3A**). To directly quantify cancer stem cells, we performed Hoechst and CD44 staining, as reported in previous studies (25,30). As shown in **Figure 3.3B-C**, enforced expression of STAT3β and STAT3α knockdown significantly decreased the Hoechst-negative cancer stem cells from 1.12% to 0.46% and 0.63%, respectively. Similarly, $CD44^{high}$ cancer stem cells were also decreased by enforced expression of STAT3β and STAT3α knockdown, from 19.2% to 12.3% and 11.6%, respectively (**Figure 3.3B-C**).

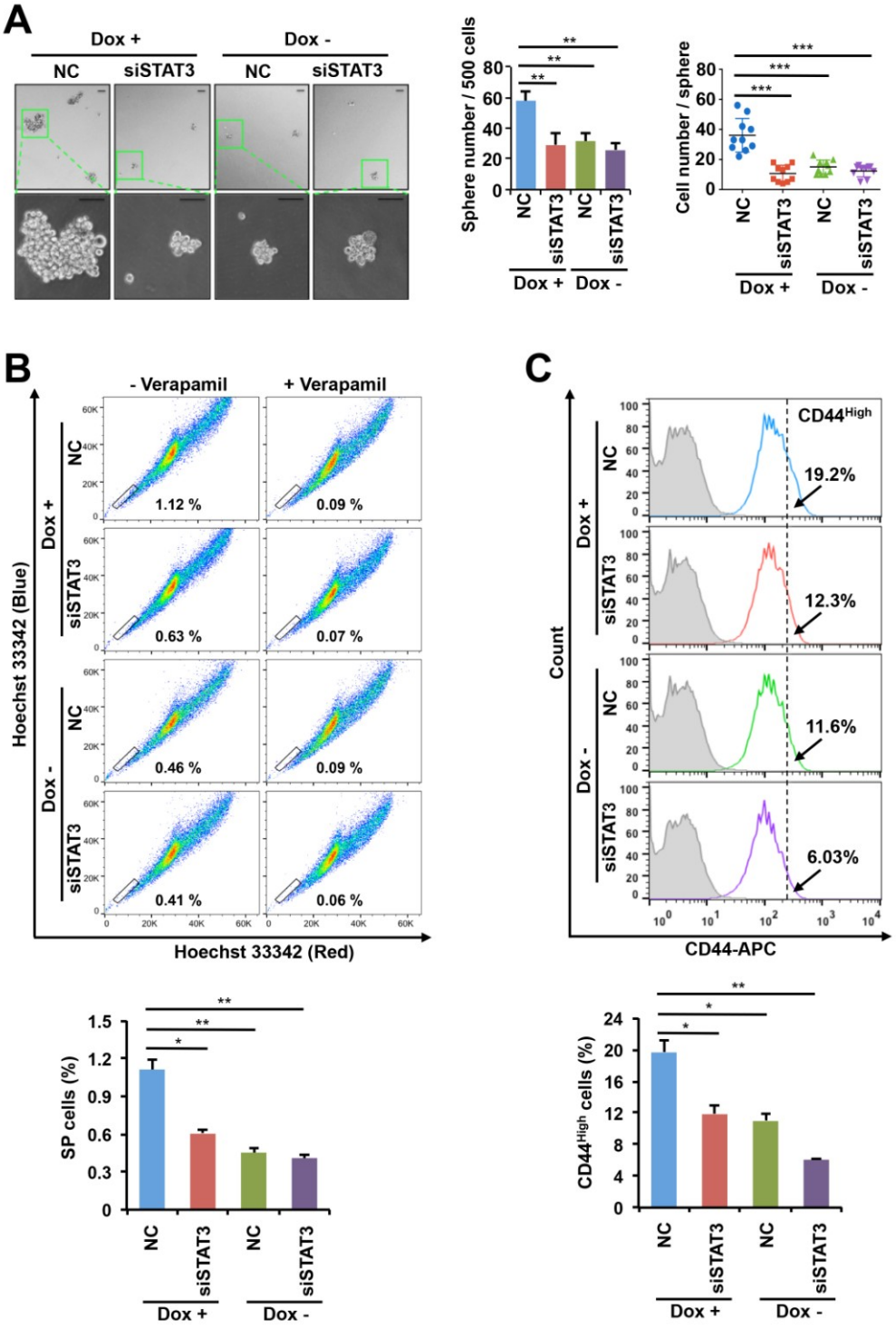

Figure 3.3 STAT3β suppresses the population of cancer stem-like cells in ESCC. (**A**) Tumorsphere formation assay was performed using EC109-STAT3β-TetOff cells (n=3). Scale bars: 50μm. (**B-C**) Hoechst 33342 dye efflux assay and CD44 staining were performed using EC109-STAT3β-TetOff cells (n=3). Grey graph indicates negative control.

3.4.4 STAT3β sensitizes ESCC cells to chemotherapy *in vivo*

The tumor suppressor function of STAT3β was further tested in nude mice xenografted with KYSE150-STAT3β-TetOff cells. As illustrated in **Figure 3.4A-B**, xenograft formation was detectable consistently on day 8, after which multiple doses of 5-FU or cisplatin was injected into these animals intra-peritoneally. We observed significant differences in tumor growth rate between animals that received doxycycline (*i.e.* low level of STAT3β) and those did not (*i.e.* high level of STAT3β) from day 14 for 5-FU and day 17 for cisplatin (**Figure 3.4B**). Under both chemotherapy regimens, xenografts with high STAT3β expression shrank significantly faster than those with low STAT3β expression ($P<0.05$) (**Figure 3.4B**). The histologic features and the expression status of STAT3β (detectable by FLAG antibody) in these xenografts are shown in **Figure 3.4C**.

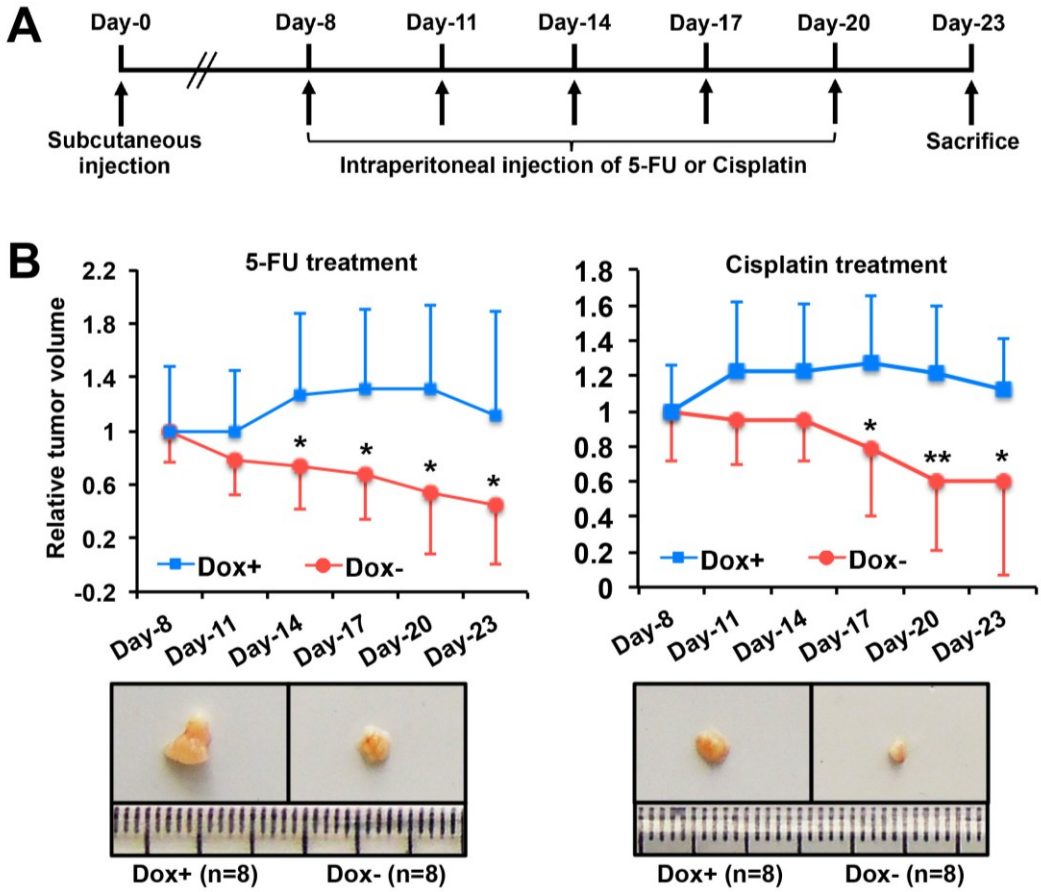

Figure 3.4 STAT3β suppresses the chemoresistance of ESCC cells *in vivo*. (**A**) A diagram showing the experimental design of the animal study, in which KYSE150-STAT3β-TetOff cells were used as a cell model. (**B**) The tumor volume changes relative to the initial tumor volume before drug treatment are plotted (n=8 in each group), and representative tumors are shown. All the data are presented as the mean ± SD, **P*<0.05, ***P*<0.01, Student's *t* test. **(Continued on the next page)**

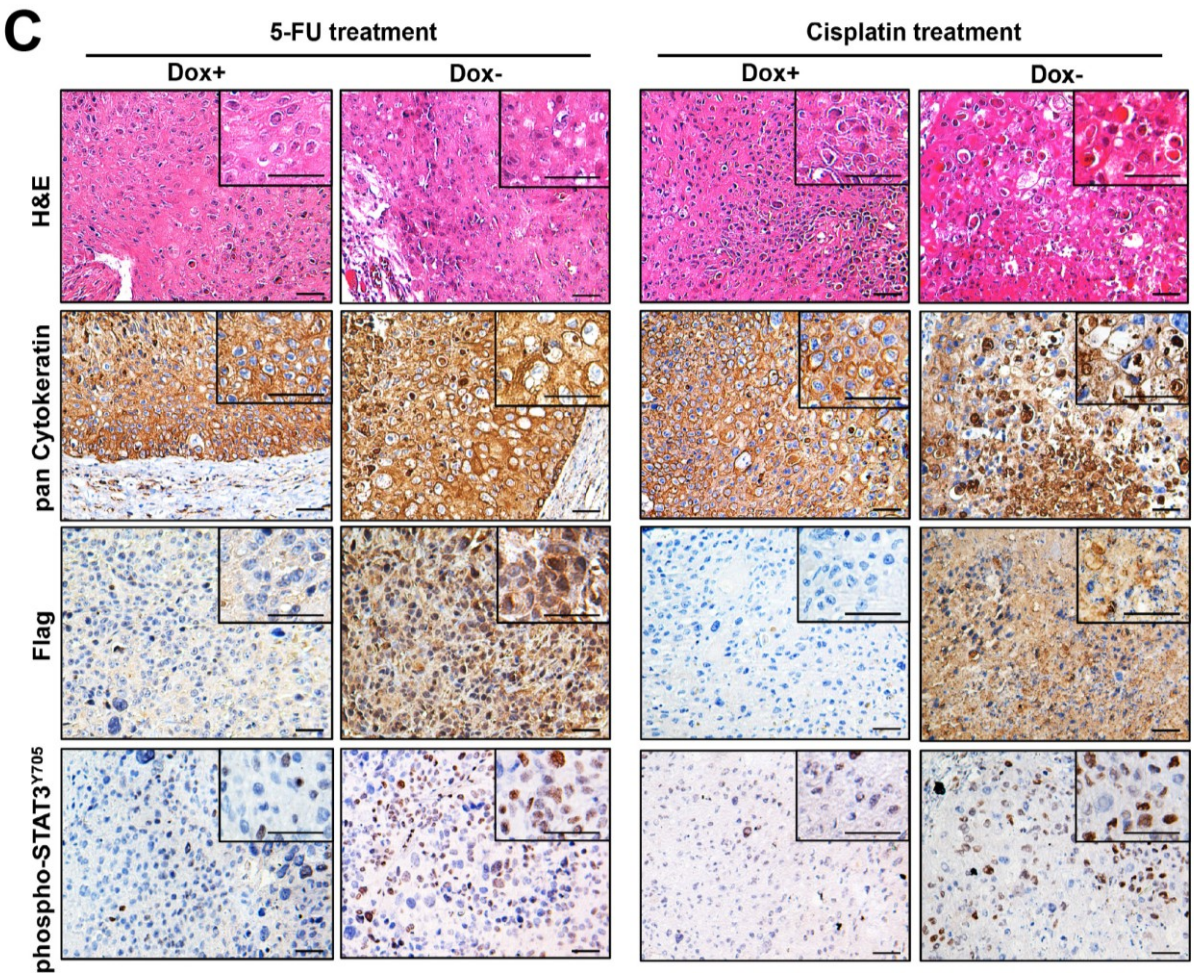

Figure 3.4C H&E staining and Immunohistochemistry were performed in mice xenografts. Scale bars: 50μm.

3.4.5 STAT3β enhances the Tyrosine705 phosphorylation and nuclear translocation of STAT3α, which is dependent on the Tyrosine705 residue in STAT3β

Despite the potent tumor suppressor function of STAT3β as shown above, we observed that enforced expression of STAT3β (controlled by doxycycline) substantially increased pSTAT3α^{Y705} both *in vitro* (**Figure 3.2A,E and F**) and *in vivo* (**Figure 3.4C**). To further validate these findings, wild-type STAT3β cDNA, mutant STAT3β^{Y705F} cDNA and STAT3 siRNAs were transiently transfected into EC109 and KYSE150 cells to manipulate the relative expression of STAT3α and STAT3β. Consistently, we found that *STAT3β* transfection again increased pSTAT3α^{Y705} levels (**Figure 3.5A**), and both enforced expression of STAT3β and STAT3α knockdown significantly decreased chemoresistance in both cell lines (P<0.01) (**Figure 3.5B**). However, Y705F mutation in STAT3β significantly abrogated its tumor suppressor effect (P<0.05) (**Figure 3.5B**). These findings suggest that the tumor suppressor effects of STAT3β may be related to its interaction with STAT3α, and Tyrosine705 is an important residue for the function of STAT3β.

Thus, we examined the interplay between these two isoforms closely. As shown in **Figure 3.5C**, enforced expression of STAT3β promoted a more sustained STAT3α^{Y705} phosphorylation upon oncostatin M (OSM) stimulation, as compared to cells transfected with an empty vector. Specifically, while the expression of pSTAT3α^{Y705} diminished to a faint level at 60 minutes after OSM exposure in empty vector-transfected cells, the pSTAT3α^{Y705} signal in *STAT3β*-transfected cells was maintained at a high level for at least 120

minutes after OSM stimulation. This effect of STAT3β was found to be dependent on its Tyrosine705 residue, as replacement by phenylalanine at this site almost completely abrogated the observed effects (**Figure 3.5C**).

Further studies using the subcellular fractionation experiment showed that the high level of pSTAT3α^{Y705} induced by *STAT3β* was evenly distributed between the cytoplasm and nucleus (**Figure 3.5D**). Furthermore, even in the absence of OSM stimulation, *STAT3β* transfection led to a substantial increase in the expression of pSTAT3α^{Y705} in ESCC cells, and the *STAT3β*-induced pSTAT3α^{Y705} was again evenly distributed between the cytoplasm and nucleus (**Figure 3.5D**). Results from confocal microscopy analysis were in line with these interpretations (**Figure 3.5E**).

Lastly, in support that the enhancing effect of STAT3β on pSTAT3α^{Y705} also occurs in patient samples, western blot studies revealed a significant correlation between STAT3β and pSTAT3α^{Y705} expression in our cohort of ESCC samples (n=91, *P*=0.019) (**Figure 3.5F and Figure 3.6**).

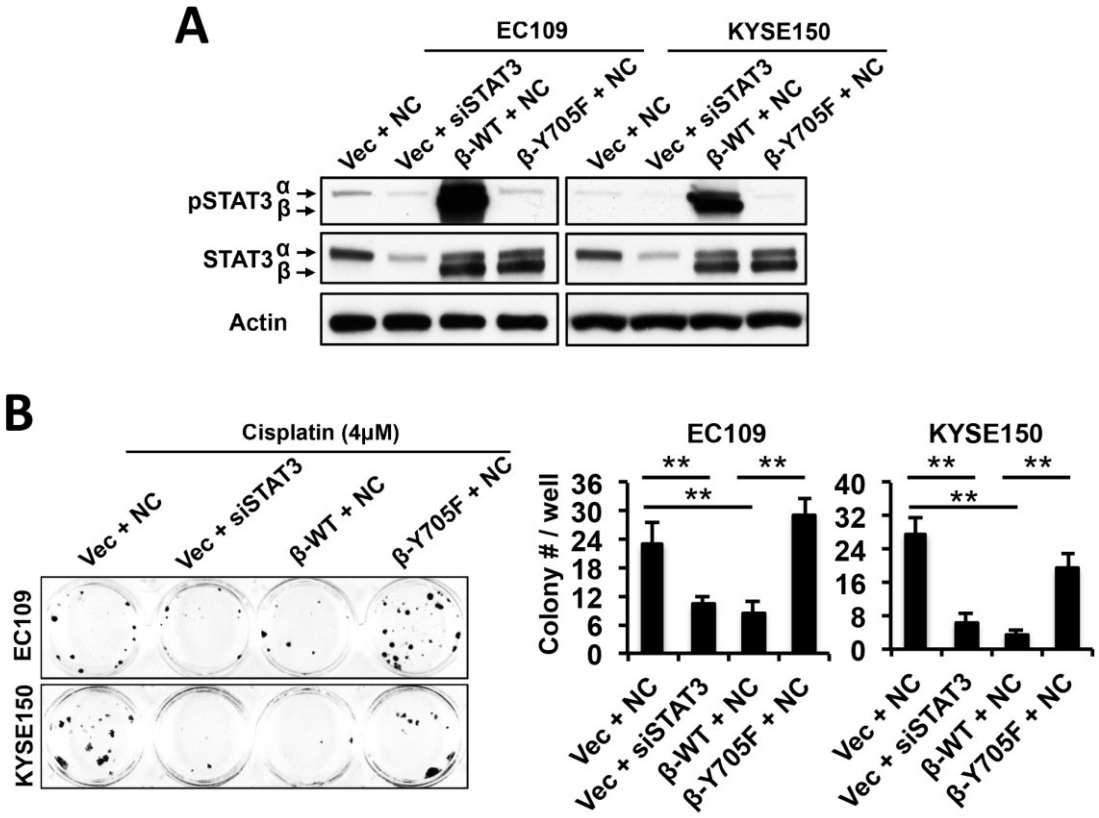

Figure 3.5 STAT3β enhances the Tyrosine705 phosphorylation and nuclear translocation of STAT3α, which is dependent on the Tyrosine705 residue in STAT3β. (**A-B**) Protein expression in the transfected cells was detected using western blots (**A**), and chemoresistance was measured using clonogenic assay (n=3) (**B**). **(Continued on the next page)**

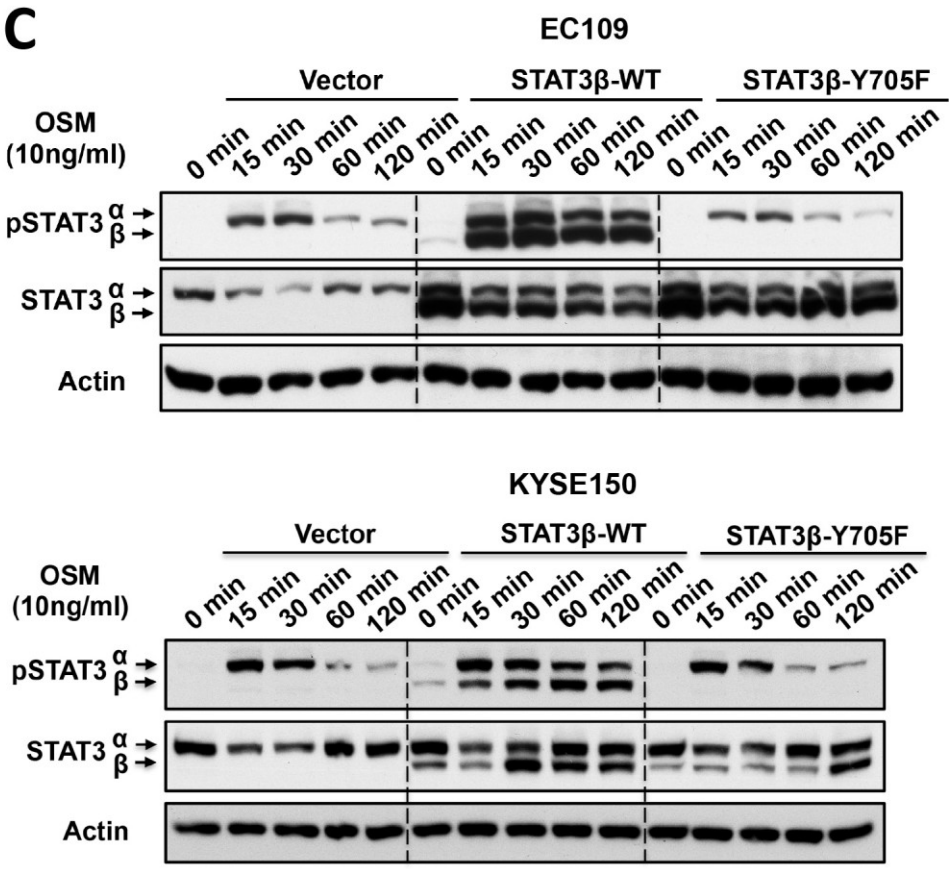

Figure 3.5C Protein expression was measured using western blots in cells treated with oncostatin M (OSM) for different times. **(Continued on the next page)**

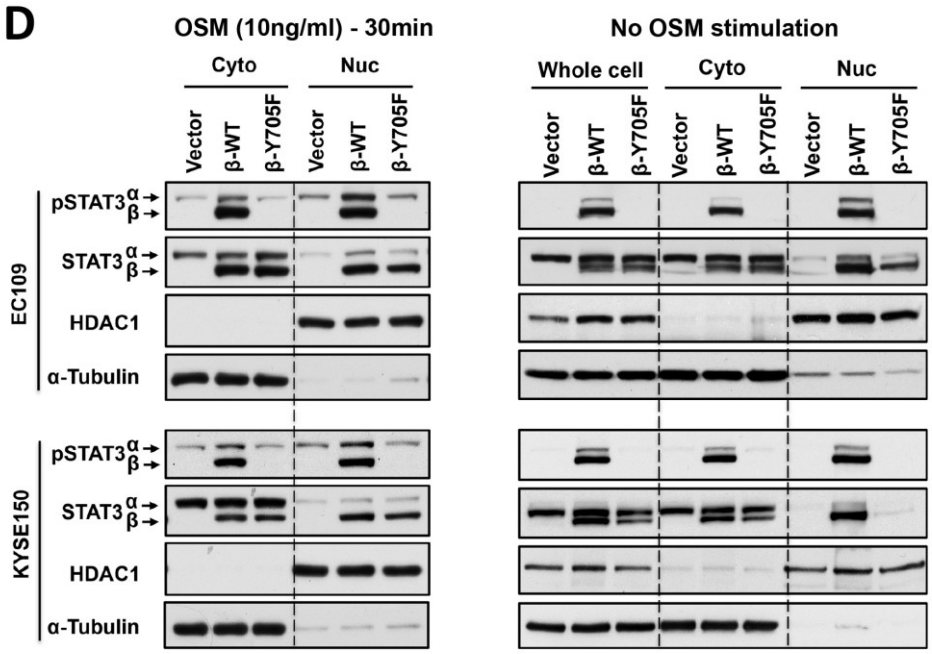

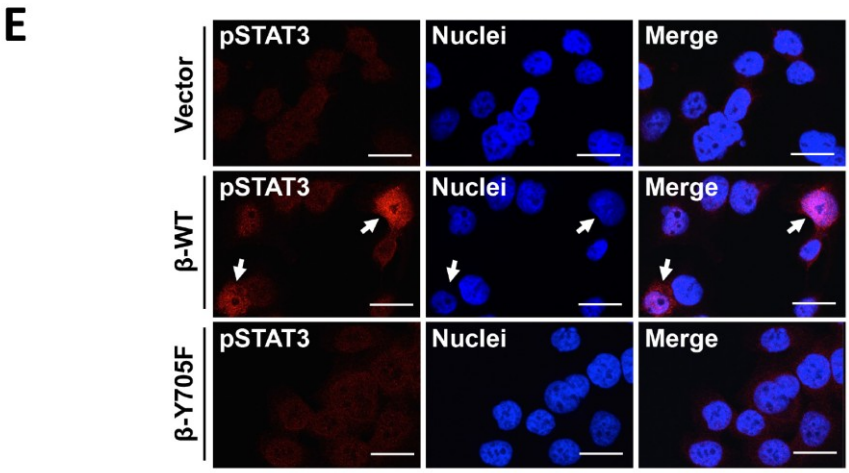

F Correlation between STAT3β and pSTAT3α in ESCC samples (n=91)

Parameters		pSTAT3α^{Y705}		Fisher's exact test
		Increase/equal	Decrease	
STAT3β	Increase	9	8	*P*=0.019
	Decrease/equal	17	57	

Figure 3.5D-F (**D**) The cytoplasmic and nuclear expression of STAT3α and STAT3β. (**E**) Confocal microscopic detection of pSTAT3^{Y705} in the transfected EC109 cells. Scale bars: 10μm. (**F**) Correlation between STAT3β and pSTAT3α^{Y705} in ESCC samples (n=91). Details are described in **Figure 3.6**.

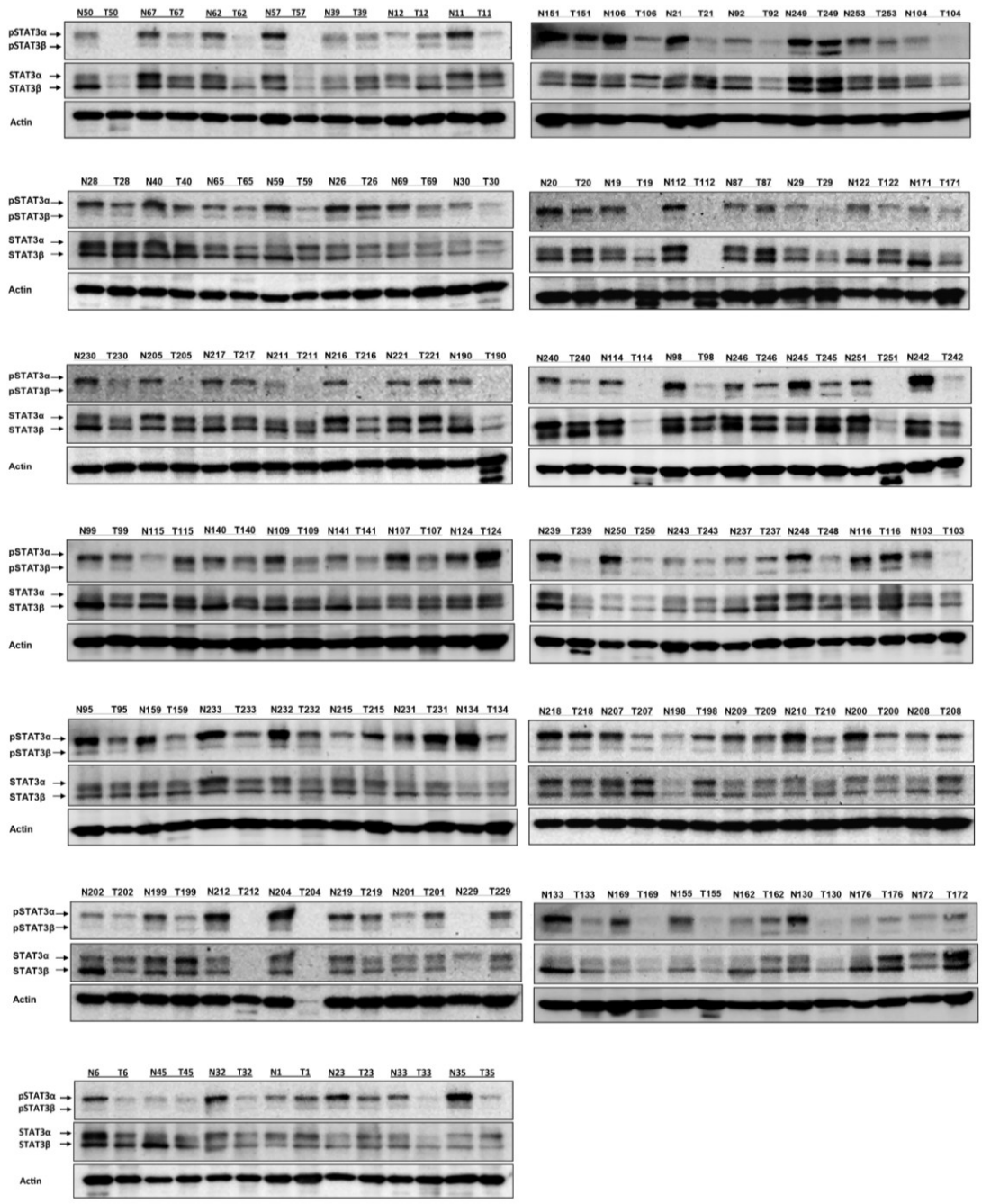

Figure 3.6 The complete Western blot data showing the expression of phospho-STAT3α/β^{Tyr705} (pSTAT3α/β) and STAT3α/β in ESCC samples. For the subsequent survival analysed, the expression changes of pSTAT3α/β and STAT3α/β in ESCC tumors compared with the cased-matched adjacent non-tumorous tissues were analyzed manually: ESCC tumors with slight, moderate or sharp increase were assigned with +1, +2 and +3, respectively; while slight, moderate or sharp decrease were assigned with -1, -2 and -3, respectively. The cases with no appreciable changes in the expression of the various STAT3 factors were assigned with 0.

3.4.6 STAT3β protects pSTAT3α^{Y705} from dephosphorylation by protein tyrosine phosphatases (PTPs)

The molecular mechanism underlying the enhancing effect of STAT3β on the expression of pSTAT3α^{Y705} remains unclear. We hypothesized that the dephosphorylation process of pSTAT3α^{Y705} is attenuated in the presence of STAT3β. Our data are in support of this hypothesis. First, as shown in **Figure 3.7A**, pSTAT3α^{Y705} expression in negative control transfected cells (both EC109 and KYSE150) was markedly increased by the treatment with a PTPs inhibitor Na_3VO_4, indicating that PTPs play an important role in the dephosphorylation of STAT3α. Second, the pSTAT3α^{Y705} expression in the negative control cells treated with Na_3VO_4 was comparable to that in the *STAT3β*-transfected cells without Na_3VO_4 treatment **(Figure 3.7A**), suggesting that STAT3β might be able to mimic the effects of Na_3VO_4 to antagonize PTPs in the dephosphorylation of STAT3α. Third, while Y705F mutation completely abolished the effect of STAT3β on enhancing pSTAT3α^{Y705} expression in the absence of Na_3VO_4, this "functional defect" of the STAT3β^{Y705F} mutant was restored by the treatment with Na_3VO_4 **(Figure 3.7A**), suggesting the importance of this amino acid residue for the function of STAT3β in antagonizing the function of PTPs in the dephosphorylation of STAT3α.

To further support these findings, compared with STAT3β, the STAT3β^{Y705F} mutant had a diminished ability to prolong the phosphorylation of STAT3α^{Y705} after OSM stimulation; again, this ‘functional defect’ of the STAT3β^{Y705F}

mutant was restored by Na_3VO_4 treatment. This observation was made in both EC109 and KYSE150 cells (**Figure 3.7B**).

The mechanism behind how STAT3β antagonizes the function of PTPs during the process of STAT3α dephosphorylation remains unknown. We hypothesized that STAT3β could interfere with the interaction between PTPs and STAT3α. To this end, we selected PTP-MEG2, a recently identified PTP that specifically interact with STAT3 to dephosphorylate $pSTAT3^{Y705}$ in breast cancer cells (31). As shown in **Figure 3.7C**, compared with empty vector transfection, STAT3β dramatically decreased the interaction between STAT3α and PTP-MEG2, whereas Y705F mutation of STAT3β diminished the effect exerted by STAT3β. Results obtained from the confocal microscopy studies are in keeping with our model (**Figure 3.7D**). We also determined whether other PTPs that have been shown to interact and dephosphorylate STAT3, including TC-45, SHP-1, SHP-2 [31], play a role in the regulation of STAT3α phosphorylation by STAT3β. Co-IP experiments were performed for this purpose, but the interaction between STAT3α and the three PTPs was not significantly changed by *STAT3β* transfection (data not shown).

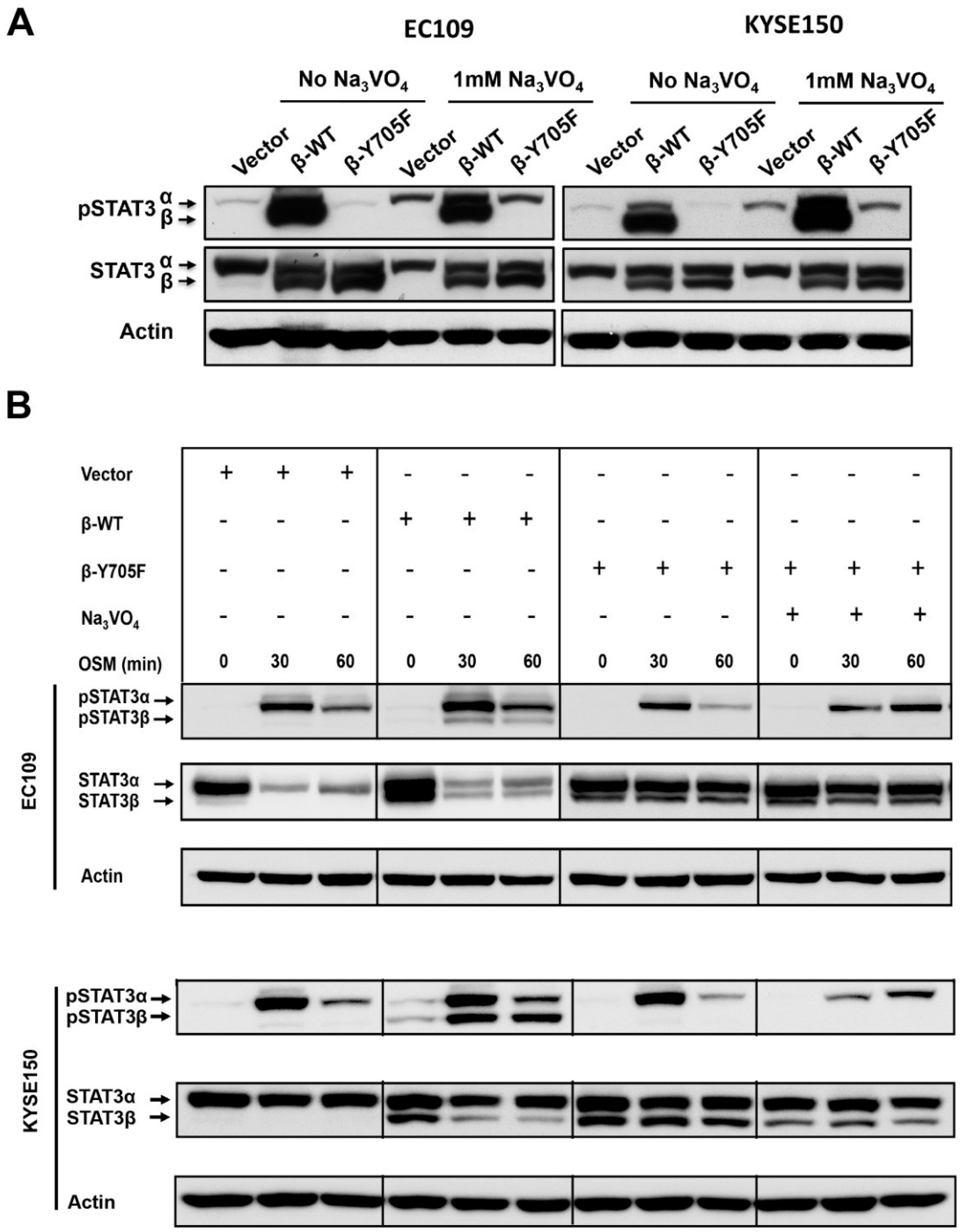

Figure 3.7 STAT3β protects pSTAT3α^{Y705} from dephosphorylation. (**A**) Transfected cells were treated with/without 1mM Na_3VO_4 for 15h, and western blot was performed. (**B**) Transfected EC109 and KYSE150 cells were pretreated with/without 1mM Na_3VO_4 for 4h before OSM (10ng/ml) stimulation. Western blot was performed. **(Continued on the next page)**

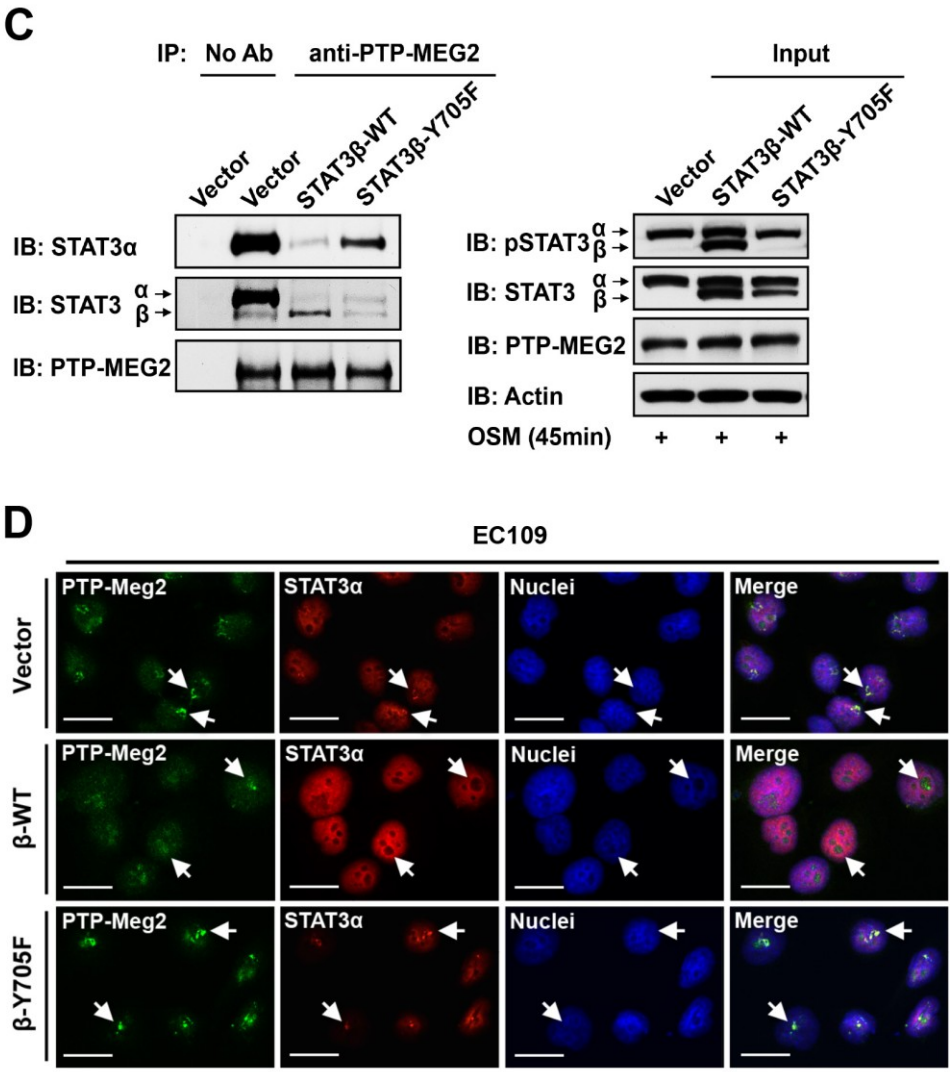

Figure 3.7C-D Transfected EC109 cells were stimulated with OSM for 45min, and co-immunoprecipitation (co-IP) (**C**) and confocal microscopy (**D**) were performed to determine the interaction between PTP-MEG2 and STAT3α. Scale bars: 10μm.

3.4.7 STAT3β enhances the DNA binding of STAT3α by forming heterodimers, whereas the transcriptional activity of STAT3α was decreased by STAT3β

The tumor suppressor role of STAT3β and the enhancing effect of STAT3β on the oncogenic pSTAT3α^{Y705} prompted us to determine how STAT3β influences the function of STAT3α in ESCC cells. First, reciprocal co-immunoprecipitation experiment showed that STAT3β was able to form heterodimers with STAT3α, and this interaction was enhanced by OSM stimulation (**Figure 3.8A**). In comparison, the functional defective STAT3β^{Y705F} mutant could not effectively form heterodimers with STAT3α (**Figure 3.8A**), suggesting that the heterodimerization is required for the function of STAT3β. We then validated this finding using confocal microscopy (**Figure 3.8B**). Specifically, upon OSM stimulation, transfected STAT3β translocated to the nuclei and overlapped with the nuclear-STAT3α, whereas the STAT3β^{Y705F} mutant was largely localized in the cytoplasm and showed no substantial co-localization with STAT3α.

We then assessed how STAT3β impacts on the transcriptional activity of STAT3α. A STAT3 reporter was used, and luciferase activity served as the readout. Since STAT3α but not STAT3β carries the domain responsible for transcription regulation, the luciferase activity detectable should reflect the transcription activity of STAT3α alone. As shown in **Figure 3.8C**, although transfection of *STAT3β* markedly enhanced STAT3α^{Y705} phosphorylation, it dramatically decreased the transcriptional activity of STAT3 as compared with negative control (P<0.001). Again, the Y705F mutation significantly

diminished the effect of STAT3β (P<0.01). Similar results were observed when these two cell lines were stimulated with OSM (**Figure 3.8C**). To further validate these observations, we repeated the same experiments using EC109-STAT3C-TetOff cells. As shown in **Figure 3.8D**, doxycycline treatment effectively suppressed STAT3C expression and decreased the STAT3 transcriptional activity by approximately 40% (P<0.01). In comparison, while transfection of STAT3β increased pSTAT3α^{Y705}, the STAT3 transcriptional activity was decreased by >80% (P<0.001).

We then asked whether the decreased STAT3 transcriptional activity induced by STAT3β was caused by a reduction in STAT3 DNA-binding ability. A pull-down experiment using a probe that contains the STAT3 consensus DNA-binding site was performed. Surprisingly, we found that STAT3β markedly promoted the DNA-binding of STAT3α, compared with the negative control and STAT3β^{Y705F} (**Figure 3.8E**). Moreover, STAT3β was also able to effectively bind to the DNA probe. To determine whether STAT3β can enhance the occupancy of STAT3α in the promoter region of its downstream target genes, ChIP-PCR was performed. PLK1, a reported oncogenic mediator of STAT3 in ESCC (24), was selected for this experiment. As shown in **Figure 3.8F,** we found that transfection of wild-type *STAT3β* but not the mutant *STAT3β^{Y705F}* markedly increased the occupancy of both STAT3α and STAT3β (FLAG-tagged) in the *PLK1* promoter. However, enforced expression of STAT3β dramatically decreased the expression of PLK1 to an extent that was comparable to STAT3α knockdown in both parental and STAT3β-TetOff cells (**Figure 3.8G**). Again, Y705F mutation in STAT3β abrogated its function

in suppressing PLK1 expression (**Figure 3.8G**). Taken together, these data indicate that the transcriptional activity of STAT3α was decreased by STAT3β, although the DNA binding of STAT3α was enhanced by STAT3β via forming heterodimers.

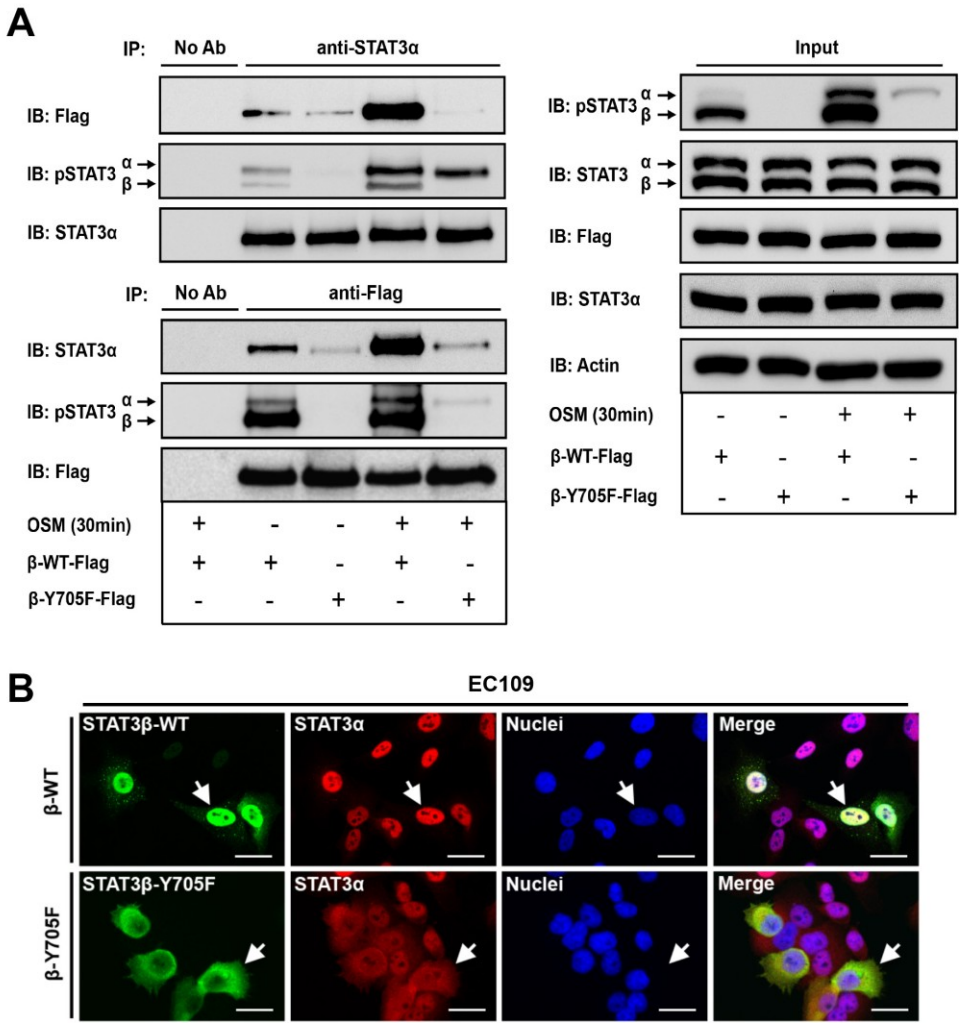

Figure 3.8 STAT3β enhances the DNA binding of STAT3α by forming heterodimers, whereas the transcriptional activity of STAT3α was decreased by STAT3β. (**A**) Reciprocal co-IP was performed to assess the interaction between STAT3α and STAT3β. (**B**) Confocal microscopy was performed to evaluate the co-localization of STAT3β and STAT3α after OSM treatment (10ng/ml 30min). Scale bars: 10μm. **(Continued on the next page)**

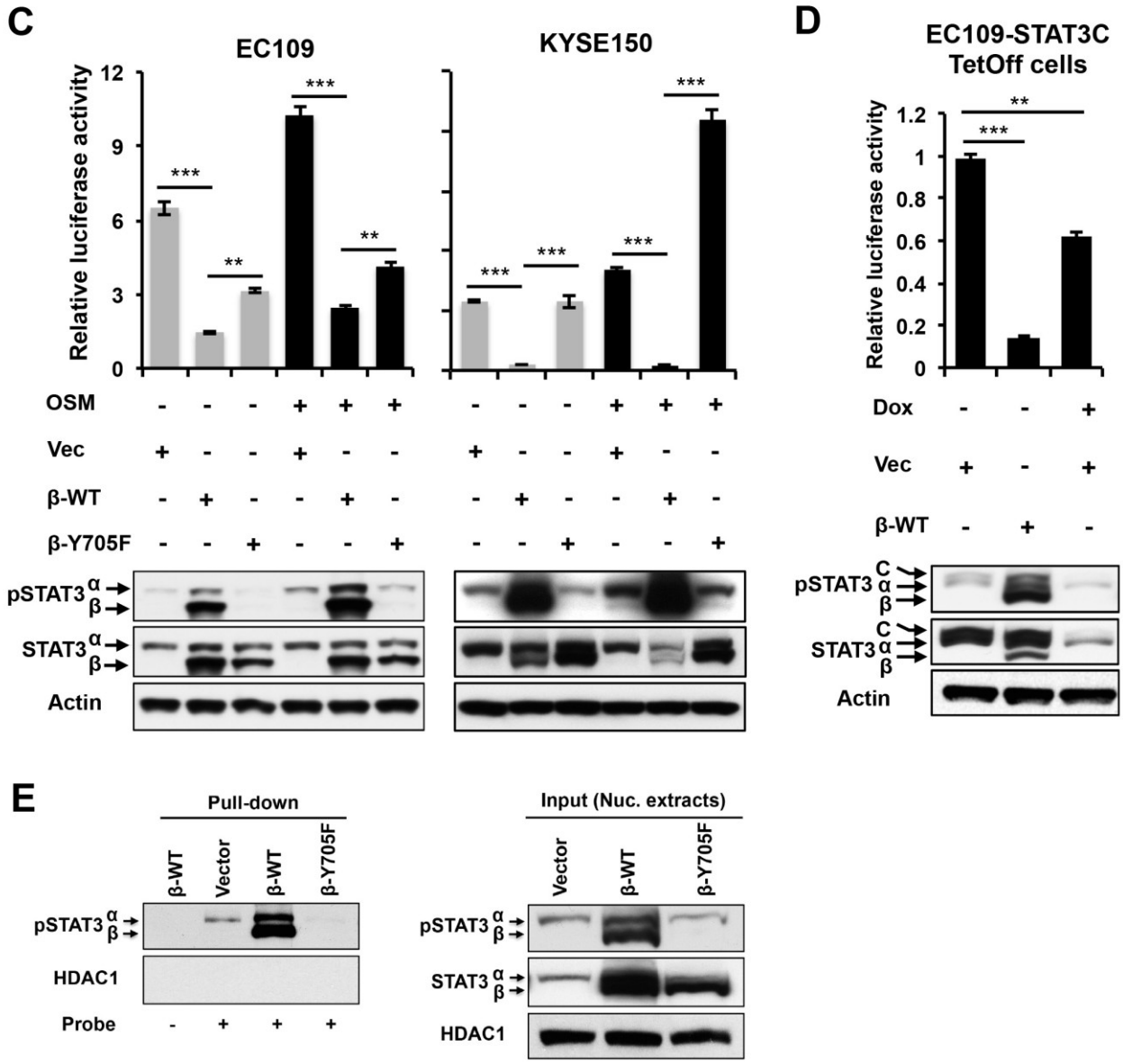

Figure 3.8C-E (**C-D**) STAT3 luciferase reporter activity was measured 48h after transfection, and western blot was performed in parallel. ***P*<0.01, ****P*<0.001, Student's *t* test (n=3). (**E**) 30min after OSM (10ng/ml) treatment, the STAT3 DNA-binding ability was determined using a pull-down assay with a STAT3 probe. **(Continued on the next page)**

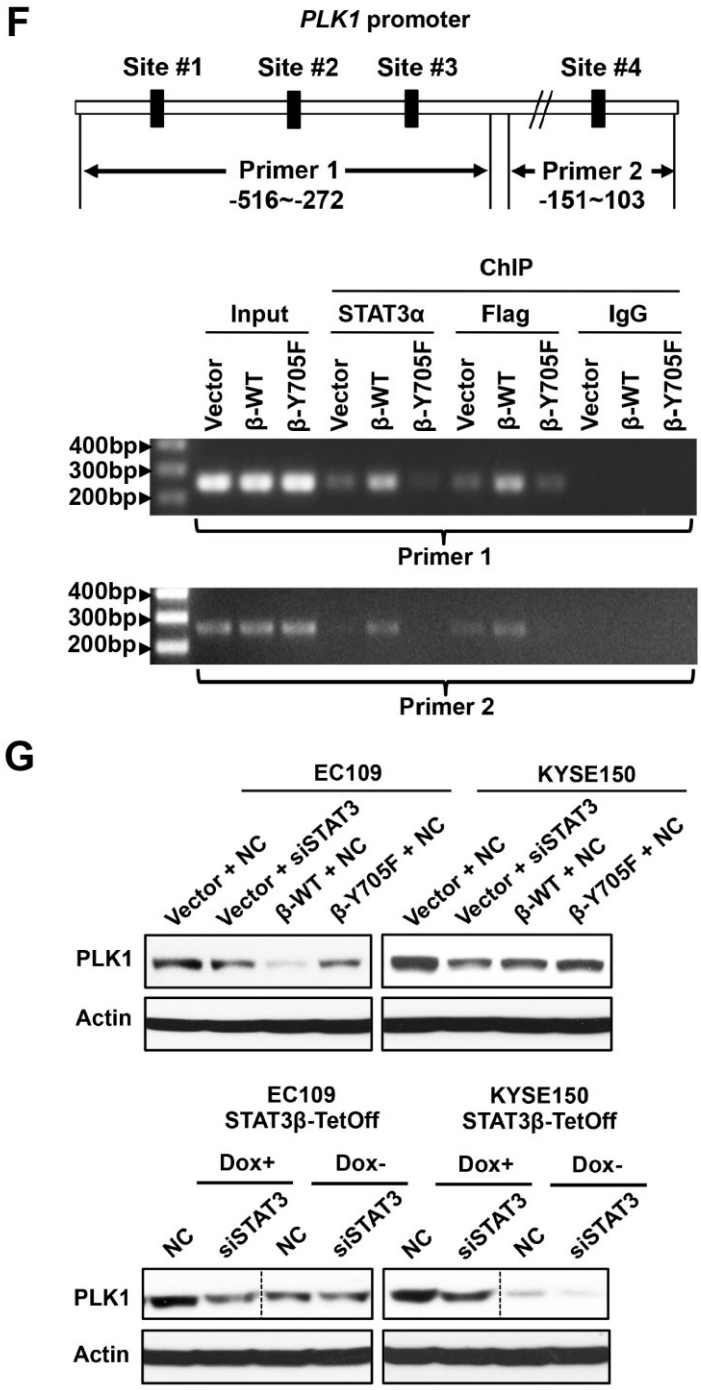

Figure 3.8F-G (**F**) Upper panel, a schematic model showing the predicted STAT3 binding sites on the PLK gene promoter. ChIP-PCR was performed to determine the occupancy of STAT3α/β in the promoter of *PLK1* in EC109 cells. (**G**) Protein expression was detected using western blots.

3.4.8 STAT3β determines the prognostic significance of pSTAT3α^{Y705} in ESCC patients

Our collected data indicates that STAT3β inhibits the transcriptional activity and oncogenic function of STAT3α while it 'paradoxically' increases the level of pSTAT3α^{Y705}. Thus, a high level of pSTAT3α^{Y705} indicates a tumor suppressive environment when STAT3β is expressed, whereas it indicates an oncogenic environment when STAT3β is negative/weak. Using western blots, we assessed the relative expressions of STAT3α and STAT3β in 91 frozen tumors, which overlapped with the initial cohort of 286 cases mentioned above (**Figure 3.9A and Figure 3.6**). Case-matched, benign esophageal tissues adjacent to the tumors were included for comparison. We also included the fascin expression levels, as fascin is known to be frequently overexpressed in ESCC (32). In 7 pairs of the randomly chosen samples from our cohort, 6 tumors showed a dramatic increase in fascin expression compared with the case-matched benign tissues, supporting the validity of our paired ESCC samples in this cohort (**Figure 3.9A**). As shown in **Figure 3.9B**, the expression of STAT3β significantly correlated with the STAT3β immunoreactivity illustrated in **Figure 3.1B (***P*=0.0001), supporting the validity of our methodology. Results of the expression status of STAT3α and STAT3β, as well as their phosphorylated forms, are summarized in **Figure 3.9B.**

In support of our model, a high level of pSTAT3α^{Y705} significantly correlated with a longer overall survival in patients with STAT3β-high tumors (n=45, *P*=0.039) (**Figure 3.9C**). In STAT3β-low tumors (n=46), while pSTAT3α^{Y705} did not significantly correlate with the overall survival (*P*=0.802) (**Figure 3.9C**),

we noted that all patients with pSTAT3α^{Y705}-high tumors did not survive over 41 months follow-up, whereas a good number of patients with pSTAT3α^{Y705}-low tumors survived past 41 months (*P*=0.031, Fisher's exact test) (**Figure 3.9D**). Lastly, in this entire group of 91 patients, pSTAT3α^{Y705} level showed a trend toward a better outcome (*P*=0.082) (**Figure 3.9E**), which can be attributed to the paradoxical enhancing effect of STAT3β on the oncogenic pSTAT3α^{Y705}.

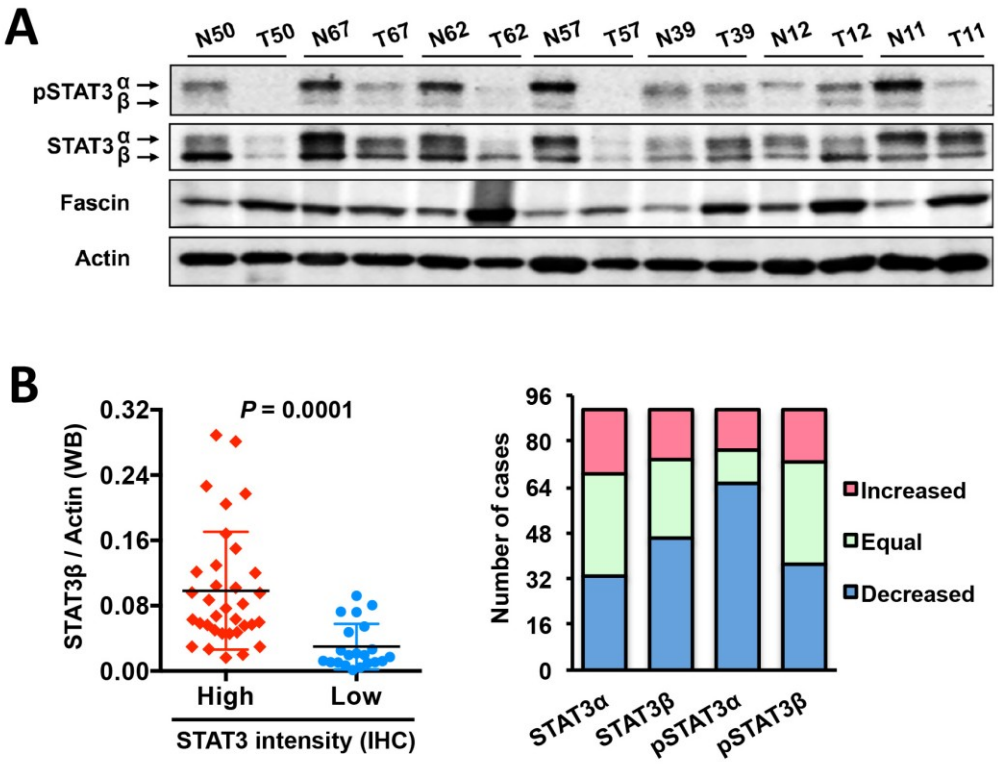

Figure 3.9 STAT3β determines the prognostic significance of pSTAT3α^{Y705} in ESCC patients. (**A**) Representative western blots showing the expression of pSTAT3α/β^{Y705} and STAT3α/β in 7/91 pairs of samples (T: tumor; N: adjacent non-tumorous tissue). The complete data and details are described in Figure 3.6. (**B**) Left panel, STAT3β expression detected by western blot correlated with STAT3β immunoreactivity illustrated in Figure 3.1; Right panel, the expression status of pSTAT3α/β^{Y705} and STAT3α/β as detected by western blot. **(Continued on the next page)**

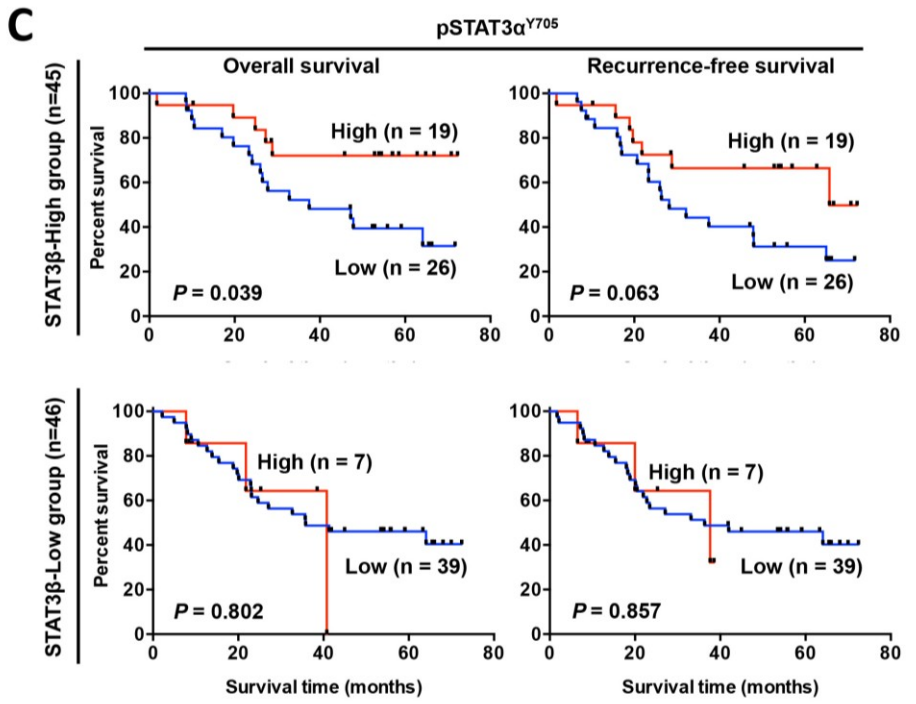

D

pSTAT3α^{Y705}-High expression correlated with shorter survival in the STAT3β-Low group patients (n=46)

	Survival < 41 months	Survival > 41 months
pSTAT3α^{Y705}-Low	20	19
pSTAT3α^{Y705}-High	7	0
Fisher's exact test	$P < 0.031$	

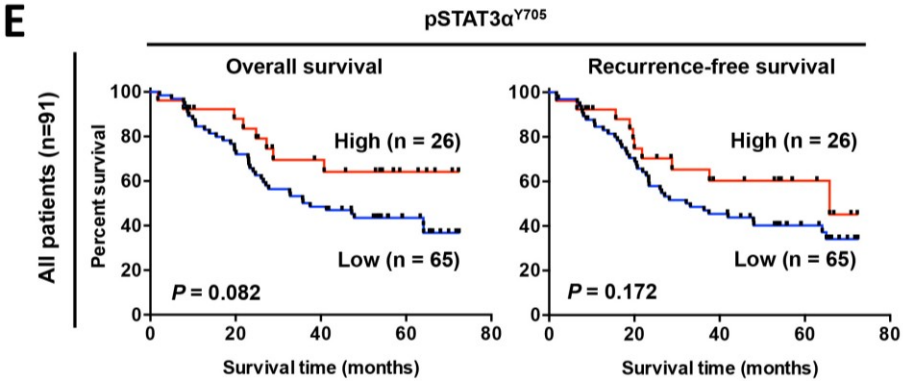

Figure 3.9C-E (**C**) Kaplan-Meier curves showing the prognostic value of pSTAT3α^{Y705} in STAT3β-High and STAT3β-Low group patients. (**D**) The correlation between pSTAT3α^{Y705} and survival time in STAT3β-Low group patients. (**E**) Kaplan-Meier curves showing the prognostic value of pSTAT3α^{Y705} in the entire group of patients (n=91).

3.5 Discussion

One of the key findings of this study is that STAT3β is a tumor suppressor in ESCC, as evidenced by the observation that enforced expression of STAT3β in ESCC cells significantly reduced colony formation, increased chemosensitivity and suppressed cancer stem cell populations. Importantly, we have delineated the key mechanisms underlying the tumor suppressor effects of STAT3β, especially in the aspects of how STAT3β interacts with STAT3α biochemically and functionally. Our data supports the hypothetical model illustrated in **Figure 3.10**. Specifically, upon cytokine (*e.g.* OSM) stimulation, at least two types of STAT3 dimers are formed, *i.e.* pSTAT3α:pSTAT3α homodimer and pSTAT3α:pSTAT3β heterodimer. Compared with the pSTAT3α:pSTAT3α homodimer, the pSTAT3α:pSTAT3β heterodimer is theoretically more stable due to the absence of the negatively charged C-terminal region in STAT3β, which has been shown to increase the stability of STAT3β homodimers (17,33). Since only monomerized pSTAT3α can be subjected to dephosphorylation by PTPs (17), the stabilizing effect of STAT3β on the STAT3α:STAT3β heterodimer blocks the interaction and dephosphorylation by PTPs. Thus, a much larger amount of pSTAT3 (as heterodimers) is preserved, which is distributed in both the cytoplasm and the nucleus. Nevertheless, the oncogenic function of the transcriptionally active pSTAT3α is sequestered in this large pool of pSTAT3 heterodimers that are still capable of binding DNA. Therefore, in the presence of sufficient STAT3β, STAT3α signaling is retarded, although the amount of $pSTAT3^{Y705}$ is markedly increased by STAT3β. In comparison, in tumors in which STAT3β is down-regulated, although $pSTAT3^{Y705}$ expression is relatively less, the

transcriptionally active and oncogenic STAT3α are relatively unchecked. In other words, whether STAT3 is oncogenic or tumor suppressive is largely dictated by the expression status of STAT3β.

The tumor suppressor function of STAT3β has not been extensively studied or published. In addition to its dominant negative effect on STAT3α, it is believed that STAT3β also may regulate the expression of a unique gene set (15,22,34-35). Nonetheless, the mechanism underlying tumor suppressor effects of STAT3β is incompletely understood, and the concept is not without challenge, since at least two studies have shown that STAT3β promotes leukemogenesis and the progression of liver cancer (36,37). Regarding the evidence supporting the tumor suppressive effects of STAT3β, we have identified only 11 studies in the literature that have discussed about this subject to varying extents. In 7 of these 11 studies, the *STAT3β* construct was only used as an experimental tool to block STAT3α, believed to act in a dominant negative fashion (20,21,38-42). In the remaining 4 studies, the main objective was to evaluate how effective STAT3β is as a tumor suppressor (18,19,22,43). Notably, only one of these studies demonstrates that STAT3β directly decreases the transcriptional activity of STAT3α (40). Besides these 11 studies in cancer cells, we are aware of 3 other studies that had evaluated the impact of STAT3β on the transcriptional activity of STAT3α in COS cells: one of these studies revealed that STAT3β significantly decreased the transcriptional activity of STAT3α (16), whereas two other studies described that STAT3β could increase the transcriptional activity of STAT3α (15,17).

While our data strongly support that STAT3β is a tumor suppressor in ESCC, we found that this isoform paradoxically increases STAT3α^{Y705} phosphorylation. A similar finding has been reported in one study using murine embryonic fibroblasts, but our present study is the first to address this phenomenon in cancer cells and to delineate the underlying mechanisms (**Figure 3.10E**). Importantly, our findings may explain the accumulating controversies regarding the tumor suppressor function of STAT3 in various cancer types (5-14). For instance, there are many publications in which the immune-detection of pSTAT3^{Y705} or nuclear STAT3 was found to significantly correlate with a better outcome (9-14). The explanations for these seemingly discrepant results have not been satisfactory or proven. In our recent review of STAT3 in cancer, we have discussed about the hypothesis that the expression status of STAT3β in cancer cells is a key determinant of the exact biologic effects of STAT3 (3). Thus, in STAT3β-negative/weak tumors, activation of STAT3 increases pSTAT3α^{Y705}, which exerts potent oncogenic effects. In contrast, in STAT3β-high tumors, although pSTAT3α^{Y705} is dramatically augmented by STAT3β, the overall oncogenic effects of STAT3 are indeed suppressed by STAT3β. In other words, without the distinction between the two STAT3 isoforms, as in the case of virtually all previously published clinicopathologic studies of STAT3, it is perceivable that one may conclude that a high expression level of pSTAT3α^{Y705} or total pSTAT3^{Y705} is oncogenic if the vast majority of the tumors in the study cohort are STAT3β-negative/weak. Alternatively, one may conclude that pSTAT3α^{Y705} or total pSTAT3^{Y705} is tumor suppressive or carries no significance if a substantial proportion of the tumors in the study cohort are STAT3β-high. In support of

this model, in our current study, in which 55.2% (158/286) of the tumors carried a relatively high level of STAT3β (*i.e.* moderate/strong STAT3β staining) as assessed by immunohistochemistry, pSTAT3α^{Y705} correlated with longer survival (**Figure 3.10D**). Thus, in the presence of high STAT3β expression, the amount of pSTAT3^{Y705} likely reflects the stabilizing effects of STAT3β on pSTAT3α^{Y705}, rather than an authentic indicator of the transcriptionally active and oncogenic pSTAT3α^{Y705}; and prognostic value of STAT3 in cancer can be fully assessed only if expression status of both STAT3α and STAT3β is known.

STAT3 has been shown to regulate cancer cell stemness in several types of cancers, including breast cancer, glioblastoma, and ESCC (3,25). For instance, in ESCC, the JAK2/STAT3 pathway was shown to increase the side population cells and CD44^{High} cells (25), two subsets of ESCC cells that have been demonstrated to have cancer stem cell features (25,30). Our study is the first to show that STAT3β suppresses cancer stemness, as evidenced by the decrease of both side population cells and CD44^{High} cells. This finding is expected, as our data show that STAT3β suppresses the transcription activity and antagonizes the oncogenic function of STAT3α in the ESCC model. Recently, a study reported that morpholinos, a type of artificial small molecules, was able to modulate the STAT3 alternative splicing process to favor the generation of STAT3β at the expense of STAT3α (22). Given that STAT3β opposes the oncogenic role of STAT3α in cancer stemness, these small molecules can be potentially used as a powerful tool to target cancer stem cells.

In conclusion, we have presented data supporting that STAT3β is a tumor suppressor in ESCC, and STAT3β can effectively suppress the oncogenic effects of STAT3α. Our results support the model that STAT3 can be both oncogenic and tumor suppressive, and the expression status of STAT3β is the key regulator of this dual role. Our study has highlighted the importance of interpreting the prognostic value of $pSTAT3^{Y705}$ with the knowledge of the expression status of STAT3β.

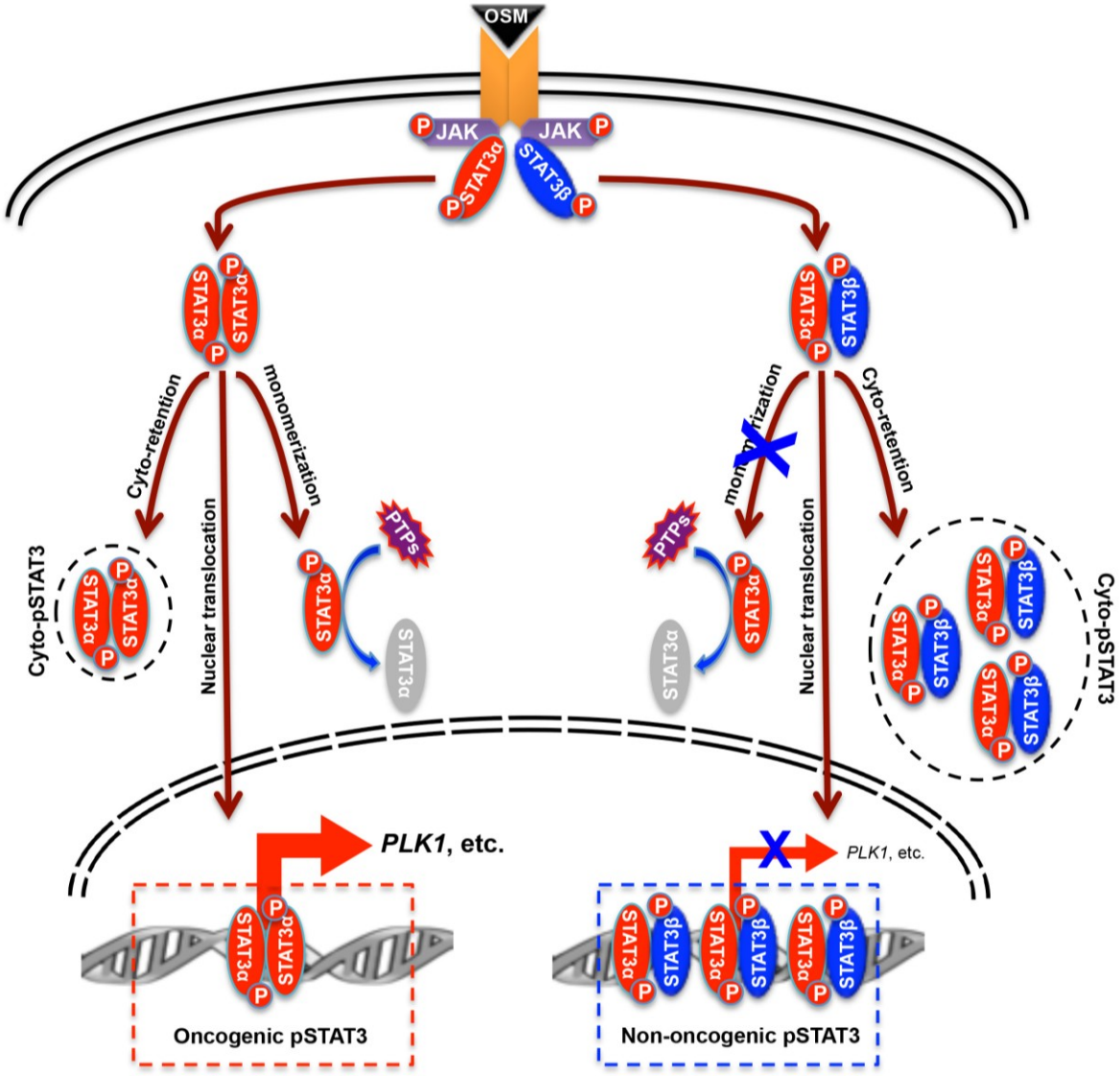

Figure 3.10 A schematic model showing how the interplay between STAT3α and STAT3β dictates the dual role of STAT3 in cancer. Upon cytokine (*e.g.* OSM) stimulation, at least two types of dimers are formed between the two tyrosine^{705}-phosphorylated STAT3 (pSTAT3): pSTAT3α:pSTAT3α homodimer and pSTAT3α:pSTAT3β heterodimer. Compared with the pSTAT3α:pSTAT3α homodimer, the pSTAT3α:pSTAT3β heterodimer is more stable, which hampers the monomerization process and thus blocks the interaction and dephosphorylation by protein tyrosine phosphatases (PTPs). Thus, a much larger amount of pSTAT3 (as heterodimers) is preserved, which is distributed in both the cytoplasm and the nucleus. Nevertheless, the oncogenic function of the transcriptionally active pSTAT3α is sequestered in this large pool of pSTAT3 heterodimers, even though its DNA-binding ability remains intact.

3.6 References

1. Yu H, Kortylewski M, Pardoll D. Crosstalk between cancer and immune cells: role of STAT3 in the tumour microenvironment. Nat Rev Immunol 2007;7:41-51.
2. Yu H, Jove R. The STATs of cancer--new molecular targets come of age. Nat Rev Cancer 2004;4:97-105.
3. Zhang HF, Lai R. STAT3 in Cancer-Friend or Foe? Cancers (Basel). 2014;6:1408-1440.
4. Bromberg JF, Wrzeszczynska MH, Devgan G, Zhao Y, Pestell RG, Albanese C, et al. Stat3 as an oncogene. Cell 1999;98:295-303.
5. Musteanu M, Blaas L, Mair M, Schlederer M, Bilban M, Tauber S, et al. Stat3 is a negative regulator of intestinal tumor progression in Apc(Min) mice. Gastroenterology 2010;138:1003-1011.
6. Lee J, Kim JC, Lee SE, Quinley C, Kim H, Herdman S, et al. Signal transducer and activator of transcription 3 (STAT3) protein suppresses adenoma-to-carcinoma transition in ApcMin/+ mice via regulation of Snail-1 (SNAI) protein stability. J Biol Chem 2012;287:18182-18189.
7. Couto JP, Daly L, Almeida A, Knauf JA, Fagin JA, Sobrinho-Simões M, et al. STAT3 negatively regulates thyroid tumorigenesis. Proc Natl Acad Sci USA 2012;109:E2361-2370.
8. Clifford JL, Menter DG, Yang X, Walch E, Zou C, Clayman GL, et al. Expression of protein mediators of type I interferon signaling in human squamous cell carcinoma of the skin. Cancer Epidemiol Biomarkers Prev 2000;9:993-997.
9. Pectasides E, Egloff AM, Sasaki C, Kountourakis P, Burtness B, Fountzilas

G, et al. Nuclear localization of signal transducer and activator of transcription 3 in head and neck squamous cell carcinoma is associated with a better prognosis. Clin Cancer Res 2010;16:2427-2434.

10. Ettl T, Stiegler C, Zeitler K, Agaimy A, Zenk J, Reichert TE, et al. EGFR, HER2, survivin, and loss of p-STAT3 characterize high-grade malignancy in salivary gland cancer with impact on prognosis. Hum Pathol 2012;43:921-931.
11. Dolled-Filhart M, Camp RL, Kowalski DP, Smith BL, Rimm DL. Tissue microarray analysis of signal transducers and activators of transcription 3(Stat3) and phospho-Stat3(Tyr705) in node-negative breast cancer shows nuclear localization is associated with a better prognosis. Clin Cancer Res 2003;9:594-600.
12. Sato T, Neilson LM, Peck AR, Liu C, Tran TH, Witkiewicz A, et al. Signal transducer and activator of transcription-3 and breast cancer prognosis. Am J Cancer Res 2011;1:347-355.
13. Hsiao JR, Jin YT, Tsai ST, Shiau AL, Wu CL, Su WC. Constitutive activation of STAT3 and STAT5 is present in the majority of nasopharyngeal carcinoma and correlates with better prognosis. Br J Cancer 2003;89:344-349.
14. Gordziel C, Bratsch J, Moriggl R, Knösel T, Friedrich K. Both STAT1 and STAT3 are favourable prognostic determinants in colorectal carcinoma. Br J Cancer 2013;109:138-146.
15. Schaefer TS, Sanders LK, Nathans D. Cooperative transcriptional activity of Jun and Stat3 beta, a short form of Stat3. Proc Natl Acad Sci USA 1995;92:9097-9101.

16. Caldenhoven E, van Dijk TB, Solari R, Armstrong J, Raaijmakers JA, Lammers JW, et al. STAT3beta, a splice variant of transcription factor STAT3, is a dominant negative regulator of transcription. J Biol Chem 1996;271:13221-13227.
17. Schaefer TS, Sanders LK, Park OK, Nathans D. Functional differences between Stat3alpha and Stat3beta. Mol Cell Biol 1997;17:5307-5316.
18. Niu G, Heller R, Catlett-Falcone R, Coppola D, Jaroszeski M, Dalton W, et al. Gene therapy with dominant-negative Stat3 suppresses growth of the murine melanoma B16 tumor in vivo. Cancer Res 1999;59:5059-5063.
19. Niu G, Shain KH, Huang M, Ravi R, Bedi A, Dalton WS, et al. Overexpression of a dominant-negative signal transducer and activator of transcription 3 variant in tumor cells leads to production of soluble factors that induce apoptosis and cell cycle arrest. Cancer Res 2001;61:3276-3280.
20. Ivanov VN, Bhoumik A, Krasilnikov M, Raz R, Owen-Schaub LB, Levy D, et al. Cooperation between STAT3 and c-jun suppresses Fas transcription. Mol Cell 2001;7:517-528.
21. Ivanov VN, Zhou H, Partridge MA, Hei TK. Inhibition of ataxia telangiectasia mutated kinase activity enhances trail-mediated apoptosis in human melanoma cells. Cancer Res 2009;69:3510-3519.
22. Zammarchi F, de Stanchina E, Bournazou E, Supakorndej T, Martires K, Riedel E, et al. Antitumorigenic potential of STAT3 alternative splicing modulation. Proc Natl Acad Sci USA 2011;108:17779-17784.
23. Jemal A, Bray F, Center MM, Ferlay J, Ward E, Forman D. Global cancer statistics. CA Cancer J Clin 2011;61:69-90.

24. Zhang Y, Du XL, Wang CJ, Lin DC, Ruan X, Feng YB, et al. Reciprocal activation between PLK1 and Stat3 contributes to survival and proliferation of esophageal cancer cells. Gastroenterology 2012;142:521-530.e3.
25. Chen X, Ying Z, Lin X, Lin H, Wu J, Li M, et al. Acylglycerol kinase augments JAK2/STAT3 signaling in esophageal squamous cells. J Clin Invest 2013;123:2576-2589.
26. Wang Z, Zhu S, Shen M, Liu J, Wang M, Li C, et al. STAT3 is involved in esophageal carcinogenesis through regulation of Oct-1. Carcinogenesis 2013;34:678-688.
27. Edge SB, Compton CC. The American Joint Committee on Cancer: the 7th edition of the AJCC cancer staging manual and the future of TNM. Ann Surg Oncol 2010;17:1471-4.
28. Bharadwaj U, Kasembeli MM, Eckols TK, Kolosov M, Lang P, Christensen K, et al. Monoclonal Antibodies Specific for STAT3β Reveal Its Contribution to Constitutive STAT3 Phosphorylation in Breast Cancer. Cancers (Basel) 2014;6:2012-2034.
29. Visvader JE, Lindeman GJ. Cancer stem cells in solid tumours: accumulating evidence and unresolved questions. Nat Rev Cancer 2008;8:755-768.
30. Zhao JS, Li WJ, Ge D, Zhang PJ, Li JJ, Lu CL, et al. Tumor initiating cells in esophageal squamous cell carcinomas express high levels of CD44. PLoS One 2011;6:e21419.
31. Su F, Ren F, Rong Y, Wang Y, Geng Y, Wang Y, et al. Protein tyrosine phosphatase Meg2 dephosphorylates signal transducer and activator of transcription 3 and suppresses tumor growth in breast cancer. Breast

Cancer Res 2012;14:R38.

32. Hashimoto Y, Ito T, Inoue H, Okumura T, Tanaka E, Tsunoda S, et al. Prognostic significance of fascin overexpression in human esophageal squamous cell carcinoma. Clin Cancer Res 2005;11:2597-2605.
33. Park OK, Schaefer LK, Wang W, Schaefer TS. Dimer stability as a determinant of differential DNA binding activity of Stat3 isoforms. J Biol Chem 2000;275:32244-32249.
34. Ng IH, Ng DC, Jans DA, Bogoyevitch MA. Selective STAT3-α or -β expression reveals spliceform-specific phosphorylation kinetics, nuclear retention and distinct gene expression outcomes. Biochem J 2012;447:125-136.
35. Maritano D, Sugrue ML, Tininini S, Dewilde S, Strobl B, Fu X, et al. The STAT3 isoforms α and β have unique and specific function. Nat Immunol 2004;5:401-409.
36. Schneller D, Machat G, Sousek A, Proell V, van Zijl F, Zulehner G, et al. P19(ARF)/p14(ARF) controls oncogenic functions of signal transducer and activator of transcription 3 in hepatocellular carcinoma. Hepatology 2011;54:164-172.
37. Ecker A, Simma O, Hoelbl A, Kenner L, Beug H, Moriggl R, et al. The dark and the bright side of Stat3: proto-oncogene and tumor-suppressor. Front Biosci 2009;14:2944-2958.
38. Niu G, Wright KL, Ma Y, Wright GM, Huang M, Irby R, et al. Role of Stat3 in regulating p53 expression and function. Mol Cell Biol 2005;25:7432-7440.
39. Burke WM, Jin X, Lin HJ, Huang M, Liu R, Reynolds RK, et al. Inhibition of

constitutively active Stat3 suppresses growth of human ovarian and breast cancer cells. Oncogene 2001;20:7925-7934.

40. Turkson J, Bowman T, Garcia R, Caldenhoven E, De Groot RP, Jove R. Stat3 activation by Src induces specific gene regulation and is required for cell transformation. Mol Cell Biol 1998;18:2545-2552.
41. Zhang YW, Wang LM, Jove R, Vande Woude GF. Requirement of Stat3 signaling for HGF/SF-Met mediated tumorigenesis. Oncogene 2002;21:217-226.
42. Bowman T, Broome MA, Sinibaldi D, Wharton W, Pledger WJ, Sedivy JM, et al. Stat3-mediated Myc expression is required for Src transformation and PDGF-induced mitogenesis. Proc Natl Acad Sci USA. 2001;98:7319-7324.
43. Marino F, Orecchia V, Regis G, Musteanu M, Tassone B, Jon C, et al. STAT3β controls inflammatory responses and early tumor onset in skin and colon experimental cancer models. Am J Cancer Res 2014;4:484-494.

Chapter 4

Reactive oxygen species (ROS) promotes the acquired stemness in esophageal squamous cell carcinoma

This chapter contains a proportion of the manuscript in prep.:

Zhang HF, Wu CS, Alshareef A, Gopal K, Gupta N, Li EM, Xu LY, Lai R. The PI3K/AKT/c-MYC axis promotes the acquisition of cancer stem-like features in esophageal squamous cell carcinoma. (2015, Submitted to The Journal of Pathology).

Zhang HF is the first author of this manuscript and performed all the experiments described herein except for the following: Wu CS helped with the development of the protocol for H_2O_2 induced RU-to-RR conversion, and the data are shown in Figure 4.3B. Alshareef A, Gopal K and Gupta N helped with the stable clone generation shown in Figure 4.1B. Zhao Q performed the MYC immunohistochestry shown in Figure 4-2G. Lai R, Xu LY and Li EM supervised the whole project.

4.1 Abstract

The presence of cancer stem cells within a tumor has been linked to aggressiveness and chemoresistance of cancer, although the biological basis of cancer stemness remains large unknown. Using a lentiviral SRR2 (Sox2 regulatory region 2) reporter, we were able to identify two distinct cell subpopulations in 3 of 3 esophageal squamous cell carcinoma (ESCC) cell lines examined. Compared with reporter-unresponsive (RU) cells, reporter responsive (RR) cells are more stem-like, with a significantly higher capacity of tumorsphere formation and a higher proportion of cells that were $CD44^{High}$, a cancer stem cell marker. Importantly, we revealed that ROS (reactive oxygen species) induced by H_2O_2 was able to convert RU cells into the stem-like RR cells. Similar to cancer stem cells in other cancer models, both RR cells and converted RR cells contained less ROS and were more resistant to cisplatin, as compared to RU cells. Sox2 did not play a significant role in the responsiveness to SRR2, since it is only weakly expressed or siRNA knockdown of Sox2 did not decrease reporter activity. We found that siRNA knockdown of MYC significantly decreased reporter responsiveness and the H_2O_2-induced RU/RR conversion. Moreover, a high-level expression of MYC was found to correlate with a shorter survival in ESCC patients (P<0.05, n=188). This study has suggested that SRR2 is a useful marker for cancer stemness in ESCC, and RU/RR conversion induced by H_2O_2 provides a useful model to study acquisition of cancer stemness.

4.2 Introduction

Cancer stem cells (CSCs) represent a small fraction of cells within a bulk

tumor that have been shown to be responsible for the initiation of various cancers, such as colon, breast, lung, prostate and pancreatic carcinomas [1]. Besides the tumor initiating capacity, CSCs have also been shown to drive chemoresistance via exploiting multiple mechanisms, including enhanced expression of ABC transporters and aldehyde dehydrogenase (ALDH), and high DNA damage response [2]. Mounting experimental evidence has documented that chemotherapy or radiotherapy only eliminates the non-CSCs but selectively preserves CSCs that are more therapy-resistant and aggressive [3-5]. These features of CSCs contribute to treatment failure and cancer recurrence, which is one of the most lethal events for cancer patients. However, our understanding of the molecular basis underlying the origin of CSCs remains limited. Recent studies have revealed that stemness can be acquired by non-CSCs, the mechanisms include the de-differentiation process driven by epithelial-to-mesenchymal transition [6-8], and the stimulation by specific tumor microenvironment such as hypoxia and inflammation [9,10]. Nevertheless, a model that can be easily used to investigate how cancer cells acquire stemness remains lacking.

Reactive oxygen species (ROS) are a group of radical and non-radical oxygen species mainly generated by the partial reduction of oxygen in the process of endogenous mitochondrial oxidative metabolism, and ROS can also be produced from interactions with exogenous materials such as environmental agents and pharmaceuticals [11,12]. Although the oxidative stress induced by excessive levels of ROS are cytotoxic due to the oxidative damage on cellular macromolecules, mild levels of ROS has been shown to activate survival and

proliferation pathways, such as the MAPK signaling pathway and the PI3K-AKT signaling pathway [11,12]. The balance of cellular ROS is tightly regulated by a wide spectrum of antioxidant proteins involved in the redox mechanism, such as glutathione, glutathione S-transferase, NADPH quinone oxidoreductase-1, copper/zinc superoxide dismutase [11,12]. Recent studies have shown that normal stem cells and cancer stem cells harbor a low-level of ROS via maintaining a high expression of antioxidants [4,13], however, ROS has also been shown to stimulate self-renewal of neural stem cells [14].

Sox2 is one of the 4 transcription factors that have been shown to reprogram somatic cells to induced pluripotent stem cells [15,16], and its expression is normally restricted to embryonic stem cells and somatic stem cells, whereas it has been reported to be frequently overexpressed in various cancers [17]. Extensive studies have linked aberrantly expressed Sox2 with multiple hallmarks of cancer, such as enhancing cellular proliferation, evading apoptotic signals, and promoting invasion and metastasis [17]. Sox2 regulatory region 2 (SRR2) is a motif (*CATTGT*) where Sox2 binds in embryonic stem cells. Using a lentiviral SRR2 reporter that carries both *GFP* and *Luciferase* genes as read-outs, our previous studies have successfully identified and purified subsets of GFP+ and GFP- cells (*i.e.* evidence of SRR2-activation and inactivation, respectively) in both breast cancer cells and anaplastic large cell lymphoma cells [18-20]. The GFP+ or reporter-responsive (RR) cells were shown to be more tumorigenic and more stem-like than the GFP- or reporter-unresponsive (RU) cells [18-20]. Since we have demonstrated that the RU and RR cells remain to be GFP+ and GFP- over 4 months [18], this can be used as

a stable and ideal model to study acquired stemness and specific molecular characteristics of CSCs.

Esophageal cancer is one of the most deadly cancers, representing the sixth leading cause of cancer-related death worldwide [21], and esophageal squamous cell carcinoma (ESCC) is a major histological subtype of this disease [22]. The lack of markers for early diagnosis and treatment renders ESCC patients a very poor prognosis, with a 5-year survival rate of approximately 14% [22]. Our understanding of the biology of CSCs in ESCC remains scarce, and only a few studies have started identifying CSC-like cells in ESCC using Hoechst dye efflux and CD44 as markers [23-25].

In this study, we used ESCC cells stably infected with the lentiviral SRR2 reporter to identify and purify RU and RR cells. Using this model, we investigated the molecular mechanism underlying the acquired stemness induced by ROS in ESCC cells.

4.3 Materials and methods

4.3.1 Patient samples

Details about the human ESCC samples used in this study have been described in Section 3.3.1 (Chapter 3).

4.3.2 Cell lines

Details about the human ESCC cell lines, *i.e.* EC109, EC1, KYSE150 and KYSE510, have been described in Section 2.3.2 (Chapter 2). Immortalized

human esophageal epithelial cell lines, *i.e.* NE3 and NECA6, were provided by Dr. Sai-Wah Tsao, University of Hongkong. The details about the culture conditions for these cell lines have been described previously [26].

The RU and RR cells derived from the ESCC cell lines and NECA6 immortalized cells were generated as previously described [18]. Briefly, these cell lines were infected with lentivirus carrying the pGreenFire1-mCMV-EF1-Puro vecor or pGreenFire1-mCMV-Sox2SRR2-EF1-Puro vector (SBI System Biosciences, CA, USA). The pGreenFire1-Sox2SRR2-mCMV-EF1-Puro vector contained three tandem-repeat of Sox2 regulatory region 2 (SRR2), which is 5'-AAAGAATTTCCCGGGCTCGGGCAGCCATTGTGATGCATATAGGATTAT-TCACGTGGTAATG-3'. The underlined sequence is the Sox2 consensus sequence. Stable cell clone were selected in media containing 2μg/ml Puromycin. After two weeks, RU and RR cells were purified from the infected cells using fluorescence activated cell sorting (FACS) as described previously [18].

To select H_2O_2-resistant RU cells, parental RU cells were treated with different concentrations of H_2O_2 (*i.e.* 0μM, 100μM, 200μM, 300μM, 400μM and 500μM) for four cycles. Specifically, each treatment lasted for 24h, and the cells were then cultured in fresh media to allow the cells to recover for 3 days between each treatment. Due to the higher sensitivity of KYSE150 cells to H_2O_2, resistant cells were acquired only with H_2O_2 doses as high as 300μM.

4.3.3 Flow cytometry (for the detection of GFP, CD44 and ROS)

For GFP detection, trypsinized cells were washed with cold PBS and were resuspended in cold PBS before the analysis using flow cytometry (BD Biosciences). 20,000 live cells were acquired in each run. For CD44 staining and detection, the details have been described in Section 3.3.10 (Chapter 3). For ROS detection, cells were cultured for 30min in media containing 5μM CellROX® Deep Red (Molecular Probes). Then, the cells were trypsinized and resuspended in cold PBS before flow cytometry analysis. All the flow cytometry data were analyzed using the Flow Jo software.

4.3.4 Luciferase measurement

The luciferase activity was measured using the luciferase assay systems kit (Promega) according to the manufacturer's instructions. Briefly, trypsinized cells were washed in cold PBS, and cell pellets were lysed using passive lysis buffer. Then, 20μl lysate were mixed with 100μl luciferase assay reagent before measuring the light produced.

4.3.5 Western blot

Details about the Western blot assay have been described in Section 3.3.12 (Chapter 3). Additional antibodies used in this project, including antibodies against c-MYC, GCLC, non-phospho-β-Catenin (active), ERK1/2 and phospho-ERK1/2$^{T202/Y204}$ were all from Cell Signaling Technology.

4.3.6 Tumorsphere formation assay

Details about tumorsphere formation assay have been described in Section 3.3.8 (Chapter 3).

4.3.7 Chemoresistance assay

Cells were plated in 96-well plates, 2000 cells/well. 24h after plating, cells were cultured in medium containing different doses of Cisplatin (*i.e.* 0μM, 1μM, 2μM, 4μM, 6μM, 8μM, 16μM and 32μM). Cell viability was measured using MTS assay (promega) four days (KYSE150) or five days (KYSE510) after treatment.

4.3.8 Immunohistochemistry

Details about Immunohistochemistry have been described in Section 3.3.16 (Chapter 3). A c-MYC antibody from Santa Cruz Biotechnology was used.

4.3.9 Statistical analysis

Details about Statistical analysis have been described in Section 3.3.18 (Chapter 3).

4.4 Results

4.4.1 Identification of two subpopulations of cells in ESCC

Using a lentiviral reporter expressing both GFP and luciferase under the control of SRR2, our previous studies have identified two phenotypically and biochemically distinct cell subsets in breast cancers [18,19]. Since our understanding of the heterogeneity of ESCC remains limited, we used this model to gain insights into the pathobiology of this disease. As shown in **Figure 4.1A**, compared with the mCMV negative control lentiviral vector infection, the three ESCC cells infected with the SRR2 lentiviral reporter

possessed 26.4%, 34.0% and 38.7% GFP+ cells, respectively. In comparison, the immortalized esophageal epithelial cell NECA6 had only 4.76% GFP+ cells. The reporter unresponsive cells (GFP-) and the reporter responsive cells (GFP+) were labeled RU and RR cells, respectively. As shown in **Figure 4.1B and 4.1C**, the sorted RR cells expressed substantially higher levels of GFP and luciferase, as compared with the counterpart RU cells. However, the two subpopulations of ESCC cells had no significant difference in cell proliferation rates **(Figure 4.1D)**.

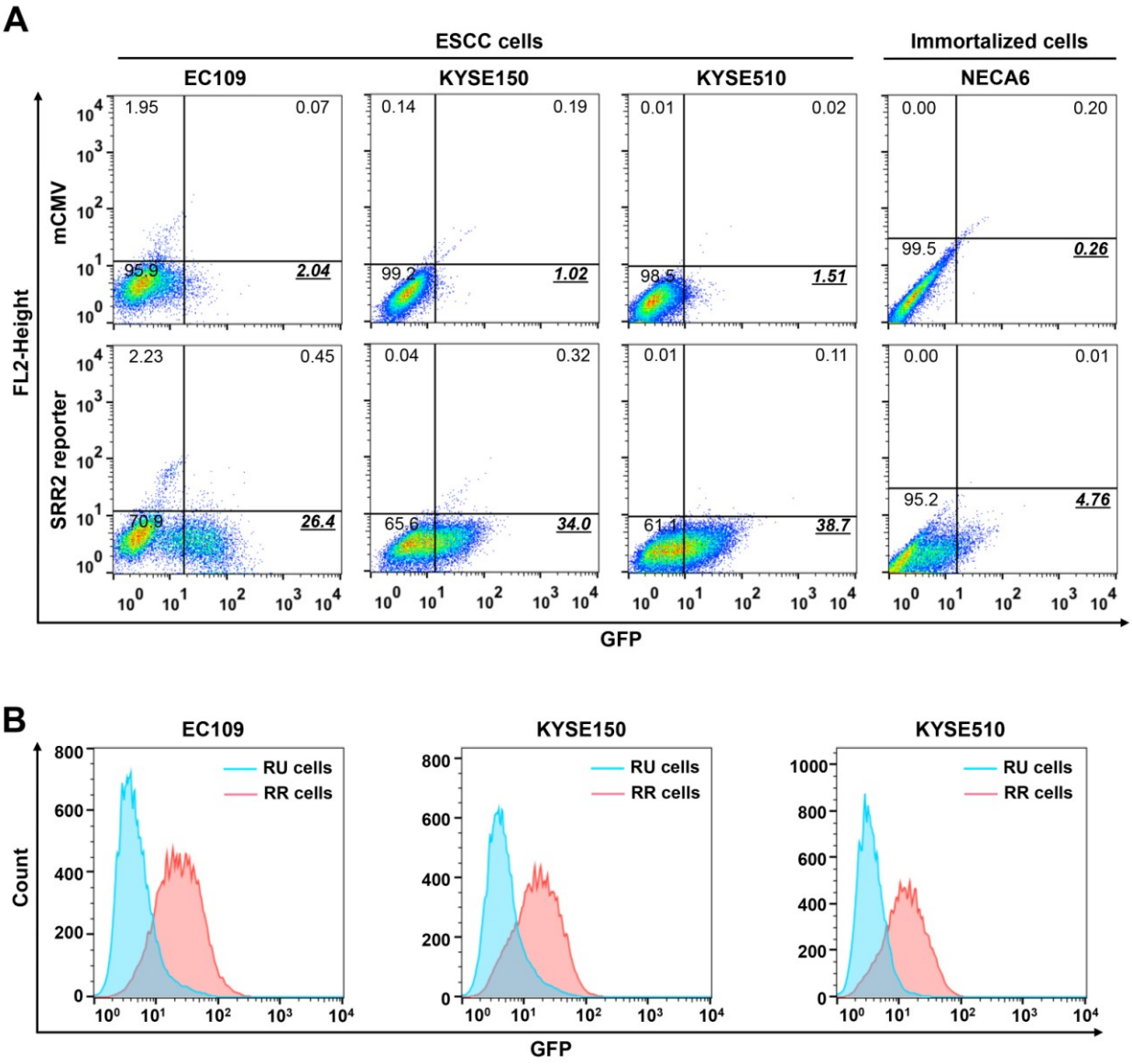

Figure 4.1 Identification of two subpopulations of ESCC cells based on the SRR2 reporter. (**A**) Flow cytometry was performed to identify the two subpopulations of cells in ESCC cell lines (EC109, KYSE150 and KYSE510) and immortalized esophageal epithelial cells (NE2) that were stably infected with the lentiviral SRR2 reporter (lower panel). Cells infected with lentivirus carrying the mCMV empty vector were used as a negative control (upper panel). (**B**) Flow cytometry was performed to sort out RU and RR cells. **(Continued on the next page)**

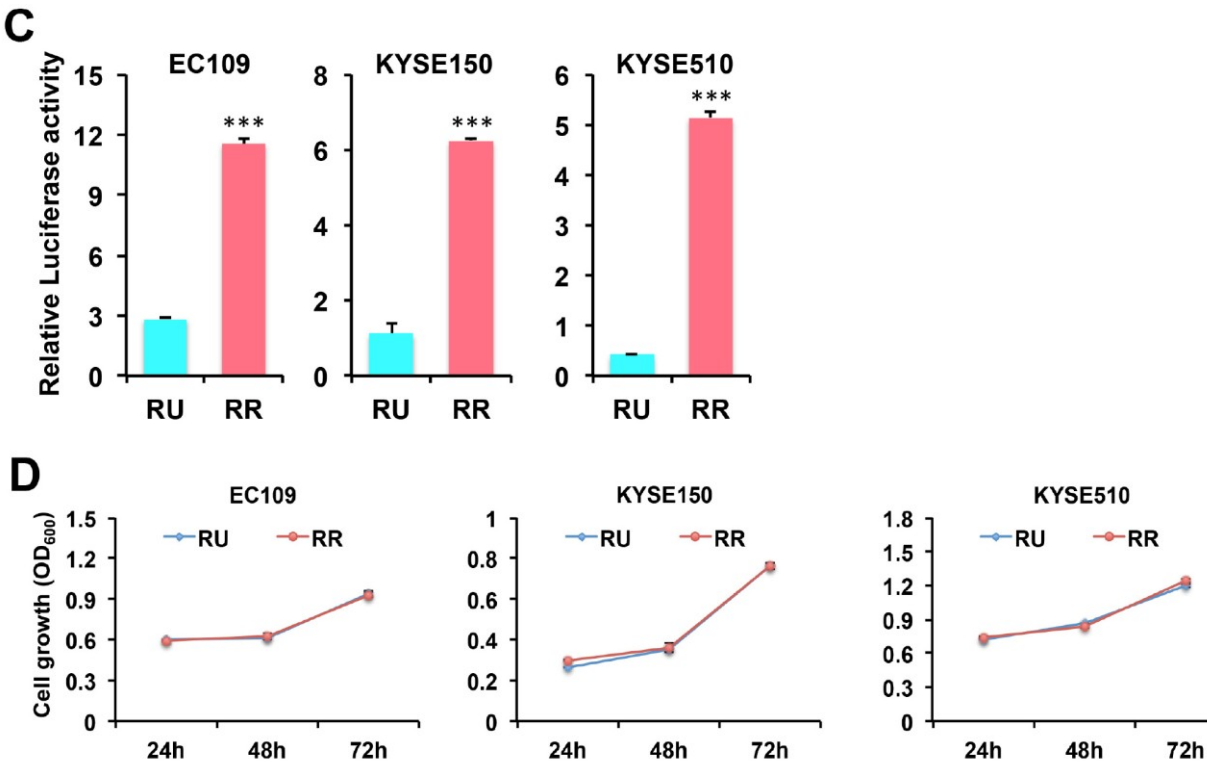

Figure 4.1C-D. (**C**) Luciferase reporter assay was performed to compare the reporter responsiveness in the sorted RU and RR cells (n=3, all *P*<0.001, Student's *t* test). (**D**) Cell growth was measured using MTS assay (n=3).

4.4.2 MYC plays an important role in determining the phenotypic difference between RU and RR cells

Our previous studies have identified Sox2 as an important determinant of the dichotomy in breast cancer cells, we thus determined its expression in a panel of ESCC and immortalized cell lines. As shown in **Figure 4.2A.B**, Sox2 protein expression was only detectable in KYSE510 cells, and its mRNA expression was also only significantly increased in this cell line compared with immortalized cells, suggesting that Sox2 may not be a key factor for this dichotomy in ESCC cells. Our previous bioinformatic analysis has revealed MYC as a putative binding protein in the SRR2 sequence [19], thus we

determined MYC expression in this panel of cell lines. As shown in **Figure 4.2A.B**, both MYC and its active form phospho-MYC^{Ser62} (pMYC) were dramatically increased in ESCC cells compared with the immortalized cells, although MYC mRNA was appreciably higher only in KYSE510 cells. To assess whether MYC and Sox2 are important factors for the dichotomy in ESCC, siRNAs were used to knockdown their expression. As shown in **Figure 4.2C.D**, MYC knockdown significantly decreased the luciferase activity in all three RR cells. However, Sox2 knockdown did not significantly influence the luciferase activity in RR cells isolated from KYSE510, the only Sox2 positive cell line.

To determine whether RU and RR cells possess different stem cell-like properties, tumorsphere formation assay, an assay that has been widely used for the isolation and propagation of cancer stem cells [27,28], was performed. As shown in **Figure 4.2E**, RR cells had a significantly higher capacity to form tumorspheres compared with RU cells in all three cell lines, and MYC knockdown dramatically mitigated the sphere-forming capacity in RR cells, and to a lesser extend in RU cells. Correlating with this, compared with RU cells, RR cells contained a much higher proportion of CD44^{High} cells, a subset of cells that have been shown to possess stem cell-like properties in ESCC [24,25], and MYC knockdown significantly decreased the percentage of CD44^{High} cells in RR cells (**Figure 4.2F**). The important role played by MYC prompted us to investigate its clinical significance in ESCC, which has been evaluated by only one study using in a small cohort of ESCC patients (n=40) [29]. Here, using a large cohort of 188 ESCC patients, a high-expression of

MYC was found to correlate with a significantly shorter overall survival in both the entire cohort (n=188, *P*=0.009) and the 30 patients who were treated with surgery plus radiation and/or chemotherapy (*P*=0.003) (**Figure 4.2G**).

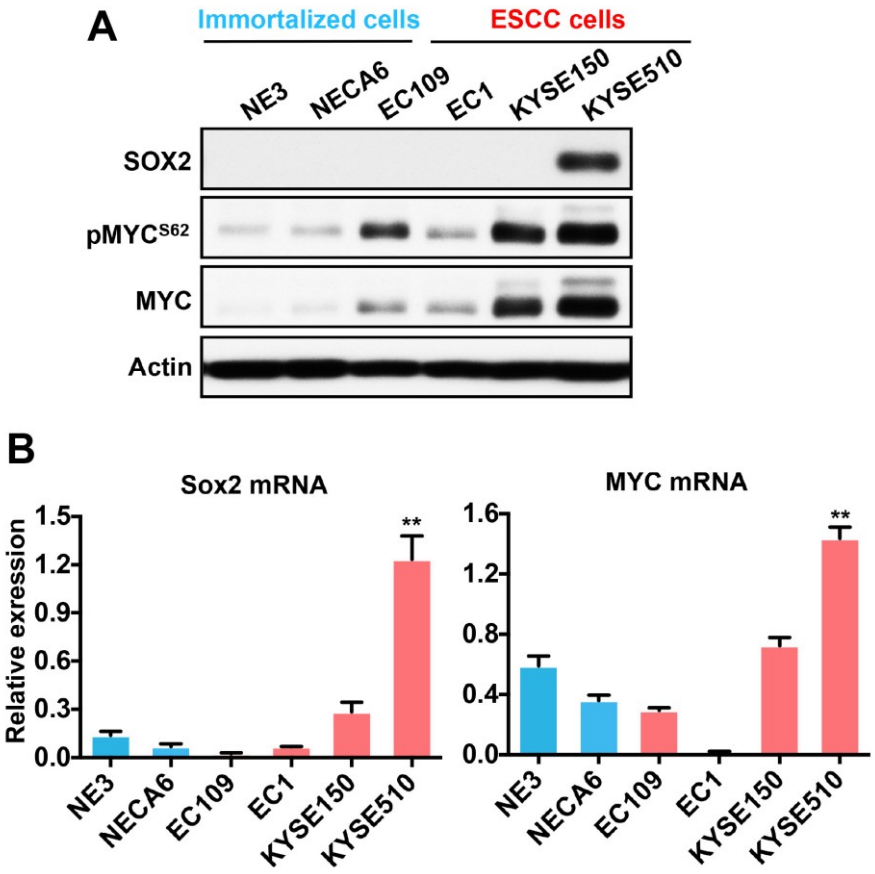

Figure 4.2 MYC plays an important role in promoting the more stem-like properties of RR cells compared with RU cells. (**A-B**) Western blot and real-time PCR was performed to assess the expression of the Sox2 and MYC in a panel of cell lines (n=3, ***P*<0.01, Student's *t* test). **(Continued on the next page)**

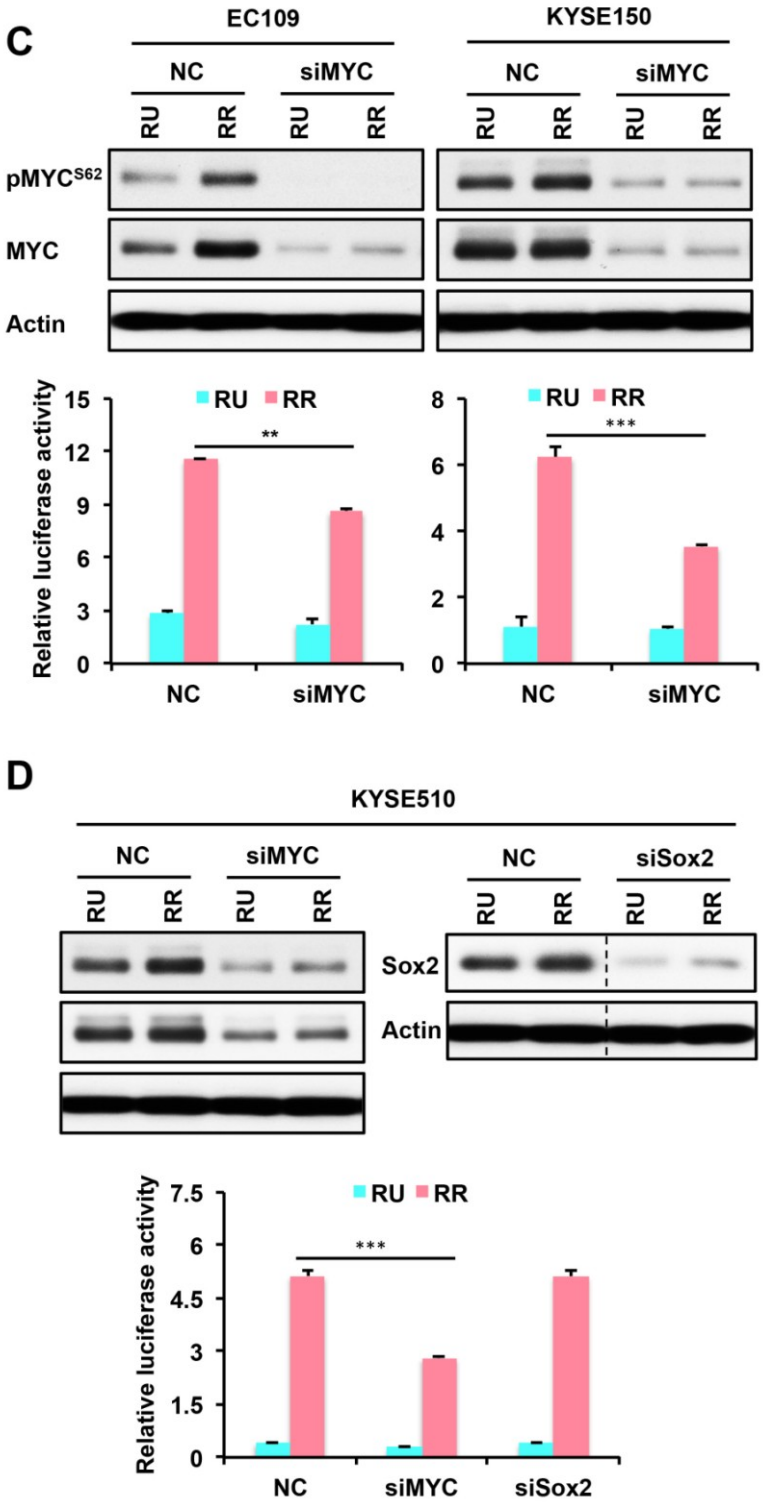

Figure 4.2C-D (**C**) The impact of MYC knockdown on the SRR2 reporter activity in EC109 and KYSE150 cells (n=3, ***P*<0.01, ****P*<0.001 Student's *t* test). (**D**) The impact of MYC and Sox2 knockdown on the Luciferase reporter activity in KYSE510 cells (n=3, ****P*<0.001, Student's *t* test). **(Continued on the next page)**

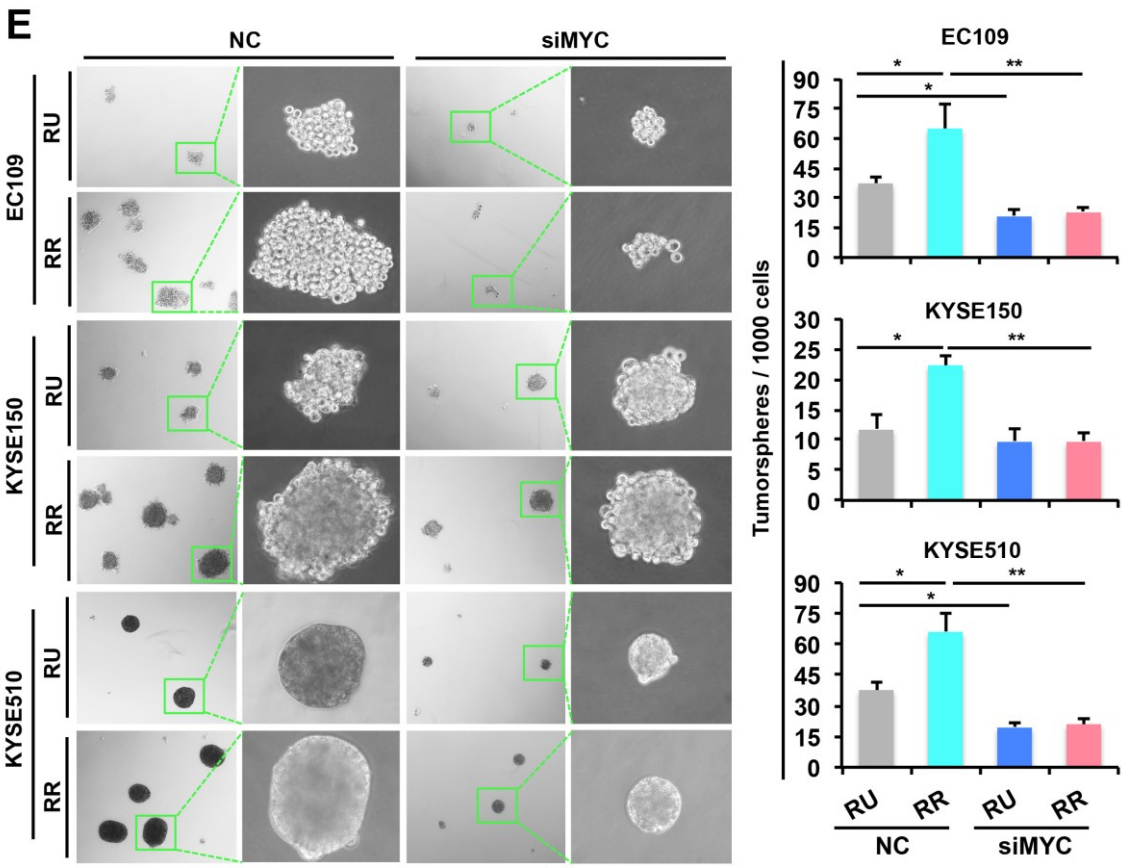

Figure 4.2E The tumorsphere formation ability of the RU and RR cells transfected with either a negative control siRNA (NC) or siMYC was determined (n=3, **P*<0.05, ***P*<0.01, Student's *t* test).

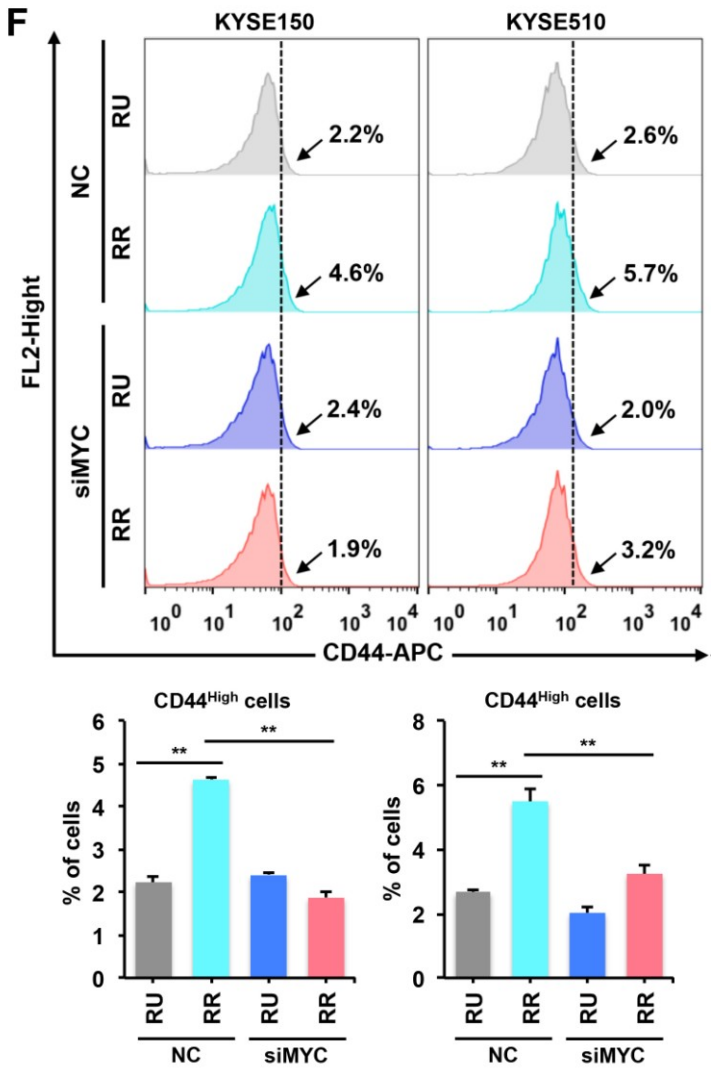

Figure 4.2F The percentage of CD44^{High} cells was identified using Flow cytometry (n=3, ***P*<0.01, Student's *t* test).

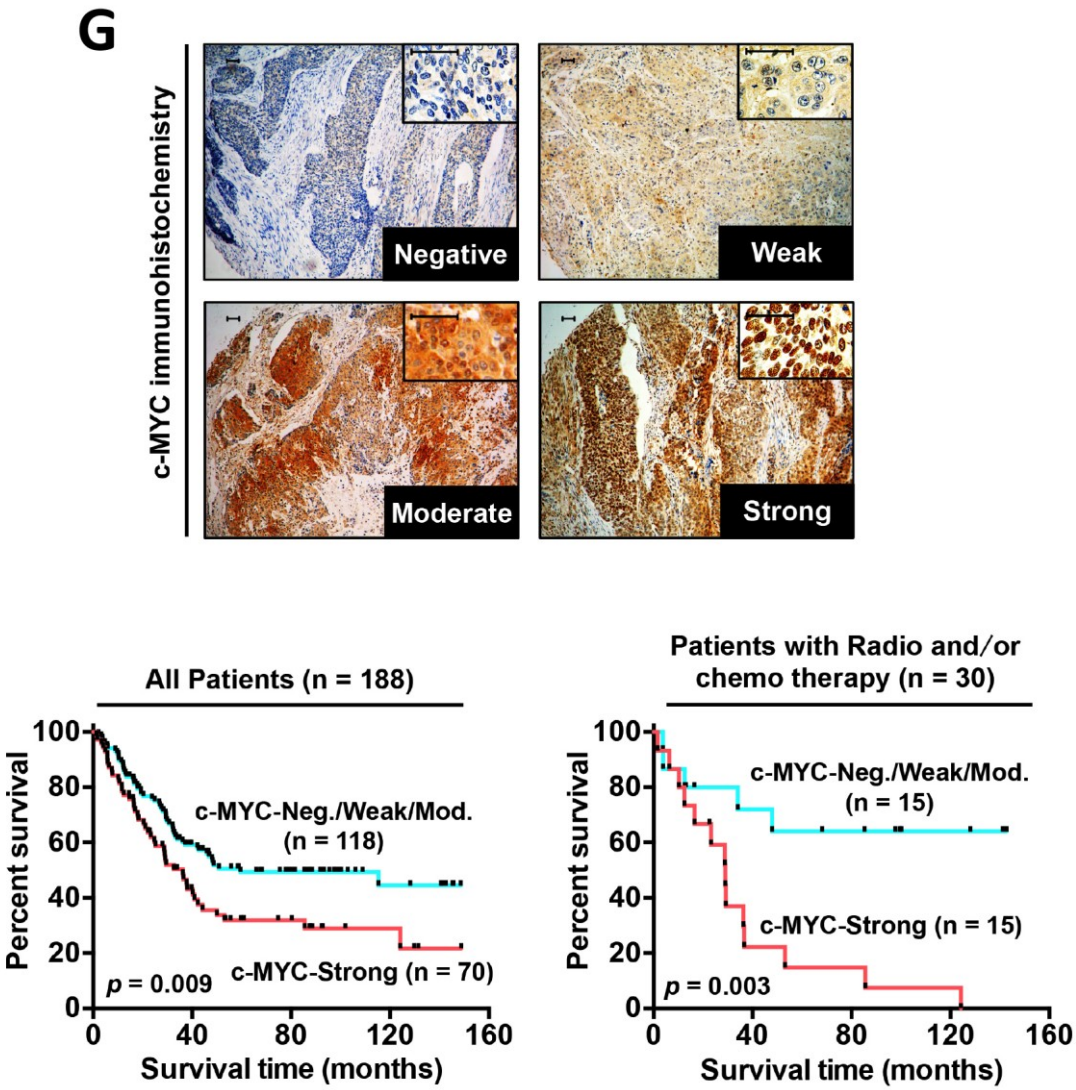

Figure 4.2G Immunohistochemistry was performed to evaluate the expression of MYC in a cohort of paraffin-embedded ESCC tumors (n=188), and representative tumors showing different MYC staining intensities are shown. Kaplan-Meier was used to determine the prognostic significance of MYC in this cohort of ESCC patients (log-rank test was used in the statistical analysis).

4.4.3 ROS induces RU to RR conversion

Although normal and cancer stem cells have been shown to maintain a low-level of ROS [4,13], recently studies discovered that ROS can stimulate self-renewal of neural stem cells [14]. To determine the role of ROS in the stemness of ESCC cells, we asked whether ROS could induce the less stem cell-like RU cells to convert to the more stem cell-like RR cells. To this end, H_2O_2 was used as an inducer of ROS for this aim, as H_2O_2 treatment significantly increased ROS levels in both KYSE150- and KYSE510-RU cells (**Figure 4.3A**). Using this model, we revealed that H_2O_2 induced RU to RR conversion in a dose-dependent manner in both cell lines, as indicated by the increase in the percentage of GFP+ cells (**Figure 4.3B**). With continuous H_2O_2 treatment, the conversion increased for four days before reaching a plateau in both cell lines, and cell viability was also decreased by H_2O_2 in a dose-dependent manner (**Figure 4.3C**). In further support of the causal role played by oxidative stress in the induction of RU to RR conversion, NAC (N-Acetyl-Cysteine), an antioxidant agent, significantly diminished H_2O_2-induced RU to RR conversion in both KYSE150 and KYSE510 cells (P<0.01) (**Figure 4.3D**).

Next, we assessed whether the converted RR cells by H_2O_2 are more stem cell-like than RU cells. To this end, by mimicking the chronic oxidative stress cancer cells experience *in vivo*, H_2O_2-resistant cells were selected, and different doses of H_2O_2 were used. Due to the different tolerance to the cellular toxicity induced by H_2O_2, resistant cells to as high as 300μM and 500μM H_2O_2 were selected in KYSE150 and KYSE510 cells, respectively. As shown in **Figure 4.4A**, the tumorsphere formation capacity of RU cells were markedly

enhanced by H_2O_2 in both cell lines, especially in KYSE510-RU cells, in which the increase was dose-dependent within the dose range of 0-300μM H_2O_2. However, the enhancing effect of H_2O_2 was mitigated in higher doses, probably due to the cellular toxicity of high ROS levels. Correlating with these observations, H_2O_2 also increased the percentage of $CD44^{High}$ cell subsets in RU cells (**Figure 4.4B**).

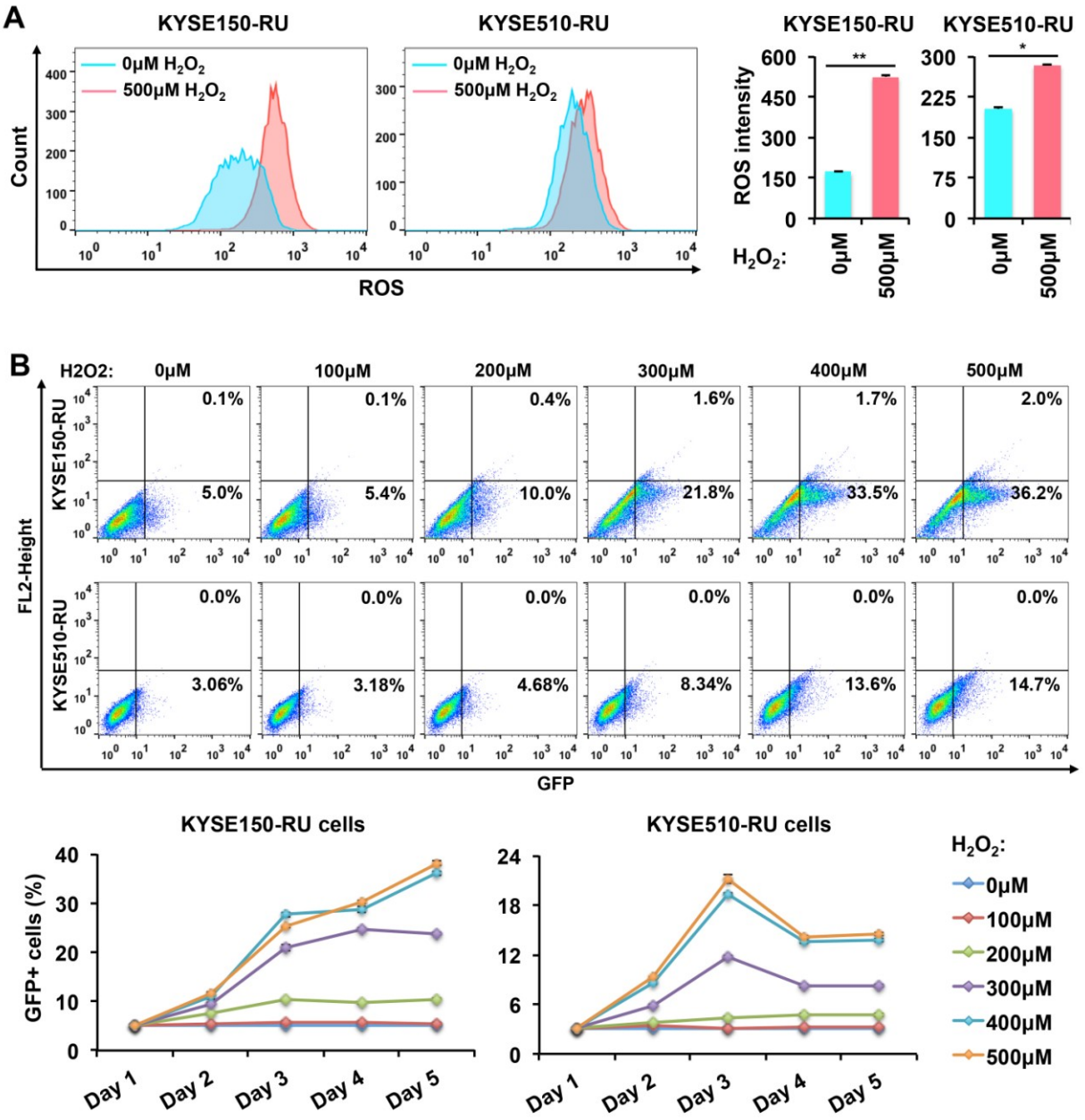

Figure 4.3 ROS induced by H_2O_2 promotes RU to RR conversion. (**A**) The cells were incubated with the indicated doses of H_2O_2 for 24h, and cellular ROS was measured by Flow cytometry (n=3, **P*<0.05, ***P*<0.01, Student's *t* test). (**B**) The RU to RR conversion induced by H_2O_2 was measured by Flow cytometry.

(Continued on the next page)

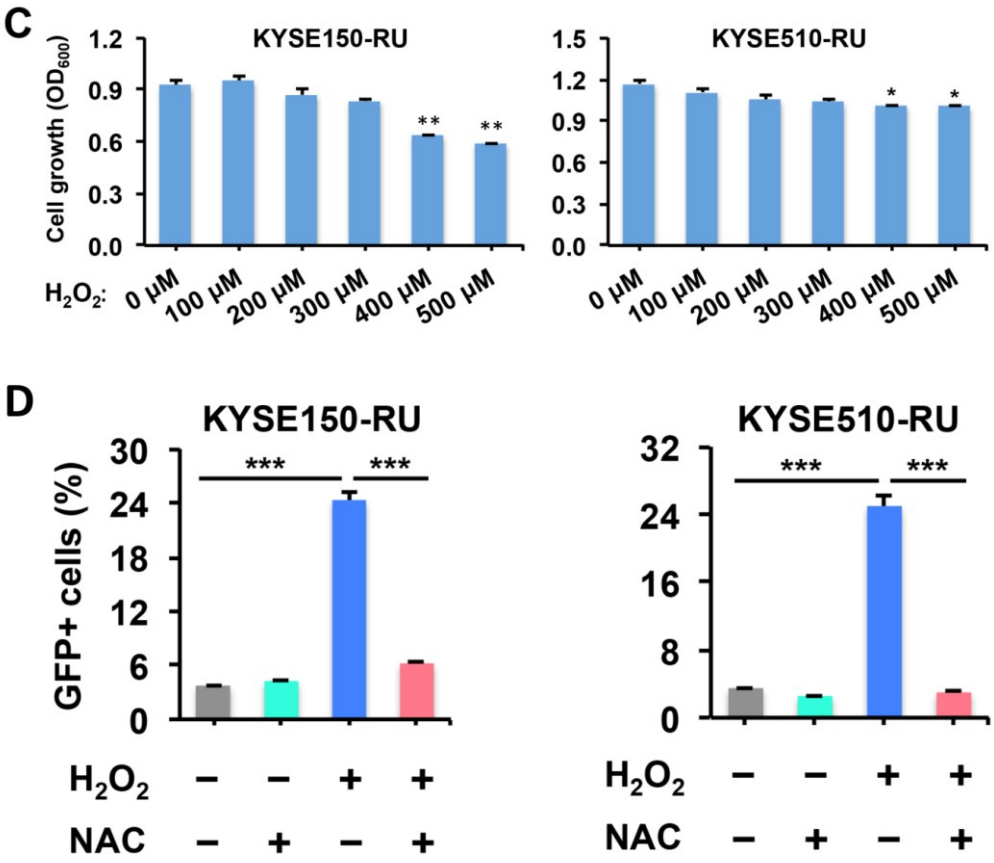

Figure 4.3C-D (**C**) MTS cell proliferation assay was performed to determine the cytotoxicity of H_2O_2 treatment (n=3, **P*<0.05, Student's *t* test). (**D**) N-acetyl-L-Cysteine (NAC), an antioxidant agent, was used to determine whether ROS is responsible for the effects of H_2O_2 in the induction of RU-to-RR conversion. (n=3, **P*<0.05, ***P*<0.01, ****P*<0.001, Student's *t* test).

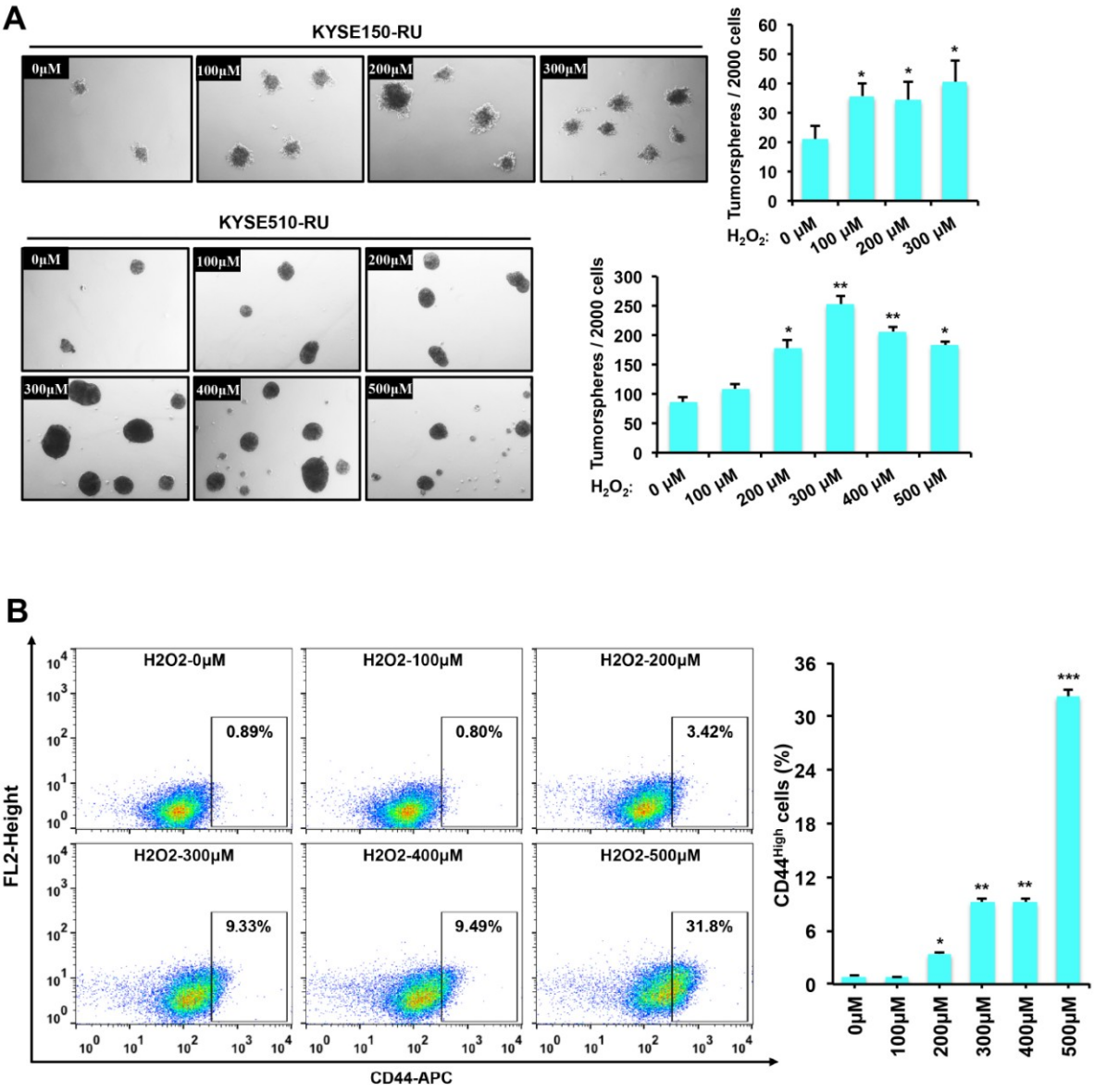

Figure 4.4 ROS-induced RU to RR conversion promotes stemness. (**A**) Tumorsphere formation assay was performed to assess the stem-like properties induced by ROS (n=3, **P*<0.05, ***P*<0.01, Student's *t* test). (**B**) CD44 expression was measured by Flow cytometry (n=3, **P*<0.05, ***P*<0.01, ****P*<0.001, Student's *t* test).

4.4.4 MYC mediates the RU to RR conversion induced by ROS

Since the data described above indicate an important role played by MYC in this dichotomy, we asked if MYC mediated the ROS-induced RU to RR conversion. Our data were in support of this hypothesis: 1) the expression of

pMYC and MYC were increased by H_2O_2 in a dose-dependent manner in both KYSE150- and KYSE510-RU cells (**Figure 4.5A**); 2) knockdown of MYC sharply abolished the RU to RR conversion induced by H_2O_2 (P<0.05) (**Figure 4.5B and 4.5C**); 3) knockdown of MYC significantly neutralized the effect of H_2O_2 on increasing $CD44^{High}$ cell population (P<0.05) (**Figure 4.5D**); 4) the tumorsphere formation capacity that was enhanced by H_2O_2 was dramatically blocked by MYC knockdown (P<0.05) (**Figure 4.5E**). Overall, these findings suggest the key role played by MYC in the RU to RR conversion induced by oxidative stress.

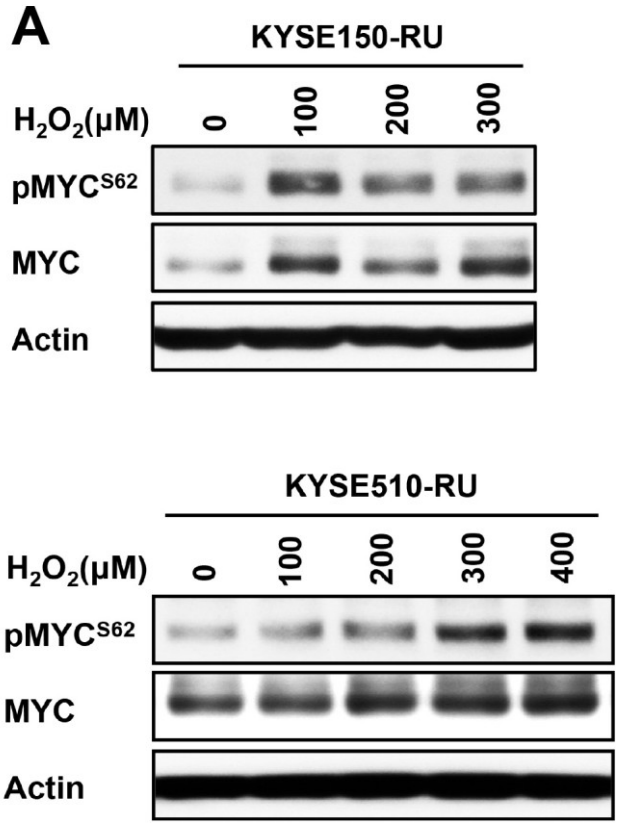

Figure 4.5 MYC mediates ROS-induced RU to RR conversion. (**A**) Western blot was performed to determine the expression levels of MYC and phospho-MYC^{S62} (pMYC^{S62}). **(Continued on the next page)**

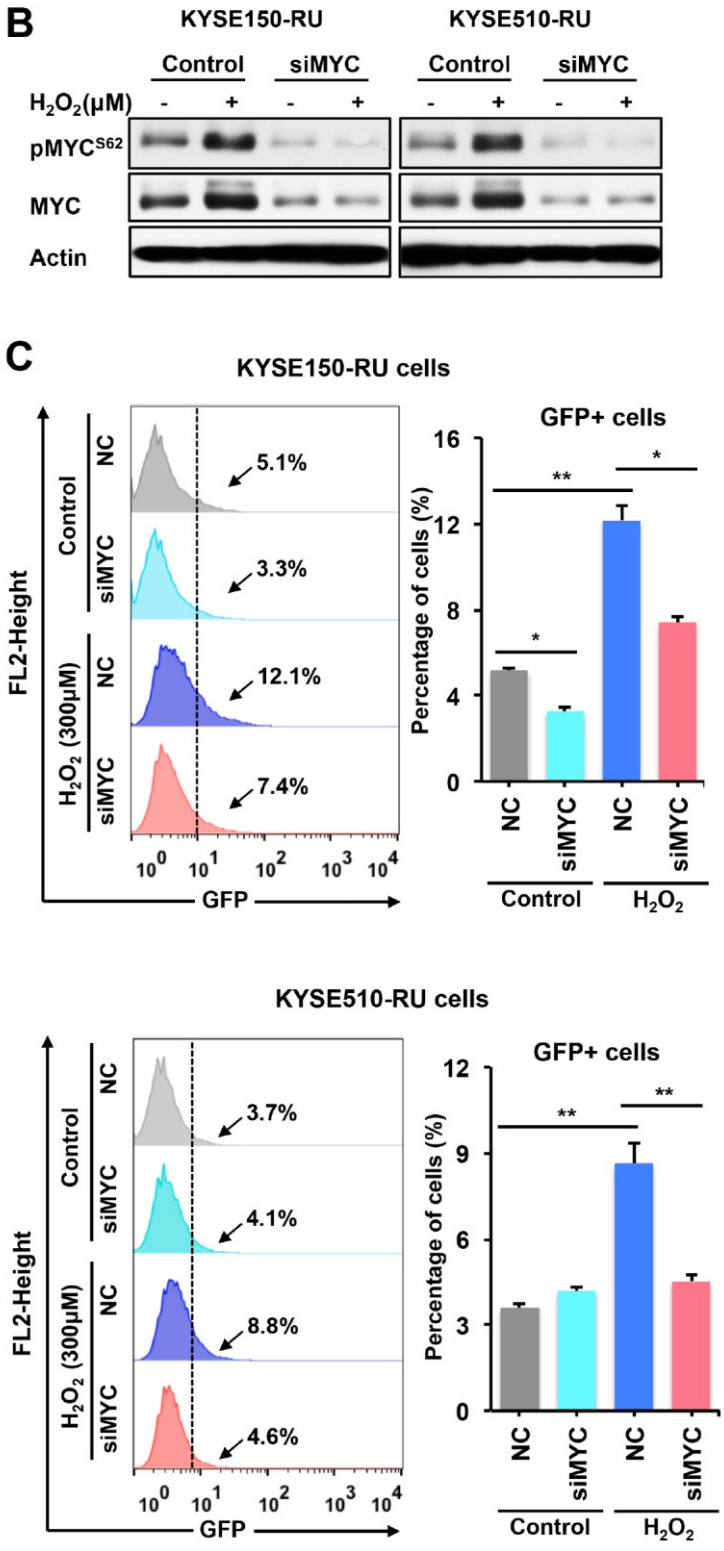

Figure 4.5B-C (**B**) Western blot was performed to detect the expression of MYC and pMYC^{S62} after siRNA knockdown. (**C**) 48h after the siRNA knockdown, GFP expression was measured by Flow cytometry (n=3, **P*<0.05, ***P*<0.01, Student's *t* test). **(Continued on the next page)**

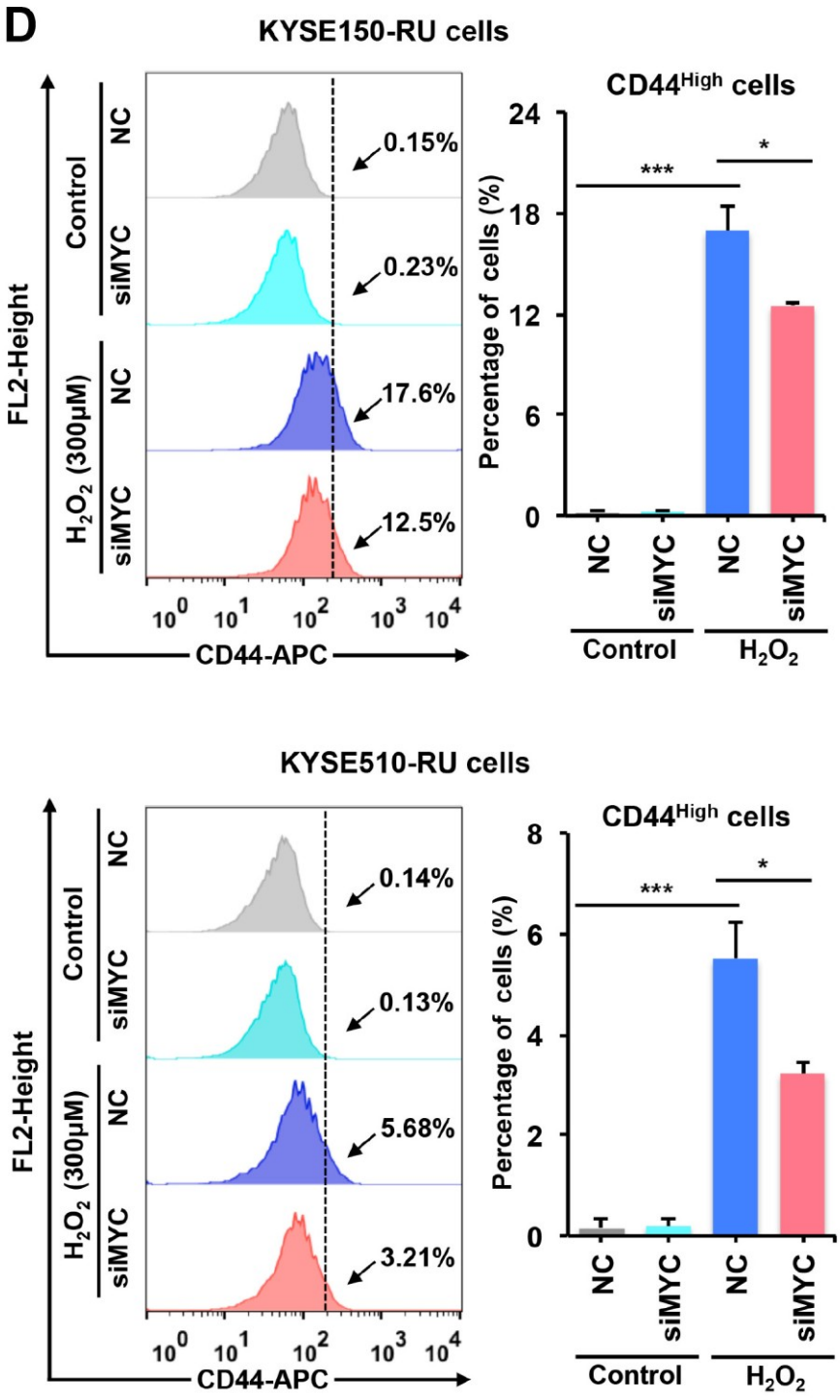

Figure 4.5D 48h after NC/siRNA transfection, CD44 expression was measured by Flow cytometry (n=3, **P*<0.05, ****P*<0.001, Student's *t* test). **(Continued on the next page)**

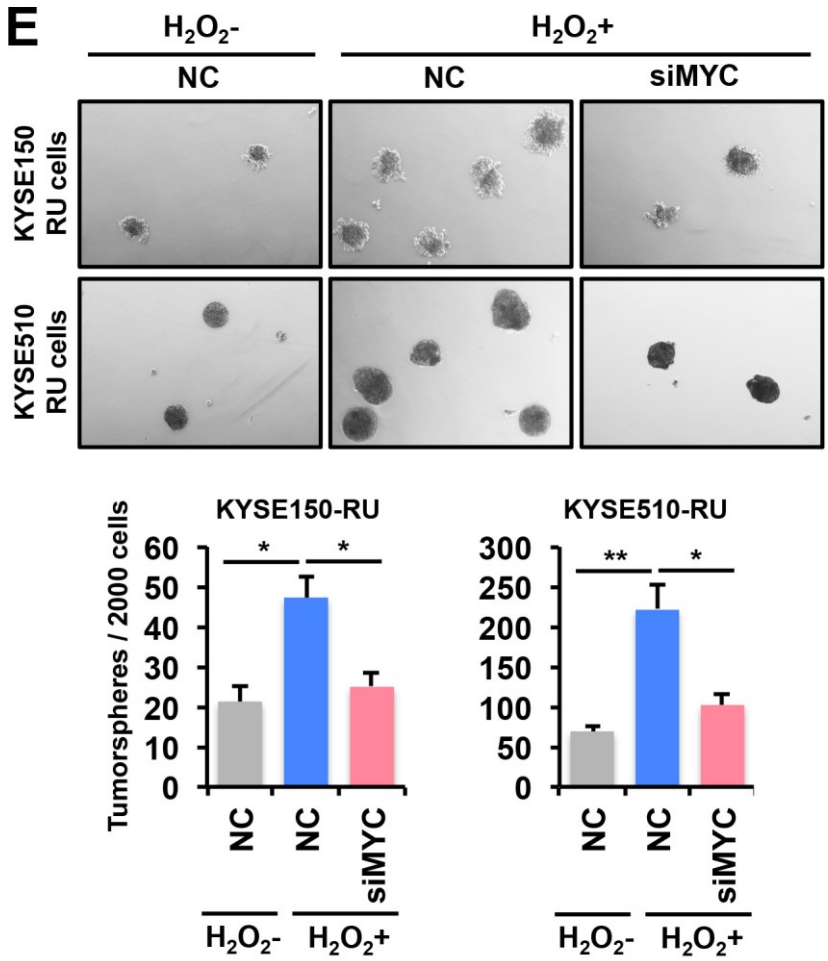

Figure 4.5E 48h after NC/siRNA transfection, tumorsphere formation assay was performed (n=3, **P*<0.05, ***P*<0.01, Student's *t* test).

4.4.5 RR cells and converted RR cells contain low ROS and are more chemoresistant

It has been reported that cancer stem cells harbor low levels of ROS [4,5,13]. In line with these findings, as shown in **Figure 4.6A**, RR cells derived from both KYSE150 and KYSE510 contained significantly lower levels of ROS compared with RU cells (P<0.05), suggesting RR cells are more cancer stem cell-like than RU cells. Moreover, although the ROS intensity was not drastically different between the whole population of parental RU and H_2O_2-resistant RU cells, cells harboring low levels of ROS (ROS^{Low} cells) are 2-fold more enriched in H_2O_2-resistant RU cells (**Figure 4.6B**). Knockdown of MYC dramatically decreased the proportion of ROS^{Low} cells within the H_2O_2-resistant RU cells, to a level that was comparable to parental RU cells (**Figure 4.6B**). These observations were made in both ESCC cell lines, indicating the key role played by MYC in the maintenance of ROS^{Low} cells.

It has been reported that MYC regulates redox balance by directly activating the transcription of both the catalytic and regulatory subunits of γ-glutamyl-cysteine synthetase, the first rate-limiting enzyme catalyzing the biosynthesis of the master antioxidant glutathione [31]. Thus, we hypothesized that γ-glutamyl-cysteine synthetase is differentially expressed in RU and RR cells. As shown in **Figure 4.6C**, both RR cells and H_2O_2-resistant RU cells expressed higher levels of GCLC, the catalytic subunit of γ-glutamyl-cysteine synthetase. Moreover, knockdown of MYC preferentially decreased GCLC expression in RR cells and H_2O_2-resistant RU cells rather than RU cells (**Figure 4.6C and 4.6D**).

ROS^{Low} cells have been shown to be more radioresistant and chemoresistant than ROS^{High} cells within the same cell line [4,5,30]. Consistent with these findings, compared with RU cells, RR cells and H_2O_2-resistant RU cells derived from both cell lines had significantly higher IC50 to cisplatin (P<0.05), a chemo-drug that has been shown to cause oxidative stress (**Figure 4.6E and F**). Moreover, knockdown of MYC significantly attenuated the chemoresistance of RR cells and H_2O_2-resistant RU cells, generating IC50 values that were comparable to RU cells (P<0.05) (**Figure 4.6E and F**).

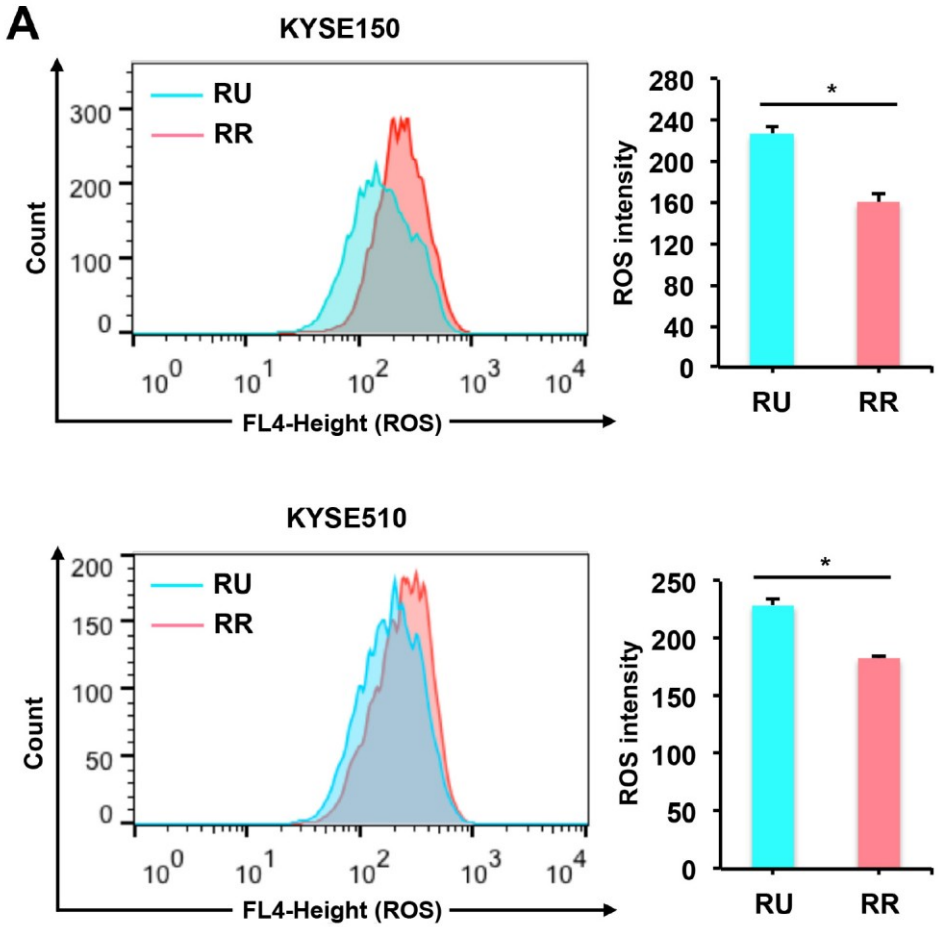

Figure 4.6 RR and converted RR cells contain low levels of ROS and are more chemoresistant. (**A**) ROS levels were assessed by Flow cytometry (n=3, **P*<0.05, Student's *t* test). **(Continued on the next page)**

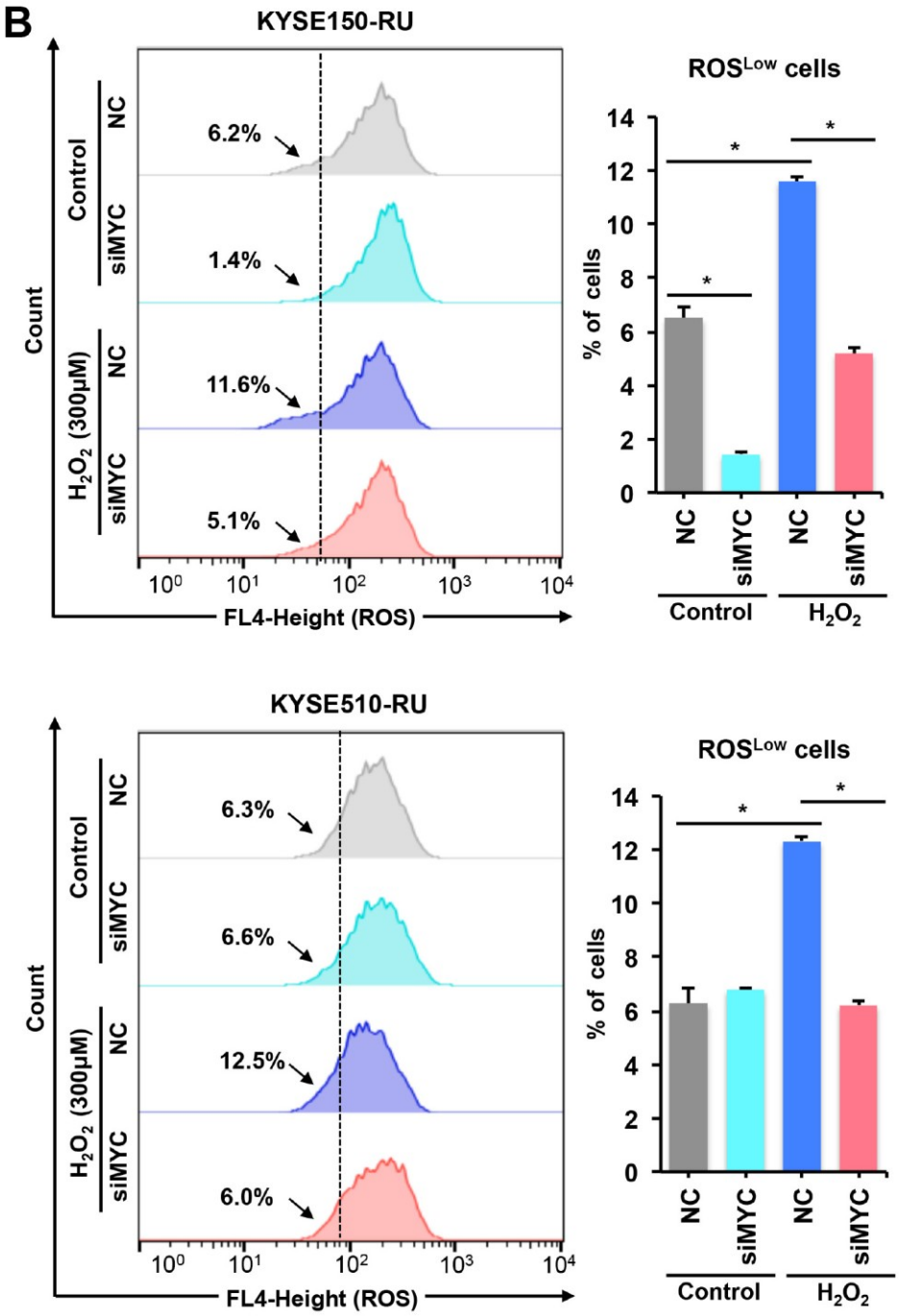

Figure 4.6B 48h after NC/siRNA transfection, ROS levels were assessed by Flow cytometry (n=3, **P*<0.05, Student's *t* test). **(Continued on the next page)**

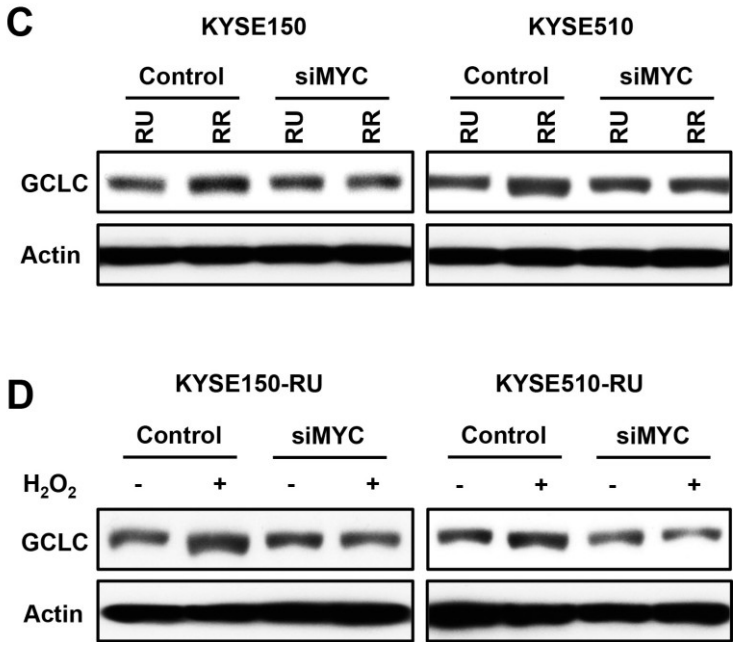

Figure 4.6C-D 48h after NC/siRNA transfection, Western blot was performed to detect protein expression. **(Continued on the next page)**

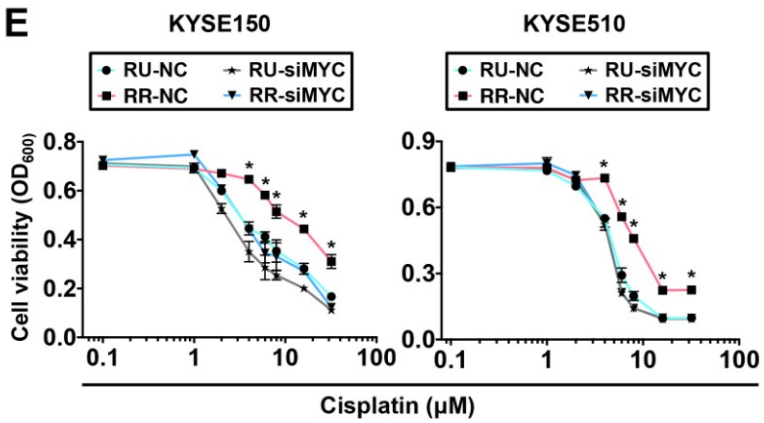

Cell lines	IC50 to Cisplatin (95% CI, μM)			
	RU-NC	RR-NC	RU-siMYC	RR-siMYC
KYSE150	6.9 (5.3−8.9)	13.4 (9.5−18.9)	5.8 (4.3−7.8)	6.6 (5.0−8.6)
KYSE510	5.4 (3.4−8.6)	9.9 (6.3−13.5)	5.1 (3.1−8.3)	5.4 (3.3−8.9)

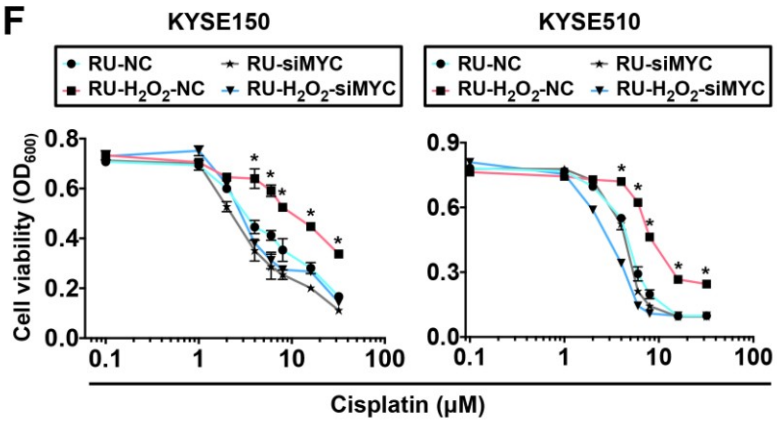

Cell lines	IC50 to Cisplatin (μM)			
	RU-NC	RU-H_2O_2-NC	RU-siMYC	RU-H_2O_2-siMYC
KYSE150	6.9 (5.3−8.9)	10.9 (8.4−14.2)	5.8 (4.3−7.8)	5.7 (4.1−7.8)
KYSE510	5.4 (3.4−8.6)	11.0 (7.0−17.3)	5.1 (3.1−8.3)	3.5 (2.2−5.3)

Figure 4.6E-F 24h after NC/siRNA transfection, the cells were plated into 96-well plates (2000 cells/well) and cultured in media containing increasing doses of Cisplatin. Four days (KYSE150) or five days (KYSE510) after drug treatment, cell viability was measured using MTS assay (n=3, **P*<0.05, Student's *t* test).

4.4.6 The PI3K-AKT pathway promotes the RR phenotype

To determine the signaling pathways that contribute to the RR phenotype, we compared the activation status of multiple signaling pathways between RU and RR cells, such as the PI3K-AKT pathway, the MAPK pathway, the JAK/STAT3 pathway, and the canonical WNT/β-catenin pathway. As shown in **Figure 4.7A**, phospho-AKT^{S473} (pAKT), a central mediator of the PI3K-AKT pathway, was expressed at a higher level in RR cells compared with RU cells in both KYSE150 and KYSE510. No significant difference was observed in the expression of pERK$^{T180/Y182}$, pSTAT3^{Y705}, or active non-phosphorylated β-catenin (both in whole cell lysates and nuclear extracts), markers of the other three pathways, respectively.

The involvement of the PI3K-AKT pathway in the dichotomy was strongly supported by the following observations: 1) LY294002, an inhibitor of the PI3K-AKT pathway, markedly decreased the luciferase activity of the SRR2 reporter in both cell lines (P<0.05) (**Figure 4.7B**); 2) the proportion of CD44^{High} cells in both KYSE150- and KYSE510-RR cells was decreased by over 50% by LY294002 compared with DMSO treatment (P<0.05) (**Figure 4.7C**); 3) the tumorsphere formation capacity of RR cells was significantly decreased by LY294002 treatment in both cell lines (P<0.05) (**Figure 4.7D**). Moreover, the PI3K-AKT pathway also promoted H_2O_2-induced RU-to-RR conversion, as pAKT expression was increased by H_2O_2 in a dose-dependent manner (**Figure 4.7E**).

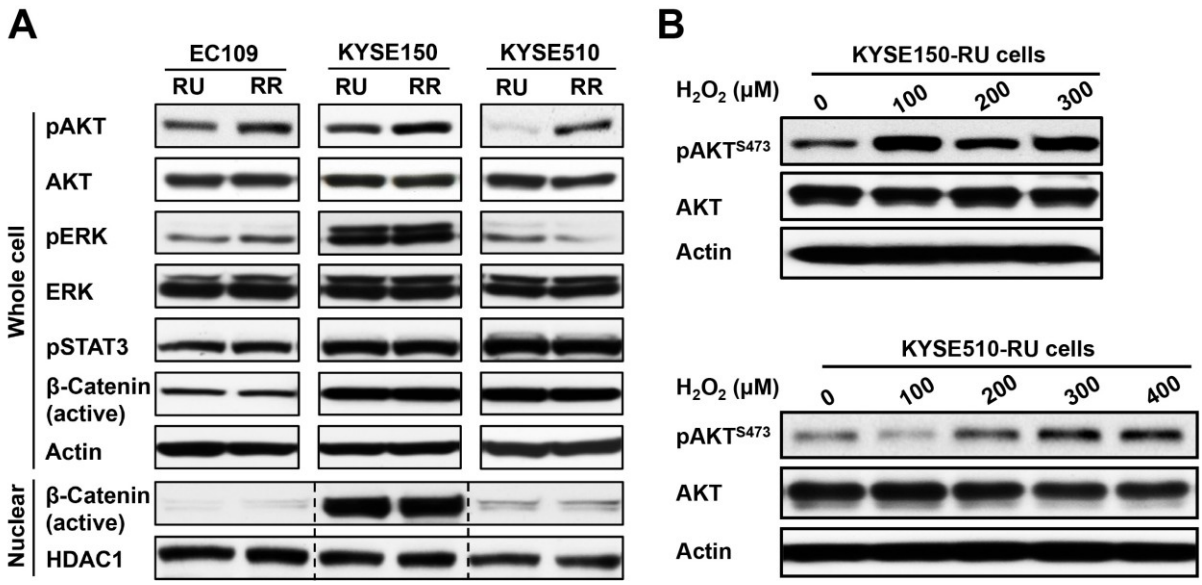

Figure 4.7 The PI3K-AKT pathway promotes the RR phenotype. (**A**) The activation status of various signaling pathways was determined by Western blot. (**B**) The expression of pAKT and AKT in H_2O_2-resistant cells was determined by Western blot. **(Continued on the next page)**

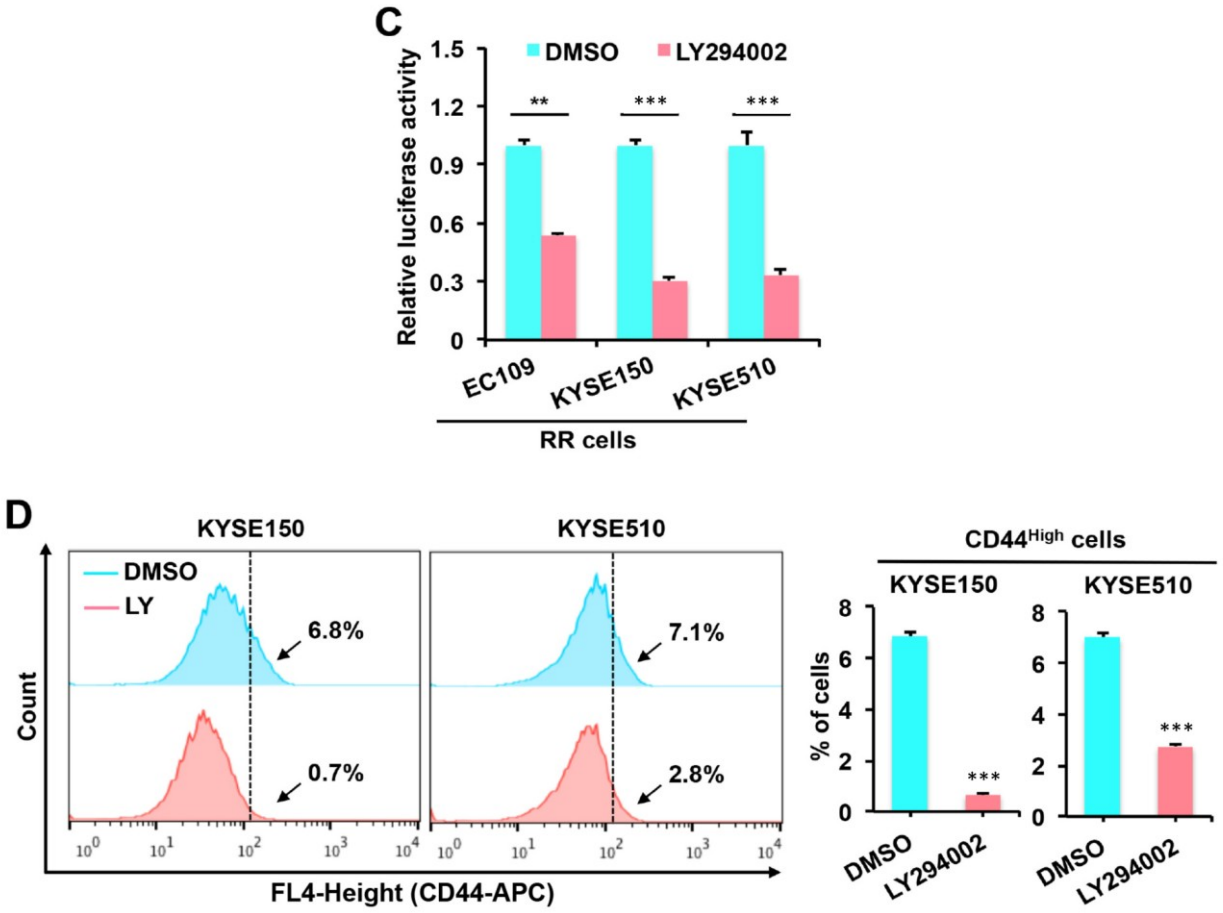

Figure 4.7C-D (**C**) 24h after DMSO or LY294002 treatment, Luciferase reporter assay was performed to determine the effect of the PI3K inhibitor LY294002 on the SRR2 responsiveness in RR cells (n=3, ***P*<0.01, ****P*<0.001 Student's *t* test). (D) 24h after LY294002 or DMSO treatment, CD44 expression was detected by Flow cytometry (n=3, ***P*<0.01, ****P*<0.001 Student's *t* test). **(Continued on the next page)**

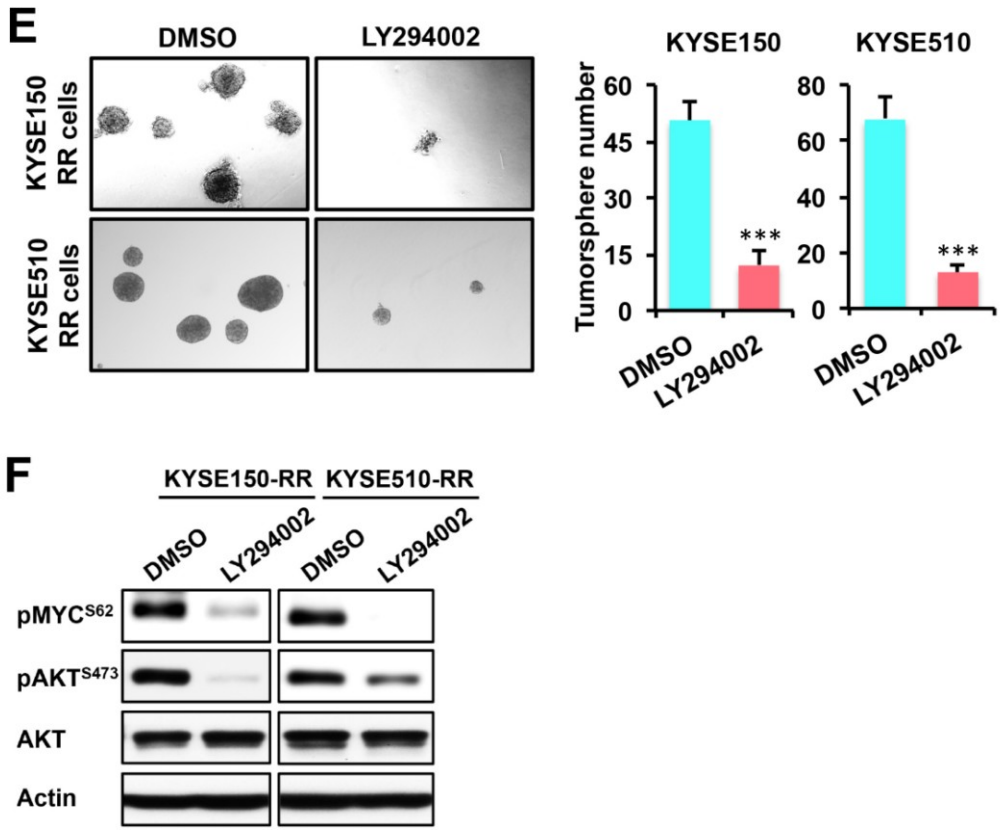

Figure 4.7E-F (**E**) Tumorsphere formation assay was performed with the treatment of DMSO or LY294002 (30μM) (n=3, ****P*<0.001, Student's *t* test). (**F**) The expression of pAKT and AKT in H_2O_2-resistant cells was determined by Western blot.

4.5 Discussion

The concept of CSC plasticity suggests that the stemness of CSCs can be acquired by non-CSCs under certain tumor microenvironment, such as hypoxia and chronic inflammation [9,10,32,33]. The EMT process that can be induced by the microenvironmental cues, such as TGF-β, IL-6, and TNF-α, has been shown to facilitate non-CSCs to gain CSC-like properties [10,33]. Given that CSCs are the major contributors of chemoresistance and relapse of cancer, understanding the molecular mechanisms underlying CSC plasticity carries great significance. To date, an ideal model for the study of CSC plasticity remains scarce. In this study, we show that the RU and RR dichotomy based on the SRR2 reporter is a useful model for gaining insights into the biology and plasticity of CSCs. Using this model, we reveal that ROS enhances CSC-like properties in ESCC by promoting the expression of MYC via the PI3K-AKT pathway, the first study that has addressed the mechanism behind the acquisition of CSC-like properties by ESCC cells.

Previous findings have demonstrated that $CD44^{High}$ cells in ESCC carry CSC-like features as indicated by a higher expression of stemness-associated factors, such as Sox2, Oct4 and NANOG, and a higher tumor initiating capacities in SCID mice [24,25]. The mechanism that regulates the generation of $CD44^{High}$ cells in ESCC remains unclear. Using the SRR2 reporter model, we found that RR cells are more CSC-like compared with RU cells, as indicated by the higher proportion of $CD44^{High}$ cells, which correlated with the stronger tumorsphere forming ability and higher chemoresistance. Importantly, the GFP and luciferase reporter carried by this cell model that monitors the

CSC-like properties, enabled us to effectively track the CSC-like cells during H_2O_2 treatment, which facilitated the identification of ROS as an inducer of the generation of $CD44^{High}$ CSC-like cells. Thus, the SRR2 model can be used as a useful model to study the CSC-plasticity.

The role played by ROS in stem cell biology remains controversial. Oxidative stress induced by a high level of ROS has been shown to suppress stemness of CSCs [34]. In support of this, recent studies have revealed that CSCs as well as normal stem cells maintain a low-level of ROS, which promotes tumorigenicity and radio/chemo-resistance [4,5,13]. Nevertheless, ROS has been demonstrated to promote stemness [14,35]. For instance, ROS induced by H_2O_2 and hypoxia was shown to promote the self-renewal and neurogenesis of neural stem cells [14]. H_2O_2-induced ROS was found to enhance the expression of stem cell factors such as OCT4, SOX2 and NANOG in malignant mesothelioma cells [35]. Data from our studies provide evidence supporting the stemness-promoting role of ROS in ESCC cells, as H_2O_2-induced ROS increased the population of $CD44^{High}$ CSC-like cells, enhanced tumorsphere formation and chemoresistance. These findings are in support of previous findings that mild levels of ROS enhance cell survival and proliferation via activating various signaling pathways, such as the MAPK pathway and the PI3K-AKT pathway [11,12].

Although our study reveals that ROS induced by acute H_2O_2 treatment promotes RU-to-RR conversion accompanied by the increase of CSC-like $CD44^{High}$ cells, chronic H_2O_2 challenge generated H_2O_2-resistant RU cells had

lower levels of ROS, a higher expression of ROS scavenger GCLC, and a higher chemoresistance, reflecting the features of CSCs reported by other studies [4,5,13]. Based on these findings, we can speculate that ROS is necessary for the initial stage of the RU-to-RR conversion or the acquirement of CSC-like properties, but after being converted to CSC-like cells, the anti-oxidant program is activated to detoxify ROS, so that CSC-like cells harbor a low level of ROS. Our findings may potentially address the controversial role of ROS in the pathobiology of cancers, *i.e.* ROS has been shown to be both oncogenic and tumor suppressive, depending on the specific contexts [36,37].

The PI3K-AKT pathway has been shown to promote CSC-like properties in various cancers, and inhibition of this pathway was shown to decrease the size of the CSC population and the tumor initiating capacity [38]. Aberrant activation of the PI3K-AKT pathway has been found to enhance the tumorigenicity and chemoresistance of ESCC [39], however, our understanding of its function in the CSC-like ESCC cells remains limited. To our knowledge, only one study has shown that the PI3K-AKT pathway is preferentially activated in the side population cells (recognized as CSC-like cells) in ESCC, and inhibition of this pathway decreases the size of the side population [40], whereas the mechanism has not been delineated. Using the SRR2 reporter model, we found that the PI3K-AKT pathway contributes to the RR phenotype as well as the ROS-induced RR phenotype. Blockade of this pathway not only diminished the SRR2 activity in RR cells but also markedly decreased the size of the $CD44^{High}$ population and the tumorsphere formation ability. Mechanism study suggests that active PI3K-AKT pathway exerts its

biological function through augmenting the expression of MYC, a critical factor in the RU/RR dichotomy in ESCC cells. GSK3β, a kinase that can be phosphorylated and inactivated by AKT, has been shown to promote MYC degradation by phosphorylating the Threonine-58 residue, which may mediate the biological function of the PI3K-AKT pathway in the regulation of MYC.

4.6 References

1. Ailles LE, Weissman IL. Cancer stem cells in solid tumors. Curr Opin Biotechnol 2007;18(5):460-6.
2. Abdullah LN, Chow EK. Mechanisms of chemoresistance in cancer stem cells. Clin Transl Med 2013;2(1):3.
3. Creighton CJ, Li X, Landis M, et al. Residual breast cancers after conventional therapy display mesenchymal as well as tumor-initiating features. Genes Dev 2009;23(18):2140-51.
4. Diehn M, Cho RW, Lobo NA, et al. Association of reactive oxygen species levels and radioresistance in cancer stem cells. Nature 2009;458(7239):780-3.
5. Chang CW, Chen YS, Chou SH, et al. Distinct subpopulations of head and neck cancer cells with different levels of intracellular reactive oxygen species exhibit diverse stemness, proliferation, and chemosensitivity. Cancer Res 2014;74(21):6291-305.
6. Mani SA, Guo W, Liao MJ, et al. The epithelial-mesenchymal transition generates cells with properties of stem cells. Cell 2008;133(4):704-15.

7. Scheel C, Weinberg RA. Phenotypic plasticity and epithelial-mesenchymal transitions in cancer and normal stem cells? Int J Cancer 2011;129(10):2310-4.
8. Chaffer CL, Brueckmann I, Scheel C, et al. Normal and neoplastic nonstem cells can spontaneously convert to a stem-like state. Proc Natl Acad Sci U S A 2011;108(19):7950-5.
9. Mohyeldin A, Garzón-Muvdi T, Quiñones-Hinojosa A. Oxygen in stem cell biology: a critical component of the stem cell niche. Cell Stem Cell 2010;7(2):150-61.
10. Shigdar S, Li Y, Bhattacharya S, et al. Inflammation and cancer stem cells. Cancer Lett 2014;345(2):271-8.
11. Ray PD, Huang BW, Tsuji Y. Reactive oxygen species (ROS) homeostasis and redox regulation in cellular signaling. Cell Signal 2012;24(5):981-90.
12. Klaunig JE, Kamendulis LM, Hocevar BA. Oxidative stress and oxidative damage in carcinogenesis. Toxicol Pathol 2010;38(1):96-109.
13. Ishimoto T, Nagano O, Yae T, et al. CD44 variant regulates redox status in cancer cells by stabilizing the xCT subunit of system xc(-) and thereby promotes tumor growth. Cancer Cell 2011;19(3):387-400.
14. Le Belle JE, Orozco NM, Paucar AA, et al. Proliferative neural stem cells have high endogenous ROS levels that regulate self-renewal and neurogenesis in a PI3K/Akt-dependant manner. Cell Stem Cell 2011;8(1):59-71.
15. Takahashi K, Yamanaka S. Induction of pluripotent stem cells from mouse embryonic and adult fibroblast cultures by defined factors. Cell 2006;126(4):663-76.

16. Takahashi K, Tanabe K, Ohnuki M, et al. Induction of pluripotent stem cells from adult human fibroblasts by defined factors. Cell 2007;131(5):861-72.
17. Weina K, Utikal J. SOX2 and cancer: current research and its implications in the clinic. Clin Transl Med 2014;3:19.
18. Wu F, Zhang J, Wang P, et al. Identification of two novel phenotypically distinct breast cancer cell subsets based on Sox2 transcription activity. Cell Signal 2012;24(11):1989-98.
19. Jung K, Gupta N, Wang P, et al. Triple negative breast cancers comprise a highly tumorigenic cell subpopulation detectable by its high responsiveness to a Sox2 regulatory region 2 (SRR2) reporter. Oncotarget 2015;6(12):10366-73.
20. Gelebart P, Hegazy SA, Wang P, et al. Aberrant expression and biological significance of Sox2, an embryonic stem cell transcriptional factor, in ALK-positive anaplastic large cell lymphoma. Blood Cancer J 2012;2:e82.
21. Kamangar F, Qiao YL, Schiller JT, et al. Human papillomavirus serology and the risk of esophageal and gastric cancers: results from a cohort in a high-risk region in China. Int J Cancer 2006;119(3):579-84.
22. Jemal A, Bray F, Center MM, et al. Global cancer statistics. CA Cancer J Clin 2011;61(2):69-90.
23. Huang D, Gao Q, Guo L, et al. Isolation and identification of cancer stem-like cells in esophageal carcinoma cell lines. Stem Cells Dev 2009;18(3):465-73.

24. Zhao JS, Li WJ, Ge D, et al. Tumor initiating cells in esophageal squamous cell carcinomas express high levels of CD44. PLoS One 2011;6:e21419.
25. Chen X, Ying Z, Lin X, et al. Acylglycerol kinase augments JAK2/STAT3 signaling in esophageal squamous cells. J Clin Invest 2013;123:2576-2589.
26. Cheung PY, Deng W, Man C, et al. Genetic alterations in a telomerase-immortalized human esophageal epithelial cell line: implications for carcinogenesis. Cancer Lett 2010;293:41–51.
27. Dontu G, Abdallah WM, Foley JM, et al. In vitro propagation and transcriptional profiling of human mammary stem/progenitor cells. Genes Dev 2003;17(10):1253-70.
28. Ponti D, Costa A, Zaffaroni N, et al. Isolation and in vitro propagation of tumorigenic breast cancer cells with stem/progenitor cell properties. Cancer Res 2005;65(13):5506-11.
29. Wang W, Xue L, Wang P. Prognostic value of β-catenin, c-myc, and cyclin D1 expressions in patients with esophageal squamous cell carcinoma. Med Oncol 2011;28(1):163-9.
30. Achuthan S, Santhoshkumar TR, Prabhakar J, et al. Drug-induced senescence generates chemoresistant stemlike cells with low reactive oxygen species. J Biol Chem 2011;286(43):37813-29.
31. Benassi B, Fanciulli M, Fiorentino F, et al. c-Myc phosphorylation is required for cellular response to oxidative stress. Mol Cell 2006;21(4):509-19.

32. Borovski T, De Sousa E Melo F, Vermeulen L, et al. Cancer stem cell niche: the place to be. Cancer Res 2011;71(3):634-9.
33. Friedmann-Morvinski D, Verma IM. Dedifferentiation and reprogramming: origins of cancer stem cells. EMBO Rep 2014;15(3):244-53.
34. Ito K, Hirao A, Arai F, et al. Reactive oxygen species act through p38 MAPK to limit the lifespan of hematopoietic stem cells. Nat Med 2006;12(4):446-51.
35. Kim MC, Cui FJ, Kim Y. Hydrogen peroxide promotes epithelial to mesenchymal transition and stemness in human malignant mesothelioma cells. Asian Pac J Cancer Prev 2013;14(6):3625-30.
36. Block K, Gorin Y. Aiding and abetting roles of NOX oxidases in cellular transformation. Nat Rev Cancer 2012;12(9):627-37.
37. Sporn MB, Liby KT. NRF2 and cancer: the good, the bad and the importance of context. Nat Rev Cancer 2012;12(8):564-71.
38. Martelli AM, Evangelisti C, Follo MY, et al. Targeting the phosphatidylinositol 3-kinase/Akt/mammalian target of rapamycin signaling network in cancer stem cells. Curr Med Chem 2011;18(18):2715-26.
39. Li B, Li J, Xu WW, et al. Suppression of esophageal tumor growth and chemoresistance by directly targeting the PI3K/AKT pathway. Oncotarget 2014;5(22):11576-87.
40. Li H, Gao Q, Guo L, et al. The PTEN/PI3K/Akt pathway regulates stem-like cells in primary esophageal carcinoma cells. Cancer Biol Ther 2011;11(11):950-8.

Chapter 5

General Discussion and Conclusions

5.1 miR-200b is a potential therapeutic tool for invasive ESCC tumors

Nevertheless, the usage of miR-200s as a therapeutic target should be performed with caution in certain types of cancers, e.g. breast cancer, melanoma, pancreatic ductal adenocarcinoma, as the role of miR-200s in these types of cancers remains still controversial **(Table 1.1)**. To be specific, although miR-200s have been shown to be potent suppressors of EMT and invasiveness **(Table 1.1)**, two studies have discovered that overexpression of miR-200s played a pro-metastatic role in breast cancer by enhancing the final colonization step of the multi-step metastasis process, which was shown to be the rate-limiting step in this malignant process in breast cancer [1,2]. Therefore, even though miR-200s are attractive targets based on their pleiotropic roles in multiple stages of cancer progression, stringent assessment of the therapeutic value and safety of targeting miR-200s should be conducted in each specific type of cancer.

After identifying the aberrant down-regulation of miR-200b in ESCC using microarrays applied to three pairs of ESCC and adjacent benign esophageal epithelial tissues [3], we have comprehensively evaluated the expression status, clinical significance, biological function both *in vitro* and *in vivo,* downstream target genes, and downstream signaling pathways of miR-200b in ESCC. The data are presented in Chapter 2. Our data collectively suggest miR-200b as a potent tumor suppressor in ESCC. Our findings support the schematic model depicted in **Figure 2-14 and 2-15**, which show that miR-200b is a key factor that regulates the adhesive and actin cytoskeletal machinery, two major driving forces of cell motility and invasiveness.

Specifically, the core components or the "engines" of the adhesive and actin cytoskeleton machineries are FAK and small GTPases (RhoA, Cdc42 and Rac1), respectively [4,5]. miR-200b suppresses the activation status of these core components by directly targeting Kindlin-2. Then, the signals are transmitted from Kindlin-2 to Integrin β1, the central node that leads to the activation of the two machineries. Moreover, Integrin β1 also connects the miR-200b-Kindlin-2 axis to the PI3K-AKT pathway, a pleiotropically acting pathway that enhances cell invasiveness.

Besides the important role played by miR-200b in suppressing the adhesive and actin cytoskeletal machineries that provide driving forces for cell invasion, our study also validated that the classic miR-200b-ZEB1/2 regulatory axis is intact in ESCC cell lines as well as in ESCC patient samples, as evidenced by the correlation between their expression and their significant prognostic values. Nevertheless, E-cadherin, the widely recognized effector of the miR-200b-ZEB1/2 axis in its regulation of EMT, does not mediate the biological function of miR-200b in the ESCC cell lines tested. Gene methylation of *CDH1* gene that encodes E-cadherin protein was found to be a barrier that blocks its regulation by the miR-200b-ZEB1/2 axis (**Figure 2-14 and 2-15**). Since ZEB proteins have also been shown to play critical roles in other traits of cancer in addition to EMT, such as cancer cell stemness, tumor angiogenesis, and chemoresistance, it is possible that the intact miR-200b-ZEB1/2 axis can exert its biological function through mechanisms other than regulating E-cadherin or the EMT process. Mounting evidence from recent studies is in support of this hypothesis [6,7].

To conclude, our data suggest that miR-200b is a potent tumor suppressor in invasive ESCC, which can be considered as a therapeutic tool to block invasiveness in ESCC.

5.2 STAT3β is an effective chemo-sensitizer in ESCC, which also dictates the opposing function of STAT3 as an oncoprotein and tumor suppressor

We have comprehensively evaluated the tumor suppressor effects of STAT3β in ESCC, which reveals that STAT3β dramatically sensitizes ESCC cells to the chemotherapy with cisplatin and 5-FU, both *in vitro* and *in vivo*. These findings were also evidenced by our clinical findings that higher expression of STAT3β was correlated with a longer recurrence-free survival in patients who have received radio-chemotherapy. Taken together, our study suggests that STAT3β can be used as a potential biomarker for the responsiveness of ESCC patients to chemotherapy, and STAT3β can be exploited as a tool to treat chemoresistant ESCC tumors. To this end, morpholinos, a type of artificial small molecules, that has been designed to modulate the STAT3 alternative splicing process to favour the generation of STAT3β at the expense of STAT3α [8], should be tested whether it can be used as a powerful tool to enhance the chemosensitivity of ESCC tumors.

In the last two decades, STAT3 has been widely recognized as an oncogene and an ideal target for cancer therapy. Nevertheless, data from both experimental and clinical studies have shown that STAT3 plays a tumor

suppressor role in multiple types of cancers. In our study presented in Chapter 3, using ESCC as a model, we comprehensively studied the interplay between the two STAT3 isoforms, STAT3α and STAT3β, and revealed a mechanism that may explain the discrepancies regarding the opposing role of STAT3 in cancer. We found that even though STAT3β attenuated STAT3 transcription activity, it substantially increased the tyrosine^{705}-phosphorylation, nuclear translocation and DNA binding/promoter occupation of STAT3α. In support of these findings, we found in ESCC patients that high STAT3β expression converts pSTAT3α^{Y705} from an unfavorable prognostic marker to a favorable prognostic marker. Moreover, we delineated the mechanism behind the STAT3β:STAT3α cross-regulation by showing that STAT3β forms heterodimers with STAT3α, thereby hampering the binding and dephosphorylation of STAT3α by PTP-MEG2, a protein tyrosine phosphatase.

The paradoxical increase in phospho-STAT3α^{Y705} induced by STAT3β carries important implications as to how the biological function and prognostic significance of STAT3 in cancers should be interpreted. Specifically, in STAT3β-low tumors, activation of STAT3 increases pSTAT3α^{Y705}, which exerts potent oncogenic effects. In contrast, in STAT3β-high tumors, although pSTAT3α^{Y705} is dramatically augmented by STAT3β, the overall oncogenic effects of STAT3 are indeed suppressed by STAT3β. In other words, without the distinction between the two STAT3 isoforms, as in the case of virtually all previously published clinicopathologic studies of STAT3, it is perceivable that one may conclude that a high expression level of pSTAT3α^{Y705} or total pSTAT3^{Y705} is oncogenic if the vast majority of the tumors in the study cohort

are STAT3β-negative/weak. Therefore, whether STAT3 is oncogenic or tumor suppressive is largely dictated by the expression status of STAT3β.

5.3 The PI3K-AKT pathway and MYC mediates Reactive Oxygen Species (ROS) induced acquired stemness in ESCC

Our understanding of the biology of cancer stem cells (CSCs) in ESCC remains scarce, and only a few studies have started identifying CSC-like cells in ESCC using Hoechst dye efflux and CD44 as markers. Moreover, although recent studies have revealed the plasticity of CSCs using models such as inducible EMT and hypoxia [9-12], a model that can be easily used to investigate how cancer cells acquire stemness remains lacking. In our study described in Chapter 4, we successfully isolated two distinct cell subpopulations in ESCC cell lines using used the SRR2 (Sox2 regulatory region 2) reporter. Compared with reporter-unresponsive (RU) cells, reporter responsive (RR) cells are more stem-like, with a significantly higher capacity of tumorsphere formation and a higher proportion of cells that were $CD44^{High}$, a cancer stem cell marker in ESCC. Using this cell model, which distinguishes stem-like properties with easily detectable GFP, we revealed that ROS induced by H_2O_2 converts RU cells into the stem-like RR cells. Similar to cancer stem cells in other cancer models, both RR cells and converted RR cells contained less ROS and were more resistant to cisplatin, as compared to RU cells. We found that MYC but not Sox2 is a crucial factor that promotes the reporter responsiveness and the ROS-induced RU/RR conversion. Furthermore, compared with RU cells, the PI3K-AKT pathway is more active in both RR cells and converted RR cells, and the blockade of which can

effectively mitigate the stem-like properties of these cells. Therefore, ROS can induce stemness in ESCC via activating the PI3K-AKT pathway and MYC expression. SRR2 is a useful marker for cancer stemness in ESCC, and RU/RR conversion induced by H_2O_2 provides a useful model to study the plasticity of cancer stemness.

5.4 Plausible intrinsic associations among deregulated STAT3β, miR-200b and stemness of ESCC

5.4.1 Possible association between the two tumor suppressors in ESCC (*i.e.* STAT3β and miR-200b)

Our studies described above underscore the pathobiological function of STAT3β and miR-200b, two tumor suppressors in ESCC. However, whether the aberrant expression of these two tumor suppressors is intrinsically linked remains unclear. A recent study revealed that activation of the STAT3 signaling pathway by Oncotatin M (OSM) in breast cancer cells promotes EMT via suppressing the expression of the miR-200b and miR-200c [13]. Since our data has shown that STAT3β suppresses the STAT3 signaling pathway, we can speculate that reduced expression of STAT3β in ESCC may contribute to the downregulated miR-200b in ESCC cells. Nevertheless, further studies are required to support this hypothesis.

5.4.2 Possible roles of STAT3β and miR-200b in suppressing cancer stem cells in ESCC

Our data have shown that enforced expression of STAT3β suppressed the cancer stem-like cells in ESCC (Figure 3.3); however, the exact mechanism remains ambiguous. Since STAT3 has been reported to be an important factor for cancer cell stemness, including glioma, breast cancers, neuroblastoma, and ESCC [14-18], we speculate that STAT3β may suppress cancer cell stemness via repressing the STAT3 signaling pathway. Data from Chapter 4 show that oxidative stress can promote stemness acquisition in ESCC cells, whether STAT3β or the STAT3 signaling pathway is involved in this process needs further investigation.

Given that STAT3β has a unique 7-amino acid in the C-terminus compared with STAT3α, STAT3β may form transcriptional complexes with a distinct set of proteins, which may confer STAT3β with biological functions that does not overlap with its dominant-negative effects on STAT3α. Thus, it is likely that STAT3β may suppress ESCC stem-like properties via STAT3α-independent mechanisms.

As described in the introduction section 1.2.2.2, the miR-200 family members are important regulators of stemness in both normal stem cells and cancer stem cells. However, the biological function of miR-200b in the regulation of stemness in ESCC cells remains unknown. Since BMI-1, one of the key downstream mediators of miR-200b in the regualtion of cancer stemness, has been shown to promote the self-renewal of ESCC stem-like cells [19], it is likely that miR-200b can mitigate ESCC stemness via targeting this protein, albeit other mechanisms may also mediate the function of miR-200b.

5.5 References

1. Korpal M, Ell BJ, Buffa FM, et al. Direct targeting of Sec23a by miR-200s influences cancer cell secretome and promotes metastatic colonization. Nat Med 2011; 17: 1101-8.
2. Dykxhoorn DM, Wu Y, Xie H, et al. miR-200 enhances mouse breast cancer cell colonization to form distant metastases. PLoS One 2009; 4: e7181.
3. Wu BL, Xu LY, Du ZP, Liao LD, Zhang HF, Huang Q, et al. MiRNA profile in esophageal squamous cell carcinoma: downregulation of miR-143 and miR-145. World J Gastroenterol 2011;17:79-88.
4. Hall,A. *et al.* (1998) Rho GTPases and the actin cytoskeleton. *Science,* 279, 509–514.
5. Webb,D.J. *et al.* (2003) Illuminating adhesion complexes in migrating cells: moving toward a bright future. *Curr. Opin. Cell Biol.,* **15,** 614-620.
6. Li X, Roslan S, Johnstone CN, *et al*. MiR-200 can repress breast cancer metastasis through ZEB1-independent but moesin-dependent pathways. Oncogene 2014;33:4077-4088.
7. Bracken CP, Li X, Wright JA, *et al*. Genome-wide identification of miR-200 targets reveals a regulatory network controlling cell invasion. EMBO J 2014;33:2040-2056.
8. Zammarchi F, de Stanchina E, Bournazou E, Supakorndej T, Martires K, Riedel E, et al. Antitumorigenic potential of STAT3 alternative splicing modulation. Proc Natl Acad Sci USA 2011;108:17779-17784.

9. Mohyeldin A, Garzón-Muvdi T, Quiñones-Hinojosa A. Oxygen in stem cell biology: a critical component of the stem cell niche. Cell Stem Cell 2010;7(2):150-61.
10. Shigdar S, Li Y, Bhattacharya S, et al. Inflammation and cancer stem cells. Cancer Lett 2014;345(2):271-8.
11. Borovski T, De Sousa E Melo F, Vermeulen L, et al. Cancer stem cell niche: the place to be. Cancer Res 2011;71(3):634-9.
12. Friedmann-Morvinski D, Verma IM. Dedifferentiation and reprogramming: origins of cancer stem cells. EMBO Rep 2014;15(3):244-53.
13. Guo L, Chen C, Shi M, et al. Stat3-coordinated Lin-28-let-7-HMGA2 and miR-200-ZEB1 circuits initiate and maintain oncostatin M-driven epithelial-mesenchymal transition. Oncogene 2013;32(45):5272-82.
14. Kim E, Kim M, Woo DH, et al. Phosphorylation of EZH2 activates STAT3 signaling via STAT3 methylation and promotes tumorigenicity of glioblastoma stem-like cells. Cancer Cell 2013;23(6):839-52.
15. Marotta LL, Almendro V, Marusyk A, et al. The JAK2/STAT3 signaling pathway is required for growth of $CD44^+$ $CD24^-$ stem cell-like breast cancer cells in human tumors. J Clin Invest 2011;121(7):2723-35.
16. Wei W, Tweardy DJ, Zhang M, et al. STAT3 signaling is activated preferentially in tumor-initiating cells in claudin-low models of human breast cancer. Stem Cells 2014;32(10):2571-82.
17. Agarwal S, Lakoma A, Chen Z, et al. G-CSF Promotes Neuroblastoma Tumorigenicity and Metastasis via STAT3-Dependent Cancer Stem Cell Activation. Cancer Res 2015;75(12):2566-79.

18. Liu K, Jiang M, Lu Y, et al. Sox2 cooperates with inflammation-mediated Stat3 activation in the malignant transformation of foregut basal progenitor cells. Cell Stem Cell 2013;12(3):304-15.
19. Yu X, Jiang X, Li H, et al. miR-203 inhibits the proliferation and self-renewal of esophageal cancer stem-like cells by suppressing stem renewal factor Bmi-1. Stem Cells Dev 2014;23(6):576-85.